Palaeozoic and Mesozoic Palaeomagnetism of South America: Results from Peru, Bolivia, Argentina, and Brazil.

Inaugural–Dissertation
zur Erlangung des Doktorgrades
an der Fakultät für Geowissenschaften der
Ludwig-Maximilians-Universität München

Vorgelegt von
Nicolas A. Rakotosolofo
Mai 2004

Acknowledgement

Table of contents

Chapter 1 Introduction

Chapter 2 Geological setting of the sampling regions

Chapter 3 Palaeomagnetic sampling and techniques

Chapter 4 A new Cretaceous palaeomagnetic pole from NE Brazil

List of Figures

List of Tables

Glossary

$\alpha_{95}°$ .... Radius of 95% confidence circle (Fisher, 1953) about mean direction

$A_{95}°$ .... Radius of 95% confidence circle (Fisher, 1953) about mean palaeopole

AP .... Argentina Precordillera

APWP .... Apparent Polar Wander Path

CRM .... Chemical remanent magnetisation

$Dg°$ .... Declination in *in-situ* (geographic) co-ordinates

$Ds°$ .... Declination in bedding-corrected (stratigraphic) co-ordinates

Dip .... Plunge of bedding in degree

Dir .... Direction of the plunging of rock's bedding in degree east

dp/dm .... Semi-axes of the 95% confidence ellipse about VGP

FA .... Famatina Range

Fm.. .... Formation

Gp .... Group

Hc .... Coercive force

Hcr .... Remanence coercivity

$Ig°$ .... Inclination in bedding-corrected (stratigraphic) co-ordinates

$Is°$ .... Inclination in bedding-corrected (stratigraphic) co-ordinates

IRM .... Induced remanent magnetisation

kg .... Precision parameter (Fisher, 1953) for *in-situ* direction

ks .... Precision parameter (Fisher, 1953) for bedding-corrected direction

K .... Precision parameter (Fisher, 1953) for mean palaeopole

MAD .... Maximum angular deviation in degree

Mrs .... Specific saturation remanence

Ms .... Specific saturation magnetisation

n .... Number of core samples

N .... Number of palaeomagnetic sites

$P_{lat}(°S)$ .... Latitude position of palaeosouth VGP in degree south

$P_{long}(°E)$ .... Longitude position of palaeosouth VGP in degree east

$\lambda(°S)$ .... Latitude position of mean palaeosouth pole in degree south

$\phi(°E)$ .... Longitude position of mean palaeosouth pole in degree east

SP .... Sierras Pampeanas (Pampean Range)

TRM .... Thermoremanent magnetisation

VFTB .... Variable Field Translation Balance

VGP .... Within-site or Sample-level Virtual Geomagnetic Pole

VRM .... Viscous remanent magnetisation

Abstract

In order to help define the apparent polar wander path for Gondwana, and to determine the palaeogeographic evolution of the Pacific margin of Gondwana, detailed palaeomagnetic studies have been carried out in several different regions of South America. In the Central Andes, sampling was carried out in Ordovician through to Early Triassic age sequences of the Subandean Zone, the Eastern Cordillera, the Altiplano, the Famatina Ranges, the Argentine Precordillera, and the Paganzo Basin. From more stable regions of South America, samples were also collected from Palaeozoic and Cretaceous age sedimentary and volcanic rocks from the Parnaíba, Araripe and Pernambuco-Paraiba Basins of NE Brazil.

Samples from more than 320 sampling sites were collected. From the majority of these samples, however, no reliable information could be obtained due to problems of remagnetisation and the magnetic instability of many sequences (factors which are not apparent in the field). Nevertheless, a number of high quality primary palaeomagnetic results were obtained and provide important information concerning the palaeogeographic evolution of western Gondwana.

For Cretaceous times, samples collected from the Sardinha Formation of north eastern Brazil yield a high quality primary direction of D= 176°, I= +05.1°; α_{95}= 2.0°; k= 355; n= 82 samples; N= 15 sites), which translates into a palaeosouth pole of λ= 84.4°S; ϕ= 090.7°E; A_{95}= 1.8°; K= 441.9. This is in agreement with the previously published well-dated Lower Cretaceous poles from Brazil. Combination of the result from Sardinha Formation with the coeval published high quality data (Q≥4) from stable South America results in a new Early Cretaceous pole located at λ= 84.3°S; ϕ= 067.7°E (A_{95}= 2.3°; K= 867). The age of this mean pole compiled exclusively from South American data is well constrained between 115 Ma and 133 Ma.

Results from the Late Palaeozoic-Lower Mesozoic rock units exposed in the southern Peruvian Andes show that the Mitu and the Copacabana Groups carry well-defined pre-folding primary remanences. The stable magnetisation of the Early Triassic Mitu Group (244 ±6 Ma) consists of a dual polarity magnetisation yielding an overall site mean of D= 349.3°; I= -35.3° (α_{95}= 4.1°; k= 351.4; n= 24 samples; N= 5 sites). This remanence passes the fold test at the 99% confidence level and the reversal tests with classification B. Combining the pole from the Mitu Group (λ= 78.6°S; ϕ= 351.9°E; A_{95}= 3.7°; K= 447) with the selected coeval published palaeomagnetic data from stable South America (Q≥3 and good age control), results in a new Early Triassic pole situated at λ= 76.5°S; ϕ= 306.2°E (A_{95}= 8.3°; K= 66.0; N= 6 studies). In opposition to the Mitu Group, the stable remanence carried by the Early Permian Copacabana Group (D= 166.1°; I= +48.9° (α_{95}= 4.5°; k= 131.5; n= 43 samples; N= 9 sites) is exclusively of reversed polarity. Positive fold test

significant at the 99% level and consistency with the Permian-Carboniferous Reverse Superchron (PCRS) confirmed the Early Permian acquisition of this remanence. Combining the pole from Copacabana Group ($\lambda= 68.2°S$; $\phi= 321.3°E$ ($A_{95}= 5.2°$; $K= 99.8$) with published data from stable South America results in a new Early Permian pole (280 ±20 Ma; $\lambda= 70.4°S$; $\phi= 341.8°E$; $A_{95}= 8.8°$; $K= 48.3$; $N= 7$ studies).

These results from southern Peru have an important implication for the palaeogeography of Pangaea. Comparison with the palaeomagnetic data from Laurussia show that both the Early Permian and the Early Triassic poles from South America do not coincide with the coeval poles from Laurussia when adopting the reconstruction parameters for Pangaea A. In contrast, palaeogeographic reconstructions based on palaeomagnetic data from South America satisfy the proposed Pangaea B in Early Permian and Pangaea A2 in Early Triassic, implying large scale dextral shear between Gondwana and Laurussia in Permian times.

For Early Carboniferous times, samples collected from the Taiguati Formation of the Bolivian Subandean Zone yields a slightly less well defined plausible Late Carboniferous remagnetisation exclusively carried by magnetite. The palaeosouth pole position ($\lambda= 58.3°S$; $\phi= 348.9°E$ ($A_{95}= 6.0°$; $K= 66$) calculated from this remanence is in good agreement with the 290-323 Ma poles from South America, Africa, and Australia. Combining the Taiguati pole with the well-dated published South American data ($Q\geq3$) result in a new mean Late Carboniferous pole situated at $\lambda= 53.0°S$; $\phi= 348.4°E$ ($A_{95}= 6.0°$; $K= 86.4$; $N= 8$ studies).

As an implication for the Gondwana APWP, the presented new Palaeozoic-Mesozoic poles define a complete Late Carboniferous to Early Triassic path for South America, and by proxy, for Gondwana. When transferred in African co-ordinates, this path suggests a palaeosouth pole that has moved southwards from northern Antarctica (Late Carboniferous) to south of Antarctica (the Early Triassic), implying a northward drift of Gondwana with an average velocity of 7.2 cm/year in Late Carboniferous-Early Permian times, and 4.6 cm/year during the whole Permian. The presented APW path for Gondwana, supports the Carboniferous to Triassic segment of the paths of Torsvik & Van der Voo (2002) and McElhinny *et al.* (2003). In contrast, the newly defined Late Carboniferous pole disagrees with the Carboniferous segment of the APW paths of Bachtadse & Briden (1990), Schmidt *et al.* (1990) and Smith (1998).

For Early Palaeozoic times, results from the Early Ordovician Umachiri Series exposed in the Altiplano (southern Peru) show pre-folding stable remanence (D= 003.6°; I= +45.5°; $\alpha_{95}= +13.5°$; $K= 84$; $n= 18$ samples; $N= 3$ sites) that passes the fold test at the 99% confidence level. Palaeolatitude information from this unit places southern Peru at a latitude of 27 ±5°S. This is coherent with the position of South American margin within the Lower

Ordovician Gondwana. The calculated palaeopole (λ= 47.7°N; ϕ= 293.7°E; A_{95}= 12.8°; K= 93.3), however, diverges from Early Ordovician poles for Gondwana. The discrepancy suggests an approximately 45° anticlockwise rotation of the sampling area. This rotation is constrained by previous study as having occurred in post-Oligocene times, and took place along a shear system that developed in northern Altiplano during the Andean deformation.

From the Argentine Precordillera, remanences carried by the Patquia, Guandacol, Los Espejos, and combined data from San Juan and La Silla Formations, are considered as being primary in origin. Results from the Late Permian Patquia Formation (D= 225.8°; I= +61.8°; α_{95}= 3.0°; k=215; n=12 samples), the Late Carboniferous Guandacol Formation (D= 194.1°; I= +59.8°; α_{95}= 4.4°; k= 279; n= 8 samples), and the Late Silurian Los Espejos Formation (D= 289.8°; I= -29.9°; α_{95}= 17.6°; k= 50; n= 20 samples, N= 3 sites) indicate an approximately 60° clockwise rotation of the Precordillera during the Cenozoic Andean orogeny. Alternatively, combined results from the Early Ordovician San Juan and La Silla Formations (D= 011.1°; I= +58.4°; α_{95}= 4.0°; k= 81.5; n= 17 samples), which passes the fold test (99%) at sample level, show that the sampling location was located at latitude 39.5 ±4°S during the Ordovician. Good agreement of this palaeolatitude situation with the position of the Precordillera with respect to the Early Ordovician Gondwana, indicate that the Argentine Precordillera was part of Gondwana since the Early Ordovician times. However, in opposition to the Late Permian to Late Silurian sequences, the Early Ordovician sequences show a net anticlockwise rotation of approximately 45°, suggesting a complex tectonic history of the Precordillera. The overall palaeomagnetic data demonstrate an up to 105° anticlockwise rotation of the Precordillera between the Early Ordovician to Late Silurian times and an approximately 60° clockwise rotation during the Cenozoic Andean orogeny. The earlier pre-Late Silurian rotation possibly take place during the Ocloyíc deformational phase that resulted in a closure of the Puna Basin.

Palaeomanetic data for the Famatina Ranges are derived from De La Cuesta Formation (Late Permian) and Suri Formation (Early Ordovician). The pre-folding remanence carried by the Suri (D= 107°; I= 31°; α_{95}= 7.1°; k= 97; n= 25 samples; N= 5 sites), which yields a palaeopole position of λ= 21.6°S, ϕ= 014.0°E (A_{95}= 4.5°; K= 293.1 in South America co-ordinates), is considered as being Early Ordovician in age. An approximately 60° clockwise rotation of the Famatina after the Early Ordovician times is deduced from this data. As result from De la Cuesta Formation (D=163.2°; I= +43.8°; α_{95}= 10.0°; k=59.5; n= 23 samples; N= 5 sites) show that Famatina was stable since Late Permian, this rotation is constrained as having occurred in Early Ordovician-Late Permian times. It may also occurred during the Ocloyíc deformation. As the palaeolatitude position of Famatina (16.5 ±3°S) calculated from Suri Formation is in agreement with its position in the Early Ordovician Gondwana, the presented results suggest that Famatina was situated at its

present position with respect to South America since the Early Ordovician times. This rule out the proposed para-autochthonous origin of the Famatina.

In summary, the new results presented provide important new data to constrain the timing of terrane accretion and deformational history of the western margin of Gondwana. They indicate coherency of the Argentine Precordillera with the south American margin in Early Ordovician times, and a subsequent complex consolidation of the margin involving large scale rotations in pre-Permian times. Further relatively large scale block rotations also occurred during the Andean orogeny. Finally, the high quality results from southern Peru clearly indicate a Pangaea B reconstruction in Early Permian times, and a Pangaea A2 type configuration in the Early Triassic, thus supporting the more recent hypotheses concerning the configuration of Pangaea and its evolution through Permian times from the B to the A configurations.

Zusammenfassung

Im Rahmen der vorliegenden Arbeit, wurden in verschiedenen Regionen Südamerikas detaillierte paläomagnetische Untersuchungen durchgeführt. Ziel dieser Arbeiten war die Erstellung einer hochauflösenden scheinbaren Polwanderkurve für Gondwana im Paläozoikum und eine Beschreibung der paläogeographischen Entwicklung des pazifischen Gondwanarandes. In den zentralen Anden wurden ordovizische bis früh-triassische Sequenzen untersucht. Im einzelnen wurden folgende Regionen detailliert bearbeitet: die Subandine Zone, die östliche Kordillere, der Altiplano, die Famatina Ketten die argentinische Vorkordillere sowie das Paganzo Becken. Zusätzlich wurden Sedimente und Vulkanite paläozoischen und kretazischen Alters auf dem südamerikanischen Kraton untersucht. Untersuchungsgebiete waren hier die Parnaíba, Araripe und Pernambuco-Paraiba Becken in Nordost Brasilien. Insgesamt wurden im Rahmen dieser Studie 1682 orientierte Proben an mehr als 320 Lokalitäten entnommen. Detaillierte paläomagnetische Experimente ergaben jedoch lediglich für einen Bruchteil dieser Kollektion zuverlässige Daten. Die Mehrheit des untersuchten Probenmaterials ist entweder remagnetisiert oder aber trägt Magnetisierungen, die als instabil zu bezeichnen sind. Dennoch konnte eine hohe Zahl paläomagnetischer Ergebnisse von hoher Qualität erzielt werden. Diese Ergebnisse liefern wichtige Parameter für das Verständnis der paläogeographischen Entwicklung Westgondwanas.

Die mesozoischen Gesteine Nordost-Brasiliens (Sardinha Formation) weisen stabile, von Magnetit getragene Remenzrichtungen auf. Diese Remanenz wurde in der frühen Kreide erworben. Die gemittelte paläomagnetische Richtung dieser Einheit (120-130 Ma) ist D= 176°; I= +05.1°; α_{95}= 2.0°; k= 355; n= 82 Proben; N= 15 Sites),was einer Pollage von λ= 84.4°S; ϕ= 090.7°E; A_{95}= 1.8°; K= 441.9 entspricht. Dieser Pol ist in guter Übereinstimmung mit bereits publizierten Daten datierter paläomagnetischen Pole der Unterkreide Brasiliens. Fasst man die Ergebnisse der Sardinha Formation mit publizierten und verlässlichen Daten gleichen Alters zusammen so ergibt sich ein neuer paläomagnetischer Pol für die frühe Kreide (115-133 Ma) des stabilen Südamerikas (λ= 84.3°S; ϕ= 067.7°E ; A_{95}= 2.3°; K= 867).

Die Einheiten der Mitu und Copacabana „Groups", aufgeschlossen in den südlichen peruanischen Anden, tragen primäre, gut definierte Remanenzrichtungen die in der frühen Trias bzw. dem frühen Perm erworben wurden. Sowohl inverse als auch normale Polarität konnten bei Proben der Mitu „Group" (244 ±6 Ma) nachgewiesen werden (D= 349.3°; I= -35.3°; α_{95}= 4.1°; k= 351.4; n= 36 Proben; N= 5 Sites). Die hohe Qualität der Daten wird durch einen positiven Faltentest (99% Konfidenz) und eine positiven Reversaltest der Kategorie B belegt. Durch Kombination dieser Daten mit bereits publizierten paläomagnetischen Ergebnissen ergibt sich ein neuer früh-

triassischer Pol von λ= 78.6°S; ϕ= 351.9°E (A_{95}= 3.7°; K= 447). Im Gegensatz zur Mitu „Group" wurden bei den Proben der früh-permischen Copacabana „Group" ausschließlich Remanenzrichtungen inverser Polarität identifiziert. Diese Tatsache legt einen Erwerb der Magnetisierung während der „Permian-Carboniferous Reverse Superchron" (PCRS) nahe. Der Faltentest ist auf dem 99% Konfidenzniveau positiv. Die gemittelte paläomagnetische Richtung von D= 166.1°; I= +48.9° (α_{95}= 4.5°; k= 131.5; n= 39 Proben; N= 9 Sites) und der damit definierte früh-permische Pol (λ= 68.2°S; ϕ= 321.3°E; A_{95}= 5.2°; K= 99.8) kann daher als zuverlässig betrachtet werden. Auch in diesem Fall lässt sich ein neuer paläomagnetischer Pol berechnen. Zusammen mit Literaturdaten ergibt sich ein Pol für das frühe Perm des stabilen Südamerika von λ= 70.4°S; ϕ= 341.8°E; A_{95}= 8.8°; K= 48.3; N= 7 Daten).

Die neuen Ergebnisse für das frühe Perm und die frühe Trias des stabilen Südamerikas haben weitreichende Auswirkungen auf die paläogeographische Rekonstruktion Pangäas. Sie sind nicht kompatibel mit Polen gleichen Alters wie sie für Laurussia bestimmt wurden, wenn man ein Pangäa A Konfiguration annimmt. Geht man allerdings von einer Pangäa B Konfiguration im frühen Perm und dem Modell von Pangäa A2 in der frühen Trias aus, so werden diese Unstimmigkeiten aufgelöst. In diesem paläogeographischen Szenario muß man von einer westwärtigen Bewegung Gondwanas relativ zu Laurussia während des Perms ausgehen. Diese Relativbewegung hat sich möglicherweise im Jura fortgesetzt, bis die Pangäa A Konfiguration, so wie sie allgemein für den Zeitraum vor dem Zerbrechen Pangäas akzeptiert wird, erreicht wurde.

Die Einheiten der „Subandine Zone" Boliviens (Taiguati Formation) lieferten keine primären Remanenzrichtungen. Allerdings konnte nachgewiesen werden, dass die ermittelte mittlere paläomagnetische Richtung (D= 149.0°; I= +54.0°; α_{95}= 5.1°; k= 46; Pol: λ= 58.3°S; ϕ= 348.9°E; A_{95}= 6.0°; K= 66) auf eine Remagnetisierung im späten Karbon zurückzuführen ist. Ein Vergleich mit Daten gleichaltriger Gestein aus anderer Regionen Südamerikas, Afrika und Australien ergibt eine sehr gute Übereinstimmung. Daher kann auch in diesem Fall ein neuer kombinierter spät-karbonischer Pol für Südamerika bestimmt werden (λ= 53.0°S; ϕ= 348.4°E; A_{95}= 6.0°; K= 86.4; N= 8 Daten).

Die neuen paläomagnetischen Pole erlauben die Erstellung einer vollständigen scheinbaren Polwanderkurve „apparent polar wander path", APWP) für Südamerika und damit indirekt auch für Gondwana. Transferiert man diesen APWP in afrikanische Koordinaten, so zeigt es sich, dass der Paläosüdpol sich von der nördlichen Antarktis (spätes Karbon) südwärts bis in die südliche Antarktis (frühe Trias) bewegt hat. Daraus ergibt sich eine nordwärtige Drift Gondwanas mit einer mittleren Geschwindigkeit von 7.2 cm/a zwischen dem frühen Karbon und dem frühen Perm. Während des Perms liegt die aus den Daten abgeleitete mittlere

Driftgeschwindigkeit bei 4.6 cm/a. Der in dieser Arbeit vorgeschlagene APWP unterstützt das Modell von Torsvik und Van der Voo (2002) und McElhinney *et al.* (2003) für das karbonische bis triassische Segment des APWPs Gondwanas. Widersprüche ergeben sich allerdings aus dem Vergleich der neuen spät-karbonischen Daten mit der APWP von Bachtadse und Briden (1991), Schmidt et al. (1990) und Smith (1998).

Um weitere Daten für den APWP Gondwanas im frühen Paläozoikums zu gewinnen wurde die Umachiri Serie (Altiplano, Süd-Peru) beprobt. Es konnte eine stabile Magnetisierungskomponente isoliert werden (D= 003.6°; I= +45.5°; α_{95}= +13.5°; K= 84; n= 18 Proben; N= 3 Sites). Der primäre Charakter dieser früh-ordovizischen Komponente wird durch einen positiven Faltentest (99% Konfidenzniveau) untermauert. Anhand der Remanenzrichtungen wurde die Paläobreitenlage von Süd-Peru mit 27 ±5°S bestimmt. Dieses Ergebnis ist konsistent mit der Lage des Randes Südamerikas innerhalb Gondwanas im frühen Ordoviz. Allerdings weicht die Pollage der Umachiri Serie deutlich vom Referenzpol Gondwanas für diesen Zeitbereich ab. Die Daten weisen auf eine Rotation des Beprobungsgebietes um 45° gegen den Uhrzeigersinn relativ zu dem stabilen Südamerika hin. Frühere Studien belegen, dass diese Rotationen nach dem Oligozän stattgefunden haben müssen. Sie stehen im Zusammenhang mit einer Scherzone, die sich während der andinen Deformation im nördlichen Altiplano gebildet hat.

Ein anderer Schwerpunkt dieser Arbeit ist mit Hilfe paläomagnetischer Methoden die komplexen tektonischen Prozesse Nordwest-Argentiniens während des Paläozoikums anhand der „Vorkordillere" und der „Famatina Ketten" zu untersuchen. Innerhalb der „Vorkodillere" wurden unter anderem die Patquia, Guandacol, Los Espejos, San Juan und die La Silla Formationen beprobt. Jede dieser Einheiten ergab primäre Remanenzrichtungen. Im Fall der San Juan und der La Silla Formation kann dies durch einen positiven Faltentest nachgewiesen werden. Sowohl die Ergebnisse der spät-permischen Patquia Formation (D= 225.8°; I= +61.8°; α_{95}= 3.0°; k=215; n=12 Proben) und der spät-karbonischen Guandacol Formation (D= 194.1°; I= +59.8°; α_{95}= 4.4°; k= 279; n= 8 Proben) als auch die Daten der spät-silurischen Los Espejos Formation (D= 289.8°; I= -29.9°; α_{95}= 17.6°; k= 50; n= 20 Proben, N= 3 Sites) deuten darauf hin, dass die „Prekordillera" um 60° mit den Uhrzeigersinn relativ zu dem stabilen Teil Südamerikas rotiert ist. Auch hier ist der Ursprung der Rotation in der känozoischen andinen Deformation zu suchen. Ältere Einheiten zeigen ein davon abweichendes Richtungsverhalten. Die Ergebnisse der früh-ordovizischen San Juan und La Silla ergeben eine Paläobreitenlage der Vorkordillere von 39.5 ±4°S. Dies ist konsistent mit ihrer Lage relativ zu Südamerika innerhalb Gondwanas im frühen Ordoviz, d. h. die Vorkodillere war zu diesem Zeitpunkt bereits ein Teil Gondwanas. Der kombinierte Datensatz der San Juan und der La Silla Formation deutet allerdings eine relative Rotation dieser Einheiten von 45° gegen dem Uhrzeigersinn hin. Daher muß von

einer Rotation von 105° (gegen dem Uhrzeigersinn) zwischen dem frühen Ordoviz und dem späten Silur ausgegangen werden. Wahrscheinlich steht sie in Verbindung mit der Ocloyíc Deformation, die zur Schließung des Puna Beckens geführt hat.

Die Ergebnisse für die „Famatina Ketten" basieren auf Untersuchungen an der De La Cuesta Formation (spätes Perm) und der Suri Formation (frühes Ordoviz). In beiden Fällen konnten stabile primäre Remanenzrichtungen isoliert werden. Vergleicht man sowohl die Daten der Suri Formation (D= 107°; I= 31°; α_{95}= 7.1°; k= 97; n= 25 Proben; N= 5 Sites) als auch die der De La Cuesta Formation (D=163.2°; I= +43.8°; α_{95}= 10.0°; k=59.5; n= 23 Proben; N= 5 Sites) mit dem jeweiligen gleichaltrigen Referenzpol des stabilen Südamerikas und Gondwanas, so stellt sich heraus, dass nur erste eine Rotation (60° mit dem Uhrzeigersinn) belegen. Wie schon bei der San Juan und der La Silla Formation ist auch hier wahrscheinlich die Ocloyíc Deformation dafür verantwortlich. Die aus den Resultaten der Suri Formation abgeleitet Paläobreitenlage der „Famatina" (16.5 ±3°S) deckt sich mit ihrer Position innerhalb Gondwanas im frühen Ordoviz. Man kann daher davon ausgehen, dass sie ihre Lage relativ zu dem stabilen Südamerika seit dem frühen Ordiviz nicht verändert hat. Damit kann im Gegensatz zu anderen Modellen ein para-autochthone Ursprung der „Famatina" ausgeschlossen werden.

Zusammenfassend liefern die Rahmen dieser Arbeit erzielten Daten wichtige Parameter für die Bestimmung des Zeitpunkts der „terrane" Akkretion und der Deformationsgeschichte am westlichen Rand Gondwanas. Basierend auf diesen Ergebnisse kann gezeigt werde, dass die argentinische Vorkordillere integraler Bestandteil Südamerikas bereits im frühen Ordoviz war. Die weitere Konsolidierung des südamerikanischen Rands war mit großmaßstäblichen, vorpermischen Rotationen verbunden. Weiter Rotationen fanden während der andinen Orogenese statt. Qualitativ hochwertige Ergebnisse für Südperu unterstützen paläogeographische Modelle vom Typ Pangäa B für das frühe Perm und Pangäa A2 Konstellationen in der frühen Trias.

Chapter 1

Introduction

The present study encompasses palaeomagnetic investigations conducted in autochthonous areas of the Central Andes (Peru, Bolivia, Argentina) and in cratonic Basins in NE Brazil. Palaeomagnetic data from sedimentary and magmatic rocks covering the whole Palaeozoic and the Early Mesozoic are presented. This investigation is essentially aimed to provide firstly, Palaeozoic palaeomagnetic data to determine the drift history of Gondwana, and also to constrain its relative palaeopositions within the Permian-Triassic Pangaea supercontinent, and secondly to further resolve problems concerning the geological evolution of the South American margin of Gondwana during the Palaeozoic times.

1.1   Gondwana and Pangaea Supercontinents

The Gondwana supercontinent is though to have developed mainly between 800 Ma to 550 Ma, as a result of episodic collisions between various cratonic fragments derived from the earlier supercontinent Rodinia (Meert & Van der Voo, 1997). Palaeozoic palaeogeography was dominated by Gondwana, which constituted more than two thirds of the entire continental crust, and include the continental masses of South America, Africa, India, Madagascar, Antarctica, and Australia. The relative palaeopositions of major continental fragments within the Gondwana reconstruction are reasonably well established. For instance, geological connections between South America and Africa within Gondwana are well-known and well-constrained age correlations between cratonic areas and geological provinces within both continents have been convincingly demonstrated (*e.g.* Cordani & Torquato, 1981). However, the drift history of Gondwana and its collisional history with Baltica and Laurentia are still unresolved.

Gondwana is believed to have joined Laurussia in Late Palaeozoic times to form the Pangaea supercontinent (*e.g.* Tait *et al.*, 2000), which existed throughout the Permian and Triassic. Pangaea developed between 360 to 270 Ma, during the Variscan Orogeny as a result of the amalgamation of Gondwana with Laurentia, Eurasia, Siberia, and other smaller continental fragments. The subsequent break-up of Pangaea and opening of the Atlantic,

Indian, and Australian-Antarctica oceans started in Early Jurassic times (approximately 180 Ma ago). The palaeogeography presented by Bullard *et al.* (1965) for the Jurassic Pangaea, known as Pangaea A configuration, in which South America and Africa are respectively facing North America and Europe (Laurentia), is well accepted as the starting point of the opening of the Atlantic Ocean and the subsequent continental drift. However, the Permian-Triassic palaeogeography remains a matter of dispute as palaeomagnetic data from Laurussia and Gondwana provide a large continental overlap when adopting Pangaea A reconstruction. Alternatively, different configuration including Pangaea A2 (Van der Voo & French, 1974), Pangaea B (Morel & Irving, 1981), and Pangaea C (Smith *et al.*, 1981) have been proposed to overcome overlap between Laurussia and Gondwana. These reconstructions place Gondwana farther to the east with respect to Laurentia, with South America facing Europe and Africa facing Eurasia.

1.2   Palaeomagnetic data from Gondwana

Depending on different interpretations and the criteria adopted when selecting palaeomagnetic results from the database, there exist two conflicting models for the Palaeozoic apparent polar wander path (APWP) of Gondwana. These models, referred to as the X and Y paths were originally proposed by Morel & Irving (1978). Despite the fact that many new palaeomagnetic data have been published since 1978, and a range of APWPs have been proposed (Fig. 1.1), these two basic schools of thought still remain. Taking into account these more recent data, both the X and Y paths have been slightly modified in the course of time. At present, the path X modified by Bachtadse & Briden (1991) and the path Y refined by Schmidt *et al.* (1990) are widely in use, though, the Y path needs further modification since a new radiometric age of the Aïr pole is now available (see Tait *et al.*, 2000).

Both the X and Y path models are in agreement that the palaeosouth pole for Gondwana was situated in northwest Africa in Early Ordovician times, in central Africa in the Latest Devonian, and in Antarctica in Late Carboniferous to Permian times (Fig. 1.1a,b). Contrarily, the Silurian-Devonian segments of the X and Y paths are significantly different. The X path, which indicates a gradual northward drift of Gondwana from Late Ordovician (ca. 450 Ma) through to Early Carboniferous (ca. 340 Ma) times, suggests that the palaeosouth pole for Gondwana shifted from northern Africa to central Africa during the Silurian and Devonian. Conversely, the Silurian-Devonian segment of the Y path of Schmidt *et al.* (1990) forms a distinct loop (Fig. 1.1b), implying that the south pole moved rapidly from

northwest Africa in Early Ordovician to southern South American in the Silurian to Early Devonian times and back to central Africa by the Late Devonian. This more complex path requires extremely high drift rates movement of Gondwana during the Palaeozoic era and collision with Laurussia in the Late Silurian-Early Devonian (ca. 415 Ma) and the Late Carboniferous (ca. 300 Ma) times.

As these models arise from different selection of the palaeomagnetic results from the database, the main controversy concerns the poles used to reconstruct these paths. The main debate focuses on the reliability of palaeomagnetic data from the Lachlan Fold Belt (LFB) of southeast Australia and the palaeopole from the Aïr complex of Niger, northern Africa, which define the Silurian-Devonian segments of the Y path proposed by Schmidt *et al.* (1990), but are regarded as not trustworthy in the X path of Bachtadse & Briden (1991). On one hand, those who support the Y path argue that the LFB has been attached to the Australian craton during the Palaeozoic era. Hence, the palaeopoles from this region are representative for Gondwana. Good agreement of the palaeomagnetic results from the LFB with the palaeopole from Aïr complex and the implied mid-Devonian segment of the path compiled from African and South American data were reported in Schmidt *et al.* (1990) as an evidence of this autochthonous model. On the other hand, those who support the X path argue that the age of magnetisation of the Aïr complex is not clearly constrained due to the lack of field tests. Based on close similarity of the Aïr pole with the secondary magnetisation from Devonian ring complexes of Sudan (northern Africa), Bachtadse & Briden (1991) consider the results from Aïr complex as being a Carboniferous remagnetisation in their X path. Furthermore, Devonian poles from LFB are not used in X path as the autochthonous nature and differential movement of the tectono-stratigraphic zones of the Lachlan Fold Belt are still unsolved. The implied rapid drift of Gondwana from Late Ordovician to Late Devonian, the collision of Gondwana with Laurussia in Early Devonian and the repeated closure and opening of the proto-Tethys Ocean, which are not obvious on geological grounds, are also used to argue against the Y path (Bachtadse & Briden, 1991; Tait *et al.*, 2000).

As the existing palaeomagnetic data are still insufficient to confidently define the APWP of Gondwana, this study was carried out to provide new data from stable South America. Palaeomagnetic investigation of the Lachlan Fold Belt were also carried out by the working group within the frame of this project in order to resolve the tectonic history of SE Australia.
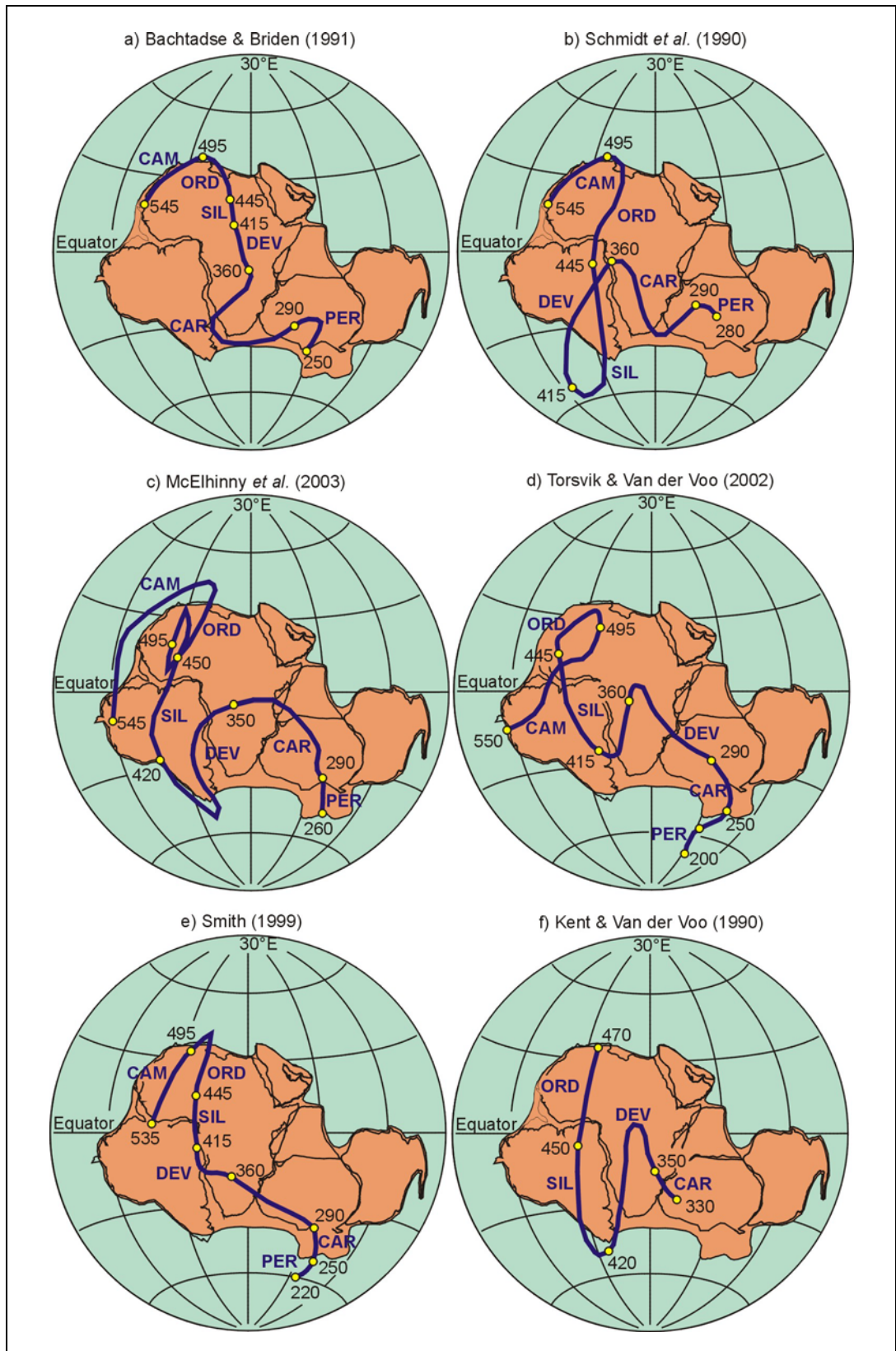
Fig. 1.1. Proposed Palaeozoic APW paths for Gondwana. Numbers adjacent to poles (yellow dots) represent age in million years. Segments of APW paths are: CAM: Cambrian, ORD: Ordovician, SIL: Silurian, DEV: Devonian, CAR: Carboniferous; PER, Permian.

In view of the palaeogeography of Pangaea, the proposed Pangaea B and C configuration provide a better match for palaeomagnetic data. However, the position of Gondwana in these configurations is not proven geologically as it implies that Gondwana must have translated westward relative to Laurentia during the Late Permian or Early Triassic times to end up with the pre-Atlantic Jurassic Pangaea type A (Fig. 1.2) As no strong evidence of major relative movement between the two supercontinents have been found, it has been discussed that the mismatch of the palaeomagnetic data in Pangaea A configuration is the result of the poor quality of the existing palaeomagnetic dataset for Gondwana (Van der Voo, 1990).

Fig. 1.2. Permian-Triassic reconstruction of Pangaea (A) after Lottes & Rowley, 1990). Notice the palaeoposition of Gondwana with respect to Laurentia and Eurasia (see text). Reconstruction parameters are: Gondwana: 24.3°N / 297.4°E / angle: -50.7°; Laurentia: 38.6°N / 049.4°E / angle: +53.4°; Eurasia: 00°N / 249.0°E / angle: -43°

1.3   Palaeomagnetic data from South America

The South American continent is composed of cratonic fragments, including the Amazonian, Sao Francisco, Sao Luiz, and Rio de la Plata cratons, which make up part of western Gondwana. Only few data from Palaeozoic rocks

exposed on these cratons can be considered palaeomagnetically reliable. The reasons are that either the age and/or structural context of the Palaeozoic sequences in the studied area are poorly constrained, or for the older data, the techniques employed do not meet modern standards for palaeomagnetic investigations. The present study takes advantage of the more recently published geological studies of various geological provinces, which provide a much better understanding of the structural evolution, as well as better age control and characterisation of the Palaeozoic sequences.

Palaeomagnetic data are now widely used to determine the widespread intra-cratonic block rotations within the Andean belt. Palaeomagnetically determined rotations are primarily based upon comparison of observed magnetic directions with that of the expected magnetic directions at the sampling location for the times under consideration. Accuracy of the reference pole position is thus fundamental to prevent misinterpretation. Concerning the Mesozoic reference poles for the South American plate, several post-Jurassic APW paths have been published (Irving & Irving, 1982; Beck, 1988; Butler *et al*., 1991; Roperch & Carlier 1992; Riley *et al*., 1993; Raposo & Ernesto, 1995), and distinct differences between the suggested reference poles for some age windows are obvious. The reference poles used to reconstruct these paths are either calculated from selected poles South American cratons, or translated from the African or North American APWP.

Chapter 2

Geological setting of the sampling regions

The South American continent comprises a number of Proterozoic cratons, namely the Guiana Shield, the Central Brazilian Shield and the Coastal Brazilian Shield. Large inter-cratonic basins, referred to as the Amazonian, the Parnaíba, the São Francisco, and the Paraná Basins, formed between these cratons in Palaeozoic times. Along the western edge of these shield and basins occur the Llanos, Iquitos-Acre-Beni, Chaco, and Pampas peri-cratonic basins (Fig. 2.1). Further west, the Andean Belt forms the western border of South America. The present palaeomagnetic investigation focuses mainly on the Palaeozoic rocks within the inter-cratonic Parnaíba Basin (NE Brazil) and those of the central part of the Andean belt (Peru, Bolivia, and northern Argentina).

2.1 The Parnaíba Basin

The Parnaíba Basin, also called Piauí-Maranhão Basin, is situated in NE Brazil within the Central Brazilian Shield (Fig. 2.1). The basin is considered to have been initiated in the Late Proterozoic by rift related graben due to the presence of Proterozoic continental rift sequence preserved within a N-S trending graben bounded by crystalline basement rocks (Milani & Thomaz Filho, 2000). According to Bellieni *et al.*, (1990) and Milani & Thomaz Filho (2000), the initial subsidence and the first marine incursion within the Parnaíba Basin occurred in Silurian times. Marine sedimentation then continued through to the Early Carboniferous. Up to 3500 meter thick marine sediments are presently preserved within the basin.

According to Milani & Thomaz Filho (2000), the Palaeozoic sedimentation began with the Silurian Sierra Grande Group and related to the global sea level rise, which took place over the whole of Gondwana. The Sierra Grande Group is interpreted to represent a complete transgression–regression cycle, that was accommodated by the initial basin subsidence. The Group comprises, from base to top, a predominantly sandstone sequence, with less important siltstone and shale, and glacial diamictite beds (Ipu Formation), a sequence of alternating grey shale, siltstone and micaceous coastal sandstone

with huge Wenlockian age conglomerate deposits (Tiangúa Formation), and a sequence of coarse-grained braided stream deposits (Jaicos Formation).
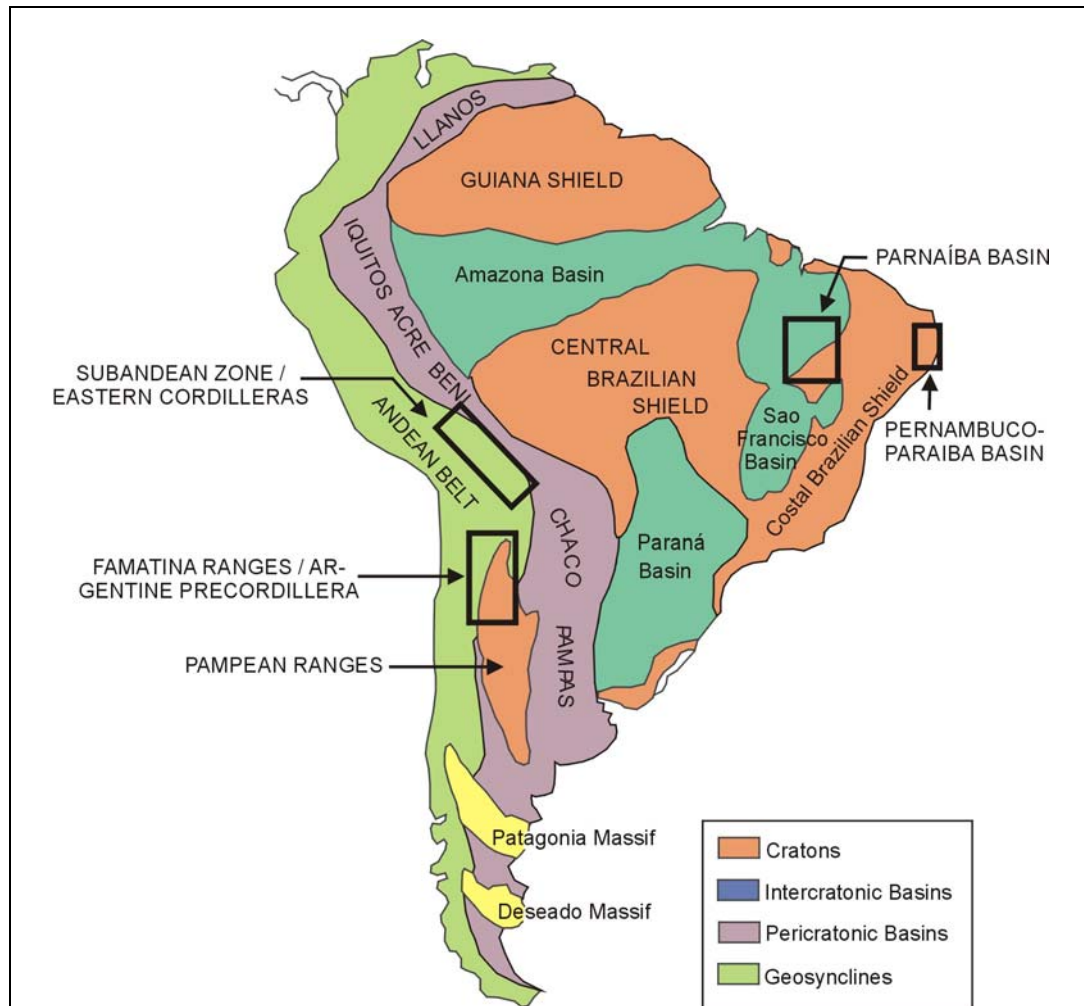
Fig. 2.1. Simplified geo-tectonic sketch map of South America (after Cordani *et al.*, 2000). Boxes represent approximate locations of the study areas.

This was followed in the Devonian by deposition of the Eifelian-Tournaisian (390-340 Ma) Canidé Group. These deposits include tide and storm-related sediments (Itaim Formation), black shales rich in organic matter (Pimenteiras Formation), fine-grained shallow marine sandstones with occasionally diamictite beds (Cabeça Formation), and a fluvial sandstones and shales (Longá Formation). The top of the Canidé Group (Poti Formation) consists of an intercalated fine-grained sandstones and shales. An Early Carboniferous age is attributed to the Poti Formation.

The overlying Carboniferous to Triassic sediments are known as the Balsas Group, which are thought to have been deposited under arid climatic conditions. The Balsas Group is subdivided into an alternating sequence of fine- to medium-grained sandstone, brown shale and occasional limestone (Piauí Formation); an alternated rhythmic oolitic limestone, white anhydrite

and yellow sandstones (Pedra de Fogo Formation); a sequence of alternated brown siltstones, medium-grained sandstones, and sporadic anhydrite beds (Motuca Formation); and aeolian sandstones (Sambaíba Formation)

During the Mesozoic, two pulses of magmatic activity affected the Parnaíba Basin. Both activities were related to the rifting precursor of the opening of the Atlantic Ocean and the subsequent separation of South America from Africa. The first magmatism occurred in the Triassic-Jurassic (Mosquito Formation) and is interpreted as being related to the rifting of the central Atlantic. The later, Early Cretaceous magmatism (Sardinha Formation) is thought to have occurred during the opening of the South Atlantic. The volcanic rocks of the Mosquito Formation is considered equivalent to the Penatecua magmatism of the Solimòes and Amazona Basins, while the Sardinha Formation is considered equivalent to northern Paraná flood Basalt.

The Jurassic sediments are represented by the Mearim Group, comprising sequences of green to red argillite and siltstone (Pastos Bons Formation) and aeolian sandstones (Corda Formation). The latter desert deposits suggest prevailing arid conditions. The overlying Cretaceous sediments (Codó, Grajaú and Itapicuru Formations) were deposited during the subsequent opening of the equatorial Atlantic Ocean.

2.2   The western margin of South America

The geological history of the western margin of South America is rather complex. After the break-up of Rodinia (800 Ma), the western border of South America corresponded to a passive margin (Cordani *et al.*, 2000). It became active and displayed convergent relationship with the Panthalassa Oceanic plate during Late Proterozoic times (Ramos, 1988; Bahlburg & Breitkreuz, 1991). Since then, various back-arc flexural and extensional basins developed along this margin (Milani & Thomaz Filho, 2000).

Terrane accretion along the western margin of South America is thought to have occurred during Late Proterozoic and/or Early to mid-Palaeozoic (*e.g.* Ramos, 1988, 1995; Astini *et al.*, 1995), and Mesozoic-Cenozoic times (Ramos, 1988; 1994). The type of accreted terrane include exotic terranes, para-autochtchonous terranes, and cratonic blocks that were part of western Gondwana during Proterozoic times, but split away and subsequently re-accreted to the margin, referred to as peri-Gondwanan terranes (Ramos & Basei, 1997; Keppie and Ramos, 1999). Terranes and suspect terranes in the Central Andes include the Arequipa-Antofalla, the Sierras Pampeanas, the Puna Oriental-Famatina, the Argentine Precordillera, the Chilenia, and the Patagonia (Fig. 2.2). Since the publication of the simplified terranes map of

Ramos (1988), various tectonic models, mainly based on geological, geochemical, and palaeontological studies of the western margin of South America, have been proposed for the timing and the accretion scenario of these terranes. Accretion models based on palaeomagnetic data also have been reported (Forsythe *et al.*, 1993; Rapalini & Tarling, 1993; Rapalini *et al.,* 1994; Conti *et al.*, 1996). However, these palaeomagnetic data are still insufficient and unconvincing.

In the Late Palaeozoic, the western margin of South America became the site of deformation events related to the subduction that led to the formation of the Gondwanides (Hercynian Orogeny), and the closure of the Tethys Ocean during the formation of Pangaea. Records of the subsequent break-up of Pangaea that resulted in large-scale extensional deformation are also recognised along this former margin of Gondwana (Ramos & Aleman, 2000). The subduction of the Nazca oceanic plate under the South American continental plate and the development of the Andean Belt followed in Mesozoic-Cenozoic. This subduction is still active at present.
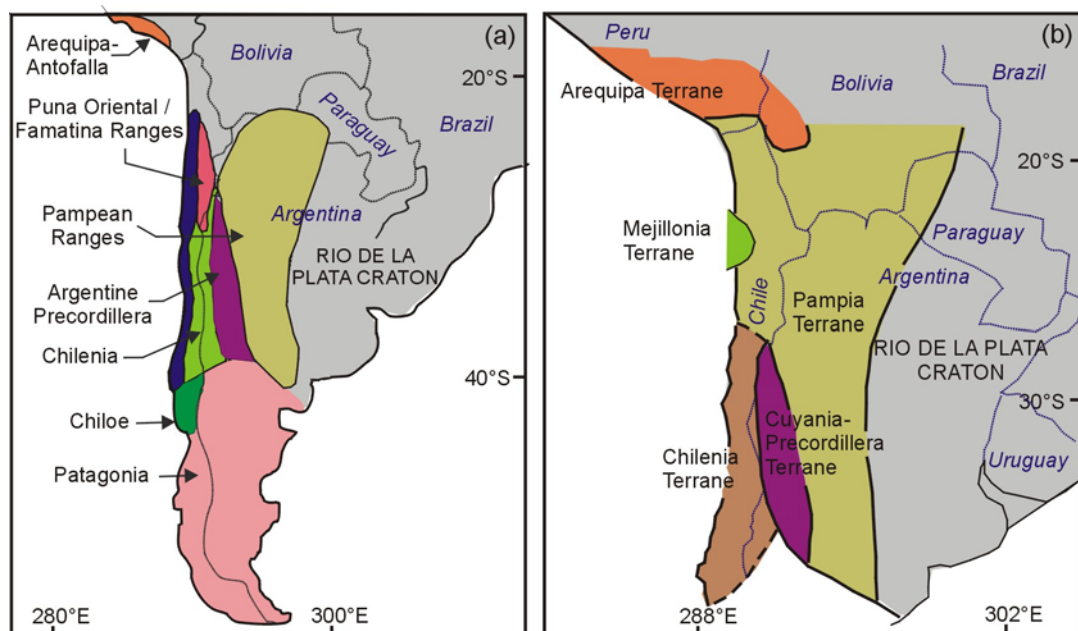
Fig. 2.2. Sketch map of terranes and suspect terranes of the western margin of South American Margin (a) from Grunow (1999); (b) from Bahlburg *et al.* (2000).

2.3   The Central Andes

The Andean Belt is an approximately 8000 km mountain Ranges that shapes the present day western border of South America. The Andes are bounded by a narrow coastal zone to the west and by the Subandean Zone to the east (Fig. 2.3). The Central Andes corresponds to the part of the Andean Belt which includes the ca. 2000 km long NW-SE trending Peruvian segment, stretching

from Peru to northern Bolivia (5°S-18°S), and the approximately 4000 km long Chilean segment, trending N-S and covering the whole western Argentina and Chile (18°S-56°S). The width of this central part of the Andes ranges between 250 km in northern Peru (5°S) to as much as 750 km in Bolivia (Jaillard *et al.*, 2000). The northern Central Andes is subdivided into various fault-bounded morpho-structural units, including from the west to the east: the Coastal Range, the Western Cordillera, the Puna-Altiplano plateau, the Eastern Cordillera, and the Subandean Zone. In its southern part, the Central Andes is subdivided into the Coastal Cordillera, the Cordillera Oriental, the Cordillera principal, the Cordillera Frontal, and the Precordillera (Fig. 2.3).

2.3.1   Pre-Andean Evolution of the Central Andes

The Palaeozoic development of the proto-Andean active margin is subdivided into three periods of alternating regional extensional and compressional regimes. As described in Jaillard *et al.* (2000), the Late Cambrian-Early Ordovician is characterised by back-arc extensional conditions resulting in a thinned crust, subsidence, rifting, and syn-sedimentary basic volcanism. This was followed by a compressional regime that led to the development of a large retroarc foreland basin. Episodic development of transpressional uplifts occurred in the Middle Ordovician to Early Carboniferous. Back-arc extensional accompanied by subsidence, rifting, and volcanism prevailed again in Late Carboniferous and Permian. Several episodes of basin development related to the pre-Andean subduction (Panthalassa oceanic crust versus Gondwana margin) and the Andean (Pacific Ocean versus present day South American plate) are known. A summary of the various sedimentary basins that developed along this margin of South America is given in Milani & Thomaz Filho (2000).

For the Central Andes between latitude 10°S and 30°S, the pre-Andean foreland basins comprise the Cambrian-Early Palaeozoic Tarija-Noroeste Basin, the Silurian-Devonian Basin in the Argentine Precordillera, and the Permian-Carboniferous Calingasta-Uspallata and Paganzo Basins. The Early Palaeozoic sediments in these basins are affected by the Late Devonian-Early Carboniferous tectonic and magmatic events that were related to Eohercynian Orogeny (Dalmayrac *et al.*, 1980). A hiatus, related to global regression occurred in Middle Carboniferous (Jaillard *et al.*, 2000). As a results, the Ordovician, Silurian and Devonian sedimentary units are directly overlain by Late Carboniferous and Permian units throughout the Central Andes (Kley & Reinhard, 1994; Isaacson & Diáz-Martinez, 1995).
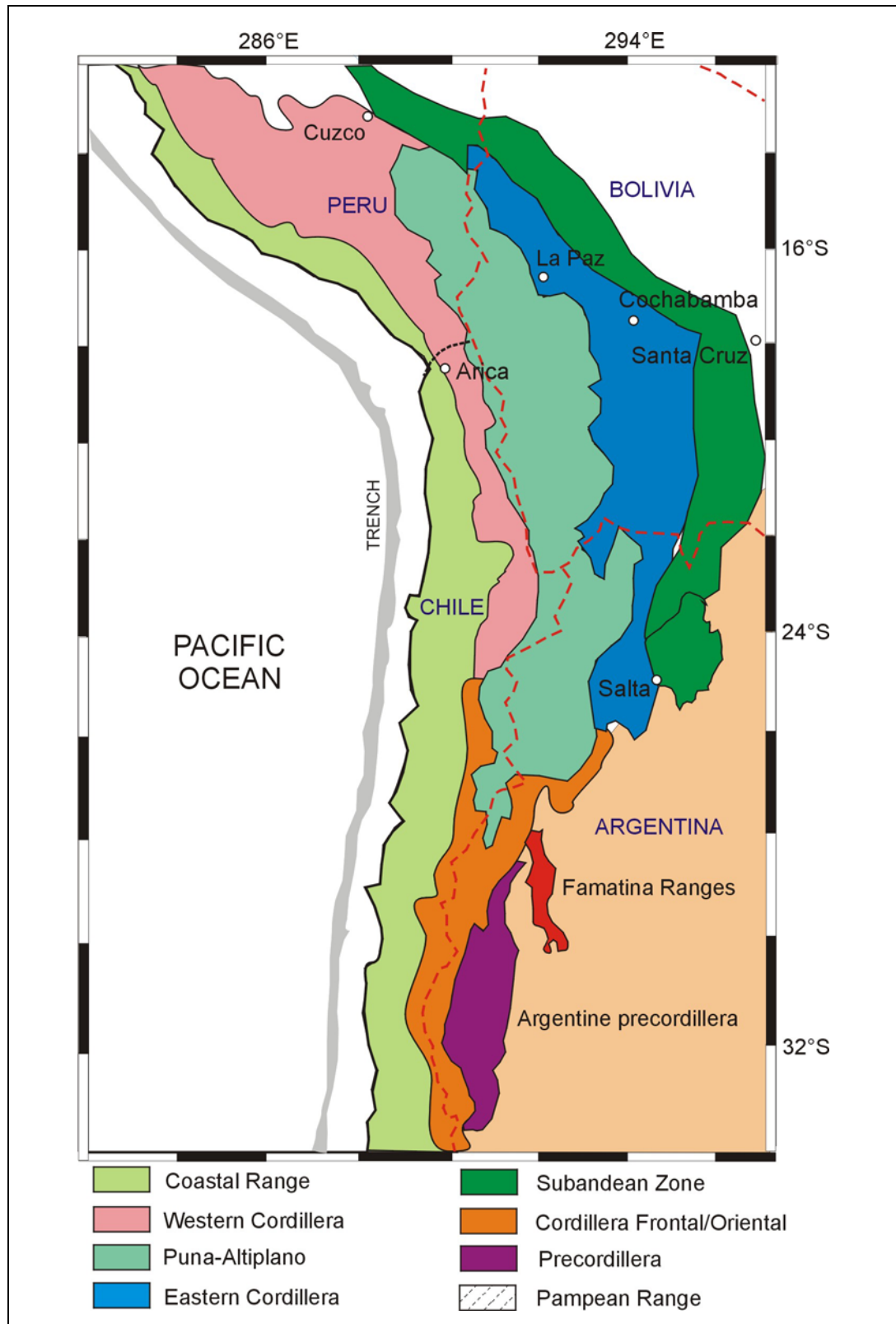
Fig. 2.3. Morpho-structural sketch map of the Central Andes (Jaillard *et al.*, 2000).

The beginning of subduction-related marginal volcanic arc activity marks the Late Carboniferous. These volcanic activities are recorded in the Peruvian and western Bolivian Andes. This was followed in the Late Palaeozoic by the regional extension during the break-up of Pangaea. This extensional regime

is interpreted to have resulted in partial rifting along the suture zone between the Arequipa-Antofalla and the Amazonian cratons (Jaillard *et al.*, 2000). The related volcanism and plutonism began in the Peruvian sector in the Late Permian-Triassic, and migrated towards the south, in Bolivia during the Middle Triassic to Early Jurassic.

2.3.2   The Peruvian Andes

The Peruvian Andes form part of the roughly NW-SE trending central segment of the Andes situated between latitude 5°S and 18°S (Fig. 2.3). It is separates from the northern Andes by the Huancabamba deflexion (in northern Peru), and from the southern segments by the Arica deflexion (northern Bolivia). The Subandean Zone and the Altiplano of the Peruvian Andes were subjected to sampling for the present palaeomagnetic investigations.

The Subandean Zone constitutes the western margin of the Madre de Dios foreland basin, which extends to the east onto the Brazilian Shield. This zone consists of a fold and thrust belt of Palaeozoic, Mesozoic and Tertiary sediments, characterised by eastward verging thin-skinned style tectonics resulting from the Cenozoic compressional regime (Gil *et al.*, 1999; Jaillard *et al.*, 2000). The Altiplano is the Peruvian section of the Puna-Altiplano plateau, which stretches about 2000 km, from southern Peru to central Argentina and forms a high plateau situated between the Eastern Cordillera and the Western Cordillera. The Altiplano has an average elevation of 3.7 km (Isacks, 1988), and width of up to 700 km. The sedimentary rocks in the Altiplano Basin include Palaeozoic, Mesozoic, and Tertiary molassic sequences, which were folded and thrusted during the early phase of the Andean compressional deformation and uplifted during the Pliocene (Jaillard *et al.*, 2000). Available evidences suggest that shortening of the continental crust, mostly occurred during the last 30 Ma was responsible for the uplift of the Puna-Altiplano (Jordan & Alonso, 1987; Jordan & Gardeweg, 1989). Allmendinger & Gubbels (1996) suggest that shortening and uplift of the Altiplano took place mainly during the last 10 Ma as a result of underthrusting of the Brazilian shield.

The Peruvian Andes comprises Late Cambrian to Early Triassic, and Cretaceous to Quaternary sedimentary and magmatic rocks. The Lowermost Palaeozoic rocks include deep marine sediments (Ollantaytambo Formation) overlain by Early Ordovician laminated black shales (San José Group) interpreted as being deposited in a large retroarc foreland sediments delimited by the Arequipa massif to the west and the Brazilian Shield to the east (Jaillard *et al.*, 2000). In the Altiplano area, the Early Ordovician sequence consists of upward-shallowing clastic marine sediments, which

include the Umachiri Series discussed in Chapter 7. Detritic and flysch-type sediments (Sandia Formation) correspond to the Late Ordovician, and thick sequence of pelitic and detritic sediments (Ananea Formation) were deposited in the Silurian. The Devonian is characterised by shallow marine deposits (Cabanillas Formation). The Early Palaeozoic marine sequence (up to 6 km thickness) is affected by the Late Devonian-Early Carboniferous regional compressional tectonic event (Eohercynian phase). The Carboniferous to Permian sedimentation was controlled by regional distension and NW-SE block faulting in a subsiding basin, with fluvial and deltaic clastic sediments (Ambo Group) at the base. Detritic and marine carbonate deposits occurred in Early Carboniferous times, and continued into the Late Carboniferous (Tarma Group) and throughout the Early Permian (Copacabana Group). This sedimentation cycle was interrupted by a compressional event, which caused gentle folding of the Palaeozoic rocks in the southern Peruvian area and development of horst/graben structures delimited by NW-SE faults in central and northern Peru (De la Cruz *et al.*, 1998). The Late Permian-Early Triassic is characterised by volcanism and plutonic activity (Mitu Group), thought to be related to the Tethyan rifting during early stage of Pangaea break-up (Kontak *et al.*, 1985; Flint *et al.*, 1993; Jaillard *et al.*, 2000).

2.3.3 The Bolivian Andes

Palaeomagnetic investigations in Bolivia were conducted in the Subandean Zone and the Eastern Cordillera. As in Peru, the Bolivian Sub-Andes is a 140 km to 150 km wide zone of foreland fold and thrust belt (Mingramm *et al.*, 1979; Díaz-Martinez, 1999). The Chaco-Beni Foreland Basin and the Eastern Cordillera delineate its eastern and western margins, respectively. The Eastern Cordillera is composed of pre-Mesozoic metamorphic rocks and subordinate Palaeozoic to Tertiary intrusive and volcanic rocks (Jaillard *et al.*, 2000). Deformation in the Eastern Cordillera is characterised by thrusting and thin to thick-skinned shortening (Díaz-Martinez, 1999).

Palaeozoic rock units present of the Subandean Zone and the Eastern Cordillera in Bolivia were deposited within the Cambrian-Early Palaeozoic Tarija-Noroeste Basin. According to Milani & Thomaz Filho (2000, and references cited therein), the Tarija-Noroeste basin is a foreland basin that developed during the subduction of Panthalassa oceanic crust under the Gondwana margin. It is an approximately 200 000 km^2 basin covering parts of southern Bolivia, Paraguay and northwest Argentina. The Tarija-Noroeste Basin contains thick sequence of Palaeozoic sediments overlying the Cambrian to Early Ordovician back-arc deposits. In the Bolivian domain, the Tacsara Supersequence represents the back-arc sediments. The Ocloyíc

orogeny ended this phase of sedimentation in Late Ordovician times, and development of foreland basin followed. The overlying sedimentary succession constitutes the Late Ordovician–Late Devonian Chuquisaca Supersequence, which comprises marine black shale (Tokochi Formation), diamictite and glacio-marine sediments (Cancañiri Formation), and turbidites (Llallagua Formation). The Silurian-Devonian part of the Supersequence include three major marine transgression-regression cycles. The shale successions of the Chululuyo, Icla, and Los Monos Formations represent the maximum flooding of these cycles, and the Santa Rosa and Huamampampa Formations represent the regressive sequences. These Early Palaeozoic sediments were folded in Late Devonian-Early Carboniferous due to the Chanic Orogeny.

The Carboniferous sediments within the basin mark the beginning of the change to a continental depositional environment. The Carboniferous-Permian succession is known as the Cuevo Supersequence (Sempere, 1995). It comprises deposits recording influence of the Early Carboniferous Gondwana glaciation (Tupambi and Tarija Formation). Conversely, tropical climate and tectonic quiescence are indicated by the Late Carboniferous sediments and the Early Permian carbonate platform of the Copacabana Group. These carbonates grade laterally to the southeast into sandy continental known as the Yaurichambi and the Cangapi Formations. Marine incursion in the Tarija Noroeste Basin during the uppermost Early Permian times is indicated by the black shale sequence of the Viticua Formation indicates.

2.3.4 The Andes of northwestern Argentina

The western margin of Gondwana corresponding to the north-western Argentinian Andes was the location of the Puncoviscana Basin in Late Proterozoic-Early Cambrian times (Aceñolaza & Duran, 1986; Aceñolaza *et al.*, 1990). The Puncoviscana Basin is variably interpreted to be a marginal continental basin that developed along the western border of the Pampia craton (Ramos & Vujovich, 1993), or a foreland basin formed during the collision of the Pampia and Rio de la Plata cratons (Kramer *et al.*, 1995). Palaeontological and geochronoligical data from the oldest sediments suggest that this basin existed between 700 Ma and 535 Ma (Ramos; 2000). The Puncoviscana Formation was deformed during the Early Cambrian Pampean orogeny, which was associated with the collision of the Mejillonia and Arequipa-Antofalla terranes (Ramos, 2000). Subduction-related magmatic activity occurred in this South American margin of Gondwana in Middle Cambrian to Early Ordovician times (510-470 Ma; Astini, 1996; Ramos, 2000).

The Puncoviscana Formation is overlain by the Late Cambrian shallow marine deposits (Méson Group) and the Early Ordovician Santa Victoria Group (Coira *et al.*, 1982). The Santa Victoria Group is variably interpreted to be oceanic back-arc sediments (Ramos, 1988) or island arc sediments (Coira *et al.*, 1999). The Early Middle Ordovician time is characterised by the Ocloyíc tectonic phase, thought by many authors to be related to the accretion of the Famatina and Precordillera terranes. The Ocloyíc phase resulted in progressive closing of the Ordovician Puncoviscana Basin and development of the volcanic arc in the Puna region (Balburg *et al.*, 2000; Ramos, 2000). The Late Ordovician clastic marine sediments overlie these Early Ordovician volcano-clastic sediments. Marine sedimentation continued in Silurian until the Middle Devonian Chaňic deformational phase. Continental alluvial deposits followed from Early Carboniferous through to Permian-Triassic times.

Palaeomagnetic investigations of the Palaeozoic rocks of the Andes of NW Argentina were carried out in the Pampean Range, the Argentina Precordillera, the Famatina Range, and the Paganzo Basin. Various models of the tectonic evolution of these morpho-tectonic units have been published. However, the proposed geological interpretations are contradicting in some cases and the evolution of this southern part of the Central Andes is not clear yet. The current knowledge concerning the evolution of these units are presented in the following sections.

a) The Pampean Ranges

Ramos (1994) defined the Pampean Ranges(Sierras Pampeanas) as a series of Precambrian crystalline blocks that accreted to the Rio de la Plata craton during the Late Proterozoic-Early Cambrian. The Pampean continental blocks (Fig. 2.2a) is interpreted to have rifted off, and partially detached from the Gondwana margin after the Late Proterozoic break-up of Rodinia (Rapela, 1998; Jaillard *et al.*, 2000; Gosen, 2001). Rifting between the Rio de La Plata craton and the Pampean terrane is thought to have resulted in the opening of the Puncoviscana Basin. Northeastward-directed subduction and progressive closure of this basin followed in Early Cambrian and continued until the collision of the Pampean block with the Rio de la Plata craton. The final collision of the Pampean block is thought to occur in late Early Cambrian and marked by the end of clastic sedimentation within the Puncoviscana Basin (Gosen, 2001) and compressive high grade metamorphism followed by isothermal uplift at 520 Ma (Rapela *et al.*, 1998). The Pampean Ranges was affected by compressive deformation related to the eastward-directed subduction of the proto-Pacific Oceanic crust during the Late Cambrian-Early Ordovician.

b) The Argentine Precordillera

The Argentine Precordillera is widely interpreted as an exotic terrane derived from Laurentia and accreted to the western margin of Gondwana in Palaeozoic times (*e.g.* Astini *et al.*, 1995; Dalziel, 1997; Pankhurst *et al.*, 1998). Different models, however, have been presented concerning the timing and its accretion scenario. On one hand, Dalla Salda *et al.* (1992) and Dalziel *et al.* (1994) proposed that during Middle Ordovician time, Laurentia collided with the Gondwana margin and transferred the Precordillera to Argentina during a Late Ordovician rifting event.

On the other hand, the faunal affinities between Laurentia and the Precordillera during the Cambrian-Early Ordovician, and the palaeontological divergence throughout the Ordovician times are interpreted by Benedetto (1998) as the result of progressive drift of the Precordillera away from Laurentia and later accretion with Gondwana. This interpretation favours the model in which the Precordillera is considered to be an independent crustal plate that travelled across the Iapetus Ocean to reach and collide with the western margin of Gondwana (Astini *et al.*, 1995; Thomas & Astini, 1996). In this scenario, the final accretion of the Precordillera is thought to have occurred during the Late Ordovician times (Ramos *et al.*, 1986, 1993; Astini *et al.*, 1995; Benedetto, 1998). However, based on pre-Carboniferous lithostratigraphy and fauna, Keller *et al.* (1998), proposed that the Precordillera was separated from Laurentia during the Ordovician, drifted slowly across the Iapetus and collided to Gondwana much later in Silurian-Devonian times.

Although, various scenarios involving the exotic origin of the Argentine Precordillera have been widely published, some authors (*e.g.* Baldis *et al.*, 1989; Aceňolaza & Toselli, 2000; Aceňolaza *et al.* (2002) propose a para-autochthonous origin of the Precordillera. Their models assume that the Precordillera was part of a hypothetical SAFRAN plateau, which developed between South America, Africa and Antarctica. A subsequent displacement along transcurrent faults is thought to have brought the Precordillera into its present location.

c) The Famatina Range

The central part of the Sierras Pampeanas is characterised by a magmatic arc of Early to Middle Ordovician age (Pankhurst *et al.*, 1998), which comprises the Famatina system and the Faja Eruptive de la Puna Oriental (Conti *et al.*, 1996). Astini *et al.* (1995) consider this arc as an oceanic island arc, which approached the Gondwana margin as a result of subduction and closure of an ocean floor. Geological data reported by Coira *et al.* (1982) and Allmendiger

(1983), and lithostratigraphic, volcanism, and palaeontological studies reported by Rapela *et al.* (1992) support the presence of this Ordovician ocean. However, based on geochemical data, Pankhurst *et al.* (1998) suggested that the Famatina Arc is a continental arc that developed on this margin of Gondwana in Early to Middle Ordovician.

On the Other hand, Conti *et al.*, (1996) suggested a para-autochthonous model based on palaeomagnetic data from the Puna-Oriental and Famatina Range. These authors suggest that both entities formed a mobile terrane that has been rotated clockwise and displaced with respect to Gondwana after the Early Ordovician. Petrological and faunistic evidence presented in Rapalini (1998) support this model.

d) The Paganzo Basin

The Paganzo basin is a foreland basin, which developed in NW Argentina during the Carboniferous (Lopez Gamundi *et al.*, 1994; González Bonorino & Ayles, 1995). The basin is situated east of the Argentine Precordillera, bounded by folded Early Palaeozoic to Early Carboniferous sediments of the Pampean range. Detailed studies of the sedimentary sequences and stratigraphic correlations indicate that sedimentation within the Paganzo basin started in the Early Upper Carboniferous (Namurian) and continued until the Middle to Late Permian (Net & Limarino, 1999; Limarino *et al*. (2002). The Late Carboniferous is interpreted as being a postglacial succession deposited during two main episodes of marine transgression, palaeotologically dated as Namurian-Westphalian and Stephanian in age. The Namurian-Westphalian transgressive sequence embraces the Guandacol, the Agua Colorada and the Malanzán Formations. The Stephanian transgression is well represented in the upper part of the Tupe Formation and in the Agua de Jagüel Formation. Limarino *et al*. (2002) subdivided the Paganzo Basin into different depositional settings, based on fossils and facies distribution. An open marine setting is suggested for the Western domain, while a marine-continental transition and a continental-dominated settings are attributed to the Central and Eastern domains, respectively.

Chapter 3

Palaeomagnetic sampling and techniques

3.1   Sampling regions

Sampling for the present palaeomagnetic investigation was carried out in NE Brazil, and in the southern Peruvian, central Bolivia and northern Argentinean Andes. Samples were collected from sedimentary and volcanic rock units covering the whole Palaeozoic era, and from some Mesozoic rock units. All sampling regions are considered autochthonous to the South American plate since the beginning of the Palaeozoic era, except for the Argentine Precordillera terrane. Samplings in NE Brazil were conducted in the Palaeozoic Parnaíba Basin and in the Mesozoic Araripe, Pernambuco-Paraiba, and Sergipe-Alagoas Basins. Samples from the Parnaíba Basin were drilled in Silurian to Devonian rock units. Cretaceous magmatic dykes and sills, and carbonate sequences were subject to sampling within the Mesozoic Basins.

Sampling within the Central Andes was carried out in the Subandean Zone, in the Altiplano, and in the Eastern Cordillera. In the Subandean Zone, sampling was made in sedimentary units covering the Early Ordovician to Early Triassic (495-240 Ma) time periods. Samples were collected in three separate regions in southern Peru and central Bolivia. Sampling in Peru was made in a continuous sequence of Late Devonian to Permian sediments (east of Cuzco), and in Devonian to Carboniferous rock units exposed more than 200 km away, in the area situated northeast of the city. In the Altiplano, sampling was made in Early Ordovician and Early Triassic sedimentary sequences exposed in the area south of Cuzco.

In the Bolivian sector, the Subandean Zone was sampled in the region west of Santa Cruz, approximately 700 km away from Cuzco. Samples from this region were drilled in Late Ordovician to Carboniferous sedimentary rocks. Samples from the Eastern Cordillera (Late Ordovician and Early Silurian) were collected in the area west of Cochabamba.

Sampling in NW Argentina was carried out within the Paganzo Basin (Carboniferous to Permian units), in the Pampean Range (Permian units), in the Famatina Range (Early Ordovician and Permian units), and in the

Argentine Precordillera (Early Devonian to Late Devonian units). A summary list of the investigated rock units is given in table 3.1, and sampling locations are shown in Figure 3.3 and 3.4. Sampling details for each rock unit are given in the relevant chapter.

3.2   Sampling methods

Field sampling was conducted in three fieldwork periods, each of 4 to 6 weeks duration. The first field sampling (August-October 2000) was carried out in Bolivia and Argentina, the second (July-August 2001) focused on southern Peru, and the third sampling period (July 2002) was carried out in NE Brazil. Sample collection was made with a portable, water-cooled, gasoline-powered drill, providing cylindrical 2.5 cm diameter core. Drill cores were mostly oriented by use of magnetic compass. Duplicate orientations using sun compass were made on some cores. Close consistency between sun compass reading and magnetic reading after adjustment by the local magnetic declination indicates the reliability of the use of magnetic compass in all sampling locations. Local magnetic declinations in the sampling region vary from 2°W (southern Peru) to 20°W (NE Brazil). All values given in this manuscript have been corrected for local deviation.

The sampling strategy was undertaken to provide continuous reliable palaeomagnetic data for the Palaeozoic era. Unweathered rocks were targeted in attempt to uncover primary magnetisations. Replicate sampling of age equivalent rock units, at location and regional level, were made to insure the homogeneity of the palaeomagnetic data. However, as rock weathering is an evident problem in the region, the resultant sampling scheme was essentially dictated by the accessibility and freshness of rock exposures. Sample collection was made preferentially in the freshest, unweathered rocks, exposed along road cuts, river sections, or within quarries when possible. For each sampling location, core samples were drilled in at least five sampling sites, and in turn, at least 5 drill cores were collected from each sampling site. Different stratigraphic levels of variable thickness and/or geographically spacing sites were considered as palaeomagnetic sampling sites, depending on the rock exposures and the weathering conditions. Spacing between samples for each rock unit was made to cover adequate time, with the purpose of averaging out the secular variation of the Earth's palaeomagnetic field.

Effort to integrate palaeomagnetic field tests was made during the field sampling, when geological field conditions allow. Consequently, it was possible to carry out fold test to the local palaeomagnetic data for some rock units. As well, core samples for conglomerate test were drilled in some units.

Application of baked contact test was possible only for the Ordovician San Bonito Formation, in which magmatic sills were present.
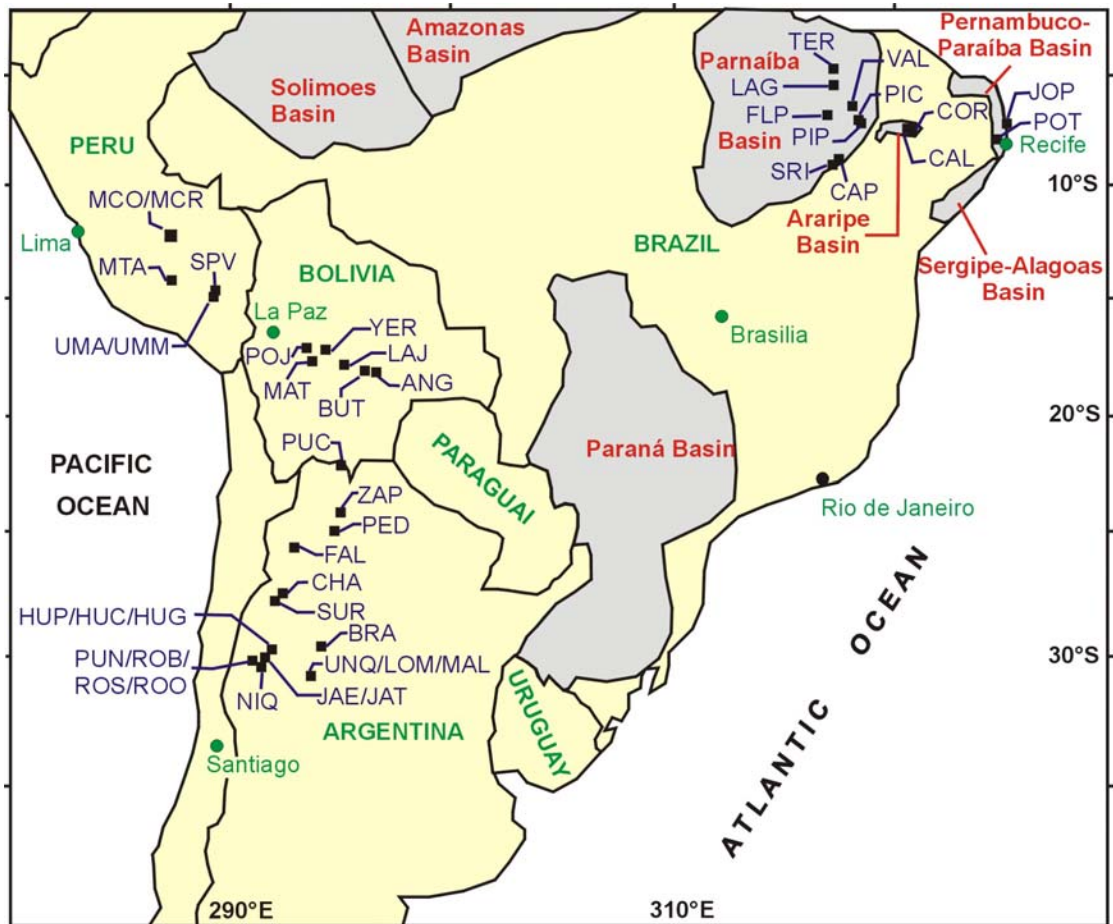
Fig. 3.1. Sketch map of South America showing all sampling locations (filled square) for the present palaeomagnetic study. Age summary of the rock units corresponding to location names are given in table 3.1.

3.3   Palaeomagnetic Measurement

Altogether, 1682 oriented cores drilled in 327 sites were collected. Each core sample was cut into two to four standard specimens, which were used for palaeomagnetic measurements. Measurements were made at the palaeomagnetic laboratory of the Geophysics section (Ludwig-Maximilians-Universität, Munich) in Niederlippach, Landshut. Laboratory experiments include measurement of the initial remanent magnetisation (NRM) of each specimen, prior to stepwise demagnetisation. Choice between the alternative demagnetisation procedures for each rock unit was made by selecting two batches of representative samples (pilot samples), which were respectively demagnetised by the use of thermal (TH) and alternating field (AF) demagnetisation techniques. Heating and cooling in magnetic field free space during thermal demagnetisation was made using Schoenstedt furnaces.

Alternating field demagnetisation was made with a 2G-AF-demagnetiser. Comparison of the demagnetisation results was made, and the demagnetisation techniques that allow isolation of magnetic direction(s) was used for further experiments.

Thermal demagnetisation technique was extensively used, as it was proved suitable for almost all investigated rock units. Demagnetisation of each specimen was made in 15 to 20 steps. Heating and cooling duration range between 40 minutes (at low temperature) to 60 minutes (at higher temperature). Measurements of magnetic direction and intensity were made with 2G-Cryogenic Magnetometer (DC-SQUID) in a field free room. After each demagnetisation step, the bulk magnetic susceptibilities were measured via a Kappa-bridge in order to check for thermo-chemical alteration. Stepwise demagnetisations generally started at 100°C, and were increased in 50°C to 100°C increments at low temperature heating steps. Heating steps at higher temperature were made in narrow increments (generally 30-20°C), and with 10°C to 5°C increments when the heating temperature approached the unblocking temperatures deduced from the pilot samples.

The demagnetisation results were analysed using orthogonal vector plots (Zijderveld, 1967) and stereographic projection. Linear (planar) demagnetisation trajectories were identified by eye, and the corresponding magnetic component was calculated using at least three successive data points. Directions of linear segments and poles to the planes were calculated using principal component analysis (Kirschvink, 1980). Within and between site mean directions were calculated according to standard methods (Fisher, 1953). Site mean directions were calculated from at least 3 sample directions. Site means lacking within-site consistency ($\alpha_{95}>15°$) were mostly rejected from further analysis. Virtual geographic pole (VGPs) were calculated from each site mean, and palaeopoles were calculated at location level.

Anisotropy of the magnetic susceptibility (AMS) was measured for the rock unit presenting doubtful palaeomagnetic data. The mineral carrier of remanence magnetisation was primarily identified based on unblocking temperature deduced from the intensity decay curve. In addition, some samples were subjected to rock magnetic tests using a variable field translation balance (VFTB). The VFTB test was to evaluate the properties of the mineral carrier of remanence by means of hysteresis curves, backfield coercivity spectra, isothermal remanent magnetisation (IRM) and saturation field. However, the low concentration of ferromagnetic minerals in many studied rock units did not permit detailed mineral properties.

Fig. 3.2. Sampling localities for all studied rock units (red dots) within the Central Andes. Details of rock units and location names are given in table 3.1.

PERIOD	AGE	ROCK UNIT (Location name)			
MIOCENE		Oriente Fm. (UMM) [1]			
CRETACEOUS		La Chonta Fm. (MCR) [1] Sardinha Fm. (FLO, OEI, PIC, LAG) [4] Gramame Fm. (JOP, POT) [4] Exu Fm. (CAL, COR) [4]			
EARLY TRIASSIC	Olenekian	Mitu Group (SPV) [3]			
	Induan				
PERMIAN	Kungurian		Pedra de Fogo Fm. (TER) [4]		
	Artinskian	La Antigua Fm. (BRA) [1] Patquia Fm. (HUP) [1]			
	Sakmarian	De La Cuesta Fm. (CHA) [1] Copacabana Group (MCO) [3]			
	Asselian				
CARBONIFEROUS	Stephanian	Tupe or Panacán Fm. (HUC) [1]	Solca Fm. (LOM) [1]		
	Westphalian	Piauí Fm. (FLP) [4]	Tarma Fm. (MTA1-6) [3]	Malanzàn Fm. (UNQ/MAL) [1]	
	Namurian				
	Visean	Taiguati Fm. (BUT) [2]	Guandacol Fm. (HUG) [1]	Cerro Fm. (RIC) [1]	
	Tournaisian	Los Monos Fm. (LAJ) [2] Iquiri Fm. (ANG) [2]			
DEVONIAN	Famennian		La Medienta Fm. (ZAP) [1] Punilla Fm. (PUN) [1]	Cabanillas Fm. ATA (1-8, and 11,12); [3]; MTC (1-7); MAM1; SIC1 [3]	
	Frasnian				
	Givetian	Pimenteiras Fm. (VAL) [4]			
	Eifelian	Itaim Fm. (CAP 7-11) [4]	Huamapampa Fm. (YER/MAT) [2]		
	Emsian	Talacasto Fm. (JAT) [1]			
	Praghian				
	Lochkovian	Acoyta Fm. (PUC) [1]			
SILURIAN	Pridoli				
	Wenlock	Los Espejos Fm. (JAE) [1]	Catavi Fm. (SAY/BOM) [2]	Tiangúa Fm. (CAP1-6, 12-15) [4]	
	Ludlow				
	Llandovery	Ipu Fm. (SRI) [4]	Cacaniri Fm. (TUN / POJ) [1]		
ORDOVICIAN	Ashgill	San Bonito Fm. (MOR) [2]			
	Caradoc	Anzaldo Fm. (POL) [2]	Yerba Loca Fm. (ROO) [1]		
	Llanvirn	Suri Fm. (SUR)			
	Arenig		San Juan Fm. (HUO)		
	Tremadoc	La Silla Fm. (NIQ) [1]	Umachiri Series (UMA1-7) [3]		

Tab. 3.1. Summary of the investigated rocks and their corresponding ages. Location names are shown in brackets (see Fig. 3.1 & 3.2). [1]Argentina, [2] Bolivia, [3]Peru, [4]Brazil.

Chapter 4

A new Cretaceous palaeomagnetic pole from northeastern Brazil

4.1   Introduction

Published Cretaceous poles for stable South American derived from palaeomagnetic data with reliability criteria Q≥3 (Van der Voo, 1990), are poorly grouped and yield mean poles with large uncertainty, especially for the Early Cretaceous (Fig. 4.1). As this is probably due age uncertainty of some data, palaeomagnetic data from well-dated rocks in NE Brazil presented in this chapter will help to refine the Cretaceous segment of the South American APW path.

The investigated rock units are exposed in the Parnaíba, Araripe, and Pernambuco-Paraíba Basins. These Cretaceous rocks were emplaced during times of rifting between the South American and African plates prior to opening of the Atlantic Ocean. Magmatic dykes and sills (Sardinha Formation), and carbonate sediments (Santana Group, Gramame Formation) deposited during marine incursions within these basins were subjected to sampling. Altogether, 166 drill cores from 31 palaeomagnetic sampling sites were collected from the Early Cretaceous Sardinha and Gramame Formations, and 70 core samples were drilled in 16 sites in the Late Cretaceous Santana Group (Tab. 4.1). Palaeomagnetic results from the Early Cretaceous (120-130 Ma; Sardinha Formation), the Late Cretaceous (65-71 Ma; Gramame Formation), and the Early Cretaceous (138-141 Ma; Santana Group are separately discussed in the following sections.
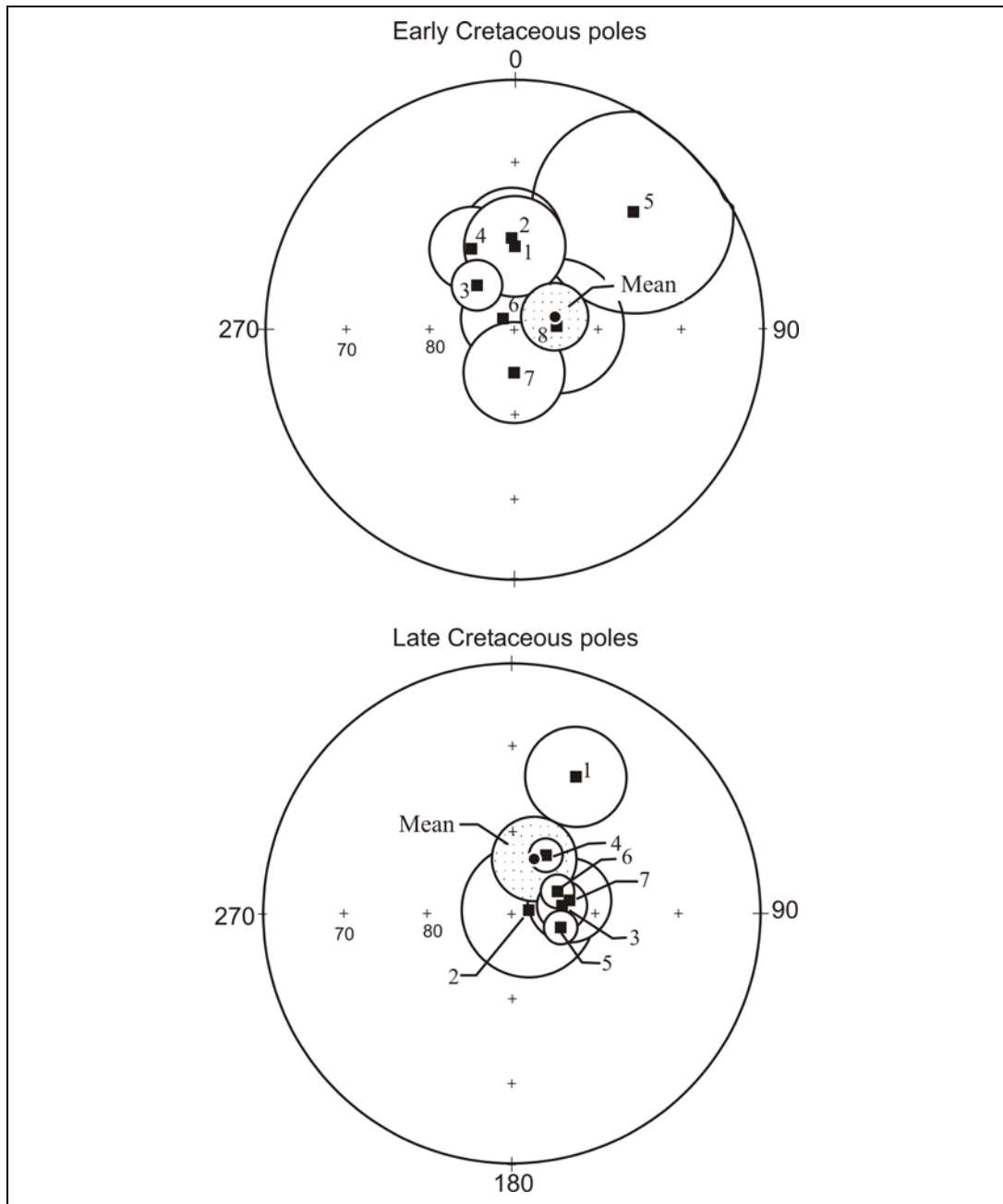
Fig. 4.1. Equal area projection of selected Early and Late Cretaceous poles from cratonic South America, and the mean poles calculated from combined South American and African poles (filled circles with stippled confidence circles) presented by Randall (1998). Early Cretaceous poles 1: Passa Quatro/Itatiaia intrusives, Brazil; 2: Patagonian Basalts, Argentina and Chile; 3: Pocos de Caldos intrusives, Brazil; 4: Sao Sabastiao Island, Brazil; 5: Cerritos Negro Volcanics, Argentina; 6: Cabo de Santo Agostinho, Brazil; 7: Cerro Barcino sediments, Argentina. 8: Cordoba Province, Argentina. Late Cretaceous poles: 1: El Salto-Almafuerte Lavas, Argentina; 2: Sierras de la Condores Group., Argentina ; 3: East Maranhao Basin volcanics, Brazil; 4: Ponta Grossa Dykes, Brazil; 5: South Parana Basin, Brazil; 6: Central Parana Basin, Brazil; 7: North Parana Basion, Brazil; 8: Rio de los Molinos Dykes, Argentina.

Rock Unit	Age (Ma)	Location	Site	S_{lat}(°S)	S_{long}(°E)	Dipdir(°)	Dip(°)	N	n
Sardinha Fm.	120-130	Floriano	FLO	6.81	317.03	164	4	6	32
		Oeiras	OEI	6.92	318.24	horizontal		2	10
		Picos	PIC	7.02	318.44	209	5	5	26
		Lagoa do Piauí	LAG	5.45	317.35	horizontal		5	27
Gramame Fm.	65-71	João Pessoa, Recife	JOP	7.14	325.11	135	3	10	50
		Poti quarry, Recife	POT	7.89	324.65	horizontal		3	20
Santana Gp.	98-121	Caldas, Juazeiro do N.	CAL	7.35	320.68	240	2	5	28
		Correntinho, Juazeiro do N.	COR	7.36	320.63	283	2	8	43

Tab. 4.1. Details of the Cretaceous rock units sampled in NE Brazil. S_{lat} and S_{long} are latitude and longitude position of the sampling location. Dipdir/dip: Dip direction (°E) and plunge (°) of the bedding attitude of the sampled unit. N: number of sites; n: number of samples (oriented drill cores). Altogether 236 samples were collected from 44 palaeomagnetic sites.
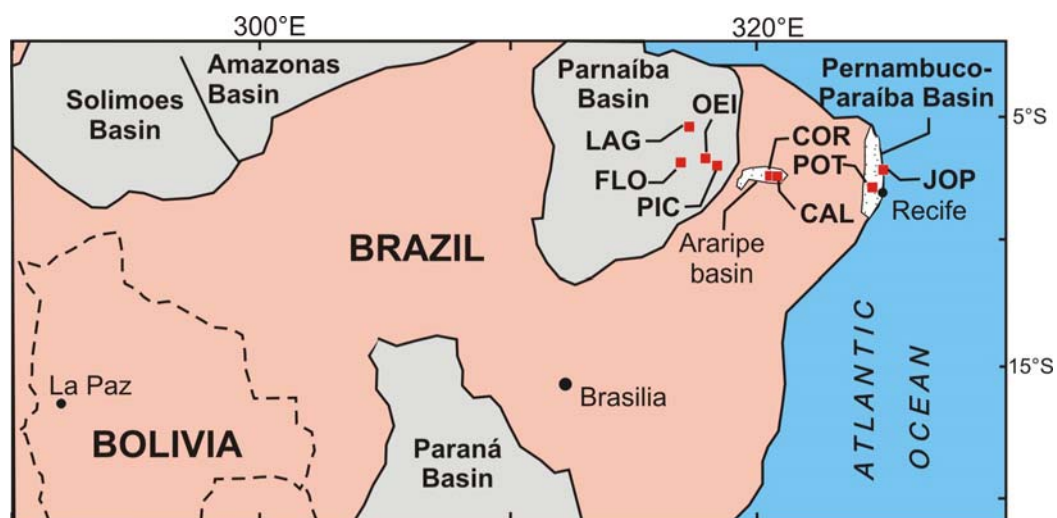
Fig. 4.2. Sketch map of the northern South America showing various cratonic basins and the sampling locations for the investigated Cretaceous rock units. Sampling locations are: Sardinha Formation: LAG, OEI, FLO, PIC; Santana Group: CAL, COR; Gramame Formation: JOP, POT. See Table 4.1 for sampling details.

4.2   Sardinha Formation (Early Cretaceous)

4.2.1   Sampling Details

The Sardinha Formation, widely exposed in the eastern Parnaíba basin. It is a part of the Late Jurassic-Early Cretaceous magmatic Series, which were emplaced in relation to the rifting that preceded the opening of the South Atlantic Ocean (Bellieni *et al.*, 1990, 1992; Almeida *et al.*, 2000). The Sardinha Formation consists essentially of extensive dykes and sills, comprising andesite-basalts and some latite-basalt intrusions (Bellieni *et al.*, 1990). A K/Ar based age of 120-130 Ma (Early Cretaceous) is attributed to

all intrusive dykes and sills exposed in the eastern part of the Parnaíba Basin (Bellieni *et al.,* 1990).

Samples from Sardinha Formation were collected at four locations in the Parnaíba Basin (Fig. 4.3; Tab. 4.1). At the sampling location north of Picos (PIC), samples were drilled in a quarry alongside the road, where, the Sardinha Formation is present as a sill within Devonian sediments. The bedding attitude of the intruded Cabeças Formation (5° towards NW) was used for tilt-correction of the palaeomagnetic data. For the unit sampled in a quarry near Lagoa do Piauí (LAG) in the area south of Teresina, the rock exposure shows an intrusive relationship with the Devonian sediments.
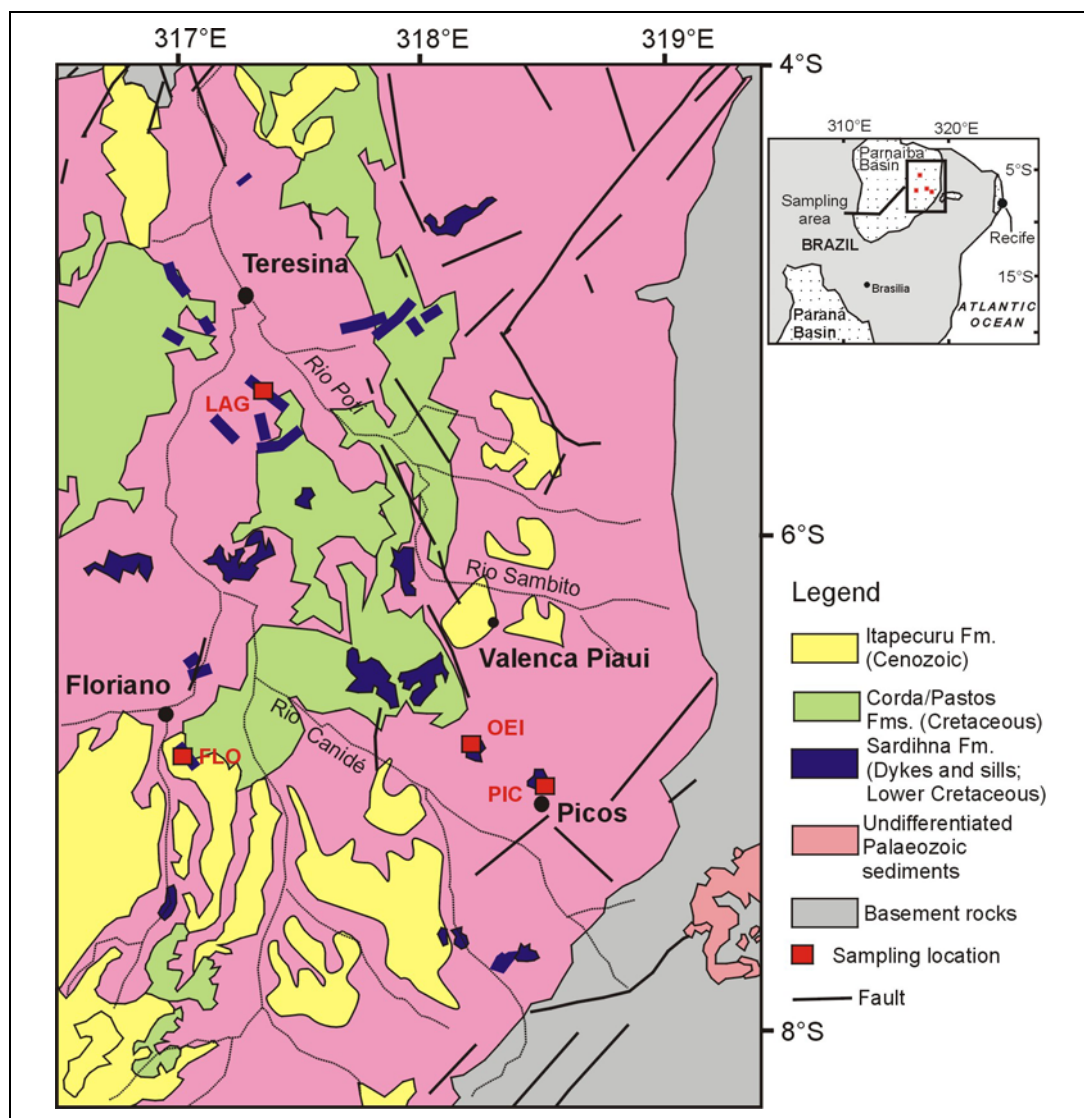
Fig. 4.3. Simplified geological map of the southeastern part of the Parnaíba Basin (NE Brazil) showing sampling locations for Sardinha Formation (PIC, OEI, FLO, LAG; see table 4.1 for details).

The stratification of the outcrop near Floriano (sites FLO1-6; Floriano-Picos highway) is not obvious and the contact with Jurassic sediments is not

exposed. However, observed planar features, which are interpreted as cooling surfaces, have similar attitudes to the bedding of the Jurassic sediments (3-6° to the SW). The sampling location near Oeiras (sites OEI1-2; Floriano-Picos highway) is assumed to be horizontal in accordance with the general stratigraphy and structure of the area.

4.2.2 Rock Magnetic Properties

The Sardinha Formation is strongly magnetised with initial NRM intensities ranging between 0.6 to 1.5 A/m. The remanence carrier in the Sardinha Formation is dominated by low coercivity magnetic mineral showing IRM curves saturated at low field (below 300mT). These minerals have low coercivity force (21 mT-32 mT) and moderate backfield coercivity (21 mT-33 m). These properties indicate that the remanence is mainly carried by magnetite. The hysteresis curves show typical loop for a population of pseudo-single domain ferromagnetic particles. This is consistent with the characteristic ratios between Mrs/Mr and Hcr/Hc, which plot within the PSD field on "Day plot" (Fig. 4.4).

4.2.3 Palaeomagnetic Results

Demagnetisation results for the samples collected near Floriano (sites FLO1-6), Picos (sites PIC1-5), and Lagoa do Piaúi (sites LAG1-5) are characterised by the presence of single component magnetisation, stable up to 590°C. Individual directions are generally identified between 400°C and 590°C by data points converging towards the origin on orthogonal projection (Fig. 4.5). This component has a southern declination and a shallowly down-dipping inclination. Intensity decay curves indicate maximum unblocking temperature at 570-580°C, suggesting magnetisation carried dominantly by magnetite. This is consistent with the rock magnetic properties discussed above.

Conversely, demagnetisation results from samples collected near Oeiras (OEI1-2) show two distinct magnetic directions: a soft component (A) generally erased below 350°C, and a high unblocking temperature direction (B), sometimes stable up to 580°C (Fig. 4.5). The component A is recognised in 12 samples and is a normal polarity magnetisation, yielding an overall sample mean of D= 356.2°; I= -13.5° (α_{95}= 6.4°) *in-situ*. This direction is similar to the expected present day magnetic dipole field at the sampling area, thus component A is interpreted as a viscous remanent magnetisation (VRM) acquired under the present geomagnetic field.

Component B is identified in 13 specimens cut from the 10 drill cores. It is a reversed polarity magnetisation with southern declination and shallow

inclination. Component B from sites OEI is similar to the direction obtain from location FLO, PIC and LAG, discussed above. The magnetic mineral carriers in the samples from OEI are also dominated by magnetite, with maximum unblocking temperature between 580-590°C.
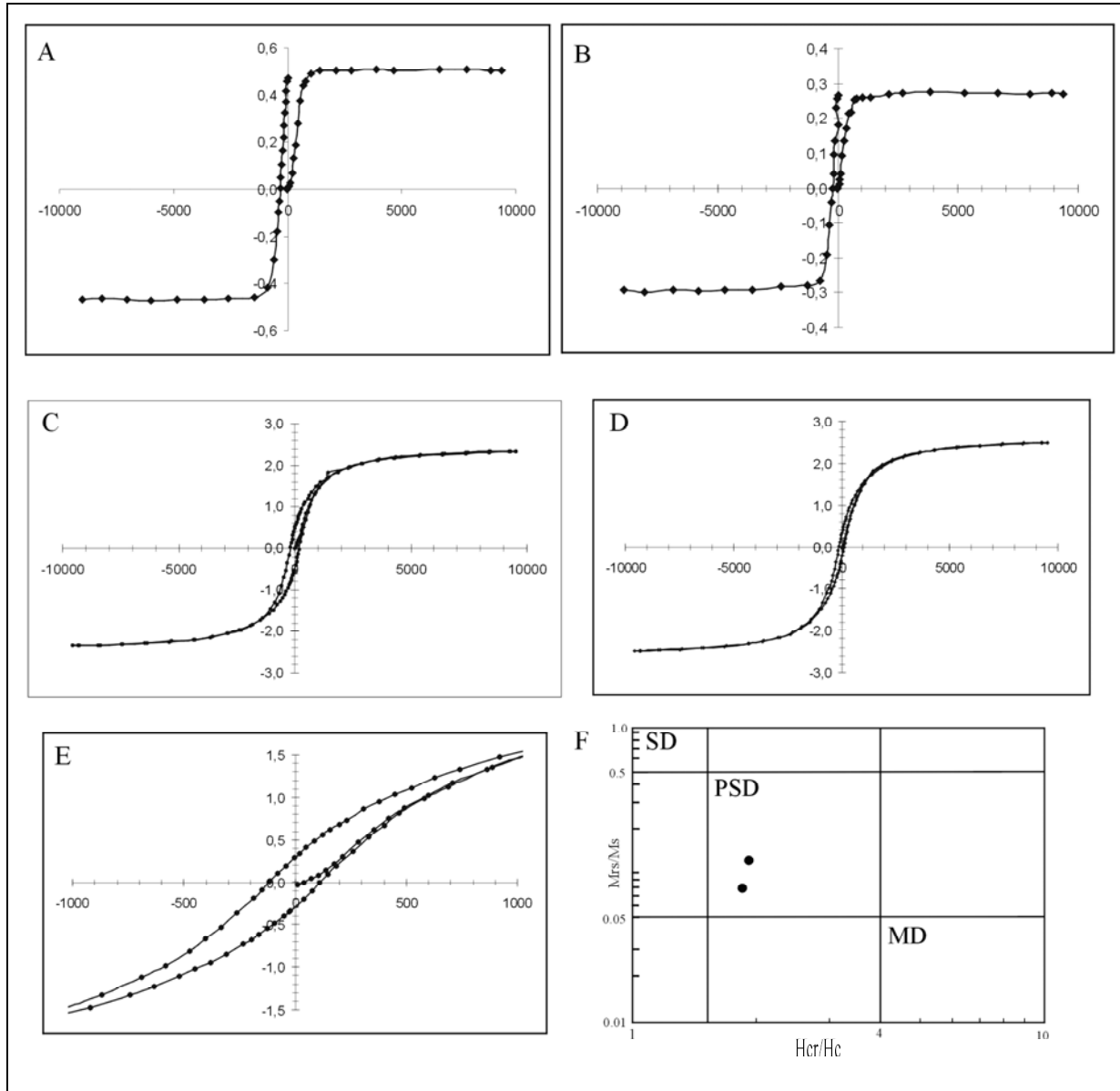
Fig. 4.4. Bulk rock magnetic properties for Sardinha Formation. A, B: isothermal remanent magnetisation (IRM) and coercivity spectra for samples from location FLO (A) and PIC (B). The IRM curves show moderate backfield values (Hcr) of 32 mT (FLO) and 22mT (PIC). Full saturation magnetisation was achieved in laboratory field. The saturation magnetisation (Ms) for samples from FLO and PIC are respectively 217 mT and 229 mT. C and D: Hysteresis loop showing that pseudo-single domain ferromagnetic minerals are the dominant magnetic carriers. E: Expanded view of the middle of the hysteresis loop (C) within ±100mT. F: Plot of the hysteresis ratios (Mrs/Ms vs. Hcr/Hc; Day *et al*.; 1977), showing the position of the samples from Sardinha Formation (dots) within the pseudo-single domain (PSD) area.
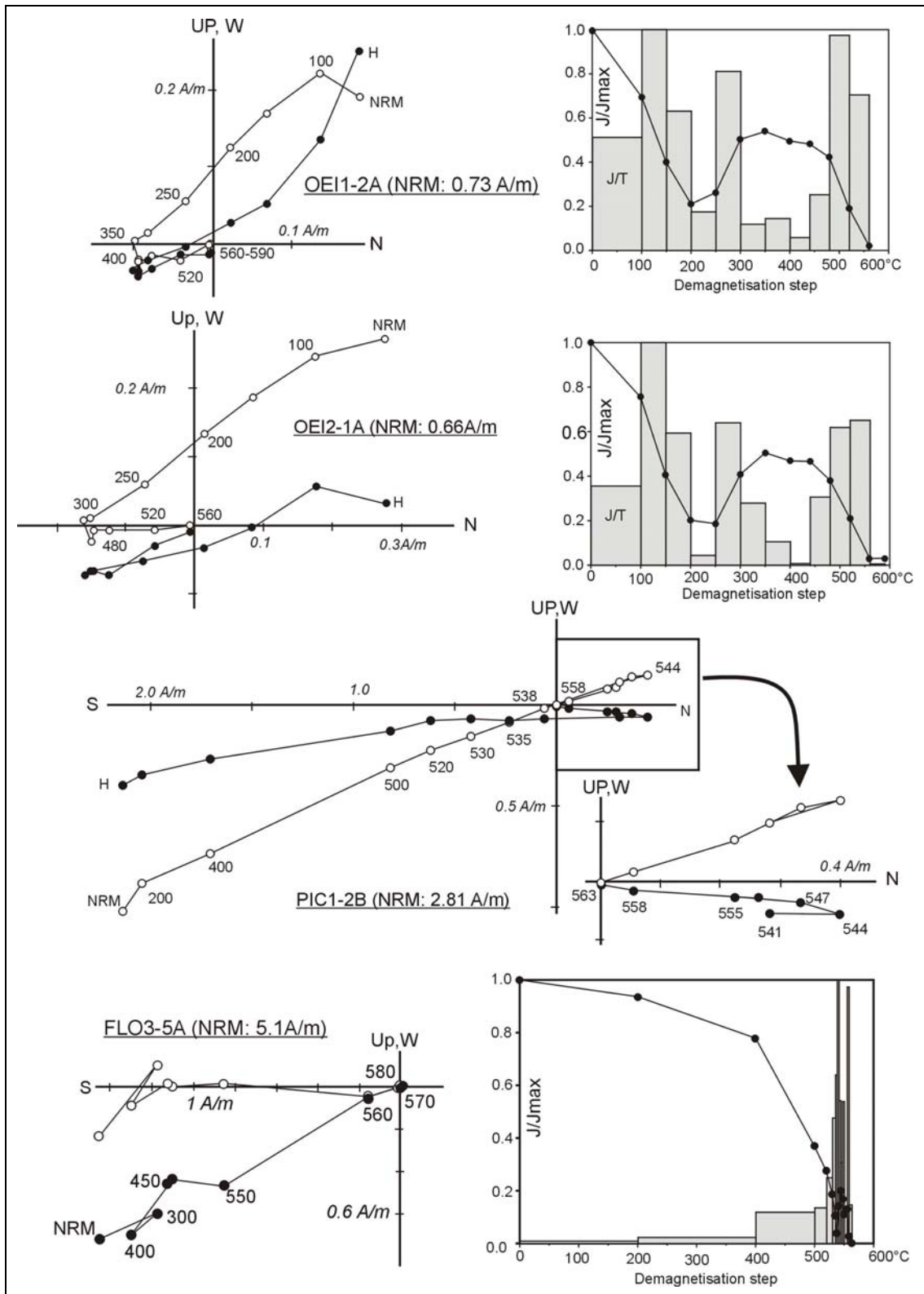
Fig. 4.5. Representative examples of demagnetisation results from Sardinha Formation. Two magnetic components are identified in samples OEI1-2A and OEI2-1A, while some samples (*e.g.* FLO3-5A) yield a single component magnetisation. Open/closed circles on orthogonal projection represent data points (*in-situ* co-ordinates) in vertical/horizontal plane.

Site	n	Dg (°)	Ig (°)	Ds (°)	Is (°)	α_{95} (°)	k	P_{lat}(°S)	P_{long}(°E)	dp	dm	dipdir	dip
FLO1	8	175.3	07.0	175.2	03.1	3.6	235	82.9	094.5	1.8	3.6	164	04
FLO2	4	181.3	08.6	181.1	04.8	5.9	240	85.5	151.1	3.0	5.9	164	04
FLO3	5	175.9	06.0	175.8	02.1	6.2	153	82.9	100.8	3.1	6.2	164	04
FLO4	4	179.9	11.9	179.7	08.1	8.9	108	87.2	130.8	4.5	9.0	164	04
FLO5	5	171.1	06.3	171.1	02.4	2.7	776	79.5	078.9	1.4	2.7	164	04
Mean	N	Dg (°)	Ig (°)	α_{95}°	kg	Ds (°)	Is (°)	α_{95} (°)	ks	λ(°S)	ϕ(°E)	A_{95}(°)	K
	5	176.7	8.0	4.4	300	176.6	4.1	4.4	303	84.2	101.2	3.9	383

Lagoa do Pauí

Site	n	Dg (°)	Ig (°)	Ds (°)	Is (°)	α_{95}°	K	P_{lat}(°S)	P_{long}(°E)	dp	dm	dipdir	dip
LAG1	4	180.0	02.4	180.2	02.2	3.3	1028	85.7	140.0	1.7	3.3	0	00
LAG2	4	174.0	03.9	174.3	04.1	5.3	297	83.4	078.0	2.7	5.3	0	00
LAG3	6	179.3	05.9	179.7	05.8	6.7	104	87.4	130.6	3.4	6.7	0	00
LAG4	3	175.5	07.7	176.1	08.5	7.7	353	85.9	064.0	3.9	7.8	0	00
LAG5	8	175.7	06.3	176.4	10.1	6.3	84	86.4	052.9	3.2	6.4	0	00
Mean	N	Dg (°)	Ig (°)	α_{95}°	kg	Ds (°)	Is (°)	α_{95}°	ks	λ(°S)	ϕ(°E)	A_{95}(°)	K
	5	176.9	06.1	5.2	591	177.0	5.8	3.8	397	86.2	88.9	2.8	740

Picos

Site	n	Dg (°)	Ig (°)	Ds (°)	Is (°)	α_{95}°	K	P_{lat}(°S)	P_{long}(°E)	dp	dm	dipdir	dip
PIC1	5	168.7	11.5	169.2	07.8	8.5	81	78.8	064.0	4.3	8.6	209	05
PIC4	5	172.3	08.8	172.7	04.9	4.2	329	81.4	080.2	2.1	4.2	209	05
PIC5	8	177.6	08.0	177.9	03.8	5.2	116	84.5	116.1	2.6	5.2	209	05
Mean	N	Dg (°)	Ig (°)	α_{95}°	kg	Ds(°)	Is (°)	α_{95}(°)	ks	λ(°S)	ϕ(°E)	A_{95}(°)	K
	3	172.9	09.5	7.3	287	173.3	05.5	7.3	283	82.1	80.5	6.9	324

Oeiras

Site	n	Dg (°)	Ig (°)	Ds (°)	Is (°)	α_{95}°	K	P_{lat}(°S)	P_{long}(°E)	dp	dm	dipdir	dip
OEI1	6	176.7	04.5	176.7	4.5	4.3	239	84.3	102.9	2.2	4.3	0	00
OEI2	7	172.2	04.0	172.2	4.0	3.5	300	80.8	080.2	1.8	3.5	0	00
Mean	N	Dg (°)	Ig (°)	α_{95}°	kg	Ds (°)	Is(°)	α_{95}(°)	kg	λ(°S)	ϕ(°E)	A_{95}(°)	K
	2	174.4	04.3	-	-	174.4	04.3	-	-	82.7	88.9	-	-

Tab. 4.2. Palaeomagnetic results from the Sardinha Formation. Sites FLO1-3: n: number of samples; N: number of sites. α_{95}° and k for site-level correspond to the tilt corrected directions. Dg/Ds and Ig/Is: Declination and Inclination in *in-situ* (g) and bedding-corrected (s) coordinates. kg/ks: precision parameter (Fisher, 1953) of the *in-situ* and bedding-corrected directions. P_{lat}(°S)/P_{long}(°E): latitude and longitude position of the site-level VGP in degrees South and East, respectively. λ(°S)/ϕ(°E): latitude (degrees south) and longitude (degrees east) position of mean palaeosouth pole. VGPs and mean palaeopole correspond to the bedding-corrected directions. The overall mean palaeosouth pole for Sardinha Formation is located at λ=84.4°S; ϕ=090.7°E (A_{95}=1.8°; K=441.9; N=15).

Altogether, the Sardinha Formation yields a stable remanence identified in 82 samples drilled in 15 sites (Tab. 4.2). The overall directions are well grouped in both sites and location levels (Fig. 4.6). The overall mean direction is D= 175.7°, I= +06.9° (α_{95}= 2.1°; k= 329.5; N= 15 sites) *in-situ* and D= 175.9°, I= +05.1° (α_{95}= 2.0°; k= 354.9°) after bedding correction. There is a slight improvement in directional grouping after bedding correction, but it provides indeterminate fold tests due to the only slight differences in bedding attitudes ($\leq 5°$; Tab. 4.1). Stepwise untilting (Enkin, 2003) on the locality-level direction shows maximum grouping at 99% untilting (Fig. 4.6e). This suggests that the remanence of the Sardinha Formation was acquired prior to the tilting.

The Sardinha remanence is unlike any expected younger magnetic direction at the sampling location, and shows consistent direction in all locations. It is, therefore, considered primary in origin. The Sardinha Formation yields a mean palaeosouth pole situated at λ= 84.4°S; ϕ= 090.7°E (A_{95}= 1.8°; K= 441.9; N= 15 sites). This pole is comparable to some published well-dated Early Cretaceous poles from Brazil (Tab. 4.3). As well, the presented new pole from NE Brazil is similar to the Early Cretaceous reference pole for stable South America derived from combined South American and African data (λ= 85°S; ϕ= 071°E; Randall, 1998; Fig. 4.7).

Rock unit	Age (Ma)	λ(°S)	ϕ (°E)	References
East Maranhao intrusive	112-124	83.6	81.0	Schult & Guerreiro, 1979
Parána Magmatic province	129-132	83.0	71.4	Ernesto et al., 1999
Serra Geral formation	131-139	83.5	100.5	Belleioni et al., 1983
Serra Geral basalts	131-139	84.6	115.4	Pacca & Hiodo, 1976
Serra Geral main Group	132-139	85.0	108.0	Ernesto et al., 1990
Sardinha Formation	120-130	83.0	88.9	This study

Tab. 4.3. Previously published Early Cretaceous poles from NE Brazil compared with the pole from Sardinha Formation. All listed data were used when calculating mean Early Cretaceous pole for South America.
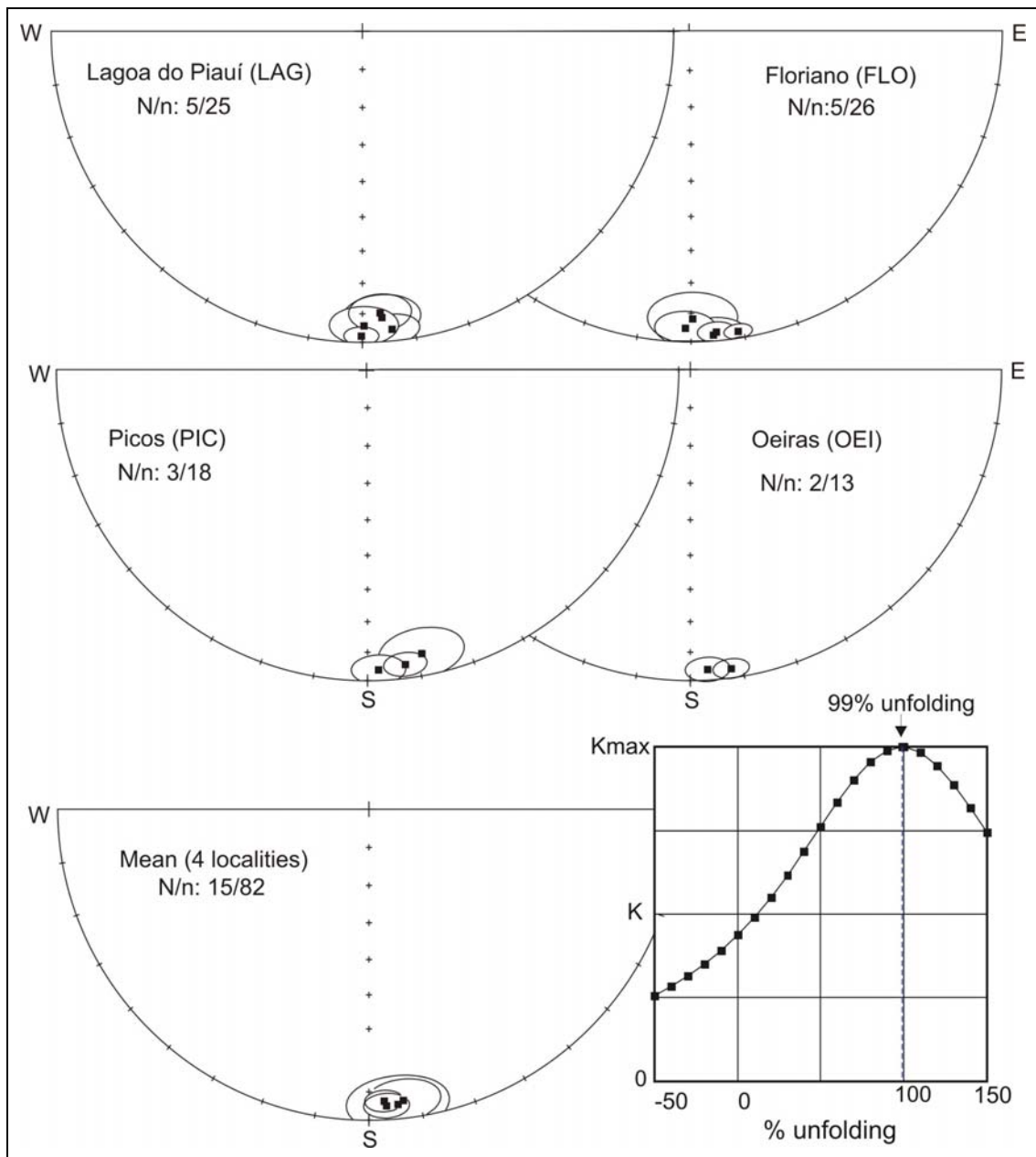
Fig. 4.6. Equal area projection of the palaeomagnetic data obtain from the Sardinha Formation. A) to D) Bedding-corrected site-level means for each sampling locality. E): Overall means for the 4 localities. N/n: number sites/samples. E) Stepwise untilting of the locality-level mean directions (N= 4). Maximum grouping is achieved at 99.2% untilting.
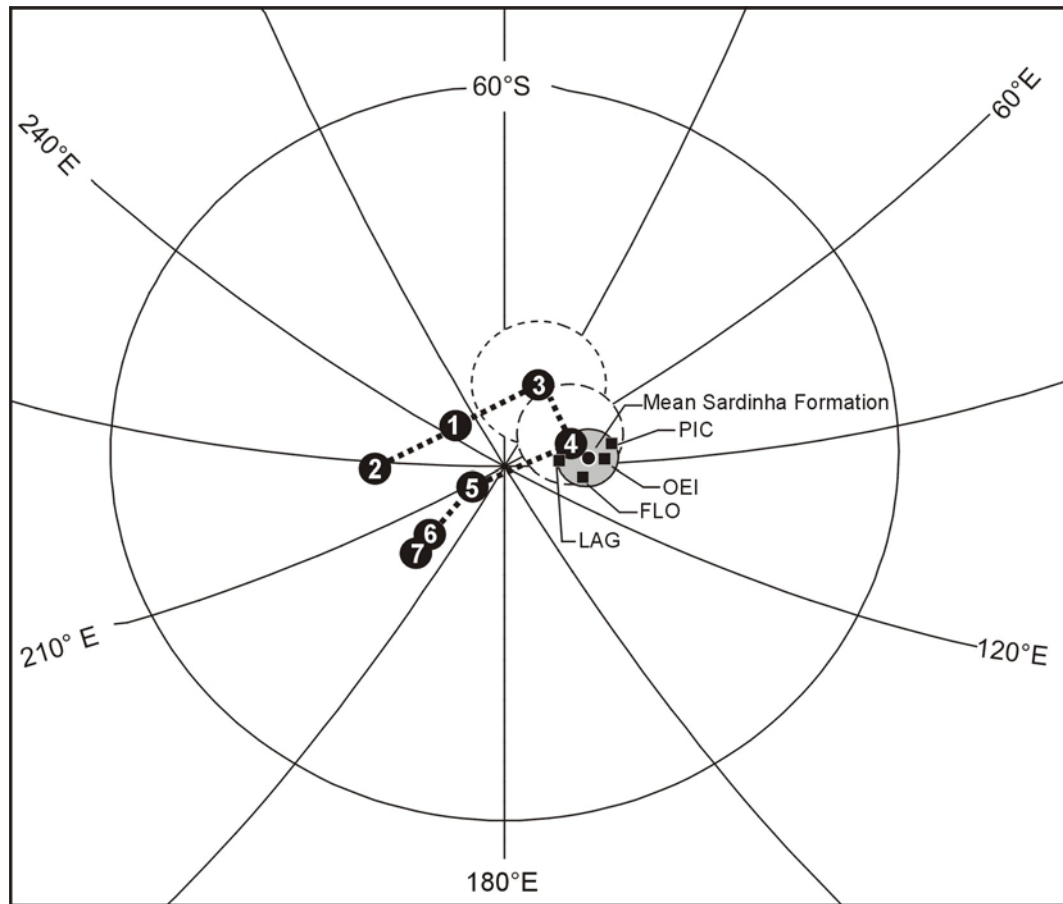
Fig. 4.7. Equal area plot of individual (square) and mean (circle with shaded confidence circle) palaeomagnetic south poles from Sardinha Formation (PIC, OEI,FLO,LAG). The Jurassic to Recent APWP for South America (Randall, 1998) is shown for comparison.1: Miocene (2-24Ma); 2: Palaeocene-Oligocene (24-66Ma); 3: Late Cretaceous (66-98 Ma); 4: Early Cretaceous (98-144 Ma); 5: Late Jurassic (144-163 Ma); 6: Mid-Jurassic (163-187 Ma); 7: Early Jurassic (187-208 Ma).

4.3   Santana Group (Early Cretaceous)

4.3.1   Sampling Details

The Santana Group was sampled within the Araripe Basin in the area north of Petrolina (Fig. 4.8). Lithologically, the Santana Group comprises sequences of fossiliferous lacustrine or lagoonal laminated carbonates (Maisey, 2000; Neumann *et al.,* 2003), and an Aptian-Albian age (98-121 Ma) has been assigned based on palynological evidence (Coimbra *et al.,* 2002). Stratigraphycally, the Santana Group rests onto the Abaiara Formation, which is dated in Neocomian (138-141 Ma) by means of palynological assemblages.

Samples for the Santana Group were collected in the Santa Rita quarry (near Caldas village) and in a quarry near Correntinho. Both locations are situated in the area south of Juazeiro do Norte (Fig. 4.8). Oriented core samples (n= 28) from the Santa Rita quarry (CAL), were drilled in massive calcareous mudstone, and finely laminated limestone beds, at the base of the quarry exposure. The unit sampled in a quarry near Correntinho (COR) consists of intercalated finely laminated calcareous sediments and mudstones overlain by sandstones. Samples from this location were drilled in calcareous limestone and muddy limestone layers. In sum, 71 oriented drill cores collected in 13 sites were investigated.
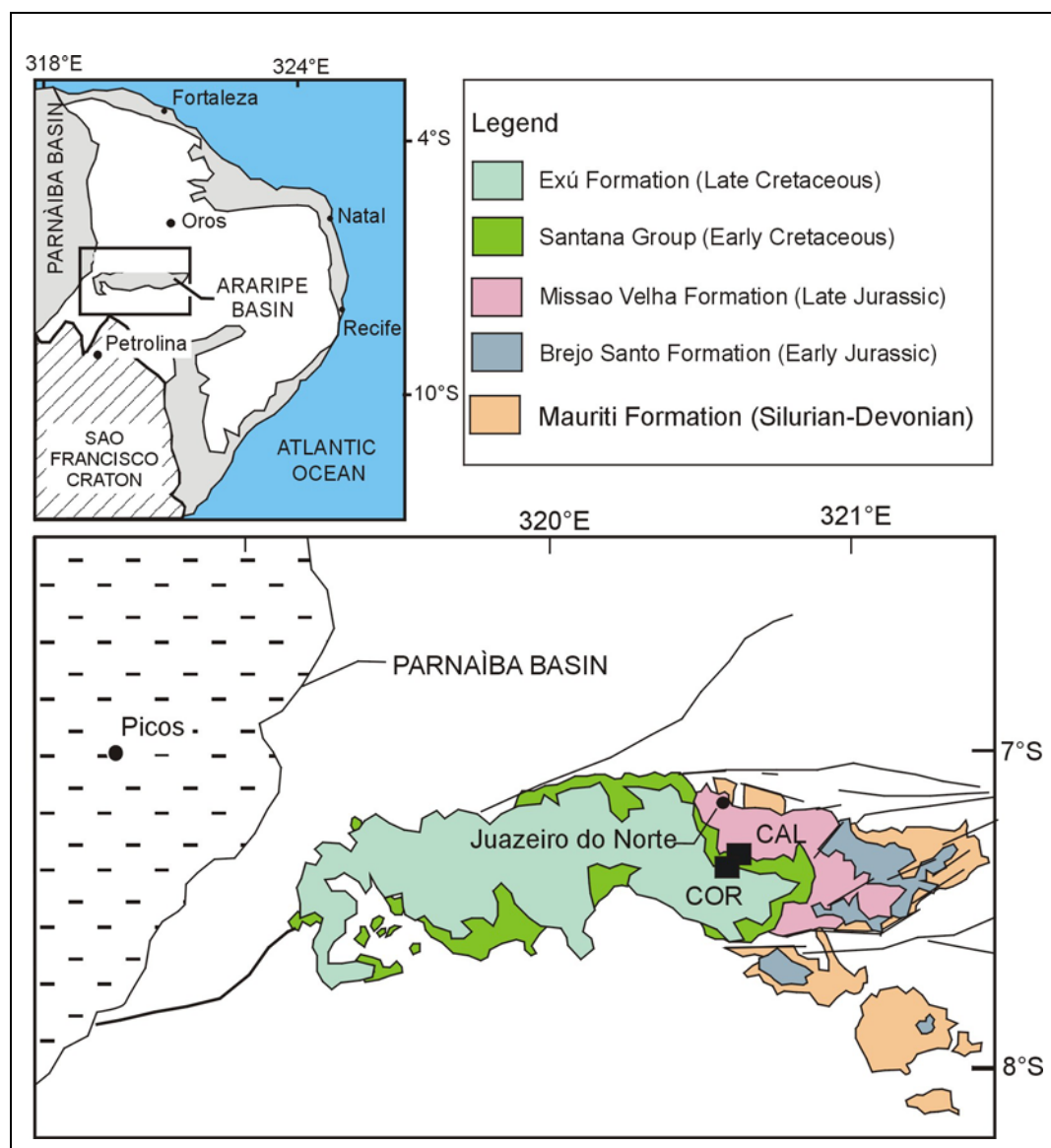
Fig. 4.8. Geological sketch map showing sampling locations for the Early Cretaceous Santana Group (Araripe Basin, NE Brazil). CAL: Santa Rita quarry (near Caldas); COR: Correntinho quarry. See table 4.1 for sampling details.

4.3.2 Palaeomagnetic Results and Interpretations

Demagnetisation results for the samples from Santa Rita quarry (sites CAL1-6) illustrate a well-defined single normal polarity magnetisation, characterised by northerly declination and shallow inclination (Fig. 4.9a). This direction is stable up to 480°C in most samples, and is identified in 20 samples from the 5 sites (Tab. 4.4). The overall directions are very well grouped at both sample and site levels (Fig. 4.9b). The site-level mean direction is D= 000.3°; I= -14.5° (α_{95}= 2.6°; k= 871) *in-situ* and D= 000.7°; I= -13.5° (α_{95}= 2.5°; k= 922) after structural-correction. There is a slight increase in statistical precision parameters after untilting, but this is not statistically significant. However, this direction is similar to the expected present day dipole field direction (D= 001.0°; I= -17.7°) at the sampling area. It, therefore likely represents an overprint acquired under the present geomagnetic field.

Samples from locality COR are very weakly magnetised (0.03-0.2 mA/m) and mostly show unstable directions during stepwise demagnetisation. However, probable stable component magnetisations are identified in 4 samples from site COR-6. Individual directions from these samples were calculated between 150°C to 390°C, from data points converging toward the origin on orthogonal projection. The calculated sample directions yield an overall mean direction D= 353°; I= -15.0°; α_{95}= 3.6°. No bedding correction was necessary as the samples were collected from flat laying sediments. This direction plots between the expected directions of the present day field (D= 338°; I= -18.0) and the dipole field (D= 001.0°; I= -17.7) at the sampling location. This low unblocking temperature magnetisation is, therefore, interpreted to be a VRM acquired under the present day field.

site	n	Dg (°)	Ig(°)	Ds(°)	Is(°)	α_{95}(°)	k	P_{lat}(°S)	P_{long}(°E)	dp	dm
CAL-1	6	358.7	-11.0	359.2	-10.1	1.8	740.4	87.6	121.2	0.9	1.8
CAL-2	4	359.5	-15.5	359.9	-14.6	2.5	494.8	89.9	014.1	1.3	2.6
CAL-3	4	000.9	-15.3	001.4	-14.2	2.6	121.0	88.6	225.5	1.4	2.7
CAL-4	3	002.1	-13.3	002.4	-12.3	13.1	90.0	87.2	205.6	6.8	13.3
CAL-5	3	000.3	-17.4	000.8	-16.3	6.9	322.0	88.7	281.4	3.7	7.1

Mean	N	Dg(°)	Ig(°)	α_{95}(°)	kg	Ds(°)	Is(°)	α_{95}°	ks	λ(°S)	φ(°E)	A_{95}(°)	K
	5	000.3	-14.5	2.6	871	000.7	-13,5	2.5	922	89.1	194.1	1.7	1927

Tab. 4.4. Summary of the palaeomagnetic data from the Santana Group sampled in the Santa Rita quarry (CAL). The listed VGPs correspond to the tilt-corrected site mean directions. n: number of samples; N=number of sites. See Tab.4.2 for table headings.
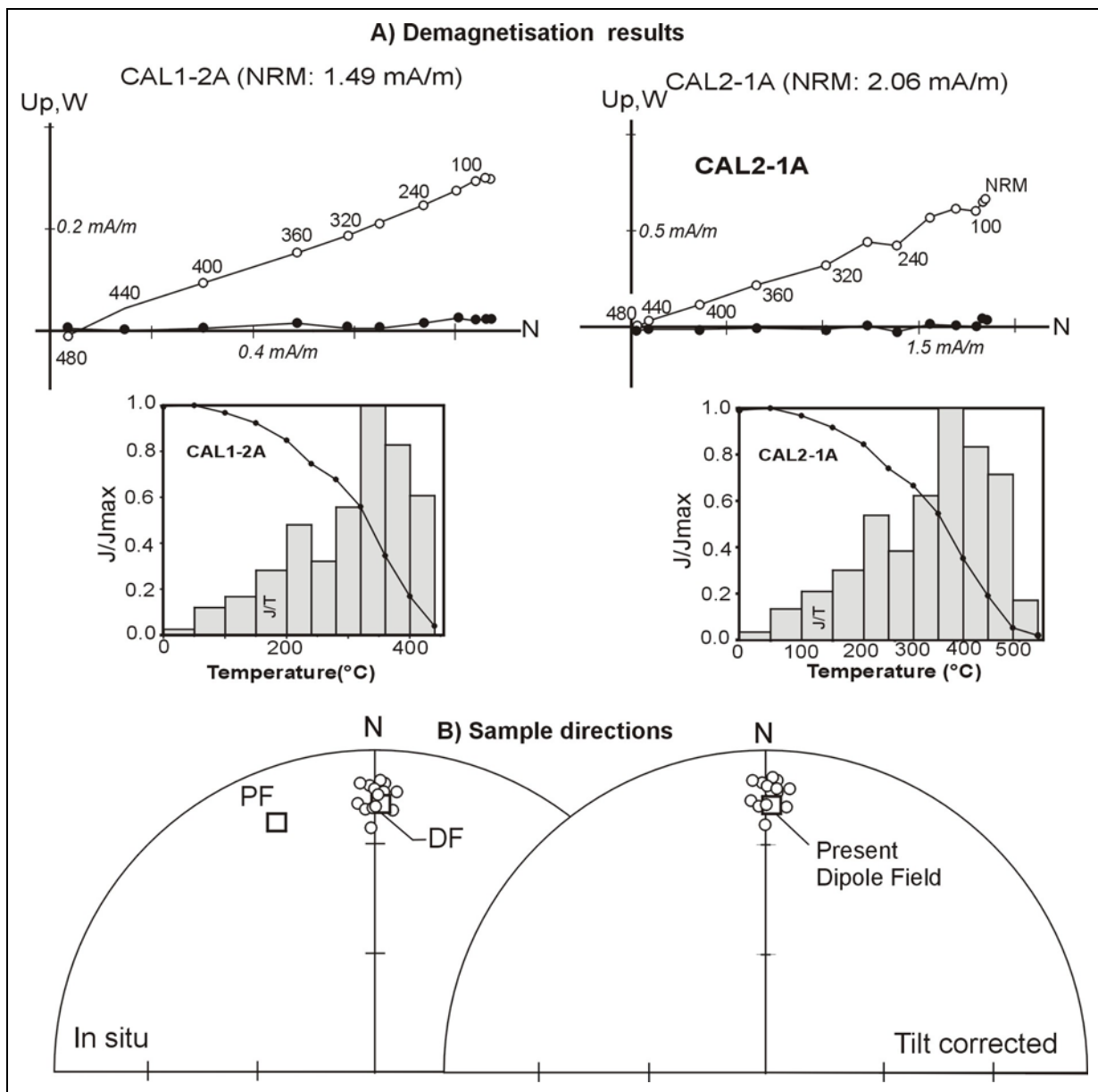
Fig. 4.9. A) Examples of thermal demagnetisation results from Santana Formation. Closed circles are projection of vector endpoints onto horizontal plane; open circles are vector end points projected onto Vertical plane (N-S). Progressive Thermal demagnetisation steps (°C) are shown adjacent to data points. **B)** Sample directions (n= 20) of the cleaned remanence. PF: present magnetic field at sampling location; DF: expected present axial dipole field.

4.4 Gramame Formation (Late Cretaceous)

The studied samples from the Gramame Formation were collected along the northeastern coast of Brazil, within the Pernambuco-Paraíba Basin. As described in Albertão & Martins (1996), the Gramame Formation was deposited in Maastrichtian (65-71 Ma) during the opening of the Atlantic Ocean and the first marine invasion into the basin Stratigraphically, the

Gramame overlies the Senonian Beberibe Formation, which, and is overlain by the Palaeocene-Oligocene Maria Farinha Formation (Milani & Thomaz Filho, 2000).

Palaeomagnetic samples were collected in two quarries located to the north of Recife. The sampling locality near João Pessoa, in the Cinescau Quarry comprises intercalated bioturbated sandy limestone and mudstone, overlain by a conglomeratic bed, with common calcite crystal and recrystallised pyrite. The sequence sampled in the Poti Quarry (POT) is situated at the top part of the Gramame Formation. This section is well known because it exposes the K/T boundary. Samples for palaeomagnetic were collected just below the K/T boundary. Altogether, 70 oriented cores of muddy and sandy limestones were collected in 13 palaeomagnetic sites.

Palaeomagnetic measurements demonstrate that the Gramame Formation is very weakly magnetised, with initial NRM intensities below 0.03 mA/m. Initial NRM directions of the samples from both locations are scattered around the expected present day field, on stereographic projection (Fig. 4.10). Demagnetisation experiments of these extremely weak samples did not provide reliable palaeomagnetic data and the results will not be discussed further.
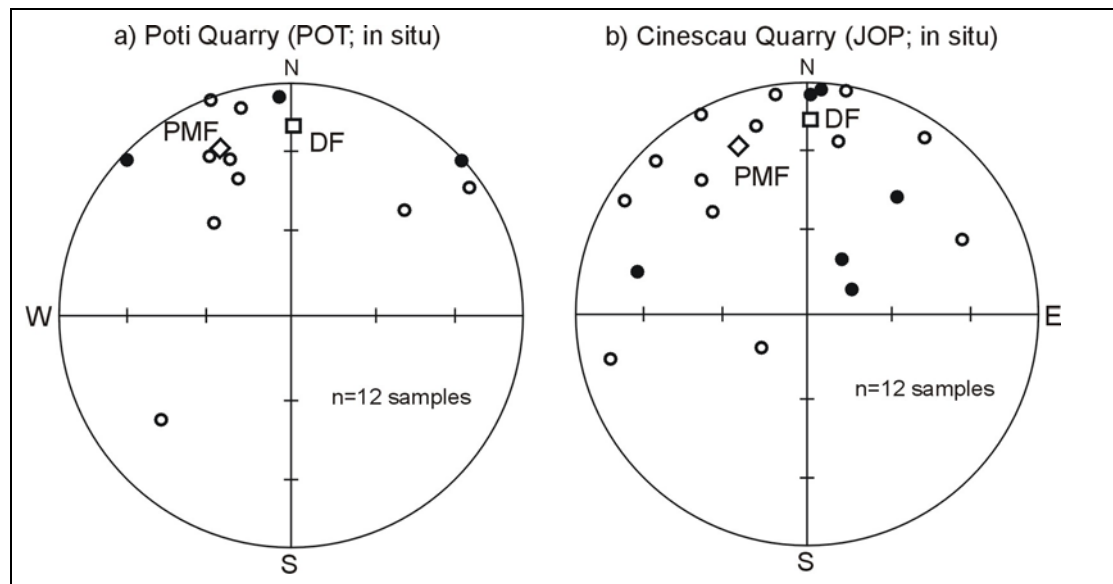
Fig. 4.10. Initial NRM directions for samples from Gramame Formation. No stable direction could be isolated from these samples. PMF and DF represent the expected present day field and dipole field at the sampling site, respectively.

4.5 Conclusion

The presented results demonstrates that the sandy and muddy carbonates of the Gramame Formation and Santana Group are not suitable for palaeomagnetic study. These units are very weakly magnetised due to the very low content of ferromagnetic minerals and relatively high content of paramagnetic clay. As a result, the total NRMs in these rocks are dominated by viscous remanent magnetisation.

Conversely, the Early Cretaceous intrusive Sardinha Formation yield a stable remanence considered primary in origin. The corresponding palaeosouth pole has a quality factor Q= 5 (out of 7), considering the reliability criteria of Van der Voo (1990). This new pole was calculated from palaeomagnetic data derived from radiometrically well dated rock (120-130 Ma; K/Ar; Bellieni *et al.*, 1990) with mean direction calculated from sufficient number of samples (82 samples from 15 sites), providing good statistical precision parameters. Tectonically, the sampling area is almost undisturbed, and the investigated units are either flat lying or only slightly tilted. Finally, this pole is distinct from younger palaeopoles, and similar to reliable Early Cretaceous poles from Brazil.

The Sardinha pole is comparable to the published highest quality poles (Q≥4) from stable South America and derived from well-dated rocks (Tab. 4.5). The combined data from the listed 6 studies suggests that the Early Cretaceous palaeosouth pole for South America was situated at λ= 84.3°S; ϕ= 67.7°E (A_{95}= 2.3°; K= 867) in Early Cretaceous (115-133 Ma). This new mean South American palaeopole is similar to the combined South American and African mean poles of Randall (1998; λ= 85.0°S; ϕ= 71.0°E; A_{95}= 4.0°) and Guena *et al.* (2000; λ= 84.8°S; ϕ= 81.8°E; A_{95}= 1.7°).

Rock unit	Age (Ma)	λ(°S)	ϕ(°E)	A_{95}°	Q	References
East Maranhão Intrusives, Brazil	124-129	83.6	81.0	1.9	4	Schult & Guerreiro (1979)
Sierra de los Condores , Argentina	115-133	86.0	75.9	3.3	5	Guena & Vizan (1998)
Alkaline Province, Paraguay	129-132	85.3	69.3	2.9	4	Ernesto *et al.* (1999)
Parana Magmatic Province, Brazil	129-132	83.0	71.4	5.0	5	Ernesto *et al.* (1999)
Ponta Grossa dyke, Brazil	127-135	82.0	30.0	2.0	6	Raposo & Ernesto (1995)
Sardinha Formation, Brazil	120-130	83.8	88.9	2.3	5	This study
Mean (N=6 studies)	**115-133**	**84.3**	**67.5**	**2.3**		

Tab. 4.5. Selected palaeomagnetic south poles for the South American plate. The listed poles are from well-dated rocks (115-133 Ma). Quality of the palaeomagnetic data (Q?4; Van der Voo, 1990) is listed.

Chapter 5

Remagnetisation of Palaeozoic rock units within the Parnaíba Basin, NE Brazil

5.1   Sampling details

Samples from the Palaeozoic sedimentary rocks in the Parnaíba Basin include 291 oriented cores drilled at 48 sites covering Silurian to Permian age rocks. The studied units include the Early Permian Pedra de Fogo Formation, the Late Carboniferous Piauí, Pimenteiras and Itaim Formations, and the Early Silurian Tianguá and Ipú Formations. Lithologies and depositional description of these units are given in section 2.1.

Samples for the Early Permian Pedra de Fogo Formation were collected from very shallowly dipping beds exposed in a quarry near José de Feritas in the Teresina area (Fig. 5.1). At least 5 core samples from each horizon, considered as palaeomagnetic sampling sites (TER1-11), were collected. Samples from the Piauí Formation were drilled on a road-cut along the Floriano-Picos highway (FLP). The exposure at this location consists of slightly tilted beds (4° towards SW) of purple-reddish laminated siltstones. The Early Devonian Pimenteiras Formation was sampled near Valença de Piauí (VAL), off the road to Teresina. Samples from this Formation were drilled in fresh layers of greenish grey fine-grained micaceous sandstones.

The Late Carboniferous Itaim Formation, the Early Silurian Tianguá and Ipú Formations were sampled in the Sierra de Capivara (CAP; Fig. 5.1) in the area near São Raimundo Notato. Samples from the Itaim Formation were drilled in intercalated finely laminated siltstone and mudstone beds (sites CAP7-11). Those from the Tangúa Formation (CAP1-6 and CAP12-15) were collected from near the contact with the overlaying Early Devonian Jaicos Formation. Sampling sites include beds of fine-grained to silty sandstones. Samples from the Ipú Formation include reddish siltstones and mudstones. In addition, twelve cores for conglomerate test were drilled in various clasts of an approximately a meter thick conglomerate at the base of the Ipú Formation.
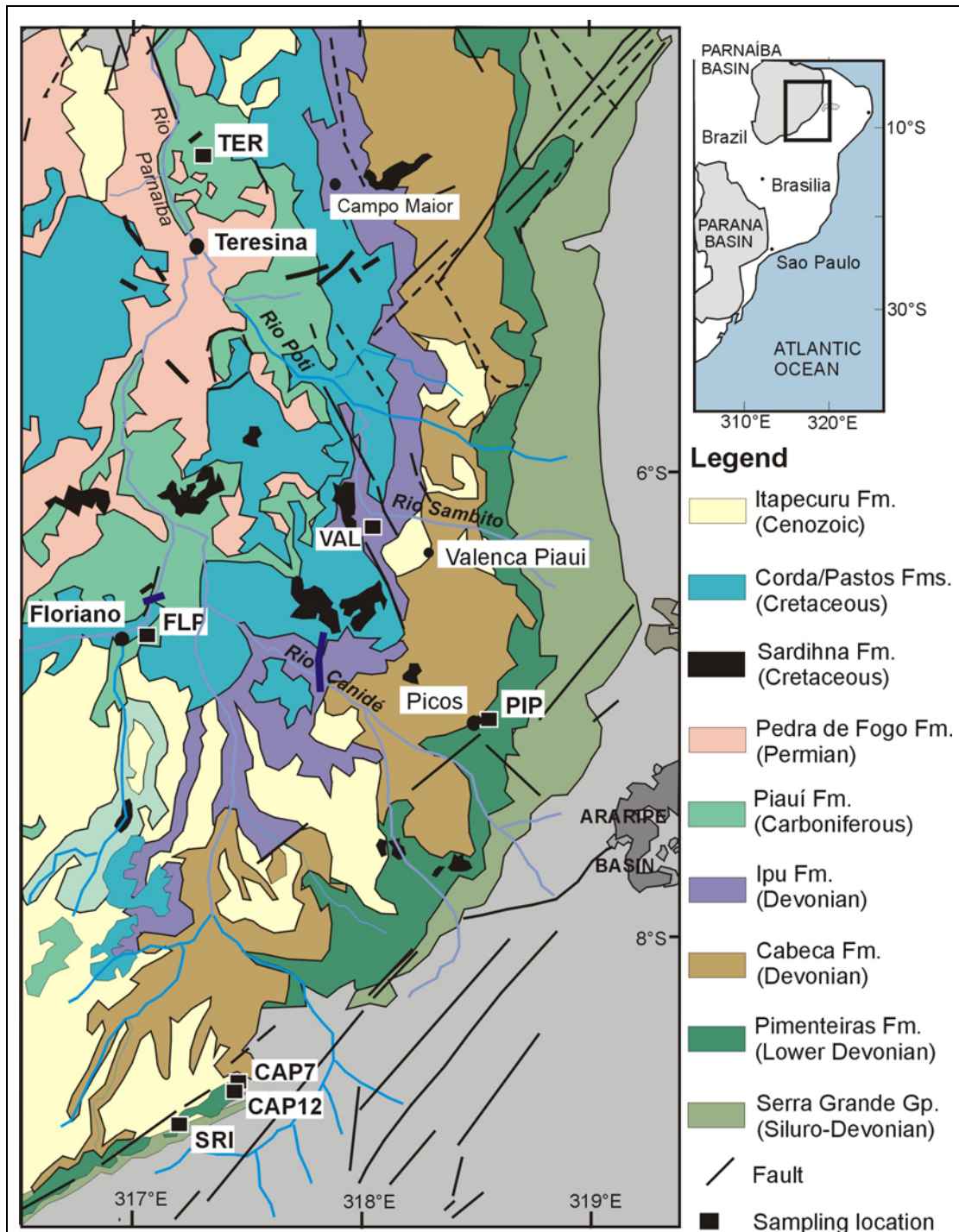
Fig. 5.1. Simplified geological map of the eastern part of Parnaíba Basin. Filled squares indicate sampling locations. Location codes and sampling details are given in Table 5.1.

Formation	Age	Location	Site	$S_{lat}(°S)$	$S_{long}(°E)$	N	n
Pedra de Fogo	E.Permian	José de Feritas, Teresina	TER	4.72	317.31	11	78
Piauí	L.Carboniferous	Floriano	FLP	6.81	317.05	5	25
Pimenteiras	M.Devonian	Valença de Piauí	VAL	6.29	318.06	10	51
Pimenteiras	M.Devonian	Picos	PIP	7.08	318.55	4	24
Itaim	M.Devonian	São Raimundo Nonato	CAP7	8.78	317.52	5	33
Tianguá	E.Silurian	Serra da Capivara	CAP12	8.78	317.51	10	60
Ipú	E.Silurian	Serra da Capivara	SRI	8.89	317.27	3	20

Tab. 5.1. Sampling details for the Palaeozoic rock units within the Parnaíba Basin. $S_{lat}(°S)$ and $S_{long}(°E)$: latitude (degrees south) and longitude (degrees east) position of the sampling sites (see Fig.5.1). N: number of sites; n: number of core samples. E: Early; M: Middle; L: Late.

5.2   Palaeomagnetic Results and Interpretation

5.2.1   Pedra de Fogo Formation (Early Permian)

Limestones from the Pedra de Fogo Formation have weak magnetisations with average intensity of 0.5 mA/m. Stepwise thermal demagnetisation, up to 600°C, of individual samples yield 2 distinct magnetic directions: a low unblocking temperature direction (A) generally identified below 300°C, and a high unblocking temperature component (B). The magnetic component A consists of a normal polarity magnetisation with northern declination and shallow inclination. It is present in almost all samples and well defined in 24 specimens cut from 17 samples. The overall *in-situ* mean direction calculated from these samples (D= 007.2°; I= -13.9°; α_{95}= 6.0°; k= 27.7), is similar to the expected direction of present day dipole field (D= 001°; I= -12.7°) at the sampling area. This direction is clearly a magnetic overprint acquired under the present day magnetic field.

The higher unblocking temperature component B direction is stable up to 600°C, and is defined by linear trends of data points, that trend toward the origin in orthogonal projection (Fig. 5.2). It is identified in 30 samples from 7 sites (Tab. 5.2). The overall B remanence is a dual polarity magnetisation characterised by north-easterly/south-westerly declination with intermediate to shallow negative/positive inclinations. Maximum unblocking temperatures of about 580°C indicate that the remanence is mainly carried by magnetite. Remanence B yields an overall site-level mean direction of D= 206°; I= -41° (α_{95}= 6°; k= 100) *in-situ*, and D= 205; I= +36° (α_{95}= 5.7°; k= 114) after bedding correction (Fig. 5.3).
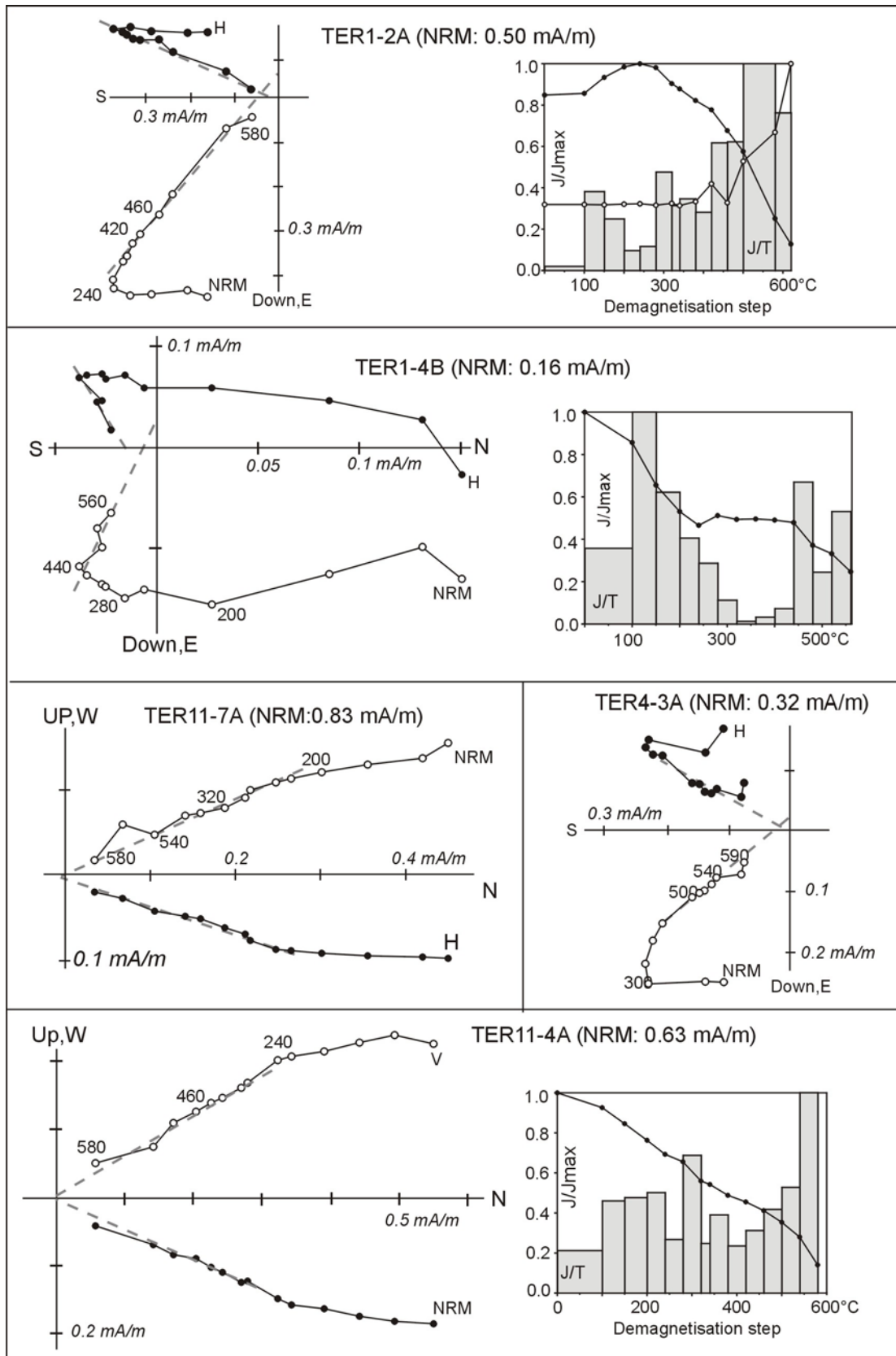
Fig. 5.2. Representative examples of demagnetisation results obtained for the Pedra de Fogo Formation. Data points in all orthogonal projections are in *in-situ* co-ordinates.
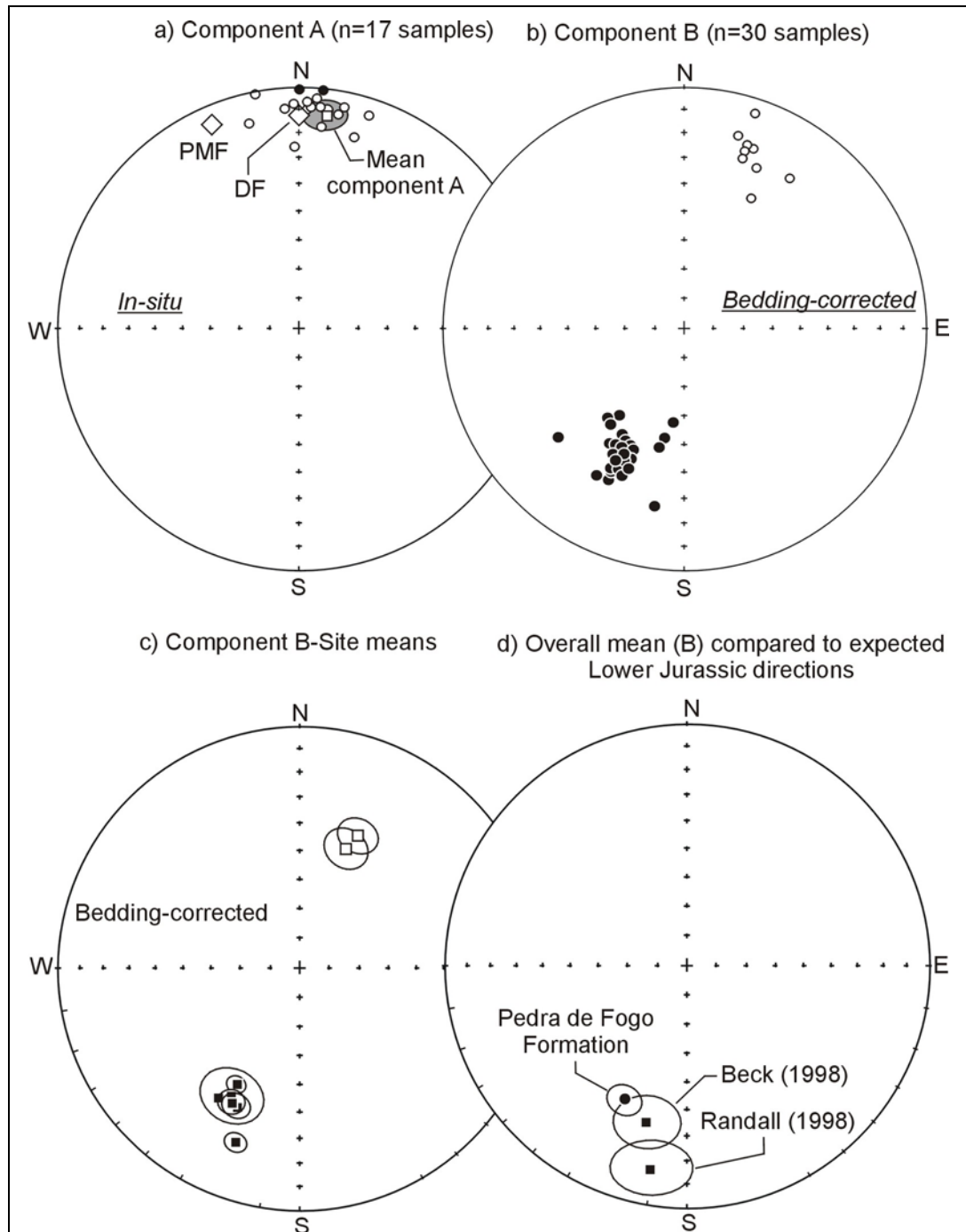
Fig. 5.3. Equal area projection of the palaeomagnetic results from the Early Permian Pedra de Fogo Formation. The expected Early Jurassic direction at the sampling location recalculated from Beck (1998) and Randall (1998) are shown (d).

The mean directions in geographic and stratigraphic co-ordinates are statistically indistinguishable at the 95% confidence level. The site mean directions, however, become more grouped after tilt correction, suggesting that the remanence is likely to have been acquired prior to tilting. Therefore, the bedding-corrected mean direction is considered for further interpretation.

The remanence B from the Pedra de Fogo Formation yields a palaeosouth pole located at λ= 60.5°S; φ= 265°E (A$_{95}$= 4.1°; K= 213; N= 7). This pole diverges from all Permian reference poles, and comparison with the younger reference poles shows close similarity with the proposed Early Jurassic pole for stable South America (Beck, 1998). The observed direction is comparable to the expected Early Jurassic magnetisation at the sampling location (Fig. 5.3d). This remanence is therefore interpreted as a magnetic overprint probably acquired in Early Jurassic times.

Site	n		D$_g$(°)	I$_g$(°)	D$_s$(°)	I$_s$(°)	α$_{95}$(°)	k	P$_{lat}$(°S)	P$_{long}$(°E)	dp	dm	Dir(°E)	Dip(°)
TER1	5	M	208.5	45.8	208.4	43.8	3.1	211	55.9	268.3	2.4	3.1	205	2
TER3-4	6	N	206.7	40.1	206.6	38.1	3.4	525	60.6	272.5	2.9	3.8	205	2
TER5-6	4	M	205.6	40.2	205.1	37.3	6.4	207	59.0	262.2	4.1	5.3	200	3
TER7-8	4	M	203.6	49.3	202.5	45.4	7.0	53	60.9	262.8	8.9	5.6	188	4
TER9	4	R	209.6	45.6	208.2	41.8	12.7	72	59.0	274.6	9.5	12.2	188	4
TER10	4	R	208.9	42.9	207.7	39.2	10.1	84	57.8	262.5	7.2	9.3	188	4
TER11	3	N	20.4	-25.5	20.2	-23.6	3.3	535	68.7	250.0	1.7	3.2	188	4

Mean	N		D$_g$(°)	I$_g$(°)	α$_{95}$(°)	k$_g$	D$_s$(°)	I$_s$(°)	α$_{95}$(°)	k$_s$	λ(°S)	φ(°E)	A$_{95}$ (°)	K
	7		205.9	41.4	6.1	99.7	205.4	38.5	5.7	114	60.5	265.4	4.1	213

Tab. 5.2. Site mean palaeomagnetic directions of the stable remanence (B) from Pedra de Fogo Formation. The listed VGPs are calculated from bedding-corrected mean directions. n/N: number of samples/sites. N, R, M designate normal, reversed and mixed polarity magnetisation.

5.2.2 Piauí Formation (Late Carboniferous)

Samples from the laminated purple siltstones of the Piauí Formation display initial NRM intensities ranging between 100 and 350 mA/m. Stepwise demagnetisation of 36 specimens cut from 25 oriented cores revealed a single magnetisation, stable up to 680°C. This direction is of reversed polarity with very shallow inclination and southerly declination values (Fig. 5.4). Maximum unblocking temperatures suggest that this remanence is carried by both magnetite (550°C<T$_b$<600°C) and haematite (T$_b$<650°C).

The overall site- mean direction (Tab. 5.3) is D= 178.7°; I= +6.4° (α$_{95}$= 2.5°; k= 951; N= 5) *in-situ* and D= 178.8°; I= +3.2° (α$_{95}$= 2.8°; k= 741) after bedding correction. There is a decrease in directional grouping after bedding correction despite the very slight difference in bedding attitude (4°) of the sampled units. This suggests a post-tilting nature of the remanence from Piauí Formation. However, the *in-situ* and bedding-corrected mean directions are statistically indistinguishable at the 95% confidence level.

When compared with the expected directions recalculated from the published Carboniferous poles for stable South America, the Piauí magnetisation deviates from all references. In opposition, the observed remanence in *in-situ* co-ordinates is similar to the magnetisation obtained from the overlying Cretaceous basaltic sill (Sardinha Formation; Fig. 5.5) exposed near the

sampling location (sites FLO1-6; section 4.3). Note that the palaeomagnetic data from the Sardinha Formation (D= 176.6°; I= +4.1°; α_{95}= 4.4°; k= 303) is considered as being a primary Early Cretaceous (120-130 Ma) magnetisation. Therefore, this similarity demonstrates that the magnetisation observed in the Piauí Formation is a Early Cretaceous overprint related to a thermal event during the intrusion of the Sardinha Formation. The Piauí magnetisation is also similar to the expected direction (D= 175.4°; I= +9.4°; α_{95}= 4.0°) recalculated from the Early Cretaceous reference pole for stable South America reported by Randall (1998). The mean palaeomagnetic south poles derived from Piauí Formation is situated at λ= 86.2°S; ϕ= 117.1°E (A_{95}= 2.5; K= 971).
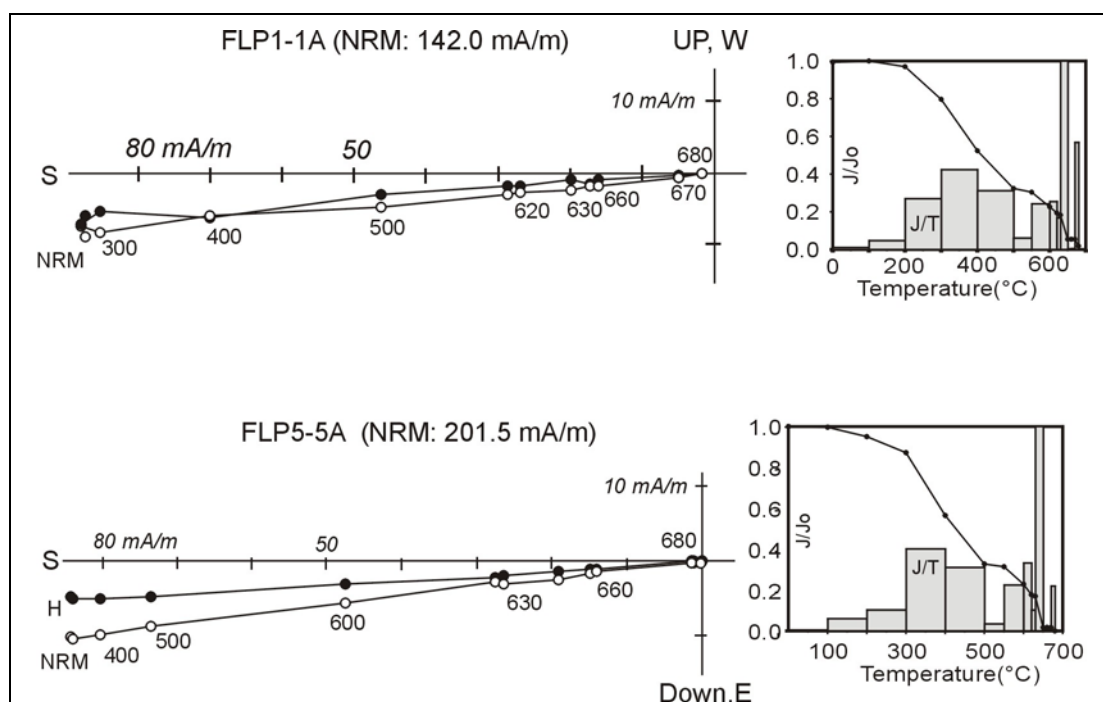
Fig. 5.4. Typical demagnetisation results from the Late Carboniferous Piauí Formation. The single reversed polarity magnetization, mainly carried by magnetite and haematite, is interpreted as being an Early Cretaceous overprint.

Site	n	D_g(°)	I_g(°)	D_s(°)	I_s(°)	α_{95}°	k	P_{Lat} (°S)	P_{Long}(°E)	dp	dm	Dip dir	Dip
FLP1	5	178.1	5.6	178.2	3.3	2.5	510	85.6	111.5	1.2	2.5	219	3
FLP2	5	180.8	4.9	180.9	2.6	4.1	218	85.6	147.5	2.1	4.1	219	3
FLP3	5	178.0	8.9	178.1	5.1	1.2	2349	87.0	96.2	0.6	1.3	194	4
FLP4	5	181.3	4.3	181.3	0.4	4.5	183	85.2	152.7	2.2	4.5	194	4
FLP5	5	178.4	8.4	175.6	4.6	2.4	634	84.8	76.1	1.2	2.4	194	4

Mean	N	D_g(°)	I_g(°)	α_{95}°	k	D_s(°)	I_s(°)	α_{95}°	k	λ(°S)	ϕ(°E)	A_{95}	K
	5	179.3	6.4	2.5	951	178.8	3.2	2.8	741	86.2	117.4	2.5	971

Tab. 5.3. Site-level palaeomagnetic data from the Piauí Formation. This remanence is likely acquired posterior to the tilting of the unit. Hence, the listed VGPs (P_{lat}/P_{long}) and mean palaeosouth pole (λ°S)/ϕ°E) were calculated from directions in *in-situ* co-ordinates. See Table 5.2 for headings explanation.
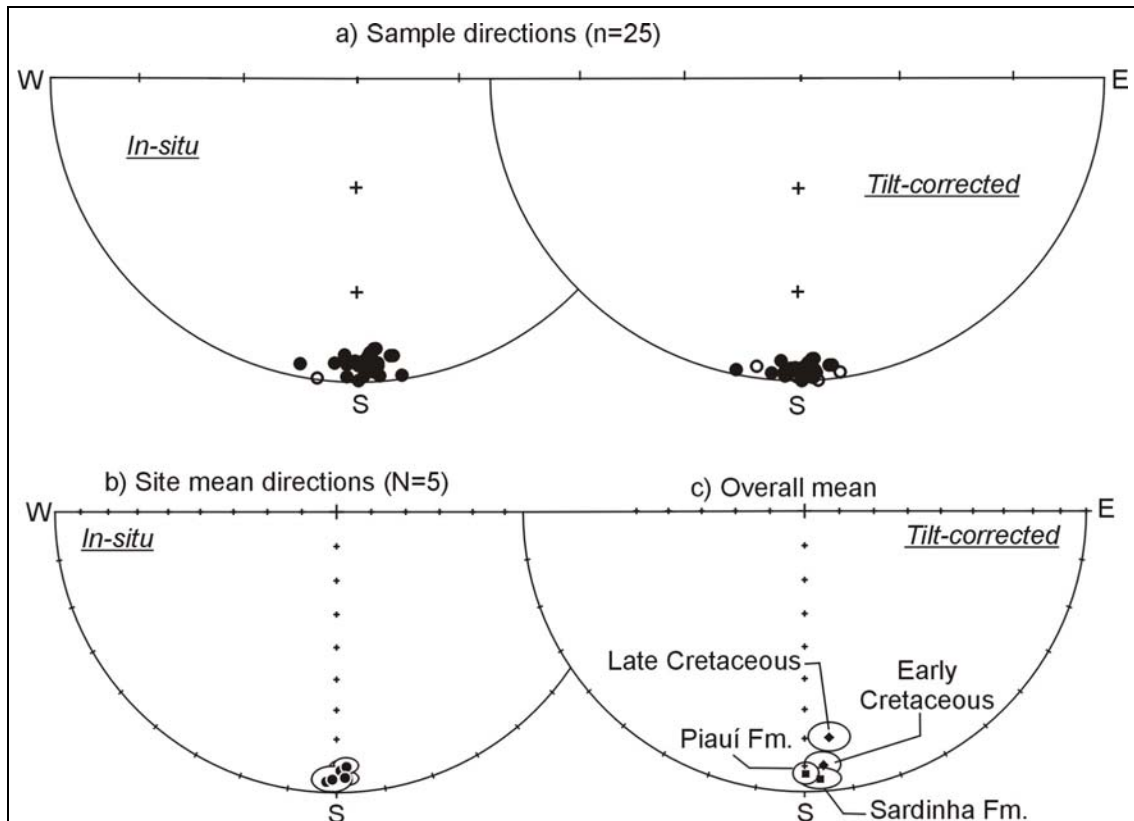
Fig. 5.5. Equal area projection of the palaeomagnetic results from Piauí Formation. **a)** *in-situ* and bedding-corrected individual directions of 25 samples. **b)** site mean directions (FLP1-5; Tab. 5.3). **c)** Overall mean direction compared with the palaeomagnetic data from the Early Cretaceous Sardinha Formation (see text) and the Late Cretaceous and Early Cretaceous reference directions (Randall, 1998) recalculated at S_{lat}= 6.8°S; S_{long}= 317.1°E.

5.2.3 Pimenteiras Formation (Early Devonian)

Samples from the Pimenteiras Formation were collected at two locations in Valença de Piauí area and in Picos (Fig. 5.1; Tab. 5.1). The fine to medium-grained sandstones collected near Valença de Piauí (sites VAL1-10) have initial NRM intensity ranging between 1.7 and 25 mA/m. Thirty-nine specimens from this location were thermally demagnetised with maximum temperatures of 700°C. Demagnetisation results of individual specimens illustrate either a single or two distinct normal polarity magnetisations (Fig. 5.6). Two component magnetisations were identified in the samples from sites VAL3, VAL4 and VAL7. The low unblocking temperature direction (A) is well identified in 11 samples, and is generally defined below 480°C in individual specimens. Component A yields an overall sample-level mean direction of D= 182°; I= +11.5° (α_{95}= 4.2°; k= 151) *in-situ*. This direction is similar to the expected present day dipole field (D= 179°; I= +15°) at the sampling location and is, therefore interpreted to be an overprint.

The high unblocking temperature component (B) has a steeper inclination and westerly declination. Maximum unblocking temperatures above 650°C in

all samples (Fig. 5.6) suggest that it is dominantly carried by haematite. This direction is well identified in 25 samples from 5 sites (Tab. 5.4), yielding an overall site-mean of D= 195.7°; I= +20.5° (α_{95}= 5.6°; k= 186). As the sampling sites are nearly flat (2-3° tilt) the *in-situ* and bedding-corrected directions are similar and statistically indistinguishable (Fig. 5.7). The mean palaeomagnetic pole corresponding to the listed 5 site-level VGPs is situated at λ= 74.5°S; ϕ= 244.0°E (A_{95}= 4.6°; K= 275).

Site	n	Dg(°)	Ig(°)	Ds(°)	Is(°)	α_{95}(°)	k	P_{Lat}(°S)	P_{Long}(°E)	dp	dm
VAL2	5	199.0	26.9	199.4	26.4	3.6	209.8	69.9	251.2	2.1	3.9
VAL3	5	200.2	18.3	200.5	17.7	6.0	66.3	70.0	238.3	3.2	6.2
VAL4	5	195.7	15.9	196.0	15.4	4.8	102.2	75.0	235.9	2.5	4.9
VAL7	5	192.9	21.5	192.8	23.5	7.0	172.2	77.2	251.1	4.0	7.5
VAL10	5	189.6	17.8	189.6	19.5	4.7	123.4	80.1	245.3	2.6	5.0
Mean	N	Dg(°)	Ig(°)	α_{95}(°)	k	Ds(°)	Is(°)	α_{95}(°)	k	λ(°S) ϕ(°E)	A_{95}(°) K
	5	195.4	20.1	5.6	186	195.7	20.5	5.8	174	74.5 244.2	4.6 275

Tab. 5.4. Site-level palaeomagnetic data from the Pimenteiras Formation. The listed VGPs (P_{lat}/P_{long}) and the mean palaeomagnetic pole position (λ/ϕ) correspond to the *in-situ* directions. See Table 5.2 for headings explanation.

The outcrop of Pimenteiras Formation in Picos (site PIP1-4; Fig. 5.1, Tab. 5.1) is relatively more weathered, comprising purple to reddish finely laminated siltstones and mudstones. Eleven samples from this location demonstrate the presence of two distinct remanences (Fig. 5.6). The low unblocking temperature remanence (A) is generally erased below 500°C. Component A yields a sample-level mean direction of D= 5.8°; I= -24.9° (α_{95}= 14.5°; k= 56). The confidence circle of this direction includes the expected present day dipole field direction in the sampling area. Therefore it is a probable magnetic overprint acquired under the present magnetic field.

The high unblocking remanence (B) yields an overall sample mean direction of D= 196°; I= +10° (α_{95}= 9°; k= 36) *in-situ*. Since the sampling sites are almost horizontal (2-3° tilting), the bedding-corrected mean (D= 196.4°; I= +8.1°; α_{95}= 9.0°) is statistically the same. This remanence is comparable to the stable remanence obtained from some sites VAL (Fig. 5.7).
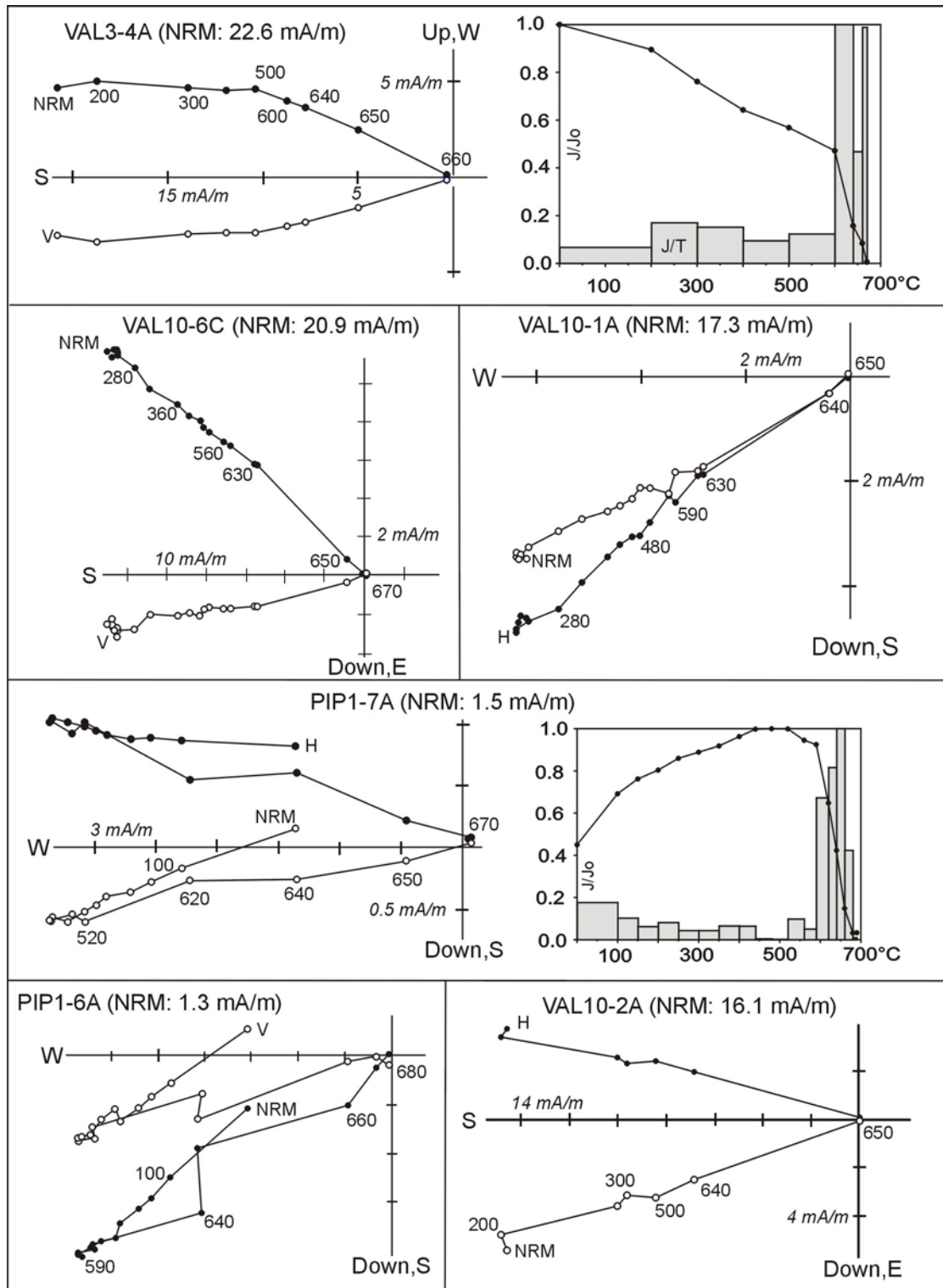
Fig. 5.6. Representative examples of thermal demagnetisation results from the Pimenteiras Formation.
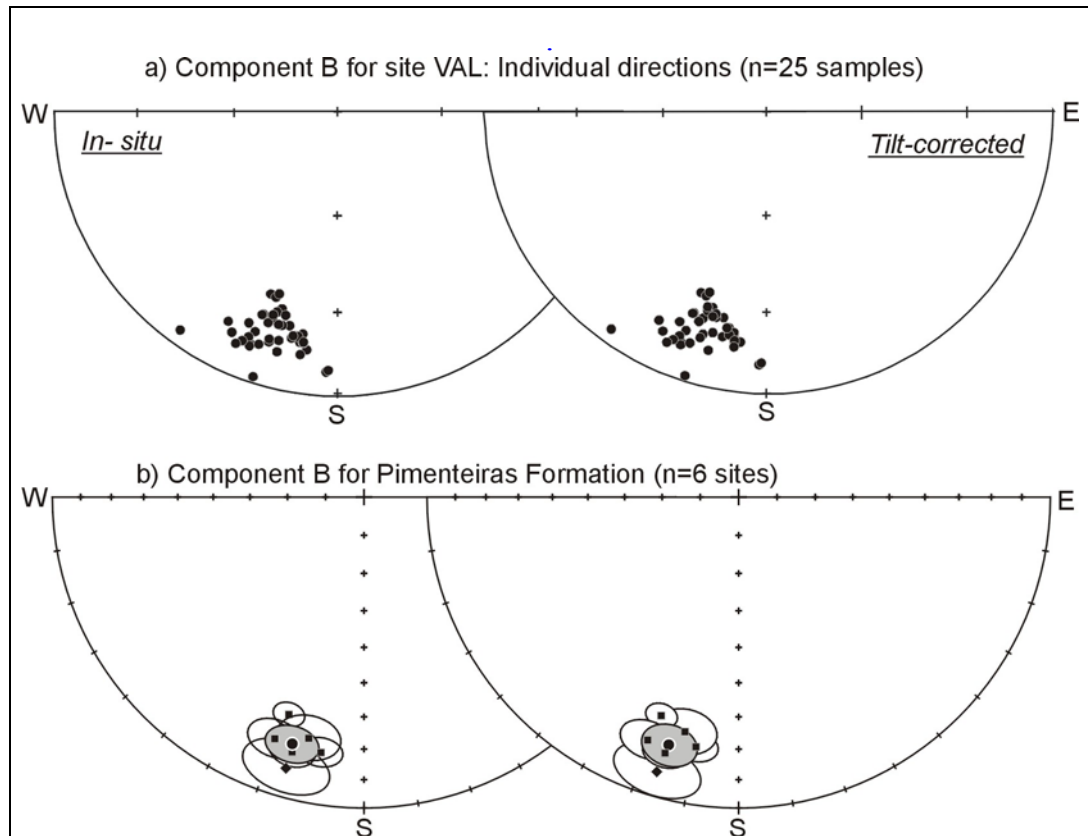
Fig. 5.7. Equal area stereographic projection of the results from Pimenteiras Formation. **a)** Distribution of individual directions for 36 specimens cut from 25 samples. **b)** Site-means (square for sites VAL and diamond for site PIP) and overall mean direction (circle with shaded confidence circle) for the high unblocking temperature component B. The overall site-mean direction (N= 6 sites) is D= 195.6°; I= +18.4° (α_{95}= 5.6°) *in-situ* and D= 195.8°; I= +18.5° (α_{95}= 6.2°) after bedding correction. Sampling details and sampling location are given in Table 5.1 and Figure 5.1, respectively.

The overall mean direction for the two locations (VAL and PIP; N= 6 sites) is D= 195.6°; I= +18.4° (α_{95}= 5.6°; k= 144.5) *in-situ* and D= 195.8°; I= +18.5° (α_{95}= 6.2°; k= 117.3) after bedding correction, and the corresponding palaeomagnetic South Pole is situated at λ= 74.6°S; ϕ= 241°E (A$_{95}$= 4.3°; N= 6). This pole diverges from all Devonian reference poles, suggesting that it may represent a post-Devonian remagnetisation. Comparison with the younger reference poles demonstrates close similarity of this pole with the Early Jurassic reference poles for stable South America reported by Randall (1998) and Gilder *et al.* (2003). The Pimenteiras magnetisation is, therefore, interpreted to be an Early Jurassic overprint. Comparison with the expected directions recalculated from the published South American poles (Fig. 5.8) illustrates that the Pimenteiras remanence is indistinguishable at 95% confidence level from the expected Early Jurassic magnetisation.
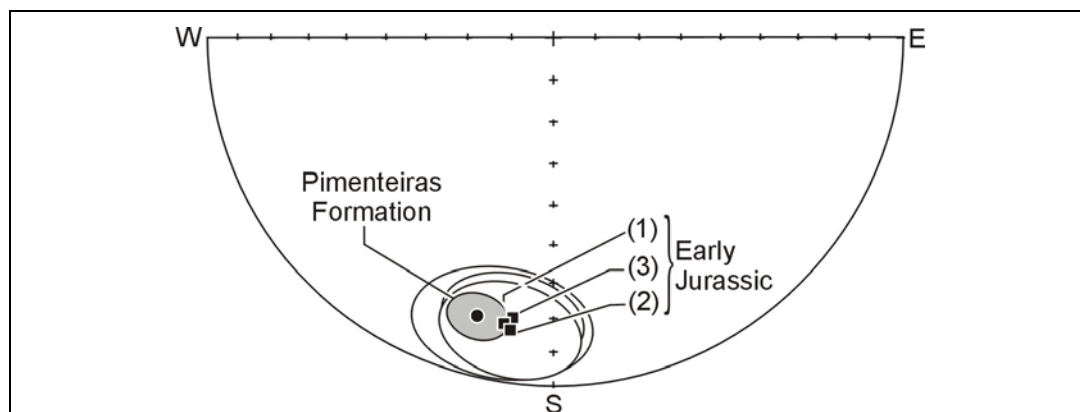
Fig. 5.8. Equal area projection of the overall mean direction from Pimenteiras Formation compared with the expected Early Jurassic directions recalculated from published reference poles for Gondwana. (1) Randall (1998); (2) Mean South America; (3)189±25 Ma, Gilder *et al.* (2003).

5.2.4 Itaim Formation (Early Devonian)

Palaeomagnetic investigations of the siltstone and mudstone units from the Itaim Formation sampled in Serra da Capivara (Fig. 5.1; Tab. 5.1) demonstrate initial NRM intensities ranging between 0.5 mA/m and 10 mA/m. Stepwise thermal demagnetisations of 35 specimens cut from 25 samples were conducted up to 680°C with the purpose of isolating the stable magnetisation. Although demagnetisation results for most samples show erratic directional behaviour, two distinct stable remanences were identified in 16 samples. Palaeomagnetic directions for individual specimens were generally calculated between 400°C and 680°C data points that apparently converge toward the origin on orthogonal projections (Fig. 5.9). The first remanence (A) consists of normal polarity with northerly declination, while the second remanence (B) is of reversed polarity with southerly declination. Unblocking temperatures above 650°C inferred from intensity decay curves suggest that both remanences are mainly carried by haematite.

The A remanence is well defined in only four samples from sites CAP-9 and CAP-10. Directions from these samples yield a mean of D= 358°; I= -22° ($\alpha_{95=}$ 9.7°; k= 91), which is similar to the expected direction of the dipole field (D= 001°; I= -20.5°) at the sampling area. The remanence A is, therefore, a clear present day magnetic overprint.

The reversed polarity remanence B is identified in 12 samples from four sites (Tab. 5.5). This remanence has steeper inclination relative to the remanence A, with an overall mean direction (N= 4 sites) of D= 176.4°; I= +40.4 (α_{95}= 4.1°; k= 495) *in-situ* and D= 176.3°; I= +35.9° (α_{95}= 4.4; k= 436) after bedding correction.
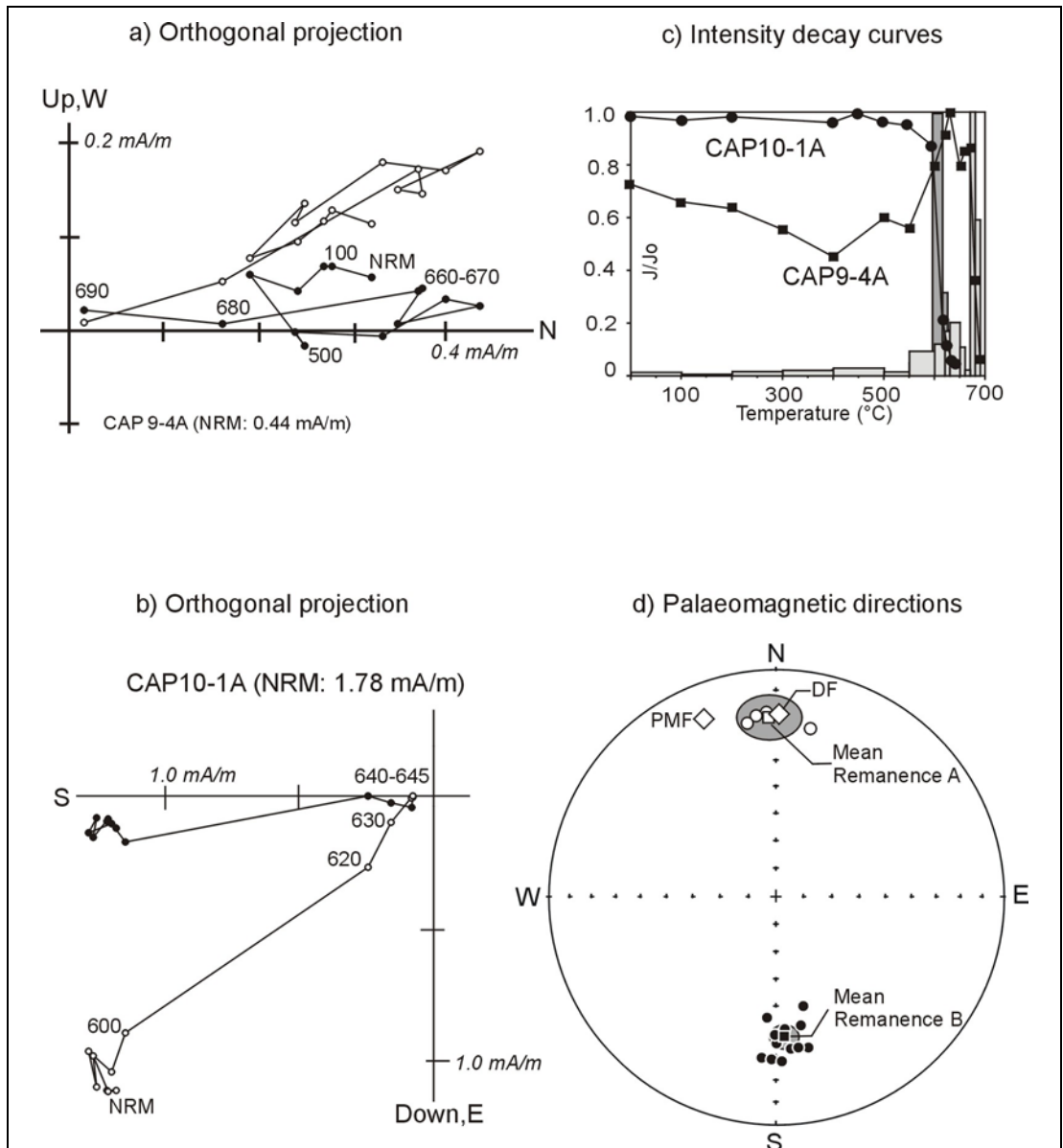
Fig. 5.9. Palaeomagnetic results from the Itaim Formation. **a)** and **b)** Representative orthogonal projections of demagnetisation results in bedding-corrected co-ordinates. **c)** Intensity decay curves during thermal demagnetisation. **d)** Equal area projection of individual sample directions (circle) and the overall mean directions (square with confidence circle) for the isolated remanence A an B. The Expected directions for the present magnetic field (PMF) and the present dipole field (DF) are shown for comparison.

The *in-situ* and bedding-corrected mean directions are indistinguishable within 95% confidence, since the bedding attitudes of all sites are almost similar and the rock unit is only slightly tilting (Tab. 5.5). However, the slight decrease in the directional clustering after bedding correction is a probable indication of the post-folding nature of this remanence. Therefore the *in-situ* direction is considered to be the true B remanence for the Itaim Formation.

| Site	n	Dg(°)	Ig(°)	Ds(°)	Is(°)	α_{95}(°)	k	P_{Lat}(°S)	P_{Long}(°E)	dp	dm
CAP-7	4	173.4	36.3	173.5	31.3	7.9	146	76.4	346.0	7.0	9.2
CAP-8	3	178.7	42.6	178.5	37.6	9.1	754	74.0	321.8	7.0	11.4
CAP-10	3	177.3	43.3	177.5	39.3	13.4	47.7	73.4	326.1	10.2	16.4
CAP-11	3	176.3	39.5	176.1	35.5	8.3	122.1	75.9	331.7	6.0	9.9
Mean	N	Dg(°)	Ig(°)	α_{95}(°)	kg	Ds(°)	Is(°)	α_{95}(°)	ks	λ(°S) ϕ(°E) A_{95}(°)	K
	4	176.4	40.4	4.1	495	176.3	35.9	4.4	436	75.1 330.7 3.4	711

Tab. 5.5. Site-level palaeomagnetic data from the Itaim Formation. The listed VGPs (P_{lat}/P_{long}) and mean palaeomagnetic pole (λ / ϕ), correspond to the *in-situ* mean directions. Notice, however, that the *in-situ* and bedding-corrected mean directions are indistinguishable at the 95% confidence level.

The palaeomagnetic south pole calculated from the 4 site-level VGPs listed in table 5.5 is situated at λ= 75°S; ϕ= 331°E (A_{95}= 3.4°; K= 711) in South American co-ordinates. This pole is similar to the mean Late Permian pole for stable South America, and when transferred in African co-ordinates, it is comparable with the 260 Ma poles for Gondwana reported in Torsvik & Van der Voo (2002) and McElhinny *et al.* (2003; Fig. 5.10). Therefore, the palaeomagnetic data from the Itaim Formation may represent a Late Permian remagnetisation. The fact that this pole deviates from all published Devonian poles for South America and for Gondwana supports the secondary origin of the remanence obtained from the Itaim Formation.
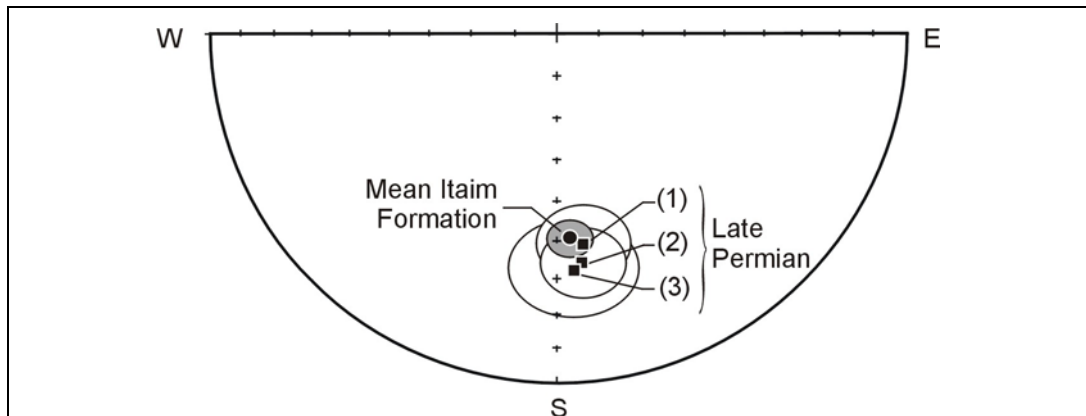
Fig. 5.10. Mean palaeomagnetic data from Itaim Formation compared with the expected direction recalculated from published poles from South America and for Gondwana. Late Permian reference directions are: (1) Mean direction calculated from published South American data. (2) 260 Ma (McElhinny *et al.*, 2003); (3) 260 Ma (Torsvik & Van der Voo, 2002).

5.2.5 Tianguá Formation (Early Silurian)

Magnetic measurements of the silty and medium-grained sandstones samples from Tiangúa show initial NRM intensity of 0.3 mA/m to 20 mA/m. Thermal demagnetisation of individual samples isolated a high unblocking temperature remanence stable up to 690°C (Fig. 5.11). Demagnetisation results of some samples demonstrate the existence of incoherent low unblocking temperature direction removed below 350°C.
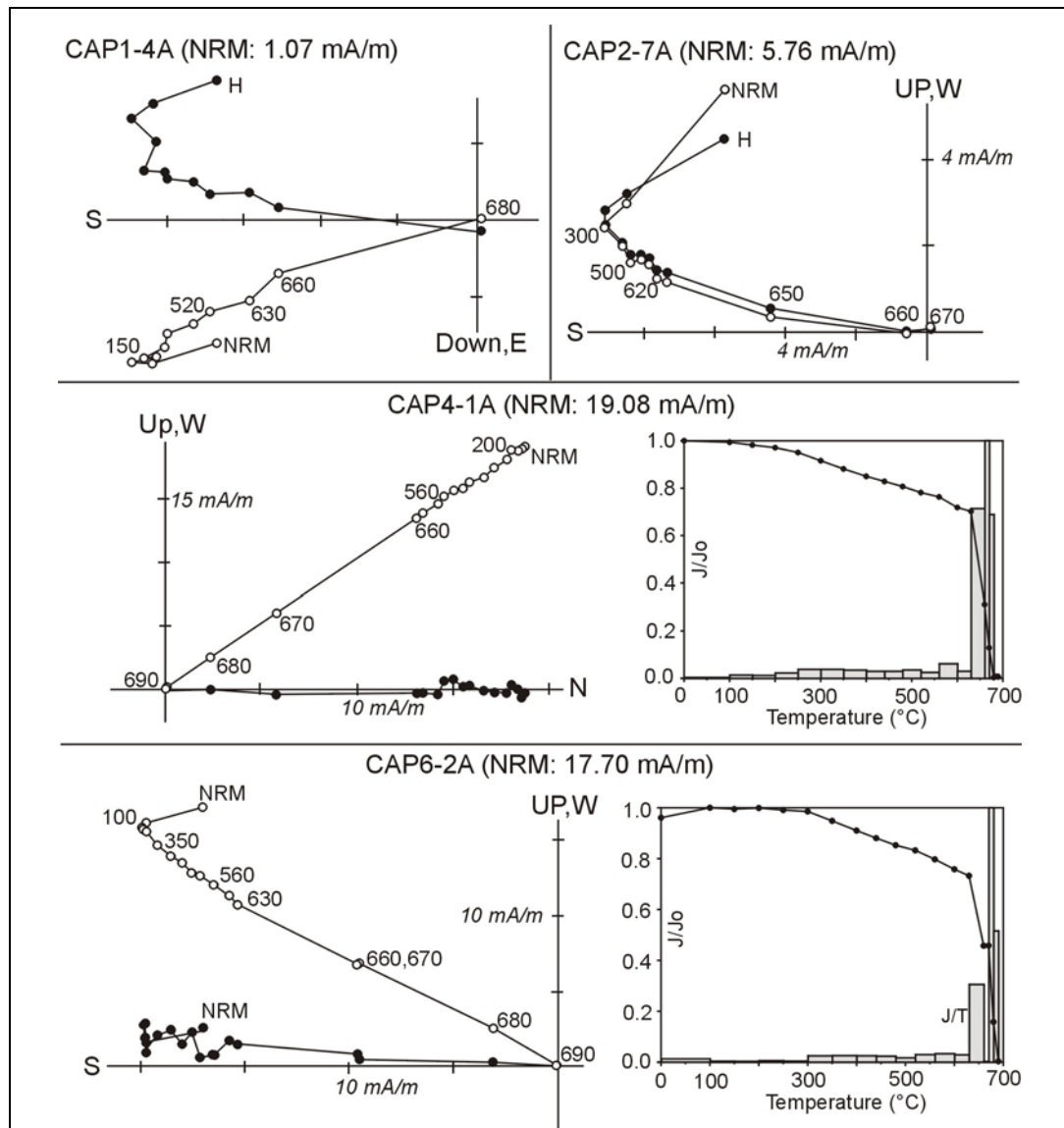
Fig. 5.11. Representative demagnetisation results from the Tiangúa Formation. Orthogonal projection in *in-situ* co-ordinates and Intensity decay curves obtain during stepwise thermal demagnetisation are shown.

The stable remanence is identified in 43 specimens cut from 25 oriented samples. This remanence is of normal polarity in 18 samples and reversed polarity in 5 samples. All directions obtained from the samples drilled in sites CAP3-5 are of normal polarity, whilst, only reversed polarity directions are

present in sites CAP4-6. Samples from sites CAP1 and CAP13-15 are characterised by the presence of dual antipodal magnetisation.

In *in-situ* co-ordinates, the sample-level mean for the normal polarity directions (D= 356.0; I= -35.7; α_{95}= 3.7°; k= 58) and that of the reversed polarity directions (D= 174.0; I= +40.5; α_{95}= 5.8°; k= 80) share a common mean direction within the 95% confidence level. This remanence passes with classification C the reversal test of McFadden & McElhinny (1990). The overall site-level mean (N= 6) is D= 353.0°; I= -36.2° (α_{95}= 6.9°; k= 95) *in-situ*. The directions obtained from Tianguá Formation are tightly grouped in *in-situ* co-ordinates, and dispersed (α_{95}= 24°; k= 14) after bedding correction (Fig. 5.12). This indicates that this remanence is a post-folding secondary magnetisation. The palaeomagnetic south pole corresponding to mean of the six site-level VGPs listed in table 5.6 is located at λ= 77°S; ϕ= 345°E (A_{95}= 6.9; K= 96). This pole is indistinguishable within the 95% confidence level from the Itaim pole (section 7.3.4). Hence, the stable remanence of the Tianguá Formation is also considered an overprint. Comparison with the expected younger direction at the sampling area is (Figure 5.13) suggests that this remanence is probably acquired in Late Permian. This dual polarity overprint, which is mainly carried by haematite with maximum unblocking temperatures above 650°C, is likely a chemical remanent magnetisation (CRM) acquired during rock weathering.

Site	n	Dg(°)	Ig(°)	Ds(°)	Is(°)	α_{95}(°)	k	P_{lat}(°S)	P_{long}(°E)	dp	dm	Dipdir	dip
CAP1	6	350.9	-31.2	349.1	-16.8	10.0	34	78.1	004.3	6.3	11.2	154	15
CAP2*	4(3)	231.2	-36.9	241.1	-38.5	38.1	9.5	-	-	-	-	154	15
CAP3	3	342.4	-30.2	341.5	-15.3	9.7	163	71.3	022.3	6.0	10.8	358	09
CAP4-5	4(1)	354.3	-36.5	353.8	-45.5	6.5	112	77.2	342.4	4.4	7.6	358	09
CAP6	4	7.0	-44.1	11.0	-50.9	4.6	97.5	71.7	297.1	3.6	5.8	136	07
CAP13	4	174.0	33.5	171.6	+27.9	5.1	144	78.8	348.3	3.3	5.8	136	07
CAP14-15	3(1)	173.6	40.6	170.4	+35.3	7.7	56.3	74.3	339.8	5.6	9.3	136	07
Mean	Dg(°)	Ig(°)	α_{95}(°)	kg	Ds(°)	Is(°)	α_{95}(°)	ks	λ(°S)	ϕ(°E)	A_{95}(°)	K		
N=6	353.2	-36.2	6.9	95	351.7	-32.2	24.1	13.9	76.9	345.3	6.9	96.0		

Tab. 5.6. Site mean palaeomagnetic data from the Tianguá Formation. n: number of samples. The number of samples from which the stable directions are calculated from remagnetisation plane (great circles) are shown between brackets. *Incoherent directions from site CAP2 are excluded.
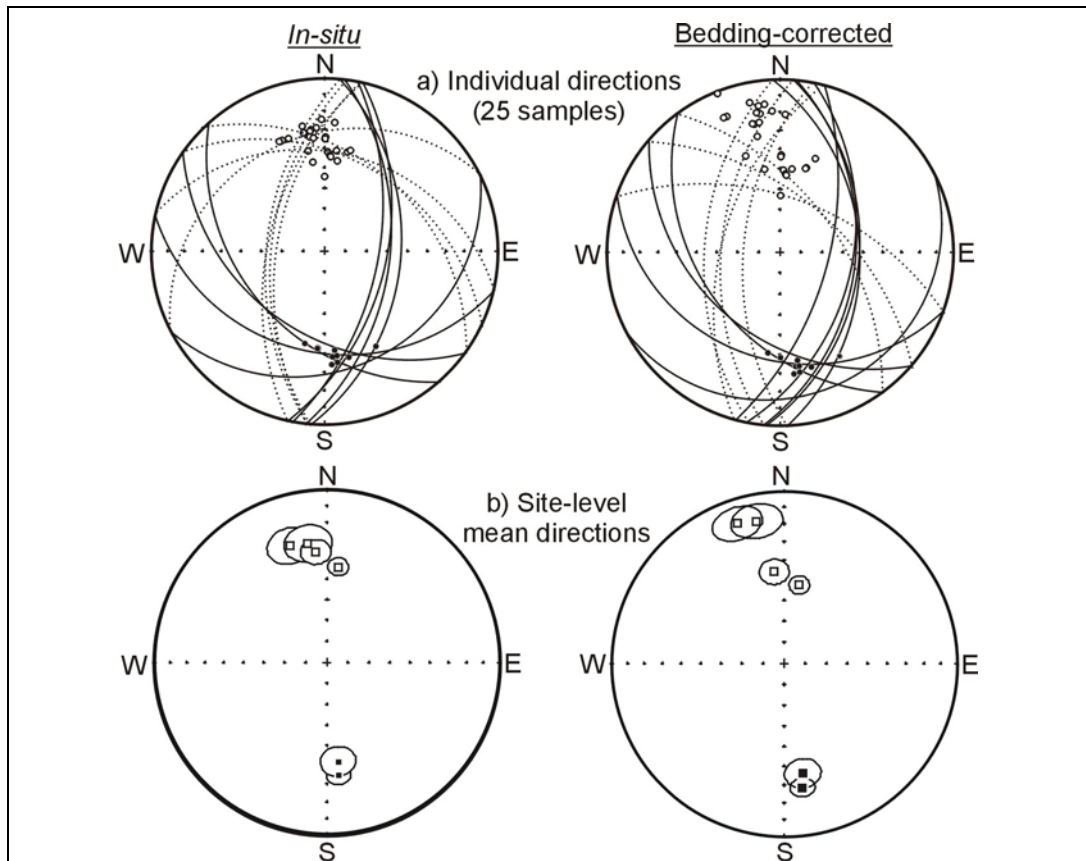
Fig. 5.12. Equal area projections of the stable remanence from the Tiangúa Formation. **a)** Individual directions from 43 specimens (25 samples) in *in-situ* and bedding-corrected co-ordinates. **b)** Site mean directions. Note that mean directions for the normal and reversed polarity magnetisations are antipodal in *in-situ* co-ordinates. Directional scattering after bedding-correction, indicating the post-folding nature of this remanence, is obvious in both sample and site levels.
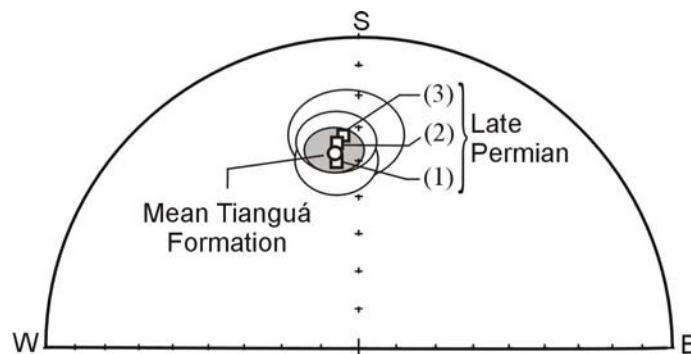
Fig. 5.13. Mean palaeomagnetic direction from Tianguá Formation compared with the published Late Permian reference directions recalculated from South American and Gondwanan published poles. Late Permian directions are: (1) Mean direction calculated from published South American data. (2) 260 Ma (McElhinny *et al.*, 2003); (3) 260 Ma (Torsvik & Van der Voo, 2002).

5.3   Summary and conclusion

The present investigations demonstrate that none of the stable remanences in the Palaeozoic sediments within the Parnaíba Basin is of primary origin. The stable remanences in these rocks are considered as being acquired in Early Cretaceous, Early Jurassic, and Late Permian times (Fig. 5.14; Tab. 5.7). The palaeomagnetic south pole position derived from the Piauí Formation is similar to the Early Cretaceous reference pole for South American and that of the overlying Sardinha Formation (120-130 Ma; section 4.3) and an Early Cretaceous age is, therefore, attributed to the stable remanence in this unit.

Secondary remanences from the Early Permian Pedra de Fogo Formation and the Early Devonian Pimenteiras Formation are probably acquired in Early Jurassic. On the other hand, the magnetic directions derived from the Devonian (Itaim Formation) and Silurian (Tianguá Formation) units in the Serra da Capivara likely represent Late Permian remagnetisations. Both the Early Jurassic and the Late Permian remagnetisations are dominantly carried by haematite, and are likely of chemical origin (CRM) related to intense weathering.

Formation	Age	Sites	$\lambda(°S)$	$\phi(°E)$	$A_{95}(°)$	N	Polarity	Age of remanence
Pedra de Fogo	Cu	TER	59	268	4.9	6	R	Lower Jurassic
Piauí	Cl	FLP	86	117	2.5	5	R	Lower Cretaceous
Pimenteiras	Dl	VAL/PIP	74.6	241	4.3	6	R	Lower Jurassic
Itaim	Dl	CAP	75.0	331	3.4	4	R	Upper Permian
Tianguá	Su	CAP	77.0	345	6.9	6	M	Upper Permian
Ipu	Sl	SRI	74	4.0	4.5	1	R	Upper Permian

Tab. 5.7. Summary of the palaeomagnetic results from the Parnaíba Basin. Age of rock units are: Cu: Upper Carboniferous; Cl: Lower Carboniferous; Dl: Lower Devonian; Su: Upper Silurian; Sl: Lower Silurian. $\lambda(°S)$ and $\phi(°E)$ are latitude and longitude position of the palaeomagnetic south pole in degrees south and east, respectively. A_{95} is the confidence circle about pole. N designates the number of site-level VGPs used when calculating mean palaeomagnetic pole. Polarities are: R: reversed (positive inclination); M: mixed (both positive and negative inclination). Probable acquisition times of remagnetisation (age of remanence) are given.
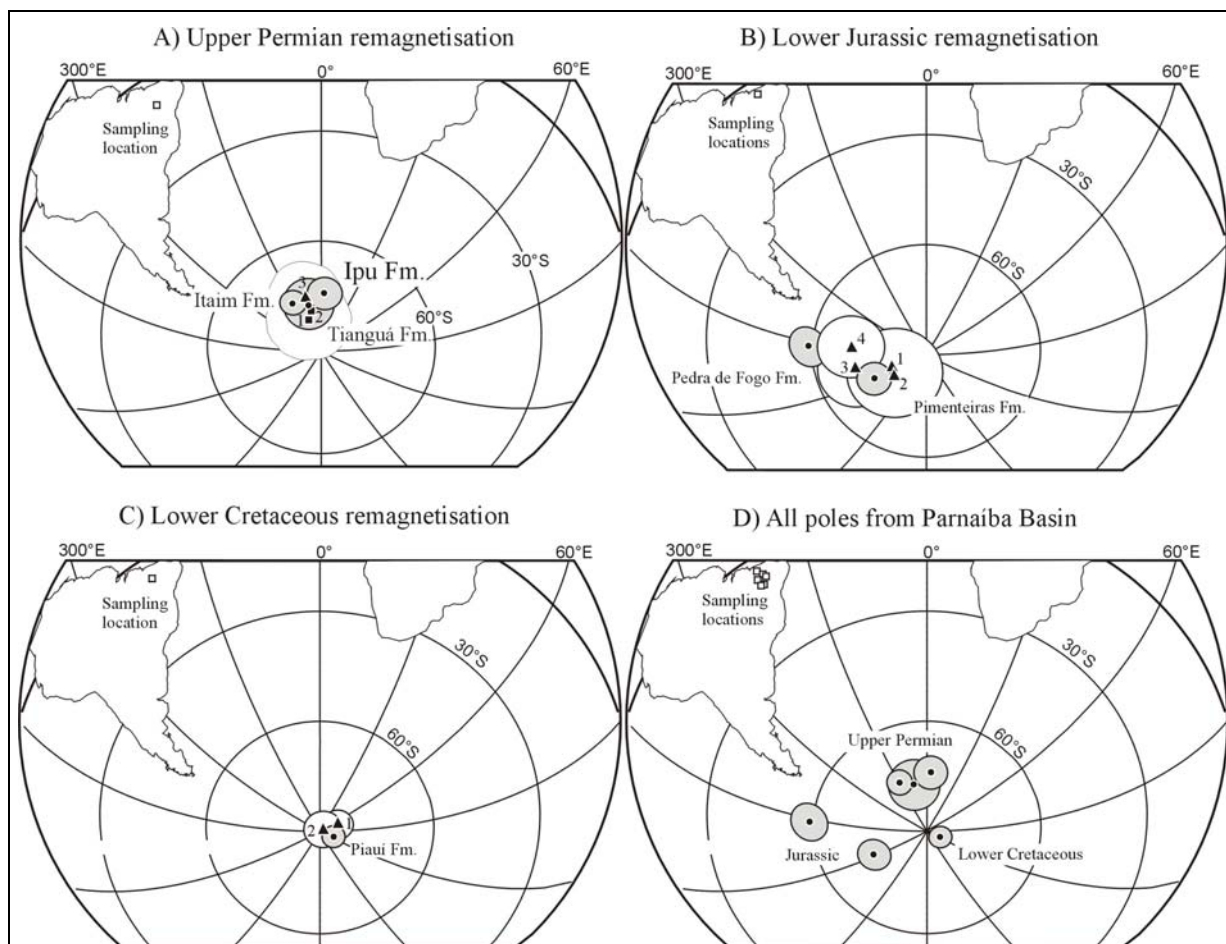
Fig. 5.14. Equal area projection of the palaeomagnetic poles from Parnaíba Basin compared with the published reference poles for stable South America (triangle) and Gondwana (square). Reference poles are: **A)** <u>Late Permian</u>: 1: Torsvik & Van der Voo (2002; 260 Ma); 2: McElhinny *et al.* (2003; 260 Ma). 3: Mean South American poles. **B)** <u>Early Jurassic</u>: 1: Randall (1998); 2: Gilder *et al.* (2003); 3: Van der Voo (1993). 4: Beck (1998). **C)** <u>Late Cretaceous</u>: 1: Randall (1998); 2: Beck (1998). The presented palaeomagnetic results demonstrate widespread Late Permian to Early Cretaceous remagnetisation of the Palaeozoic sedimentary rocks in NE Brazil.

Chapter 6

Permian-Triassic palaeomagnetic data from southern Peru: implication for Pangaea reconstructions

---

6.1   Introduction

The Pangaean supercontinent, which existed throughout Permian and Triassic times, developed as a result of the amalgamation of Gondwana with Laurasia, Siberia, and other smaller continental fragments. The geometry of this supercontinent, however, remains a matter of discussion, as the palaeogeographic reconstructions based on published Permian-Triassic palaeomagnetic data disagree with the Jurassic Pangaea configuration proposed by Bullard *et al.* (1965), referred to as Pangaea A. The Pangaea A configuration, in which South America and Africa (Gondwana), are placed facing North America and Europe (Laurentia) respectively, is a well-accepted starting point of break-up of the supercontinent during Early Jurassic times (ca.180 Ma), and the subsequent opening of the Atlantic Ocean. However, for Permian-Triassic times palaeomagnetic data from Laurussia and Gondwana provide misfits and large continental overlaps when adopting this reconstruction.

Alternative reconstructions for the Permian-Triassic Pangaea, such as the Pangaea B (Morel & Irving, 1981), and Pangaea C (Smith et al., 1981) have been proposed to overcome this problem. In these models, Gondwana is placed farther to the east, with South America facing Europe and Africa facing Eurasia to avoid continental overlap. Pangaea B and C reconstructions provide a better match for the published palaeomagnetic data, but they are not supported geologically as Gondwana's position relative to Laurussia implies a large east-west relative translation between the two supercontinents during the Triassic, to end up with the Jurassic Pangaea A.

However, the mismatch of the palaeomagnetic data in Pangaea A configuration has been considered by some authors (*e.g.* Van der Voo, 1993; Rochette & Vandamme, 2001) to be the result of the poor quality of the existing palaeomagnetic dataset from Gondwana and/or inclination

shallowing in sediments. Alternatively, Van der Voo & Torsvik (2001) and Torsvik & Van der Voo (2002) suggested that this mismatch is the results of significant contributions of non-dipole components of the Earth's geocentric dipole field in Late Palaeozoic-Mesozoic times. On the other hand, some authors argue that high quality data from Gondwana are trustworthy and Pangaea actually evolved from B to A configuration during the Late Permian (Muttoni *et al.*, 2003).

Therefore, additional reliable palaeomagnetic data from Gondwana is required to resolve the Pangaea problem. The reliability of previously published Permian-Triassic published data from South America is, however, questioned. This is because older palaeomagnetic studies do not satisfy many criteria required by modern standard palaeomagnetic investigation. Furthermore, the majority of them do not fulfil the three most important criteria of Van der Voo (1990), including well-determined age constraints, sufficient number of samples, and adequate demagnetisation and/or positive field test.

Palaeomagnetic investigations of well-dated Early Triassic and Early Permian rock units in southern Peru were carried out in an effort to contribute high-quality data to this contest, and data obtained from the volcanic rocks of the Mitu Group and from the carbonate sequence of the Copacabana Group are discussed in this chapter. The results presented are obtained from the investigation of 83 oriented core-samples drilled in 16 sites (Tab. 6.1).

Rock Unit	Age (Ma)	Location	Site	S_{lat}(°S)	S_{long}(°E)	N	n
Mitu Group	238-250[1]	Altiplano	SPV1-3	14.64	289.24	3	17
Mitu Group		Altiplano	SPV4-5	14.48	288.99	2	10
Copacabana Group	290-270[2]	Subandean Zone	MCO	12.23	287.18	11	56

Tab. 6.1. Sampling details for the Early Triassic and Early Permian rock units in southern Peru. S_{lat}(°S)/ S_{long}(°E) are geographic coordinates of the sampling location. N/n. number of sampling sites/drill cores. [1] Age based on K/Ar (Latorre & Oros; 2000). [2] Age based on palynology (De la Cruz, 1998).

6.2 Mitu Group (Early Triassic; Altiplano)

6.2.1 Sampling

Samples from the Mitu Group were collected in the northern Altiplano, in the area south of Cuzco (Fig. 6.1). The Mitu Group is a continental volcano-sedimentary rift sequence deposited during the early stage of Pangaea break-up (section 2.3.2). The Group is largely composed of volcanic units and molassic sediments derived from intense erosion of a structurally elevated

area formed during the Hercynian deformation (Jaillard *et al.*, 2000). A Late Permian-Early Triassic age has been assigned to the Mitu Group based on radiometric ages reported by Kontak *et al.* (1985) and Palacios *et al.* (1993). More recently, a K/Ar age of 244±6 Ma was determined for the volcanic units exposed in the sampling area (near Santa Rosa; Latorre & Oros ; 2000).
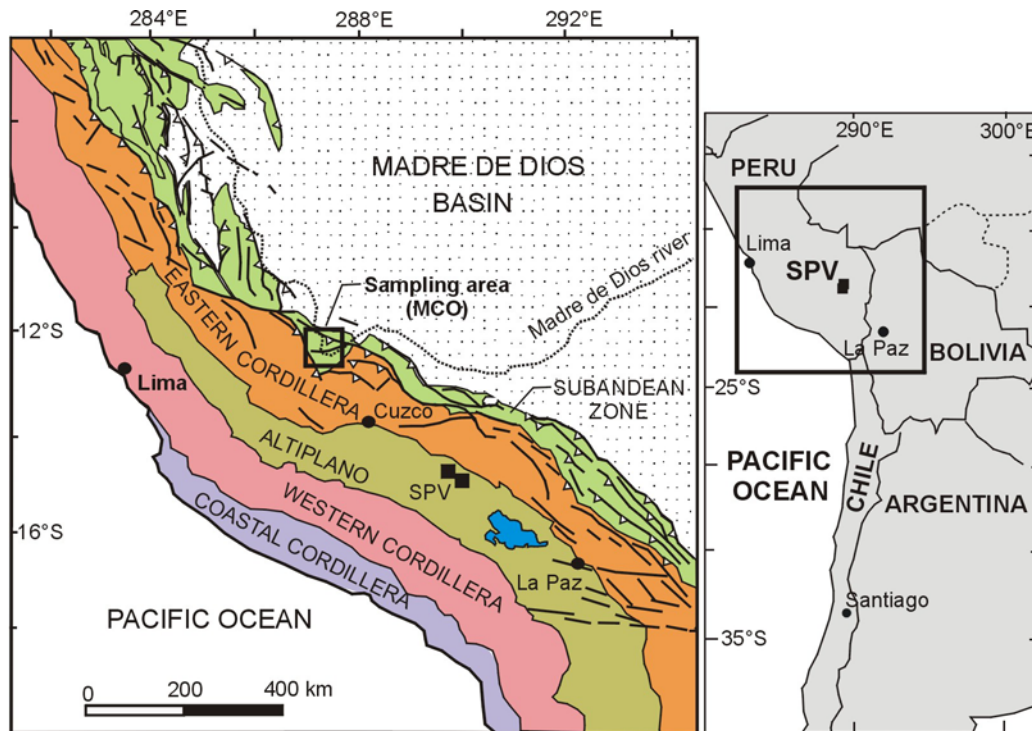
Fig. 6.1. Simplified structural map showing different morpho-structural units in the Peruvian–Bolivian Andes and the sampling location for the Early Triassic volcanics of the Mitu Group (SPV) and the Early Permian Copacabana Group. Box in location map (inset) represents sampling area.

Sampling was carried out in two locations situated 30 km apart in the southern Peruvian Altiplano. Although the volcanic units of the Mitu Group are widely exposed in this area, outcrop selection was dictated by the existence of palaeohorizontal control. Altogether, 27 cores were collected from the volcanic units composed of grey to brown or violet porphyritic andesite. Sampling in the area near the village of Santa Rosa (14.64°S; 289.24°E) was carried out in an approximately 10 m thick, well-bedded volcanic sequence dipping towards the southwest. Seventeen separately oriented samples were collected from three horizons, considered as palaeomagnetic sites (SPV1, SPV2 and SPV3). Orientations of the sampled beds were determined by standard methods using a magnetic compass. The exposure at the second sampling location (14.48°S; 288.99°E) consists of massive volcanic lava conformably overlain by Cretaceous sandstones. Ten samples, gathered in two palaeomagnetic sites (SPV4 and SPV5), were collected in this location. The palaeohorizontal was determined from the bedding attitude of the conformably overlying Cretaceous sediments.

6.2.2   Results

Samples from sites SPV1, SPV2 and SPV3 have initial NRM intensities ranging between 18 mA/m to 150 mA/m. Lower intensities (1.5 to 8 mA/m) were observed for the samples from sites SPV4 and SPV5. Most of the samples were totally demagnetised at 700°C. Some samples, however, maintain approximately 5% of the initial NRM after final demagnetisation step. Decay of remanence intensity during demagnetisation of the samples from all sites demonstrate unblocking temperatures generally above 660°C, frequently with large intensity break between 500°C and 580°C demagnetisation steps, suggesting contribution of both haematite and magnetite as remanence carriers. There is no change in magnetic direction during demagnetisation steps over the unblocking temperature of magnetite (Fig. 6.2c), suggesting that magnetite and haematite carry identical stable remanences (B).

Demagnetisation of samples from sites SPV4 and SPV5 revealed two magnetic directions. The first direction, which is identified in 13 core samples, has intermediate unblocking temperature and was calculated from linear trend of demagnetisation data points below 560°C, which do not converge towards the origin in orthogonal projection (Fig. 6.2b,e). This magnetic direction (A) is exclusively of reverse polarity with south-southwest declination and intermediate inclination. The overall sample-mean direction is D= 182.7°; I= 41.3° *in-situ* and D= 197.1°; I= 23.8° after bedding correction (n= 10 samples; α_{95}= 10.5°; k= 22.1). When compared to expected Mesozoic and younger directions at the sampling location, the *in-sit*u direction is statistically similar to the expected 24-66 Ma reference path (Randall, 1998; Fig. 6.3a), while the bedding-corrected direction deviates from all references. The A-remanence is, therefore, presumed to be a post-folding overprint magnetisation probably acquired in Palaeocene-Oligocene times.

The high unblocking temperature remanence (B) is generally identified between 500°C and 700°C. This direction is well defined by demagnetisation data directed towards the origin in orthogonal projection (Fig. 6.2). Individual directions were identified in 39 specimens cut from 24 core samples with individual directions calculated from linear demagnetisation data points trending towards the origin in orthogonal projection. Great circles method was used to calculate individual directions for three samples in which A and B directions overlap.
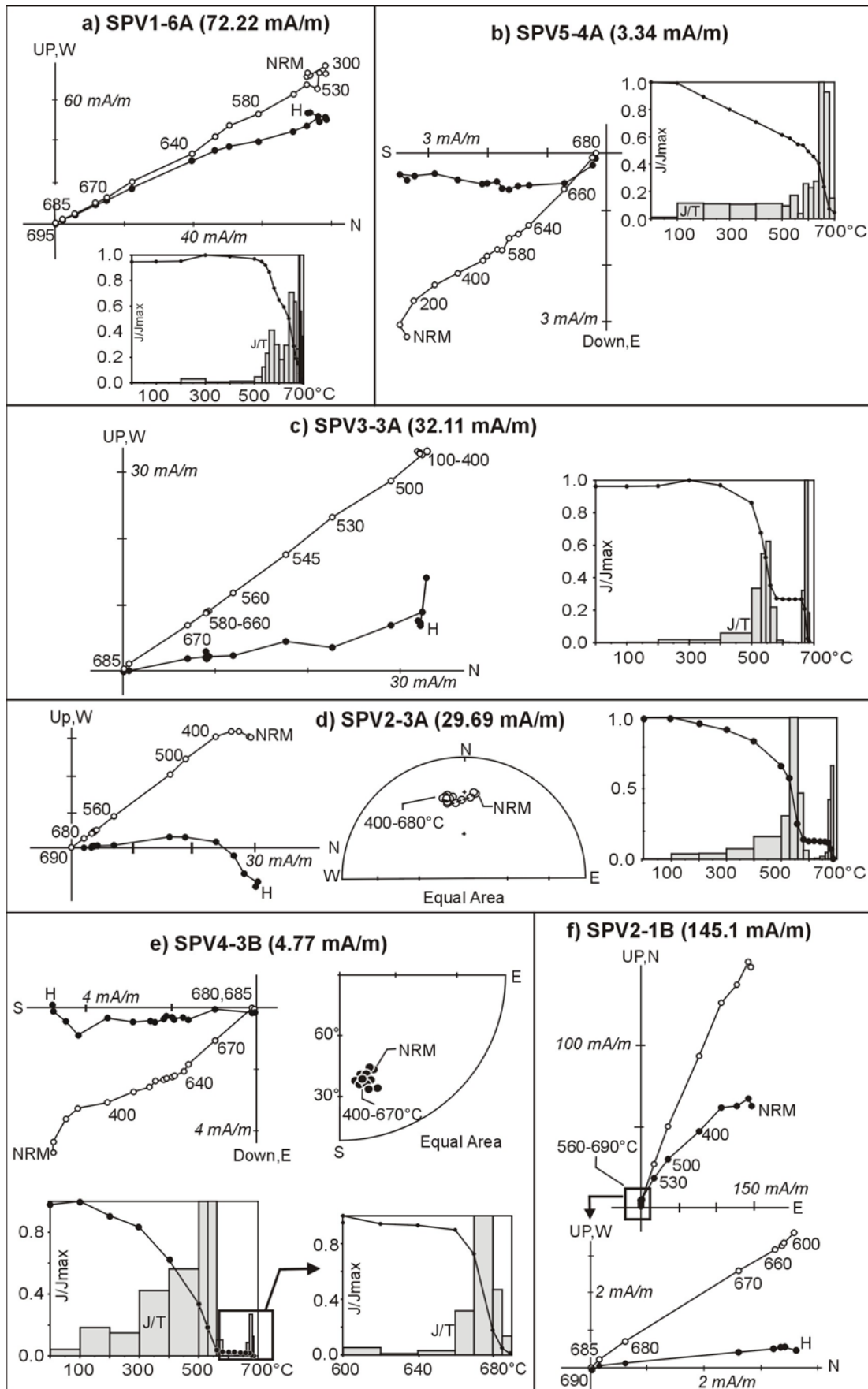
Fig. 6.2. Representative examples of thermal demagnetisation results from the Mitu

Fig. 6.2 *(cont.)* Group. Orthogonal projection and intensity decay curves of samples from sites SPV1 to SPV5 are shown with typical examples of equal area projection (samples SPV2-3 and SPV2-3). Numbers adjacent to data points indicate demagnetisation steps in degrees. In orthogonal projections, closed/open circles are projection onto horizontal/vertical plane. Initial NRM intensities are given adjacent to the projections. X and Y-axes of the intensity decay curves correspond to the demagnetisation step (temperature in °C) and the ratio J/Jmax, respectively. Decay of the NRM intensity during demagnetisation is shown in solid line. Boxes represent the intensity removed after each step. Sample names (e.g. SPV1-6A) include site number (1), core number (6) and specimen number (A). All results are shown in bedding-corrected co-ordinates.

The stable high unblocking temperature remanence (B) is identified in all 5 sites and with dual polarity (Fig. 6.3). Sample directions from sites SPV4 and SPV5 are clustered in a south-southeast declination and intermediate positive inclination, yielding an overall sample-mean D= 150.5°; I= 35.8° (α_{95}= 4.5; k= 118.4) *in-situ* and D= 169.5°; I= 31.8° (α_{95}= 4.5; k= 118.4) after bedding correction. The remanence from sites SPV1-3 is of normal polarity and characterised by a moderate negative inclination with westerly declination *in-situ*, and a northerly declination with moderate negative inclination in bedding-corrected co-ordinates. The mean directions for these three sites is D= 286.1°; I= -46.1° (α_{95}= 12.8°; k= 94.3) *in-situ* and D= 349.3°; I= -36.9°; α_{95}= 6.9°; k= 429.1) after bedding correction. The B remanence isolated in the Mitu Group is statistically different from direction A at the 95% confidence interval.

Altogether, the *in-situ* means for the normal and reversed polarity directions are not antipodal, yielding an overall mean direction with large uncertainty (D= 304.9°; I= -44.4°; α_{95}= 18.7; k= 17.7; N= 5). Directional grouping increases significantly following bedding correction, providing a positive fold test (McElhinny, 1964) significant at the 99% confidence level (N= 5; k-ratio= 19.85). The samples yield a bedding-corrected mean direction of D= 349.3°; I= -35.3° (α_{95}= 4.1°; k= 351.4) and a positive reversal test with classification B (McFadden & McElhinny, 1990), with observed angular deviation (γ_o) equal to 3.7°, a critical angular deviation (γ_c) equal to 9.0°. The overall mean palaeosouth pole calculated from site level VGPs (N= 5; Tab. 6.2) is located at λ= 78.6°S; φ= 351.2°E (A_{95}= 3.7°, K= 447) and λ= 44.2°S; ϕ= 69.1°E when rotated into South African co-ordinates according to the reconstruction parameters of Lottes & Rowley (1990).
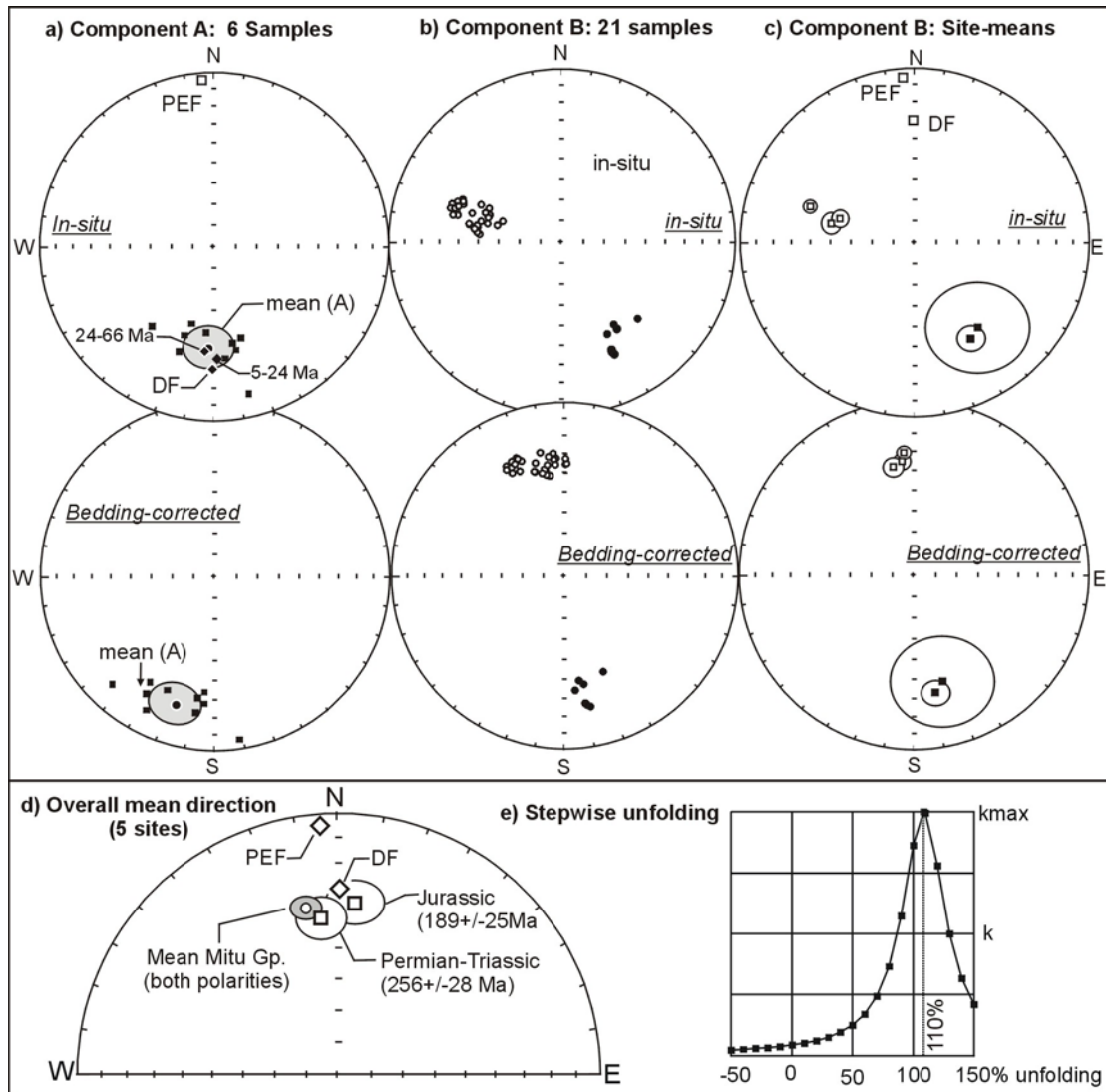
Fig. 6.3. Equal area projection of the palaeomagnetic data from the Mitu Volcanics. **a)** Distribution of the low unblocking temperature direction (A) from sites SPV4 and SPV5 in *in-situ* and in bedding-corrected co-ordinates. **b)** Distribution of individual B remanences from 36 specimens (21 samples) in *in-situ* and bedding-corrected co-ordinates. **c)** *in-situ* and bedding-corrected site mean directions along with the corresponding circles of confidences. **d)** Mean direction (both normal and reversed polarities) compared with the expected Permian-Triassic direction (P-T; 256±28 Ma; Gilder *et al.*, 2003) at the sampling location (S_{lat}= 14.5°; S_{long}= 289°E). **e)** Variation of the precision parameter k during stepwise unfolding. The stable remanence (B) from Mitu volcanic passes the fold test of McElhinny (1964) and the reversal test of McFadden & McElhinny (1990).

a) Mean directions for remanence B

Sample	Dg(°)	Ig(°)	Dg(°)	Is(°)	MAD(°)	P_{lat} (°S)	P_{long} (°E)	dp	dm
SPV4-1	190.6	52.2	207.9	31.2	8.5	69.3	263.1	8.0	11.7
SPV4-2	198.1	45.4	210.1	22.9	2.3	69.0	238.4	1.9	2.9
SPV4-3	190.4	43.3	203.6	23.3	1.7	75.5	248.4	1.3	2.1
SPV4-4	187.3	38.9	199.5	20.2	1.3	79.8	247.3	0.9	1.5
SPV5-2	217.6	41.5	223.3	15.4	4.9	53.4	289.0	3.7	6.0
SPV5-3	198.3	36.4	206.9	14.5	5.8	71.6	219.8	3.9	6.8
Mean (n=6)	Dg(°)	Ig(°)	Ds(°)	Is(°)	α_{95}(°)	k	P_{lat}(°S)	P_{long}(°E)	A_{95}(°) K
	197.2	43.4	208.6	21.4	8.1	69	70.6	235.5	6.3 10.1

b) Mean directions for remanence B

Site	S_{lat}(°S)	S_{long}(°E)	n	Dg(°)	Ig(°)	Ds(°)	Is(°)	α_{95}(°)	k	P_{lat}(°S)	P_{long}(°E)	dp	dm	DipDir	Dip
SPV1	14.64	289.24	5	288.3	-36.9	345.3	-40.2	1.8	676	73.9	346.3	1.3	2.1	230	62
SPV2	14.64	289.24	6	286.7	-52.4	353.4	-34.0	3.0	235	82.5	346.2	2.0	3.4	217	62
SPV3	14.64	289.24	5	282.8	-48.8	348.8	-36.3	4.8	161	77.9	350.4	3.2	5.6	217	62
SPV4	14.48	288.99	3	153.0	36.5	171.9	31.2	8.2	123	81.8	0.9	5.1	9.1	242	28
SPV5	14.48	288.99	3	146.1	36.8	166.7	34.6	14.6	72	76.5	357.5	9.6	16.8	242	28
Mean directions			N	Dg(°)	Ig(°)	α_{95}(°)	kg	Ds(°)	Is(°)	α_{95}(°)	ks	λ(°S)	ϕ(°E)	A_{95}	K
Normal Polarity			3	286.1	-46.1	12.8	94.3	349.3	-36.9	6.9	322.5	-	-	-	-
Reversed polarity			2	149.6	36.7	12.1	427.5	169.4	32.9	12.1	429.1	-	-	-	-
Overall mean			5	304.9	-44.4	18.7	17.7	349.3	-35.3	4.1	351.4	78.6	351.9	3.7	447

Tab. 6.2. Palaeomagnetic results from the Mitu Group. Heading explanation are as follows: S_{lat}/S_{long}: latitude and longitude of the sampling site in degrees south and east, respectively; n: number of samples; Dg°/Ig°: declination/inclination of the magnetic remanence in *in-situ* (geographic) co-ordinates. Ds°/Is°: declination/inclination in bedding-corrected (stratigraphic) co-ordinates; α_{95}: calculated radius of cone of 95% confidence about the mean direction (Fisher, 1953); k: Fisher (1953) precision parameter; P_{lat}(°S)/P_{long}(°E): latitude/longitude of VGP corresponding to the bedding-corrected site mean directions, dp/dm: semi-axes of the oval of 95% confidence about VGP. Dir/Dip: dip direction/dip of bedding plane; kg/ks: precision parameter k for the *in-situ*/bedding-corrected site mean direction; λ (in degrees south) and ϕ (in degrees east): latitude and longitude of the mean palaeosouth pole calculated from site level VGPs. The overall mean pole rotated in African co-ordinates is λ=44.2°S; ϕ=69.1°E.

6.2.3 Interpretation

The component A (D= 182.7°; I= 41.3°; α_{95}= 10.5°; k= 22.1; n= 10 samples) is interpreted as a post-folding remagnetisation. Comparison with the expected Triassic and younger directions at the sampling location (Lat= 14.5°S; Long= 289°E) show that remanence A is very similar to the expected Paleocene-Oligocene (24-66 Ma; Randall, 1998) direction (D= 184°; I= 41°). Although the large confidence circle for component A also include the expected Oligocene-Miocene (5-24 Ma; Randall, 1998) reference direction for stable South America, the observed inclination is 6° steeper than the recalculated Oligocene-Miocene direction (D= 178°; I= 35°). This remanence is also significantly different from the expected present geocentric axial dipolar field (D= 360°; I= -30°) and the present day field (D= 357°; I= -4°) in southern Peru. Therefore the component A from Mitu Volcanics is interpreted as being acquired in Paleocene-Oligocene times. This component yields a palaeopole situated at λ= 80.4°S; ϕ= 273.0°E (dm= 7.8°; dp= 12.8°).

The high unblocking temperature remanence (B) from Mitu Volcanics passes the fold test and the reversal test and, therefore, was acquired prior to the folding of the unit during the Cenozoic deformation of the Andes. The corresponding palaeosouth pole (λ= 78.6°S; ϕ= 351.9°E; A_{95}= 3.7°, South American co-ordinates) is comparable with the previously published data from stable South America with quality index Q≥3 (Fig. 6.4; Tab. 6.3). The Mitu Volcanics (MV) pole also falls within the 95% confidence circle of the Early Triassic (235±14 Ma) and Permian-Triassic (256±28 Ma) mean pole for stable South America reported in Gilder *et al.* (2003). The agreement of the palaeomagnetic data from Mitu Volcanics with these reference poles suggests that the sampling location did not experience significant rotation since, at least, the Early Triassic. This finding is incompatible with the Late Permian to Early Jurassic palaeomagnetic data reported in Gilder *et al.* (2003), which indicate systematic post-Oligocene anticlockwise rotation in the sampling area. For this reason, an examination of both the component A (Palaeocene-Oligocene) and component B (Early Triassic) directions from the Mitu Volcanics was made. Accordingly, although assuming an anticlockwise a rotation of 20° brings the component B direction at close to the expected Early Jurassic direction for stable South America, this rotation results in departure of the Palaeocene-Oligocene magnetisation (component A) away from all post-Triassic reference directions. Thus, a post-Oligocene rotation is irrational when considering the whole palaeomagnetic data from the Mitu Volcanics. This is an indication of the magnetic stability and reliability of directions obtained from the Mitu Group.

	Rock unit	Age (Ma)	λ_{am}(°S)	ϕ_{am}(°E)	λ_{af}(°S)	ϕ_{af} (°E)	α_{95}°	Tests	Ref.
AR	Amana Redbeds	235-245	83.0	317.0	48.3	069.1	12.0	-	(1)
HF	Horcajo Formation	235-256	72.4	264.8	59.2	053.2	12.0	-	(2)
MG	Mitu Group, Peru	242-256	71.4	303.6	47.5	051.3	5.7	F+ R+	(3)
MV	Mitu Group, Volcanics	242-256	78.5	351.2	41.5	068.6	3.7	F+ R+	(4)
QA	Quebrada Alumbera	241-256	67.0	290.0	50.9	042.9	10.0	-	(5)
CM	Choique Mahuida Formation	250-270	75.0	344.0	39.8	064.0	10.0	-	(6)
	Mean Permian-Triassic	235-270	76.5	306.2	48.3	058.9	8.3	K=66.0	

Tab. 6.3. Late Permian-Early Triassic palaeomagnetic data from South America with quality index Q≥3 and good age constrain. λ_{am}(°S)/ϕ_{am}(°S): pole position in South American co-ordinates. λ_{af}(°S)/ϕ_{af}(°S): position of pole in African co-ordinates following the reconstruction parameters of Lawer & Scotese (1987). References are: (1) Valencio *et al.* (1977); (2) Rapalini & Vilas (1991); (3) Gilder *et al.* (2003); (4) This study; (5) Valencio & Vilas (1985); (6) Conti & Rapalini (1990). The mean pole in African co-ordinates is located at λ=48.3°S; φ=058.9°E. F+: positive fold test; R+: Positive reversal test.
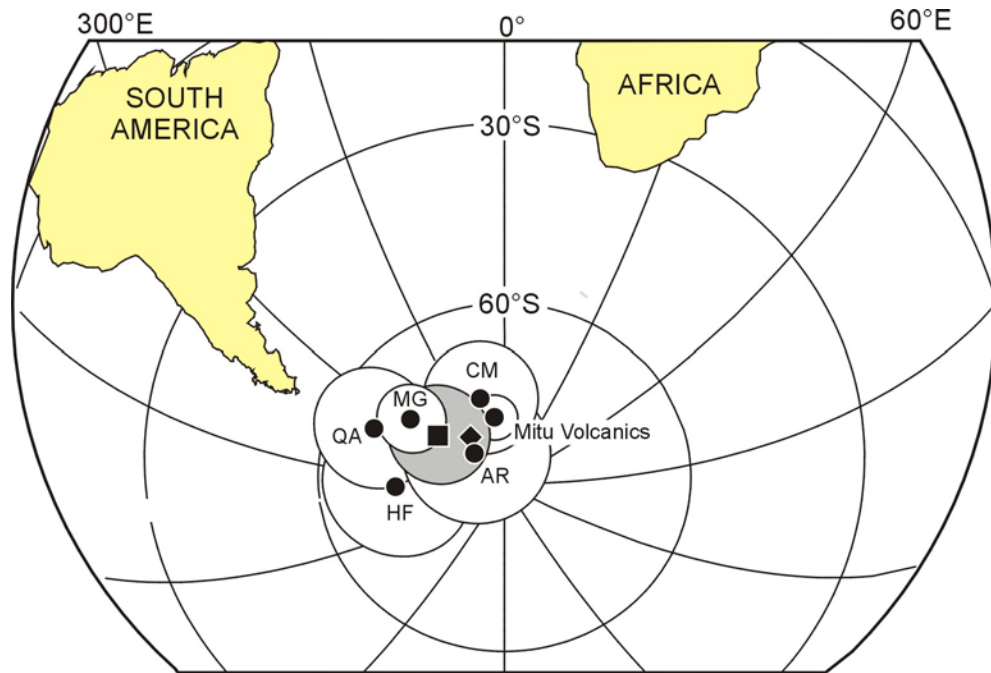
Fig. 6.4. Equal area projection showing palaeosouth pole position for the Mitu Group and those from selected (Q≥3) published Permian-Triassic and Early Triassic data from stable South America. The overall mean palaeopole for South America (λ= 76.5°S; φ= 306.2°E) calculated from the 6 plotted poles (see Tab 6.3) is presented by square with confidence circle filled in grey. Diamond represents mean Early Triassic (235±14 Ma) pole for South America compiled by Gilder *et al.* (2003).

Considering all palaeomagnetic data listed in Table 6.3, the combined Permian-Triassic data from South America yield a palaeosouth pole located at λ= 76.5°S; φ= 306.2°E (A$_{95}$= 8.3°; K= 66.0). This pole is not significantly different from the mean Early Triassic (235±14 Ma; λ= 79.0°S; φ= 288.4°E) and Late Permian (256±10; λ= 74.0°S; φ= 290°E) poles for South America

compiled by Gilder *et al.* (2003) and Van der Voo (1993), respectively. The Combined Early Permian pole is situated at λ= 48.3°S; ϕ= 58.9°E (A95= 8.3°) when transferred into African co-ordinates, according to the reconstruction parameters of Lawver & Scotese (1987). Within the error limits, this is in good agreeement with the Early Triassic segments of the APW paths for Gondwana of Torsvik & Van der Voo (2002), and Bachtadse & Briden (1991).
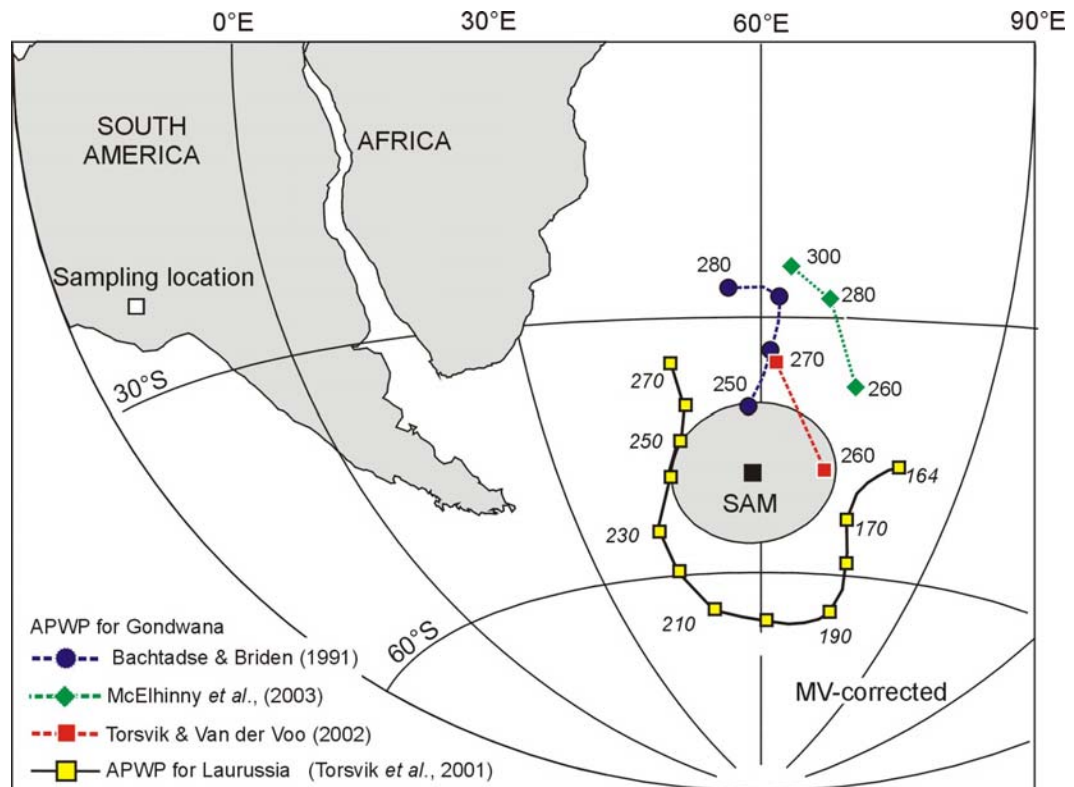
Fig. 6.5. Position of the Early Triassic palaeomagnetic south poles from Mitu Group (square with grey confidence circle) compared with sections of the proposed APWPs for Gondwana and Laurussia.

6.3   Copacabana Group (Early Permian; Subandean Zone)

6.3.1   Sampling

Sampling for the Copacabana Group was carried out in the Subandean Zone (Fig. 6.1), which consists of fold-thrust belt of Palaeozoic, Mesozoic and Tertiary sediments (section 2.3.2). Sampling was conducted at Pongo de Mainique, along the Urubamba River (Fig. 6.6). In this area, the Copacabana Group consists of an approximately 800 meters thick carbonate sequence of fossiliferous grey micritic, nodular, detritic limestones, and calcareous sandstones. The Copacabana Group is dated as Asselian-Early Sakmarian

(275-290) based on palaeotological and palynological studies (De la Cruz *et al.*, 1998; Quiňones, 1990; Azcuy *et al.,* 1992). Stratigraphically, the Copacabana Group conformably overlies the Tarma Group, and is, in turn, overlain by the Rio Tambo Formation. Both the Tarma Group and the Rio Tambo Formation are biostratigraphically well dated as Late Carboniferous and late Early Permian in age (De la Cruz *et al.*, 1998 and references therein). Structural features in the sampling area are dominated by NW-SE folds and faults associated with the regional Late Hercynian compression that affected the Copacabana, Tarma and Ambo Groups (De la Cruz *et al.*, 1998; Jaillard *et al.*, 2000), and folds and faults associated with the Andean deformation (De la Cruz *et al.*, 1998).

Core samples from the Copacabana Group were collected from different layers, on both limbs of an approximately 20 meter folded carbonate sequence, with fold axis dipping 15° towards west (Figs. 6.6, 6.7). Fifty-six cores were drilled in nodular limestone, detritic limestone, and calcareous sandstone beds. Additional samples from La Chonta Formation (Late Cretaceous) were sampled at the same location to provide tectonic control of the sampling area. The La Chonta Formation comprises fossiliferous marine carbonate succession, palaeontologically dated as Coniacian-Santonian (83-89 Ma; De la Cruz *et al.*, 1998 and references therein). Samples from this Formation include 14 drill cores, collected in an approximately 3 meters thick sub-vertical bedded limestone. No further sampling was possible due to limited outcrop exposure.

6.3.2   Palaeomagnetic Results and Interpretations

Carbonate rocks from Copacabana Group are generally weakly magnetised, with initial NRM intensities ranging from 0.04 mA/m to 0.5 mA/m. Stepwise demagnetisations of the specimens cut from the 56 collected samples yield two distinct magnetic directions. The lower unblocking temperature direction (A) completely removed after heating to 270°C, is generally defined between 100°C and 250°C (AF: 5-20mT). It can be isolated in a total of 38 samples and yield an overall site mean direction of D= 006.3°; I= -20.1° (α_{95}= 5.9°; k= 80.6; N= 8) in *in-situ* co-ordinates. Bedding correction disperses the directional distribution into two groups on both sample and site level (Fig. 6.9), indicating the post-folding acquisition of this magnetisation. As this direction is carried by low unblocking temperature minerals (≤300°C) and because individual directions cluster at the proximity of the expected dipole field direction at the sampling locality, it may represent a viscous remanent magnetisation acquired under the present day magnetic field. The overall mean south pole (COP-A) calculated from the eight VGPs listed in table 1 is located at λ= 83.9°S; ϕ= 198.4°E; A_{95}= 4.1°.
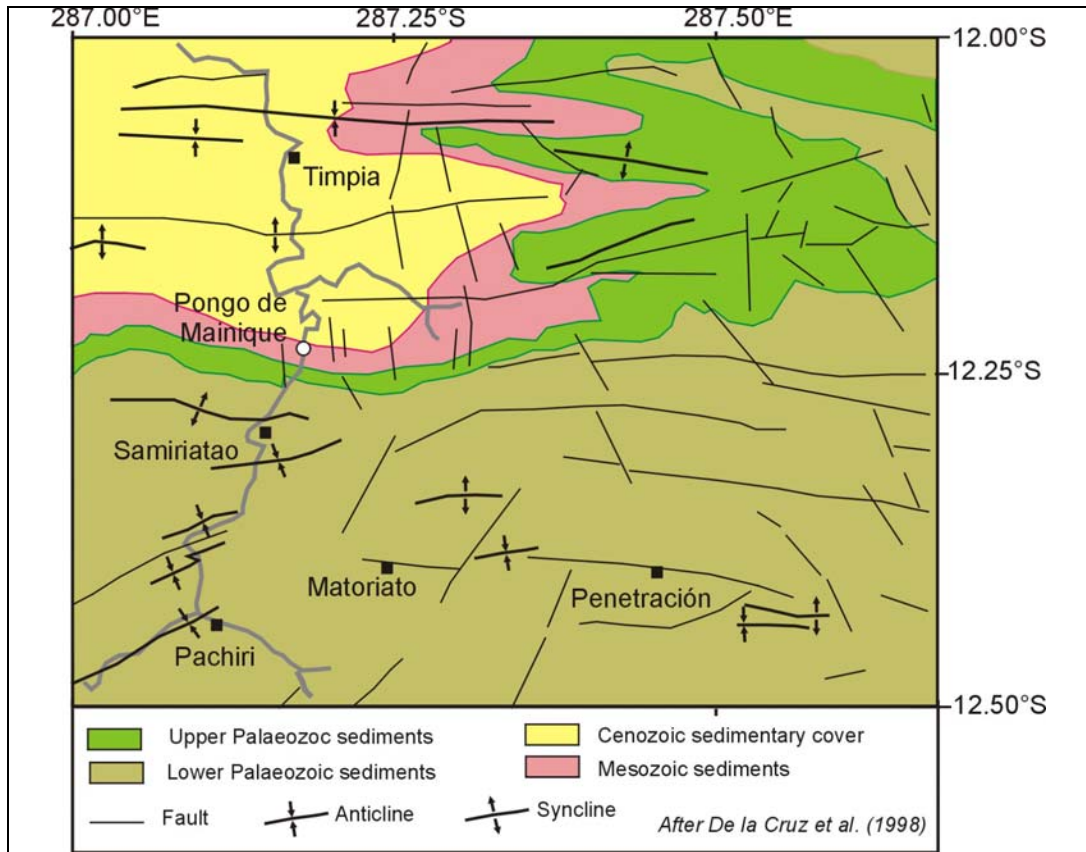
Fig. 6.6. Simplified geological map of the sampling area for Copacabana Group (box in Fig. 6.1). Circle symbol represents sampling locality (12.2°S/287.2°E).

Fig. 6.7. Photograph of the folded carbonate unit sample at Pongo de Mainique. Numbers indicate bedding horizons from which at least 5 core samples were collected. Samples collected from the same bed are grouped in a palaeomagnetic sampling site. The plunge of the fold axis (15° toward NW) was taken into consideration when correcting palaeomagnetic data.

The high unblocking temperature direction B is identified in 29 samples from 9 palaeomagnetic sampling sites. It is well defined by linear decay of demagnetisation data points showing minor directional change and reaches, or is clearly directed toward, the origin in orthogonal projection (Fig. 6.8). Individual sample directions were calculated from, minimally, the 5 last demagnetisation steps above 250°C (AF: 20mT). The majority of the specimens are totally demagnetised between 480°C and 520°C (AF= 90mT), suggesting a remanent magnetisation carried dominantly by titanomagnetites. In contrast to the A magnetisation, sample and site level directions of the B remanence are distributed into two distinct groups in in-situ co-ordinates, but clustered in a southerly declination with positive inclination after bedding correction (Fig. 6.9). The overall site-mean direction (N= 9) is D= 159°; I= 0.2° (α_{95}= 94°; k= 2.7) in-situ, and D= 166°; I= 49° (α_{95}= 4.5°; k= 132) after bedding correction (Tab. 6.4). This direction passes the fold test of McElhinny (1964; K-ratio= 82.03) and that of McFadden (1990), both at the 99% level of confidence. Stepwise unfolding shows maximum grouping of the site mean directions at 101±8% (k= 236.3; α_{95}= 3.4°; Enkin, 2003; Fig. 6.9). Because the folding of the unit is attributed to the late Hercynian compression event (De la Cruz *et al.*, 1998; Jaillard *et al.*, 2000), the B remanence is thought to have acquired during, or shortly after, rock deposition. The site-level VGPs corresponding to the bedding-corrected directions (Tab. 6.4) yield an overall mean palaeosouth pole (COP-B) located at λ= 68°S; ϕ= 321°E; (A_{95}= 5°; K= 100; N= 9). COP-B is situated at λ= 41°S; ϕ= 51°E when rotated into South African co-ordinates according to the reconstruction parameters of Lottes & Rowley (1990).

The overlying Late Cretaceous La Chonta Formation, sampled to provide tectonic control has NRM intensity ranges between 3.1 mA/m and 4.6 mA/m. Thermal demagnetisation up to 690°C of the 14 collected samples yield a well-defined stable magnetisation. Individual directions were calculated from linear trajectories of the vector components between 250°C to 650°C, clearly converging towards the origin in orthogonal projection (Fig. 6.10a). Unblocking temperature above 650°C indicates haematite as primary remanent carrier. However, occasional slight inflection in the intensity decay curves between 400 and 550°C also suggests a contribution from magnetite in the remanence matrix. The negligible change in magnetic direction after 570°C suggests that magnetite and haematite carry the same remanence. The sample directions (n= 14) from La Chonta Formation (LCF) yield an overall mean of D= 184.3°, I= -44.5° (α_{95}= 2.4°; k= 182.2) in-situ, and D= 182.9°; I= 37.7° (α_{95}= 2.0°; k= 256.1) after bedding correction. No change in directional grouping was expected as all samples were collected from unit of uniform structural attitude.

a) Component A

Site	n	Dg(°)	Ig (°)	α_{95}(°)	k	Ds(°)	Is(°)	α_{95}(°)	k	P_{lat}(°S)	P_{long}(°E)	dp	dm
MCO1	6	1.2	-34.8	13,5	25.7	213.1	-83.2	13,5	26	82.9	277.9	8.9	13.5
MCO2[*]	3	8.5	-24.6	18.8	44.2	365.5	-72.6	18.8	44	-	-	-	-
MCO3[*]	4	5.5	-37.9	21.8	18.8	27.3	-79.3	21.8	19	-	-	-	-
MCO4	5	7.0	-14.9	7.6	102.7	7.1	14.4	7.6	103	81.7	164.0	4.0	7.8
MCO5	3	8.8	-11.9	9.3	176.5	8.1	23.6	9.3	177	79.3	162.5	4.8	9.5
MCO6	9	10.9	-10.0	3.4	233.3	9.3	26.2	3.4	233	77.1	164.5	1.7	3.4
MCO7	6	4.9	-25.0	12.7	28.7	189.7	-75.1	12.7	29	85.1	208.7	7.3	13.6
MCO8[*]	8	3.8	-17.1	25.5	98.1	200.3	-81.7	25.5	98	-	-	-	-
MCO9	2	9.8	-23.2	7.4	57.2	153.9	-77.1	7.4	57	80.4	197.6	4.2	7.9
MCO10	6	1.3	-16.7	8.2	68.2	202.5	-85.0	8.2	68	86.1	126.5	4.4	8.5
MCO11	8	5.3	-25.9	5.7	96.5	179.5	-73.1	5.7	97	84.6	213.4	3.3	6.2
Mean	N	Dg(°)	Ig(°)	α_{95}(°)	k	Ds(°)	Is(°)	α_{95}(°)	k	λ(°S)	ϕ(°E)	A_{95}(°)	K
	8	6.3	-20.3	6.2	80.6	-	-	-	-	83.6	183.6	4.1	185.9

b) Component B

Site	n	Dg(°)	Ig(°)	α_{95}(°)	k	Ds(°)	Is(°)	α_{95}(°)	k	P_{lat}(°S)	P_{long}(°E)	dp	dm
MCO3	6	168.8	4.5	10.5	29.9	161.3	47.4	4.4	127	66.1	331.3	3.7	5.7
MCO4	5	108.6	52.8	5.4	136.4	149.9	49.7	1.8	614	56.7	339.1	1.6	2.4
MCO5	3	88.5	63.2	11.4	50.8	162.3	56.3	9.1	33	60.7	317.0	9.5	13.1
MCO6	5	92.8	66.9	7.6	67.5	162.5	54.1	9.0	144	62.5	319.6	8.9	12.6
MCO7	5	167.1	-34.6	5.7	121.1	165.0	42.0	7.7	1001	71.4	334.9	5.8	9.4
MCO8	3	172.7	-32.2	10.1	65.0	170.3	45.5	9.9	87	72.6	317.4	8.0	12.6
MCO9	5	177.8	-29.7	5.1	149.4	176.3	48.0	6.3	150	72.8	298.3	5.4	8.2
MCO10	6	176.1	-26.6	5.5	110.3	173.3	50.8	6.4	110	69.7	303.9	5.8	8.6
MCO11	5	171.9	-38.6	4.8	168.1	172.3	43.8	5.9	168	74.7	314.5	4.6	7.4
Mean	N	Dg(°)	Ig(°)	α_{95}(°)	k	Ds(°)	Is(°)	α_{95}(°)	k	λ(°S)	ϕ(°E)	A_{95}(°)	K
	9	158.5	0.2	94.4	2.5	166.1	48.9	4.5	131.5	68.2	321.3	5.2	99.8

Tab. 6.4. Palaeomagnetic results from the Copacabana Group. **a)** Component A direction corresponding to the low unblocking temperature magnetisation from the Copacabana Group. This magnetisation is assumed as being a present day overprint. The listed VGPs and mean palaeomagnetic poles are calculated from the *in-situ* directions. **b)** Component B corresponding to the stable direction considered being a primary Early Permian remanence. The listed VGPs and mean palaeomagnetic poles were, therefore, calculated from the bedding-corrected directions. Table headings are: Site: palaeomagnetic site code; n: number of samples used for analysis. Dg/Ig and Ds/Is: declination/inclination in degrees; g and s stand for geographic coordinates (*in-situ*) and stratigraphic coordinates (bedding-corrected), respectively; α_{95}: calculated radius of cone of 95% confidence about the mean direction (Fisher, 1953); k: Fisher precision parameter; P_{lat}(°S) and P_{long}(°E): latitude and longitude position of the calculated VGP for individual site; λ (°S) and ϕ (°E): latitude and longitude position of the resultant palaeomagnetic south pole calculated from site-level VGPs, respectively; latitude is in degrees south and longitude is in degrees east; dp/dm: axes of oval of 95% confidence about the palaeomagnetic pole. A_{95}: radius of the 95% confidence cone about the palaeomagnetic pole, in degrees. [*]Palaeomagnetic sites yielding large confidence circles ($\alpha_{95} \geq 15$) and not used when calculating mean-site direction.
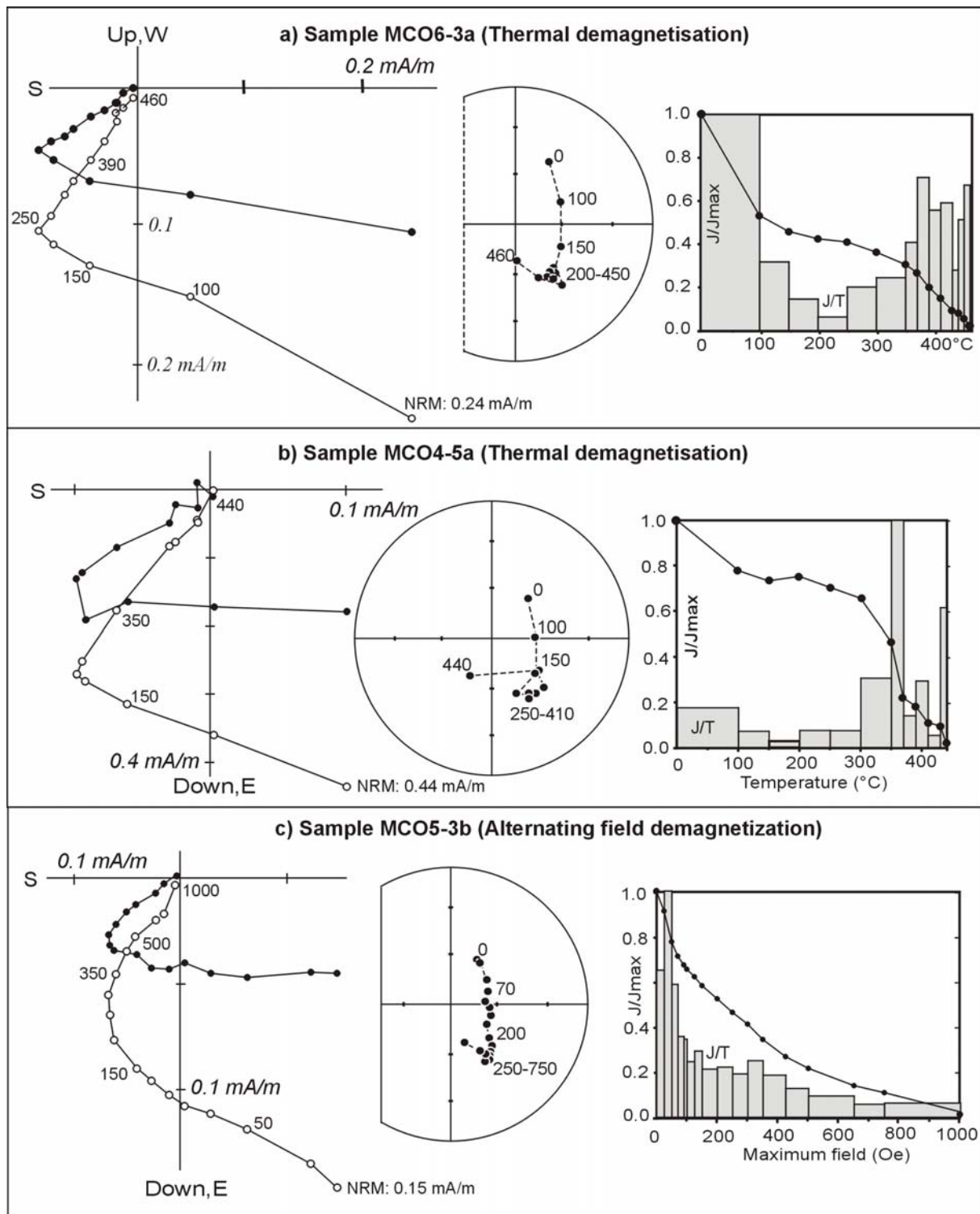
Fig. 6.8. Examples of stepwise demagnetisation results of the Copacabana Group in bedding-corrected co-ordinates. The orthogonal projections show two well-defined magnetic directions, with high unblocking temperature direction B defined within the 250°C to 480°C temperature range. Open/close circles represent data points in the horizontal/vertical plane. Initial NRM intensities for samples MCO6-3a and MCO11-5a are 0.24 and 0.43 mA/m respectively.
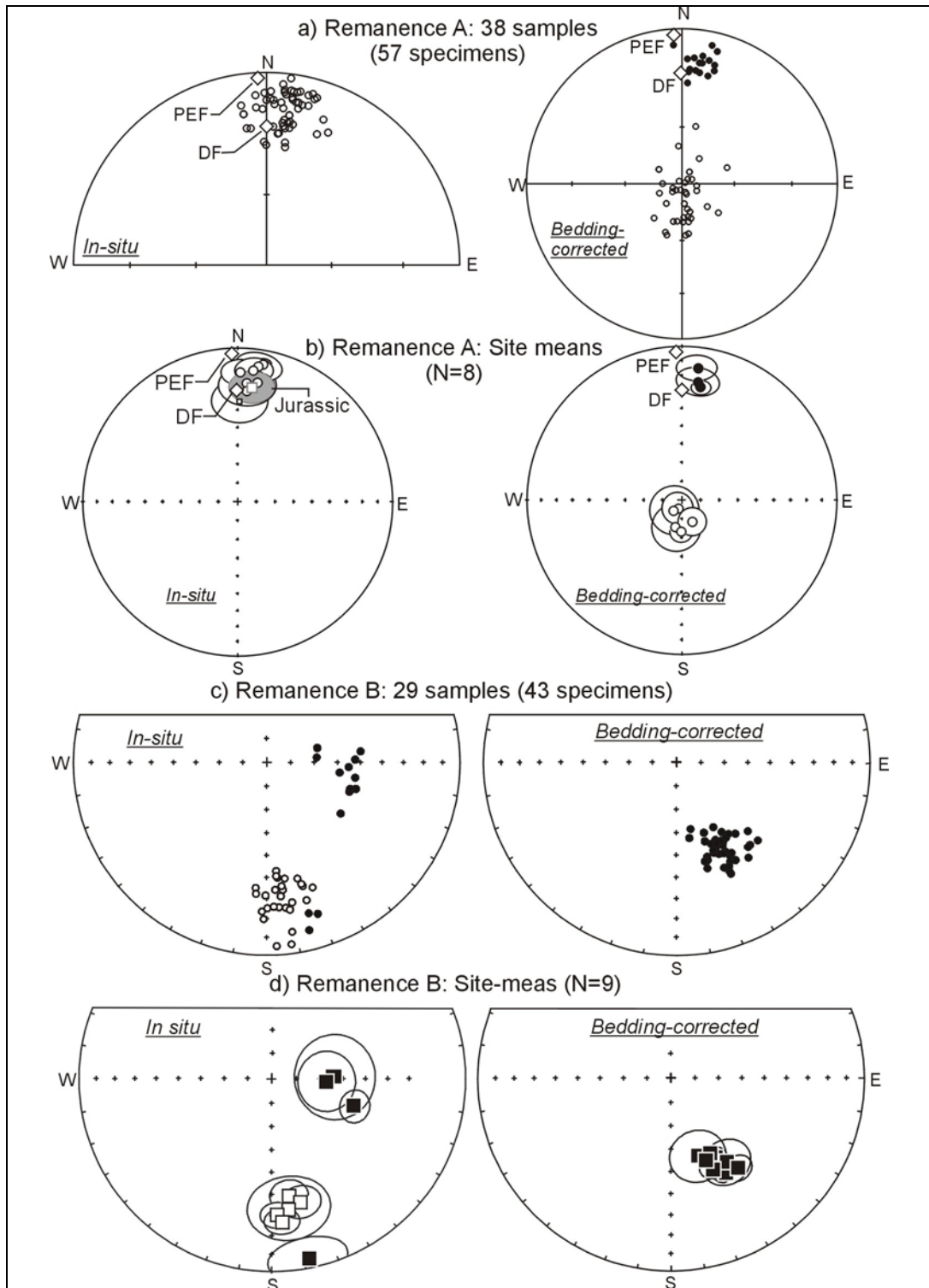
Fig. 6.9. Equal area stereographic projection showing distribution of sample and site mean directions for the magnetic overprint A and the stable remanence B from the Copacabana Group. Confidence circles (α_{95} in degrees) for site-mean directions are shown. Remanence B (D= 166.1°; I= 48.9°; α_{95}= 4.5°; k= 131.5; Bedding-*corrected*) is considered as being a primary Early Permian magnetisation, whilst the A remanence (D= 006.3°; I= -20.3°; α_{95}= 6.2°; k= 80.6; *in-situ*) is interpreted as a recent magnetic overprint. PEF: present magnetic field at the sampling area; DF: present magnetic dipole field.

Due to limited outcrop, no field test could be carried out to constrain the relative age of the LCF magnetisation. However, the in-situ direction (southern declination with intermediate inclination) is not similar to the expected Cretaceous or to any younger directions for stable South America. The bedding-corrected direction, however, is similar to Eocene-Oligocene expected directions. The magnetisation of the La Chonta Formation is, therefore, considered Cenozoic pre-folding and a probable Eocene-Oligocene remagnetisation. The palaeosouth pole position corresponding to the bedding-corrected direction (λ= 80.7°S; ϕ= 270.2°E; dp= 1.4; dm= 2.5) is similar to the 24-66 Ma pole of Randall (1998), and plots between the 30 to 67 Ma poles presented by Roperch & Carlier (1992), Van der Voo (1993) and Beck (1998; Fig. 6.10c). This indicates that the sampling area was not rotated during the Andean deformation.

6.3.3 Rock Magnetic Properties

The IRM acquisition results obtained from VFTB experiments are rather noisy due the low magnetic intensity of the carbonates from Copacabana Group. However, they clearly illustrate that representative samples are saturated by application of a field ranging between 0.9 and 1.0 Tesla. Back-field coercivity curves indicate coercivity of remanence (Hcr) about 0.4 Tesla (Fig. 6.11a,b). The hysteresis loops for these samples are characterised by a negative slope at high fields, indicating contribution of diamagnetic carbonate minerals (Fig. 6.11c,d). After removal of the diamagnetic contribution, the reduced hysteresis loops show constricted loops referred to as "wasp waisted" loops (Fig. 6.11e,f), indicating superposition of single domain (SD) and super-paramagnetic (SP) particles. This loop is characterised by high Mrs/Mr ratio, ranging between 0.28 and 0.34, and high Hcr/Hc ratio within about 5 to 6. The Mrs/Mr value ($\geq$0.05) is characteristic of fine-grained single domain magnetic carrier, whilst the high Hcr/Hc ($\geq$4) is characteristic of coarse-grained multi-domain particles. As a result of these unusual values, the ratio of Mrs/Ms versus Hcr/Hc plot out of the expected values for SD, PSD and MD on Day plot (Day, 1977). However, the values of the Mrs/Ms versus Hcr/Hc for Copacabana Group fall on the trend of values for remagnetised limestones, in which Late Carboniferous-Early Permian secondary magnetisation are carried by very fine grain magnetites (Jackson, 1990). This confirms that the stable remanence of the Copacabana Group is carried by fine SD magnetite particles. Variation of the bulk remanence magnetisation during successive heating up to 700°C, followed by cooling to room temperature (Fig. 6.12) show irreversible thermoremanent curves, suggesting mineral transformation after heating above the 590-600°C. The Curie temperature calculated from the thermoremanent behaviour

ranging between 454 to 583°C is characteristic for magnetite mineral carriers.
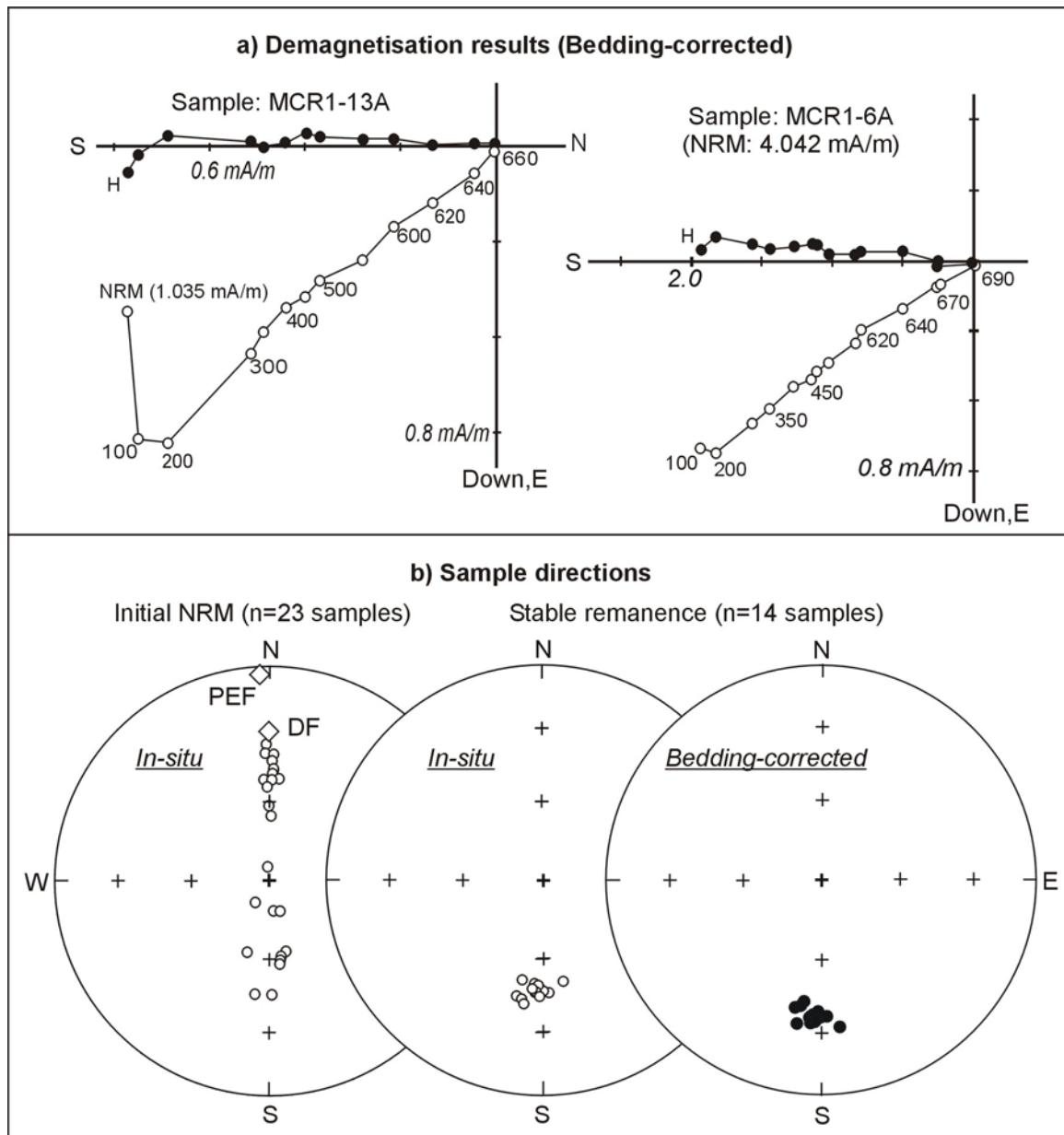
Fig. 6.10. Palaeomagnetic results from the Late Cretaceous La Chonta Formation. **a)** Examples of demagnetisation results from representative samples. Stable directions of individual samples were generally calculated from 300°C to 690°C data points. **b)** Equal area stereographic projection showing distribution of the initial NRMs and stable directions from individual samples.
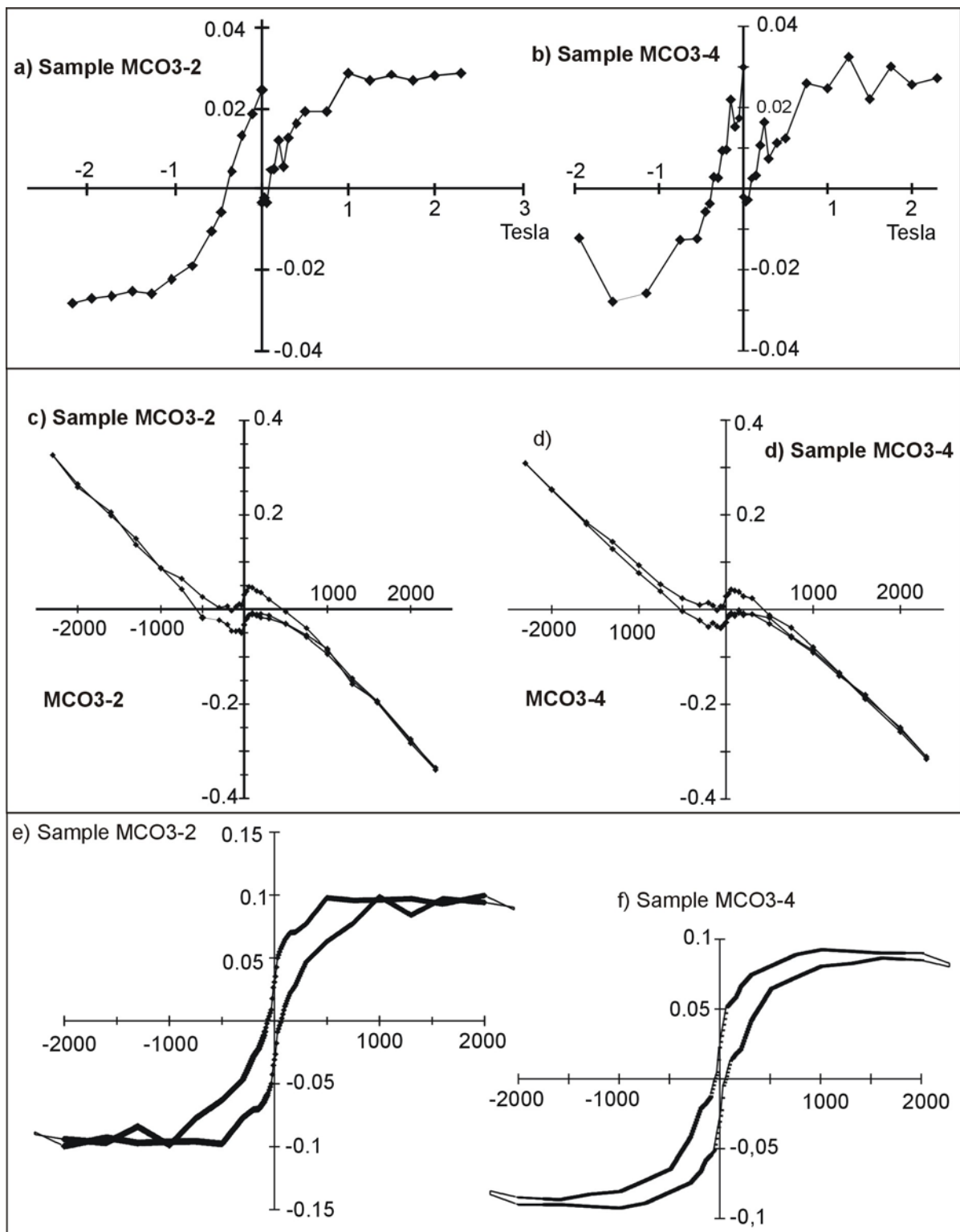
Fig. 6.11. Result of rock magnetic test for representative samples from Copacabana Group. **a)** and **b)** IRM and backfield results showing noisy data points but with obvious saturation. **c)** and **d)**: Original hysteresis loops illustrating dominance of diamagnetic minerals. **e)** and **f)** Reduced hysteresis loops obtain after removal of the paramagnetic and diamagnetic contributions.
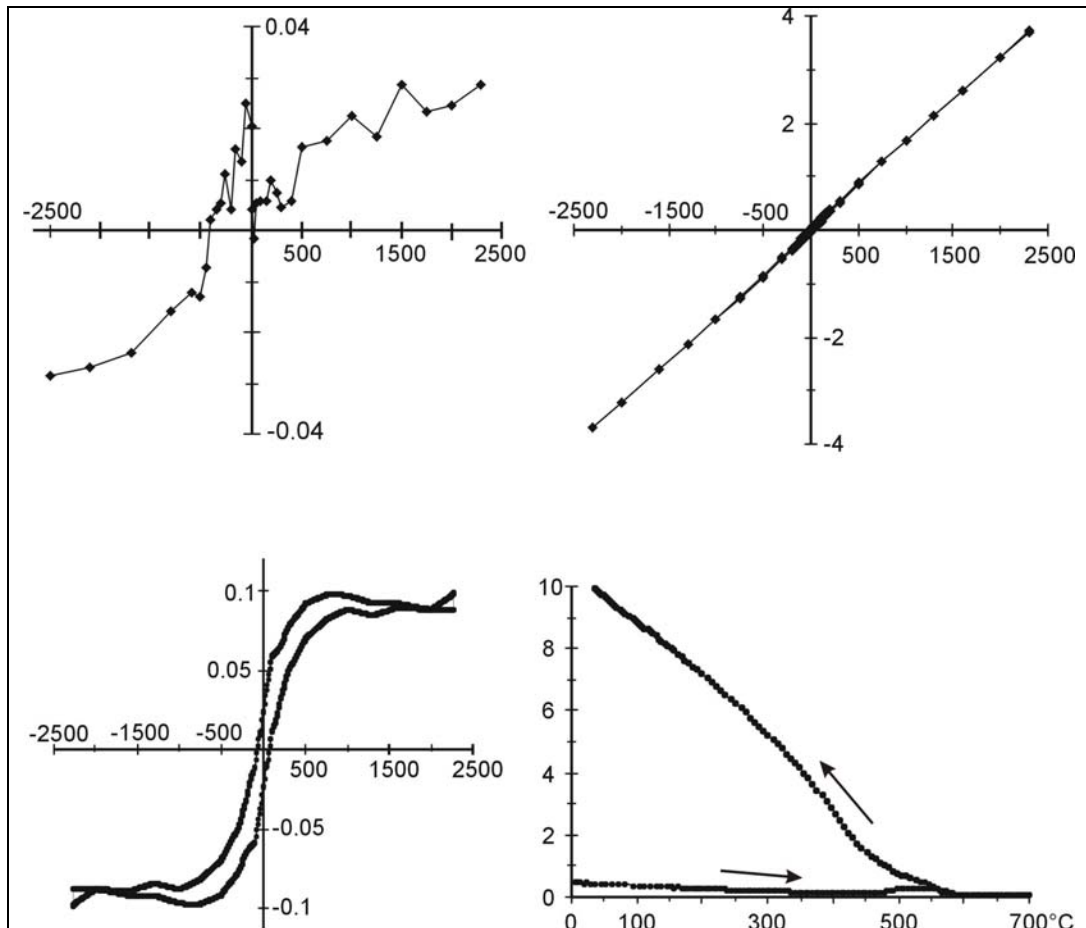
Fig. 6.12. Results of rock magnetic tests for some samples from Copacabana Group. Dominant contribution of paramagnetic mineral is obvious in the original hysteresis loop. The reduced loop is similar to that observe in Fig. 6.11.

6.4   Discussion

Based on positive fold test and the palaeomagnetic data from the La Chonta Formation, the component B magnetisation of the Copacabana Group (269-290 Ma) is considered to be a primary remanence representing the Early Permian magnetisation for stable South America. The Early Permian south pole position corresponding to this remanence is situated at $\lambda= 68.2°S$; $\phi= 321.3°E$ ($A_{95}= 5.2°$; K= 99.8). Considering the previously published Early Permian pole from South America with quality index $Q\geq3$ (Van der Voo, 1990) listed in Table 6.5 and plotted in figure 6.13, the combined data suggests a palaeosouth pole located at $\lambda= 70.4°S$; $\phi= 341.8°E$ ($A_{95}= 8.8°$; K= 48.2).

	Rock unit	Age (Ma)	λ_{am}(°S)	ϕ_{am}(°E)	λ_{af}(°S)	ϕ_{af} (°E)	α_{95}°	Tests	Ref.
LCF	La Colina Formation, Los Colorados	260-299	74	313	45.8	056.3	3.1	-	(1)
MPU	Middle Paganzo II, Los Colorados upper beds	271-299	74	308	47.1	055.5	3.0	-	(2)
MPH	Middle Paganzo II, Huaco	271-299	63	356	27.5	060.1	7.5	-	(2)
TAM	Tambillos Formation	271-285	78.9	319.6	46.5	063.6	5.2	Fo	(3)
MPL	Middle Paganzo, Los Colorados lower beds	271-299	59.5	357.5	24.1	059.1	2.5	-	(2)
TUN	Tunas Formation, synfold	276-299	63	13.9	24.6	068.5	4.8	F+	(4)
COP	Copacabana Group	269-290	68.2	321.3	40.6	051.2	5.2	F+	(5)
	Mean Early Permian pole	**260-299**	**70.4**	**341.8**	**36.7**	**059.6**	**8.8**	**K=48.3**	

Tab. 6.5. Early Permian palaeomagnetic data from South America with quality index Q≥3 and good age constrain. λ_{am}(°S)/ϕ_{am}(°S): pole position in South American coordinates. λ_{af}(°S)/ϕ_{af}(°S): position of pole in African coordinates following the reconstruction parameters of Lawver & Scotese (1987). References: (1) Thompson (1972); (2) Embleton (1970); (3) Rapalini & Vilas (1991); (4) Tomezolli & Vilas (1999); (5) this study. F+: positive fold test; Fo: Inderteminate fold test.
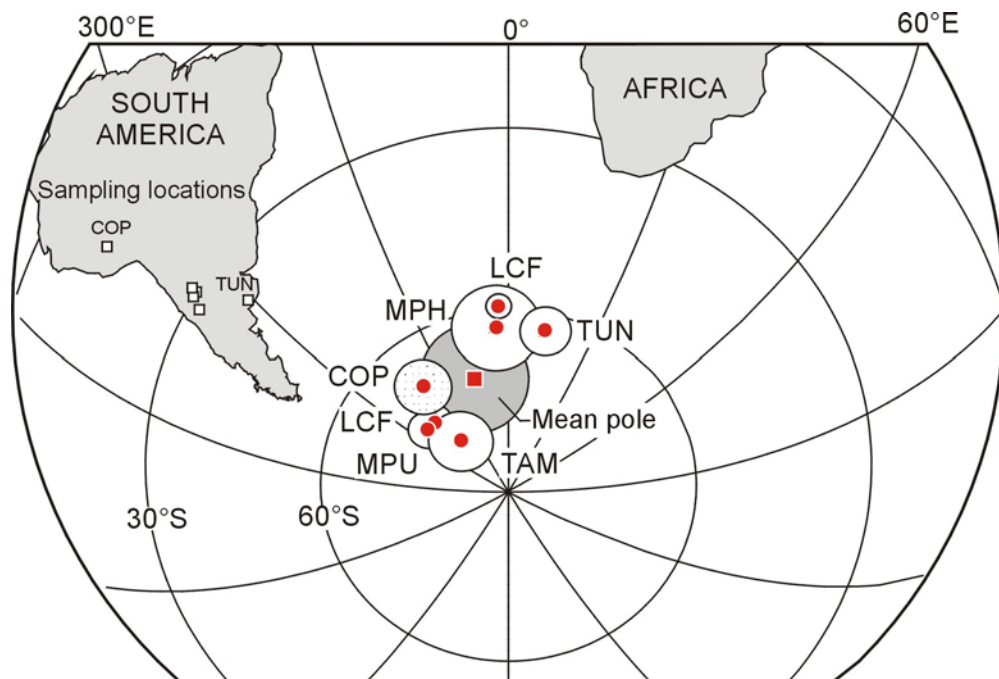
Fig. 6.13. Equal area projection of the palaeomagnetic south pole from Copacabana Group (COP; stippled confidence circle) compared with published Early Permian poles for stable South America (circles) with quality factor Q≥3 (Van der Voo, 1990). All poles are plotted in South American co-ordinates.

In order to select the most reliable published data and with the purpose of computing an Early Permian mean pole for Gondwana, the online Global Palaeomagnetic Database (GPMDB version 4.5, October 2003) was inspected. As a result, six data from Africa and three data from Australia (Tab. 6.6) were confirmed to be of high quality with well-determined Early Permian age (256-290 Ma), sufficient number of samples, and adequate demagnetisation and/or positive field test.

	Rock unit	Age (Ma)	λ(°S)	ϕ(°E)	α_{95}(°)	Tests	Ref
Africa							
CH	Chougrane red beds	256-290	32.2	064.1	4.7	F+	(1)
LT	Lower Tiguentourine Formation	280-300	33.8	061.4	4.1	-	(2)
AB	Abdala Formation, lower unit	271-299	29.0	057.0	3.0	-	(3)
AL	Upper El Adeb Larache Fm.	284-307	38.0	057.0	2.0	-	(4)
DW	combined data Dwyka System	260-303	25.0	067.0	12.0	F+	(5)
JN	Jebel Nehoud Ring Complex	278-282	46.9	068.0	5.1	-	(6)
Australia							
MLI	Mount Leyshon Intrusive	279-287	43.0	137.0	3.0	C+	(7)
FBV	Featherbed Volcanics	280-305	43.0	131.0	5.0	-	(8)
TIC	Tucker Igneous Complex	283-291	47.0	143	3.0	F+	(7)

Tab. 6.6. Previously published high quality Early Permian palaeomagnetic results from Africa and Australia. λ(°S) and ϕ(°E) are latitude and longitude positions of pole in locale (African and Australian) co-ordinates. α_{95}: statistical parameter according to Fisher (1953). F+: positive fold test; C+: positive contact test. References are: (1) Daly & Pozzi (1976); (2) Derder *et al.* (1994); (3) Merabet *et al.* (1998); (4) Henry *et al.* (1992); (5) Opdyke *et al.* (2001); (6) Bachtadse *et al.* (2002); (7) Clark & Lackie (2003); (8) Klootwijk *et al.* (1993).

When plotted in African co-ordinates, the overall Early Permian poles from South America, Africa and Australia are widely dispersed (Fig. 6.14). As palaeogeographic fits between Gondwana continents may cause such inconsistency between palaeomagnetic poles, it is important test the reconstruction parameters commonly used for transferring palaeomagnetic data from South America and Australia into the Gondwanan co-ordinates. Calculating the "great circle distance" (GCD in degrees) between palaeomagnetic poles is a common procedure to measure the goodness of fits between two continents. For this purpose, the mean palaeomagnetic poles for South America and Australia were transferred into African co-ordinates according to the reconstruction parameters of Lawver & Scotese (1987) and Lottes & Rowley (1990), respectively. For Africa, all poles from northwest and northeast African were transferred into central African co-ordinates following Lottes & Rowley (1990) and a mean was calculated from all high quality data listed in Table 6.6. This Early Permian African mean pole (λ= 28.8°S; ϕ= 65.5°E; A_{95}= 6.0°; K= 124; N= 6 studies) is used as a reference pole. The mean Australian pole (λ= 44.4°S; ϕ= 136.9°E; A_{95}= 7.4°; K= 279) calculated from the three listed studies and the newly defined Early Permian pole for South America (λ= 70.4°S; ϕ= 341.8°E; A_{95}= 8.8°; K= 48.2; N= 7 studies) were used for comparison.
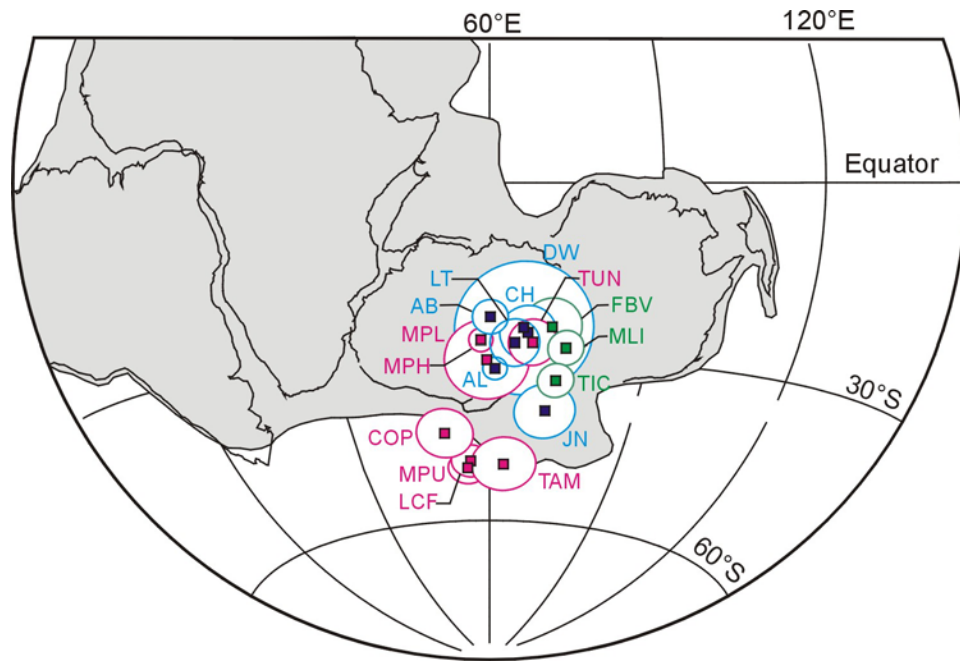
Fig. 6.14. Equal area projection showing distribution of the selected published Early Permian poles from South America (red) and high quality poles from Africa (blue) and Australia (green) in central African co-ordinates. Palaeomagnetic data from northwest and northwest Africa, South America, and Australia were transferred in African co-ordinates according to the reconstruction parameters of Lottes & Rowley (1990). See tebles 6.4 and 6.5 for details.

The GCDs between the South American and African poles, and that between the Australian and African poles are listed in Table 6.7. Accordingly, the Lottes & Rowley (1990) fit between South America and Africa has the highest GCD (11.8°) and is the least appropriate for the Early Permian palaeomagnetic data. The low GCDs for South America/Africa (9.3°) and Australia/Africa (6.3°) are obtained by using the reconstruction parameters of Lawver & Scotese (1987). Therefore, Early Permian poles for Gondwana support the South/Africa/Australia fit of Lawer & Scotese (1987). In another words, Early Permian poles from Gondwana are in better agreement when adopting these reconstruction parameters.

For this reason, the palaeogeography reconstruction parameters of Lawver & Scotese (1987) are used for calculating a mean pole for Gondwana. As the authors consider Africa as being a single continent, the mean pole for Africa was recalculated. This results in a slightly different pole situated at $\lambda= 34.2°S$; $\phi= 62.9°E$ ($A_{95}= 7.1°$). Using this pole as a reference reduces the GCD between the Africa pole and the mean poles for South America (3.7°) and Australia (8.3°). The Early Permian mean pole position for Gondwana calculated from all 16 studies listed in Table 6.8 is $\lambda= 34.8°S$; $\phi= 063.0°E$ ($A_{95}= 4.6°$; $K= 64.5$; Fig. 6.15.). This pole position is not significantly different from the mean Early Permian poles compiled by Bachtadse *et al* (2002), Torsvik & van der Voo (2002); McElhinny *et al* (2003).

South America-Africa

Reconstruction Parameter	λ(°S)	ϕ(°E)	GCD(°)	Reference
45.5°N / 327.8°E / +58.2°	36.7	059.6	9.3	Lawver & Scotese (1987)
46.82°N / 329.46°E / +55.8°	39.5	059.4	11.8	Lottes & Rowley (1990)

Australia-Africa

Reconstruction Parameter	λ(°S)	ϕ(°E)	GCD(°)	Reference
(1) 1.58°S / 039.02°E / -31.29° (2) 7.78°S / 328.58°E / +58.0°	31.3	072.2	6.3	Lawver & Scotese (1987)
29.26°S / 302.81°E / +54.02°	28.7	073.4	6.9	Lottes & Rowley (1990)

Tab. 6.7. Position of the mean Early Permian south poles from South America and Australia in central African coordinates when adopting the reconstruction parameters of Lawver & Scotese (1987) and Lottes & Rowley (1990), respectively. GCD (Great circle distance in degrees) between African-South American and African-Australian mean poles. Rotations of northwestern Africa (7.8°) and northeastern Africa (6.3°) relative to central Africa (Lottes & Rowley, 1990) were assumed when calculating the mean African pole (λ=28.8°S; ϕ=065.5°E, Central African coordinates). (1) and (2) are reconstruction parameters for Australia/East Antarctica and East Antarctica/Africa, respectively.
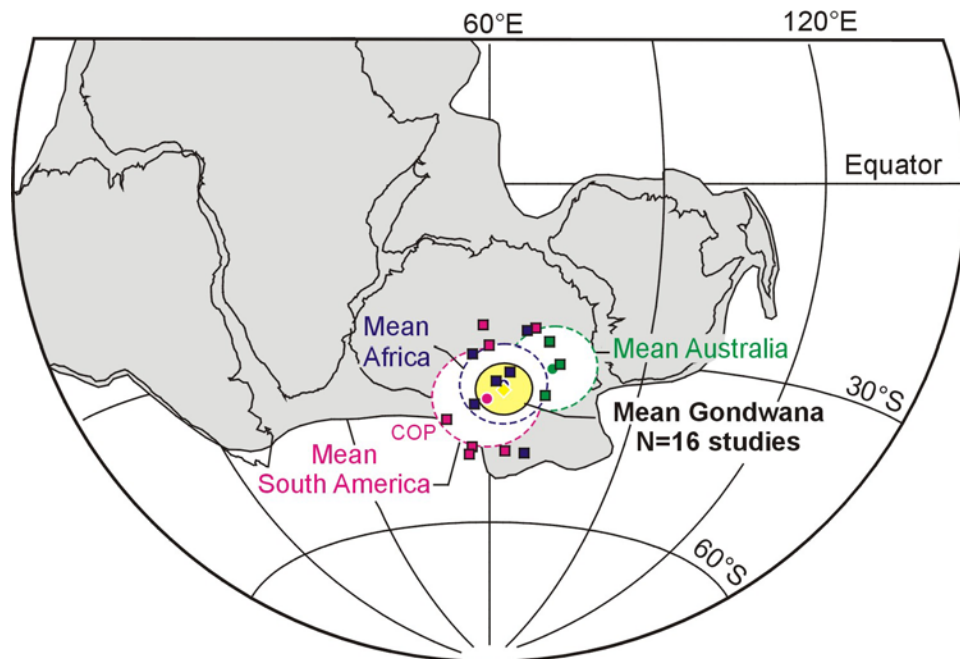
Fig. 6.15. Equal area projection showing distribution of individual (square) Early Permian poles from South America (red) and high quality poles from Africa (bleu) and Australia (green), and the calculated mean poles for Africa (λ= 34.2°S; ϕ= 62.9°E; A_{95}= 7.1°), South America and Australia (circle with A_{95} presented by discontinuous line). Palaeopole from South America (λ= 36.7°S; ϕ= 59.6°E; A_{95}= 8.8°) and Australia (λ= 31.3°S; ϕ= 72.2°E; A_{95}= 7.4°) were transferred into African co-ordinates following the Lawver & Scotese (1987) reconstruction parameters. The overall mean pole for Gondwana calculated from all 16 poles (Tab. 6.7) is located at λ= 34.8°S; ϕ= 63.0°E; A_{95}= 4.6°).

	Rock unit	Age (Ma)	λ(°S)	ϕ(°E)	α_{95}(°)	Tests	References
Africa							
CH	Chougrane red beds	273±18	32.2	64.1	4.7	F+	Daly & Pozzi (1976)
LT	Lower Tiguentourine Formation	290±10	33.8	61.4	4.1	-	Derder *et al.* (1994)
AB	Abdala Formation, lower unit	285±14	29.0	57.0	3.0	-	Merabet *et al.* (1998)
AL	Upper El Adeb Larache Formation	295±11	38.0	57.0	2.0	-	Henry *et al.* (1992)
DW	Dwyka Formation, combined data	282±21	25.0	67.0	12.0	F+	Opdyke *et al.* (2001)
JN	Jebel Nehoud Ring Complex	280±2	46.9	68.0	5.1	-	Bachtadse *et al.* (2002)
Australia							
MLI	Mount Leyshon Intrusive Complex	283±4	30.7	73.6	3.0	C+	Clark & Lackie (2003)
FBV	Featherbed Volcanics	293±13	26.8	71.4	5.0	-	Klootwijk *et al.* (1993)
TIC	Tucker Igneous Complex	287±4	36.2	71.4	3.0	F+	Clark & Lackie (2003)
South America							
LCF	La Colina Formation, Los Colorados	280±20	45.8	56.3	3.1	-	Thompson (1972)
MPU	Middle Paganzo II, Los Colorados upper beds	285±14	47.1	55.5	3.0	-	Embleton (1970)
MPH	Middle Paganzo II, Huaco	285±14	27.5	60.1	7.5	-	Embleton (1970)
TAM	Tambillos Formation	278±7	46.5	63.6	5.2	Fo	Rapalini & Vilas (1991)
MPL	Middle Paganzo, Los Colorados lower beds	285±14	24.1	59.1	2.5	-	Embleton (1970)
TUN	Tunas Formation, synfold	288±11	24.6	68.5	4.8	F+	Tomezolli & Vilas (1999)
COP	Copacabana Group	280±11	40.6	51.2	5.2	F+	this study
Mean (Gondwana)		**Mean age**	λ(°S)	ϕ(°E)	α_{95}(°)	**K**	
		282±25	34.8	063.0	4.6	64.5	N=16 studies

Tab. 6.8. List of previously published high quality Early Permian data from Africa and Australia and Early Permian palaeomagnetic poles with quality index Q≥3 from South America. λ(°S) and ϕ(°E) are latitude and longitude position of south pole transferred in African coodinates according to the reconstruction parameters for Gondwana proposed by Lawver & Scotese (1987).

6.5   Conclusions

The Copacabana Group provides a reversed polarity pre-folding remanence that achieves a positive fold test and interpreted as being a primary Early Permian magnetisation. Combination of the palaeomagnetic data from the Copacabana Group with the coeval previously published data from stable South America yields a mean Early Permian pole situated at $\lambda= 36.7°S$; $\phi= 059.6°E$ ($A_{95}= 8.8°$; $K= 48.2$; $N= 7$ studies). Although individual poles for Gondwana are widely dispersed, this pole (in African co-ordinates) is comparable with the mean palaeopoles from Africa and Australia. Combination of the Early Permian and Permian-Carboniferous palaeomagnetic data from South America, Africa and Australia ($N= 16$ studies) yields a mean pole located at $\lambda= 34.8°S$; $\phi= 063.0°E$ ($A_{95}= 4.6°$).

This pole suggests a palaeoposition of Gondwana relative to Laurussia similar to that in the Pangaea B configuration (Fig. 6.16). A large mismatch between the Gondwanan and Laurussian poles, and an unacceptable continental overlap is observed when adopting the Pangaea A reconstruction. Therefore, the palaeomagnetic pole compiled from stable South American, African and Australian data demonstrate that the disagreement of the palaeomagnetic data from Gondwana with the Pangaea A reconstruction is not the result of poor quality of Permian palaeomagnetic dataset. Based on the palaeomagnetic data from redbeds, Carbonates, and extrusive volcanic rocks of South America, which show no significant inclination difference, inclination shallowing in sediments apparently does not play a role in the mismatch of palaeomagnetic data. Thus, high quality palaeomagnetic data from Gondwana, which clearly indicate a palaeogeography supporting an Early Permian Pangaea B configuration, are trustworthy.

The combined Early Triassic results from South America, on the other hand, supports the Pangaea type A2 reconstruction of Van der Voo & French (1974). Hence, the overall Permian-Triassic palaeomagnetic data suggest a palaeogeography evolving from an Early Permian Pangaea B to an Early Triassic Pangaea A2 (Fig. 6.16). In another words, the overall data from South America indicate westward translation of Gondwana in Permian times. Further high quality data are still required, however, to improve the rather scattered Permian-Triassic palaeomagnetic data set for Gondwana.
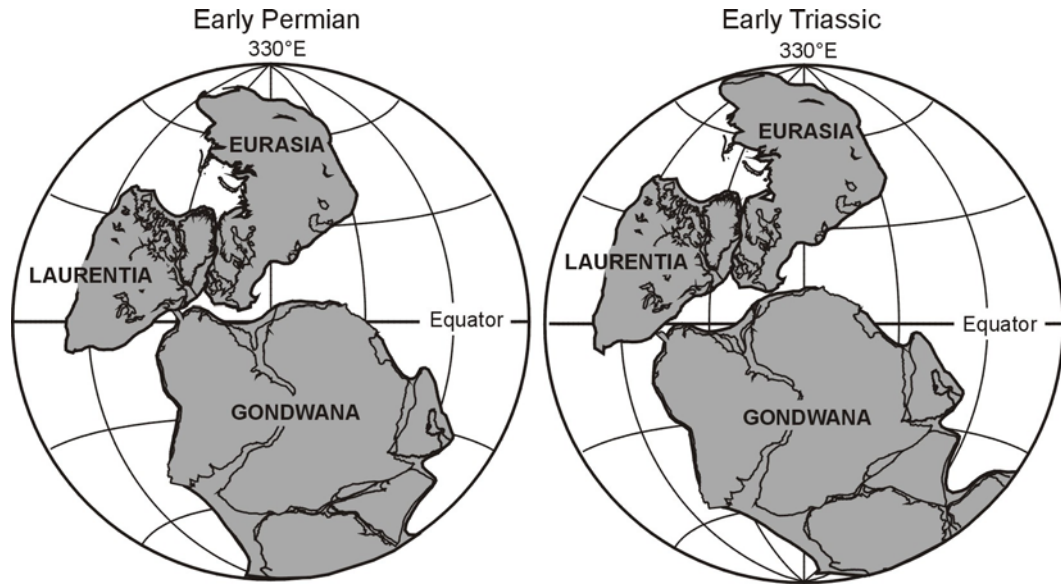
Fig. 6.16. Palaeogeographic reconstruction of Pangaea based on the Early Permian pole (λ= 34.8°S; ϕ= 063.0°E) and the Early Triassic pole (λ= 76.5°S; ϕ= 306.2.0°E) for Gondwana compiled in this study. Palaeoposition of Laurentia are based on poles from Van der Voo (1993). Reconstruction parameters used for continents within Gondwana are from Lawver & Scotese (1987), and that for Eurasia and Laurentia is from *Royer et al.* (1992). Notice that the Early Permian reconstruction is similar to the Pangaea B palaeogeography proposed by Morel & Irving (1981), while the Early Triassic palaeogeography supports the Pangaea A2 of Van der Voo & French (1974).

Chapter 7

Early Ordovician palaeomagnetic Data from the Altiplano, southern Peru

7. 1   Sampling

As discussed in section 2.3.2, clastic marine sediments dominate the Early Ordovician sedimentary units in southern Peruvian Altiplano. Sampling for the present study was made in the Umachiri Serie, exposed at the vicinity of Umachiri village (south of Cuzco; S_{Lat}= 14.9°S; S_{Long}= 289.2°E). This series consists of greenish marine sandstones, which were folded during the Late Devonian Caledonian orogeny. Forty-one core samples drilled in various levels (7 sites) were collected from both limbs of a large-scale folded sandstone unit. Samples from this unit include massive, fine to medium-grained sandstones dominantly reddish violet (UMA1), green violet (UMA5), or green (UMA2-4 and UMA6-7) sandstones. Based on the field observation, purple and reddish rocks are more weathered, whilst the green ones are the least altered.

7. 2   Palaeomagnetic Results and Interpretation

Initial NRM intensities of the samples from Umachiri Serie range variably between 0.4-1.0 mA/m and 10-400 mA/m. Demagnetisation experiments of these samples yield two distinct high unblocking temperature components. Both directions have positive inclination (reversed polarity) and characterised by southerly (Component A) and northern (Component B) declinations, respectively (Fig. 7.1).

The A remanence is identified in 9 samples from site UMA1 and UMA6. This component is carried mainly by haematite in the samples from UMA1, and calculated from the 510-670°C data points that do not converge toward the origin in orthogonal projection. Conversely, in some samples from site UMA6, this component is carried by magnetite with unblocking temperature of about 580°C. Individual specimen directions from UMA6 were calculated from best-fit lines, some of which converge towards the origin in orthogonal projection. The overall sample mean direction of the component A is D= 180.6°; I= +35.2° (α_{95}= 8.4°; k= 38.2) *in-situ* and D= 233.1°; I= +62.6° (α_{95}= 8.4°; k= 38.2) after bedding correction (Fig. 7.2). As the confidence circle of

the *in-situ* mean direction includes the expected dipole field at the sampling area (D= 180°; I= +31°), this remanence is interpreted as a post-folding present day overprint. Notice that the mean direction in bedding corrected co-ordinates deviates from all directions calculated from reference poles younger than Early Ordovician.
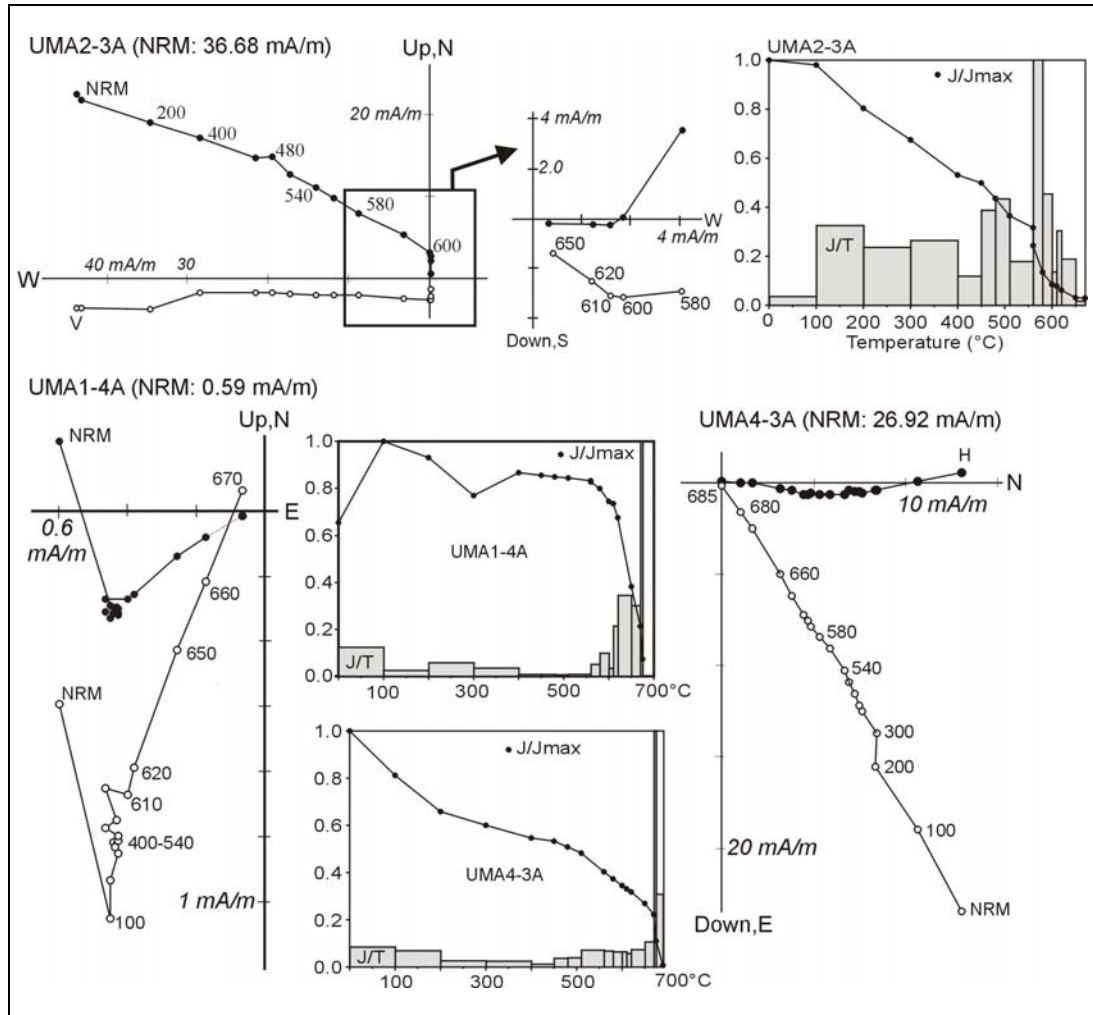
Fig. 7.1. Thermal demagnetisation results of representative samples from Umachiri Series. Closed/open circles are projection onto horizontal/vertical planes. Numbers adjacent do data points in orthogonal projections represent temperature steps in °C.

The B remanence is isolated in 18 samples from sites UMA2, 4, and 7. Individual directions were calculated either from samples having single or bi-component magnetisation (Fig. 7.1). The overall directions yield a site mean of D= 026.3°; I= +56.6° (α_{95}= 97°; k= 4.4) *in-situ*, and D= 003.6°; I= +45.5 (α_{95}= 13.5°; k= 84; N= 3 sites) after bedding correction Tab. 7.1; Fig. 7.2). This remanence passes the fold test of McElhinny (1964) at the 99% confidence level. The optimal directional grouping (Enkin; 2003) is achieved at 98.5±17.5 unfolding. This component was, therefore, acquired before

folding of the Umachiri Serie, which is thought to have occurred in mid-Devonian times

Site	n	Dg(°)	Ig(°)	Ds(°)	Is(°)	α_{95}(°)	k	λ(°N)	ϕ(°E)	dp	dm	Dipdir	Dip
UMA-2	8	063.8	60.3	005.1	37.1	9.2	37.3	54.0	297.3	6.3	10.8	327	50
UMA-4	4	341.7	22.8	355.9	52.2	13.1	50.1	42.1	284.6	12.3	18.0	137	34
UMA-7	6	070.9	60.5	008.8	46.7	10.2	44.1	46.3	300.5	8.5	13.6	325	43
Mean	N	Dg(°)	Ig(°)	α_{95}(°)	kg	Ds(°)	Is(°)	α_{95}(°)	ks	λ (°N)	ϕ(°E)	A_{95}(°)	K
	3	026.3	56.6	97.6	4.4	3.6	45.5	13.5	84.0	47.7	293.7	12.8	93.3

Tab. 7.1 Site-level palaeomagnetic data for the B remanence from the Umachiri Series. λ(°N) and ϕ(°E) are latitude (in degrees north) and longitude (in degrees east) positions of VGPs corresponding to the bedding-corrected site mean directions. λ and ϕ stand for latitude (degrees north) and longitude (degrees east) position of the mean palaeomagnetic pole calculated from the 3 listed VGPs.

The overall mean palaeopole for the Umachiri Serie B direction is situated at λ= 47.7°N; ϕ= 293.7°E (A_{95}= 12.8°; K= 93; Tab. 7.1) in South American co-ordinates, and λ= 28.3°N; ϕ= 307.8°E when rotated into African co-ordinates (Lottes & Rowley, 1990). This pole is situated far west from the Ordovician reference poles, and it diverges from the Cambrian-Ordovician segment of the APWP for Gondwana.

7. 3   Discussion and Conclusion

When transferred into African co-ordinates according to the reconstruction parameters for Gondwana (Lawver & Scotese, 1987), and compared with the high quality data from for Gondwana (Fig. 7.3), the palaeopole from Umachiri Series (λ= 28.3°N; ϕ= 307.8°E; in African co-ordinates) diverges from the cluster of Ordovician reference poles. However, the palaeolatitude position of southern Peru calculated from the results from Umachiri Series (27±5°S) is in agreement with that predicted from the Gondwana APW path, indicating vertical axis rotation of the sampling locality with respect to stable Gondwana. Comparison of the results from Umachiri Series with the reference Early Ordovician directions (Fig. 7.3) suggest that the sampling area has experienced an approximately 45° anticlockwise rotation since Early Ordovician times. This rotation is consistent with the Late Permian to Early Jurassic palaeomagnetic data reported in Gilder *et al.* (2003). These authors suggested that the rotation of the sampling area is related to a post-Oligocene left-lateral fault system that developed during the Andean orogeny.
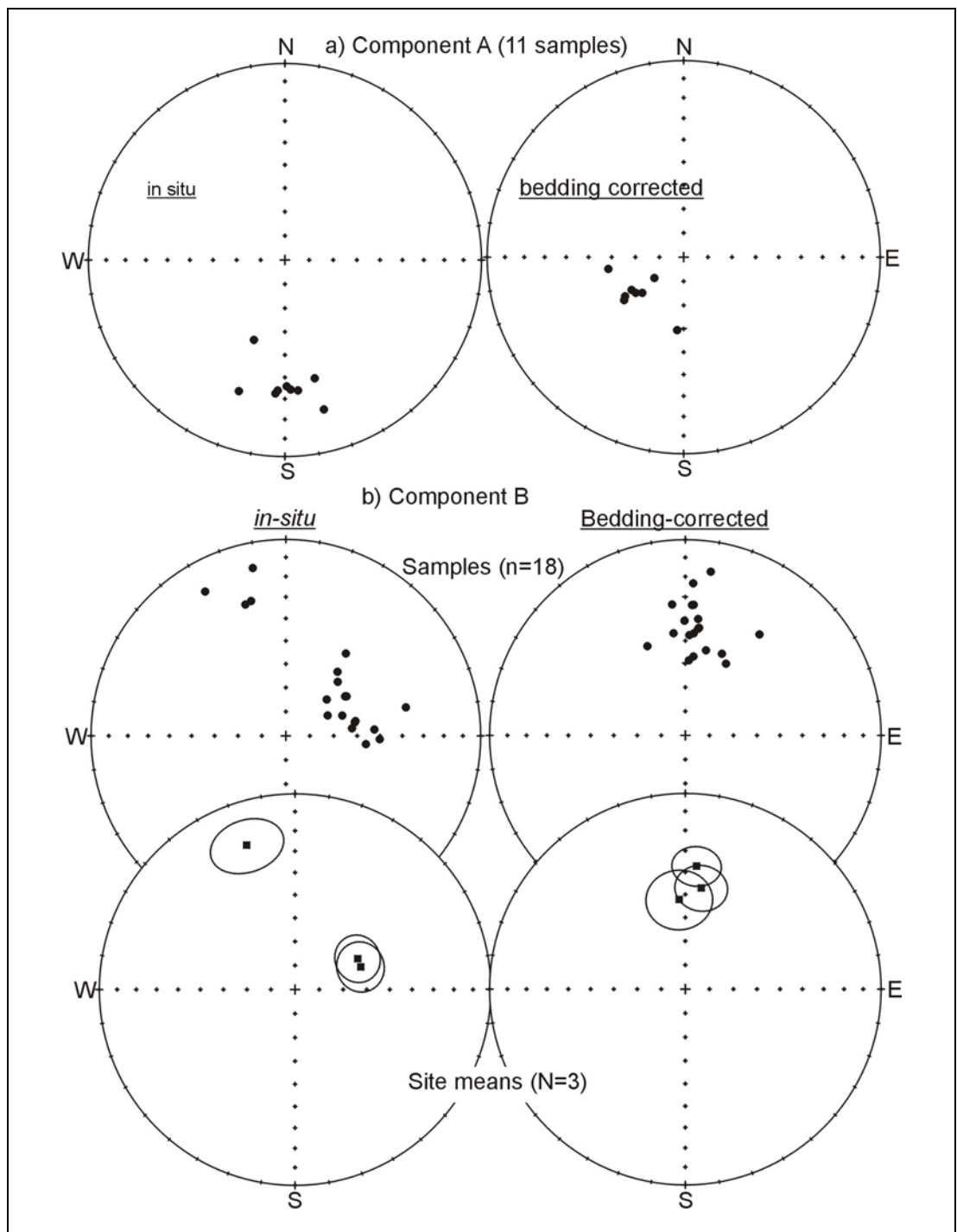
Fig. 7.2. Equal area projection of the palaeomagnetic results for Umachiri Formation. **a)** Distribution of individual sample directions for component A in *in-situ* and bedding-corrected co-ordinates. **b)** *In situ* and bedding corrected distribution of individual samples and site mean directions for component B. The 95% circles of confidences for site-means are shown.

a) palaeomagnetic pole (South African Coordinates)

b) Palaeomagnetic directions
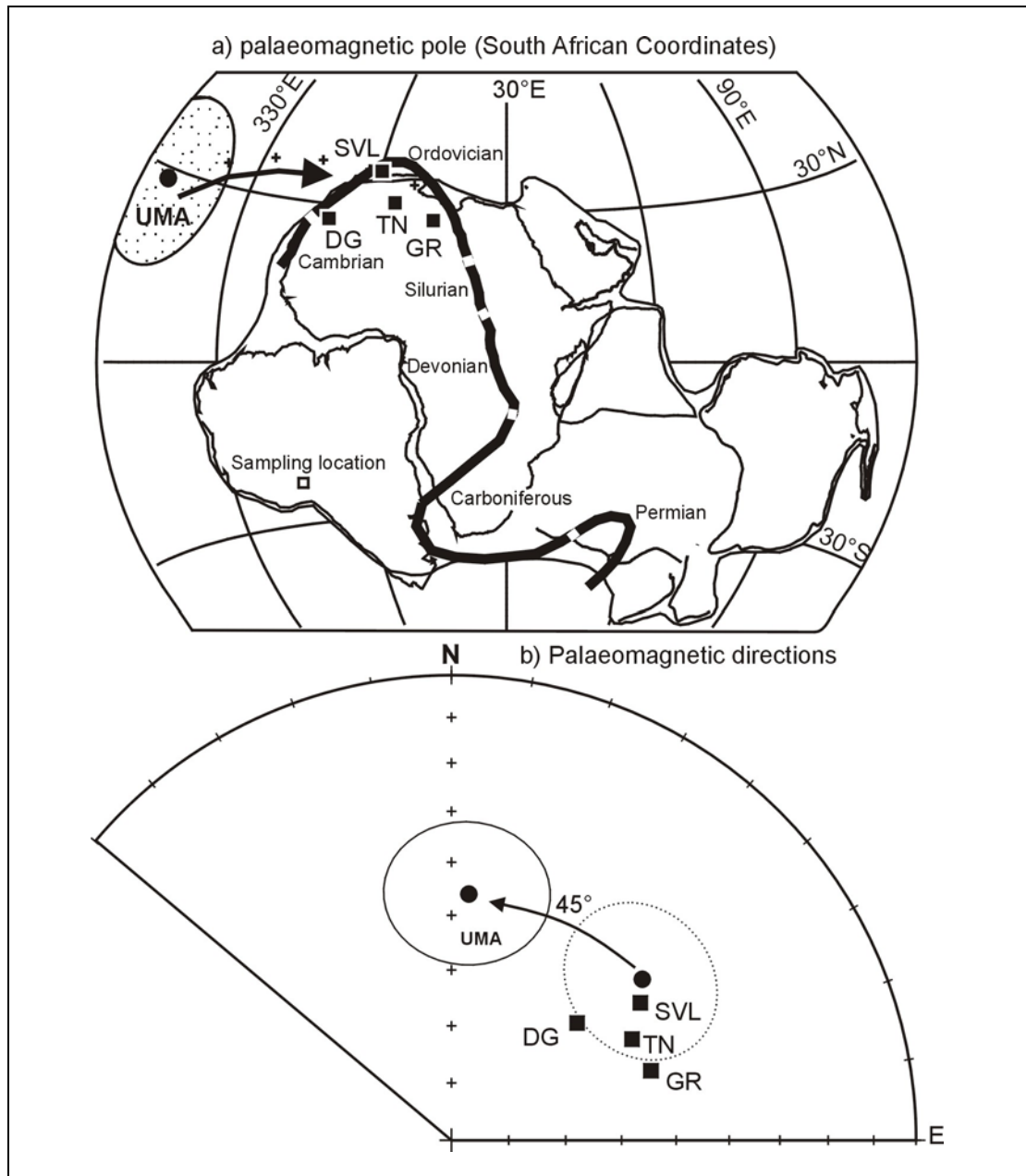
Fig. 7.3. a) Position of the pole from Umachiri Series (UMA: λ= 28.3°S; ϕ= 307.8°E; A_{95}= 13.5°) along with the reference Ordovician poles for Gondwana. **b)** Equal area projection of the mean palaeomagnetic direction from Umachiri Series (UMA; component B) compared with the expected Ordovician direction at the sampling locality (Sl_{at}= 14.9°S; S_{long}= 289.2°E). Reference directions were recalculated from published poles for Gondwana: DG= Damara Granites (Corner & Henthorn, 1978); GR= Graafwater Formation. (Bachtadse *et al.*, 1987); SVL= Southern Victoria Land (Grunow, 1995); and TN= Teall Nunatak (Lanza & Toarini, 1998). Arrow indicates that the palaeomagnetic data from Umachiri coincides with the Ordovician data for Gondwana if an approximately 45° anticlockwise rotation of the sampling area is considered.

Chapter 8

Palaeomagnetic results from Ordovician to Carboniferous Sediments of the Subandean Zone and the Eastern Cordillera

8.1   Introduction

This chapter focuses on palaeomagnetic investigations conducted on Early Ordovician to Early Carboniferous sedimentary units exposed in the Peruvian and Bolivian Subandean Zone and in the Bolivian Eastern Precordillera. Nomenclature and depositional histories of these sediments are given in sections 2.3.3 and 2.3.4. The units sampled in the southern Peruvian Subandean Zone include the Carboniferous Tarma and Ambo Groups, and the Early Devonian Cabanillas Group. In the Subandean Zone of Bolivia, the studied units include the Carboniferous Taiguati and Los Monos Formations, and the Devonian Iquiri and Huamampampa Formations. The Late Ordovician Anzaldo, Cacaňiri and San Bonito Formations were sampled in the Eastern Cordillera (Bolivia). Altogether, 539 oriented core samples (101 sites) were collected from mostly fresh, grey fine and/or medium-grained sandstones and shales.

Unfortunately, demagnetisation experiments of 643 specimens cut from these cores provided unimpressive palaeomagnetic results. With the exception of the probable primary Carboniferous remanence derived from Taiguati Formation, the studied rock units yield only overprint magnetisations and/or unstable directions. The rock units, which provided more or less consistent palaeomagnetic results are listed in table 8.1 and discussed separately. A short discussion of the palaeomagnetically unreliable results from the other studied rock units is given in section 8.1.4. The presented information may be helpful for future palaeomagnetic investigation in these areas.

Formation	Age	Location	Site	S_{lat}(°S)	S_{long}(°E)	N	n	n*
Taiguati	Ce	Mairana, Bolivia	BUT	18.15	296.07	4	18	30
Los Monos/Iquiri	Ce-Dl	Lajas, Santa Cruz, Bolivia	LAJ	18.13	296.35	17	94	94
Iquiri	Dl	Angostura, Santa Cruz, Bolivia	ANG	18.18	296.45	5	26	78
Huamapampa	Dm	Mataral, Santa Cruz, Bolivia	MAT	18.14	295.74	8	44	36
Huamapampa	Dm	Yerba Buena,Santa Cruz, Bolivia	YER	17.99	295.92	9	47	61
Anzaldo	Ol	Kakairi river, Cochabamba, Bolivia	KAK	17.62	293.63	6	33	48

Tab. 8.1. Sampling details for Palaeozoic rock units from the Subandean Zone and the Eastern Cordillera that provide consistent palaeomagnetic data. Age of rocks are: Ce: Early Carboniferous; Ce-Dl: Early Carboniferous-Late Devonian; Dl: Late Devonian; Dm: Middle Devonian: S_{lat}(°S) and S_{long}(°E) are latitude and longitude position of the sampling location (see Fig. 8.1). N: number of palaeomagnetic sampling sites; n: number of studied core samples; n*: number of specimens demagnetised.
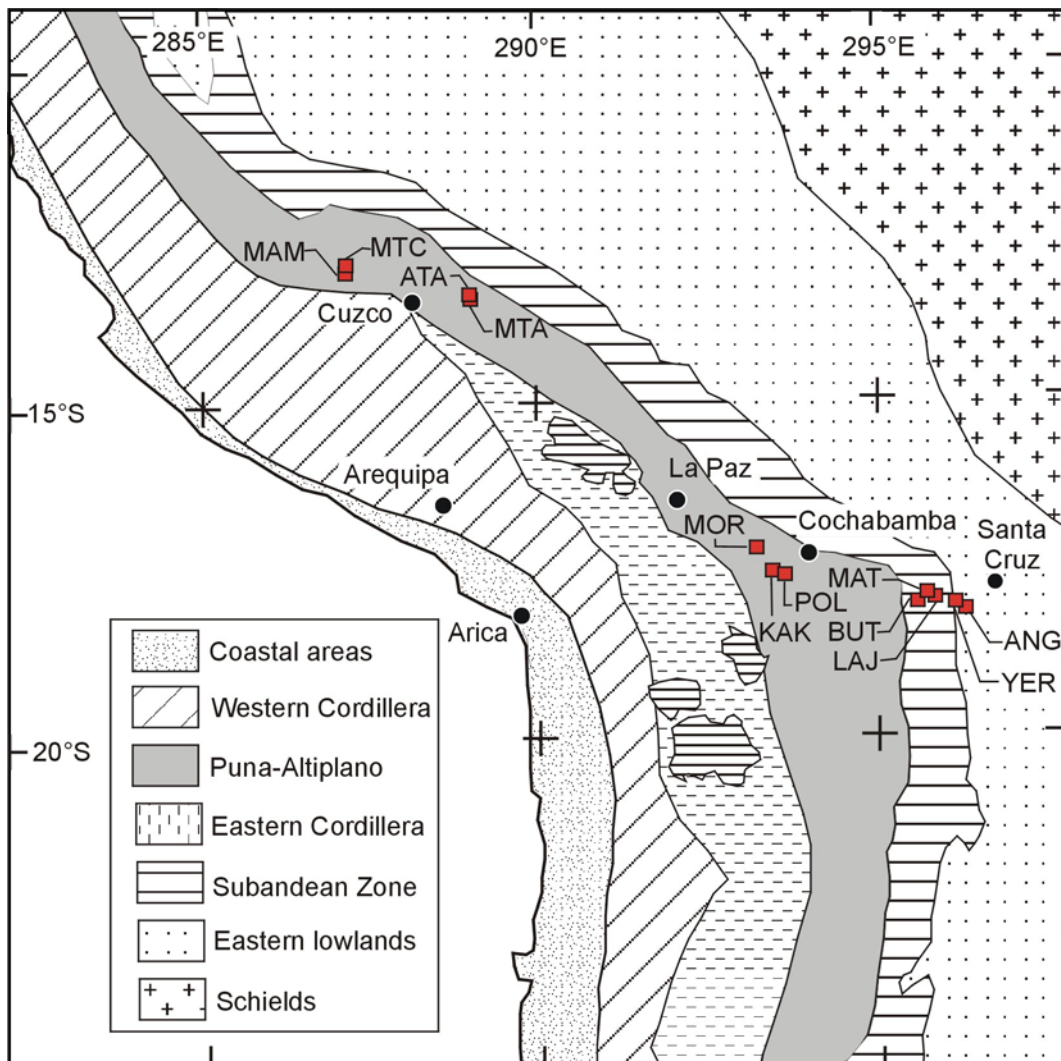
Fig. 8.1. Simplified morpho-structural sketch map of the Central Andes showing sampling locations (square) for the investigated sedimentary units. MAM: Ambo Group; MTC: Cabanillas Group; ATA: Tarma Group; MOR: San Bonito Formation; KAK/POL: Anzaldo Formation; MAT/YER: Huamampampa Formation. LAJ: Los Monos/Iquiri Formations; BUT: Taiguati Formation; ANG: Iquiri Formation. Sampling details are listed in Table 8.1 and 8.9.
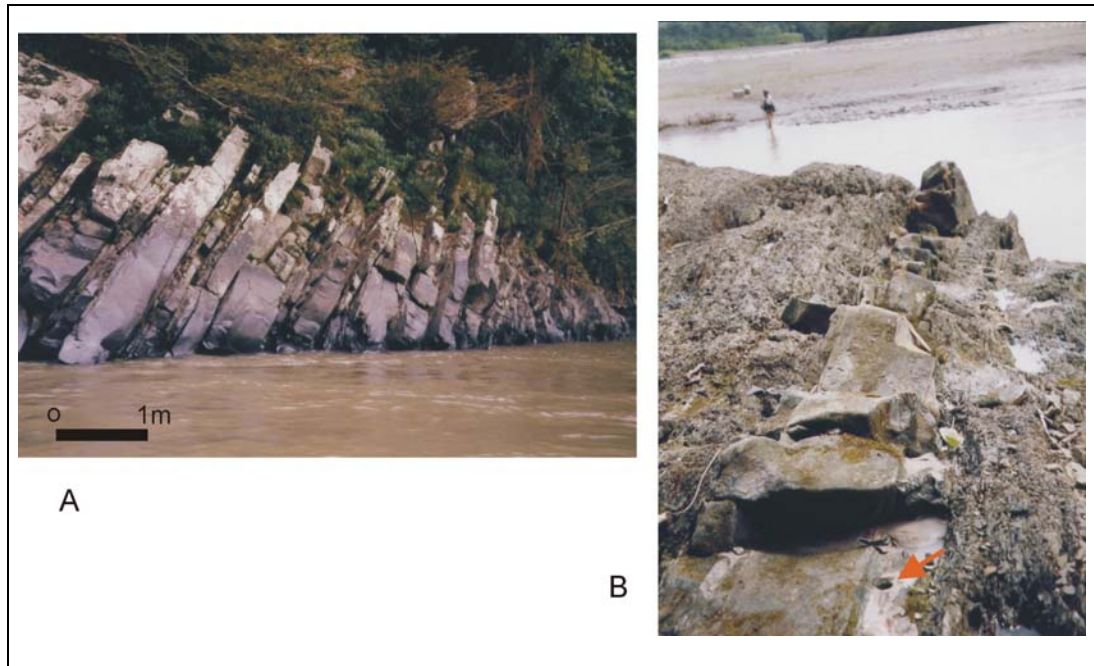
Fig. 8.2. Outcrop photographs: **A**: Ambo Group. Intercalated massive sandstone and shales. Pongo de Mainique, Urubamba River section. **B**: Cabanillas Group. Grey shales and massive sandstone beds. Arrow points on drill hole (2.5 cm in diameter). Flank of Alto de Dios River.

8.1.1 Taiguati Formation (Early Carboniferous, SAZ, Bolivia)

Previously published palaeomagnetic data from Taiguati Formation have been interpreted as being a Tertiary remagnetisation (Libarkin et al. 1998). However, the authors considered these sediments to be red-beds, though the occurrence of haematite is clearly a secondary feature due to weathering. For this reason, the same outcrop was resampled in an attempt to reveal the primary remanence in fresh less haematised parts of the exposures. The sampled unit is exposed on a road cut near Mairana (Santa Cruz-Cochabamba high way; Fig. 8.1; Tab. 8.1). It consists of alternating shales, mudstones, thinly bedded and massive sandstones, and diamictite beds. These rocks are dominantly reddish in colour due to haematisation. However, less weathered grey siltstones and fine-grained sandstone are also present at the location, and in the current study these beds were primarily targeted when sampling the unit. Samples from red siltstone and mudstone beds were also collected and analysed for comparison. The investigated samples from the Taiguati Formation include 18 oriented cores drilled in four sites involving grey and pinkish-grey siltstones, pink massive sandstones and mudstones, and red shales.

Thermal demagnetisation of 43 specimens was conducted in 15 to 18 steps with maximum temperature of 700°C. Demagnetisations results from the samples drilled in intensely haematised red shale (site BUT2) yield a single

reversed polarity remanence (Fig. 8.3). This magnetisation is identified in 11 samples and is stable up to 660°C. Unblocking temperature above 650°C indicates that the remanence is mainly carried by haematite. The overall sample-level mean direction is D= 146.3°; I= +08.9° (α_{95}= 3.6°; k= 163) *in-situ* and D= 171.3°; I= +24.2° (α_{95}= 3.6°; k= 163) after bedding correction. Comparison with the expected magnetisation at the sampling area suggests that this remanence was acquired in the Late Cretaceous, prior to the Andean deformation.

Demagnetisation results of individual samples from sites BUT-3, 4 and 5 demonstrate that the less haematised pink and grey shales and siltstones contain two distinct reversed polarity magnetisations. These remanences are dominantly carried by magnetite and hematite, respectively, based on intensity decay curves (Fig. 8.3). The remanence (A) carried by haematite has southeasterly declination and a very shallow inclination in *in-situ* co-ordinates and northerly declination after bedding-correction. As individual sample directions for the haematite remanence is dispersed around the expected Cenozoic direction (Randall; 1998), this magnetisation is interpreted as CRM overprint acquired during rock weathering.

The remanence (B) carried by magnetite is identified in 18 samples from these three sites. It yields an overall mean direction of D= 115.2°; I= +1.7° (α_{95}= 5.3°; k= 43) *in-situ* and D= 149.4°; I= +54.0° (α_{95}= 5.1°; k= 46) after bedding correction (Fig. 8.3). Directions from the more weathered samples BUT5-4 and BUT5-5, which are highly dispersed from other directions, were excluded when calculating the mean. There is a slight improvement in statistics after bedding correction but this is not statistically significant due to the only slight variation in structural attitude between the sites. However, the mean direction in *in-situ* co-ordinates diverges from all expected younger directions, whilst the bedding-corrected direction is comparable with the reference Late Carboniferous directions recalculated from published poles for Gondwana. For these reasons, the magnetite remanence (B) is considered pre-folding, and the bedding-corrected mean direction is, therefore, considered for further discussion.

The palaeomagnetic south pole corresponding to the remanence B is situated at λ= 58.3°S; ϕ= 348.9°E (A$_{95}$= 6.0°; K= 66) and λ= 27.9°S; ϕ= 53.8°E when rotated into South African co-ordinates (Lottes & Rowley, 1990). This pole position is comparable with some high quality Late Carboniferous poles from Africa (Fig. 8.5).
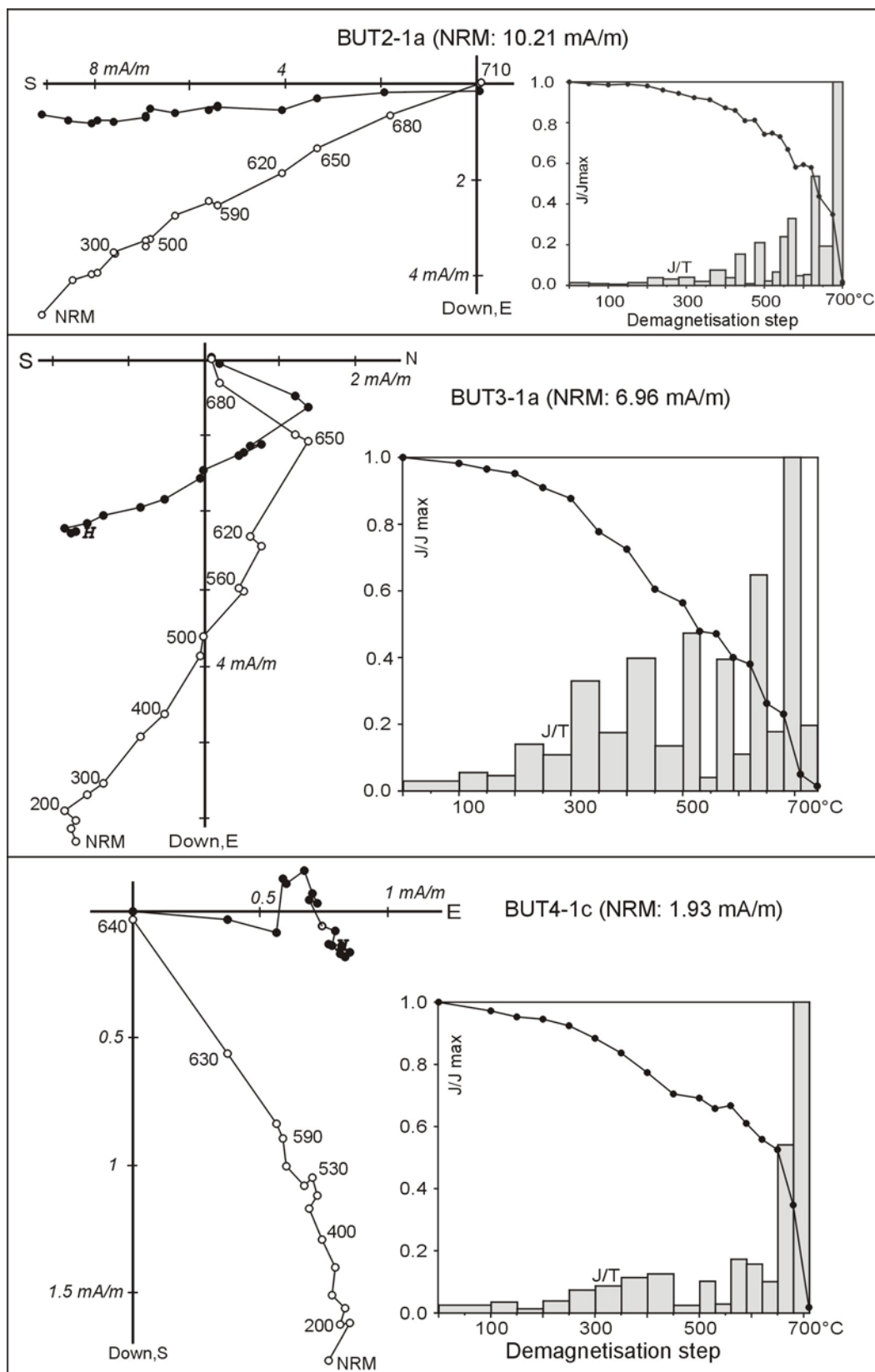
Fig. 8.3. Representative examples of demagnetisation results from the Taiguati Formation (Subandean Zone, Bolivia). Orthogonal projections represent directions in bedding-corrected co-ordinates.
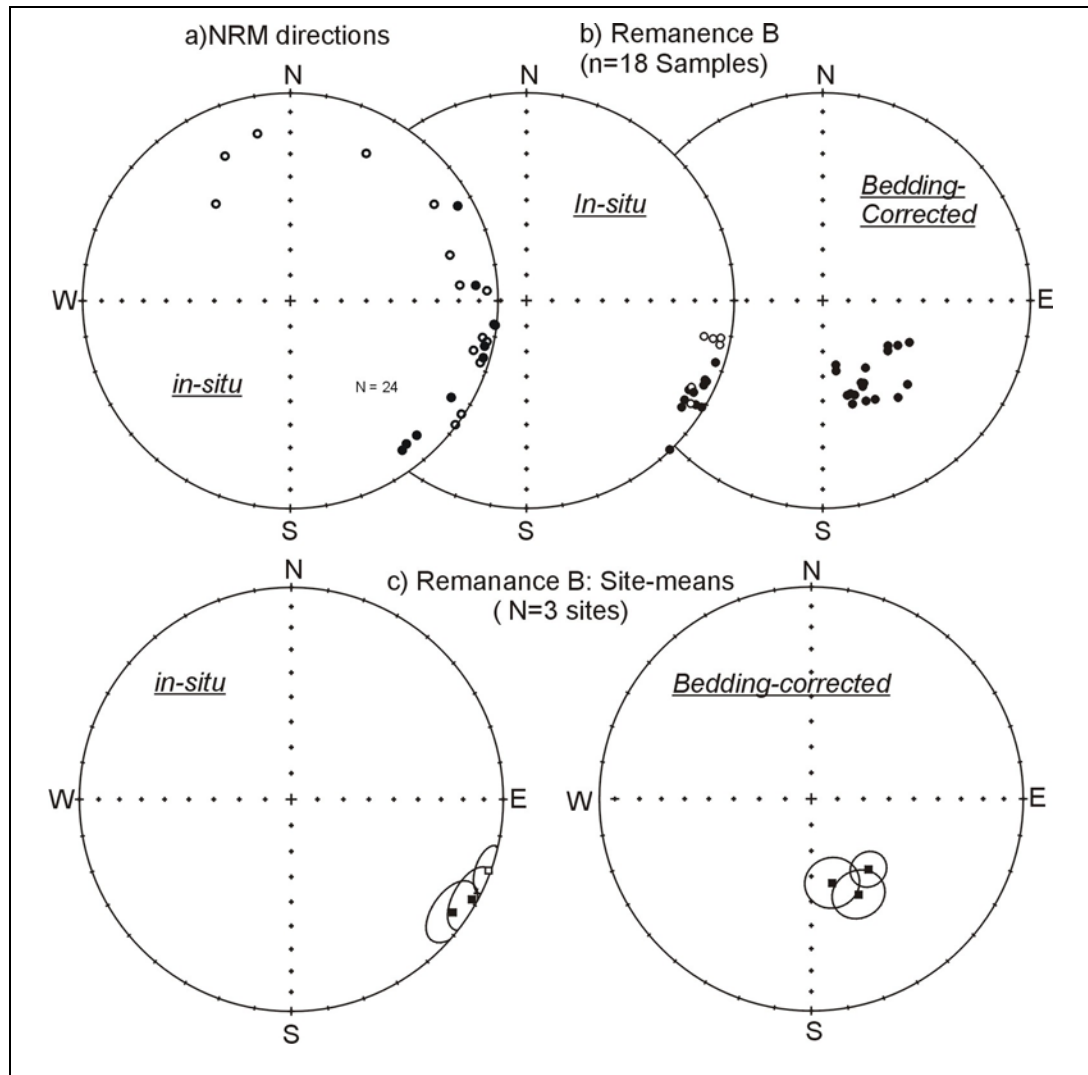
Fig. 8.4. Equal area projection of the palaeomagnetic results from Taiguati Formation. **a)** Distribution of the initial NRM directions of individual specimens. **b)** and **c)** distribution of individual directions (n= 18 samples) for the isolated remanence B in i*n-situ* and bedding-corrected co-ordinates, respectively. Site-level mean directions (BUT3, BUT4, BUT5) along with their 95% circle of confidence.

Site	n	Dg(°)	Ig(°)	Ds(°)	Is(°)	α_{95}(°)	k	P_{lat}(°S)	P_{long}(°E)	dp	dm	Dipdip	Dip
BUT3	4	119.0	2.9	153.7	48.2	9.7	91.1	63.6	356.4	8.3	12.7	259	73
BUT4	10	109.7	-1.2	141.0	54.7	6.9	49.5	51.6	12.7	6.9	9.8	259	73
BUT5	4	125.0	7.7	166.1	56.3	10.1	83.8	67.7	351.8	10.2	14.2	277	70
Mean		Dg(°)	Ig(°)	α_{95}(°)	kg	Ds(°)	Is(°)	α_{95}(°)	ks	λ(°S)	ϕ(°E)	A_{95}(°)	K
	18	115.2	1.7	5.3	43	149.4	54.0	5.1	46	58.3	348.9	6.0	65.8

Tab. 8.2. Site-level palaeomagnetic data (remanence B) from Taiguati Formation. This remanence is considered pre-folding, hence the listed VGPs (P_{lat}/P_{long}) correspond to bedding-corrected site-mean directions. The palaeomagnetic pole (λ°S/ ϕ°E) represents mean of the three VGPs.

This finding disagrees with Libarkin *et al.* (1998) who suggested that the Taiguati Formation carry only a Tertiary overprint. The magnetite remanence, described above, is clearly not a Tertiary magnetisation and does not coincide with the direction presented by these authors from the same location. However, as Libarkin *et al.* (1998) considered these sediments to be red-beds, they may have only sampled the red sandstones and shales. It is, therefore, not surprising that they identified only young remagnetisation from these more weathered rocks. The results from this study show that the grey and pinkish-grey samples yield a possible Late Carboniferous remagnetisation.
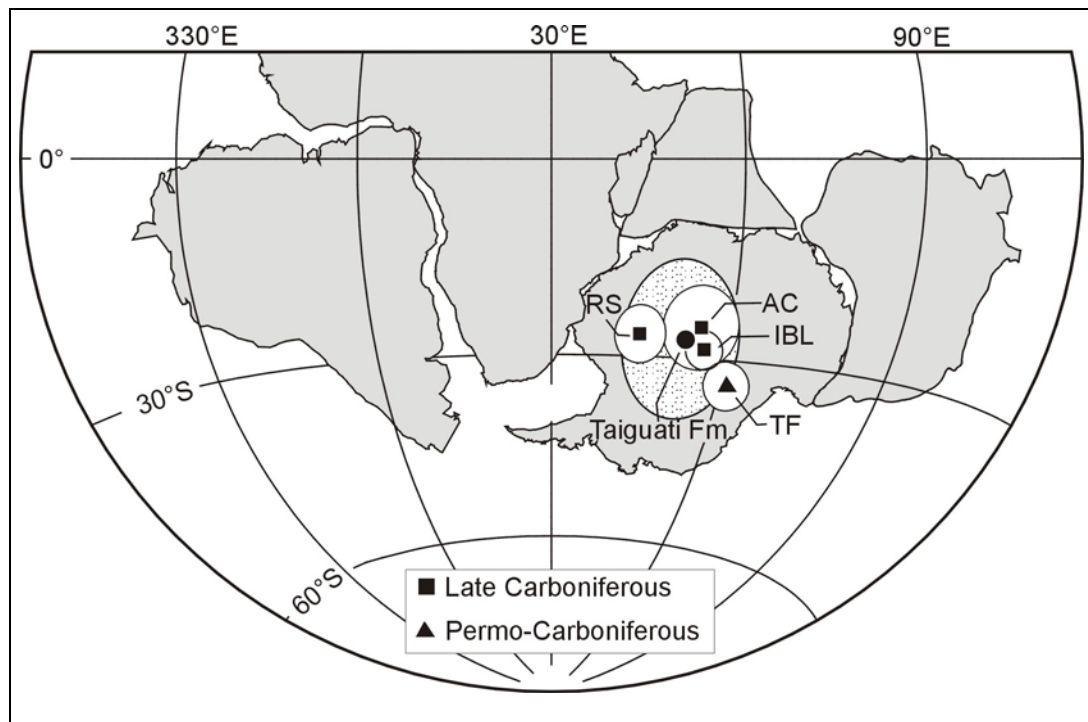
Fig. 8.5. Equal area projection showing position of the Taiguati pole (in African co-ordinates) compared with selected published high quality poles from Africa. The confidence circle for the Tiangua pole includes all Carboniferous poles from Africa. AC (307-324 Ma): Ain Ech Chebbi, Algeria (Daly & Irving, 1983); IBL (303-311 Ma): Illizi Basin, lower Formation (Henry *et al.*, 1992); TF (280-300 Ma): Tiguentourine Formation (Derder et al., 1994). RS (mid-Carboniferous): Reggane basin (Derder et al., 2001).

8.1.2 Iquiri-Los Monos Formations (Late Devonian-Early Carboniferous, Subandean Zone, Bolivia

The Early Carboniferous Los Monos Formation was sampled in southern Bolivia (LAJ). The fine- and medium-grained sandstones exposed on this locality were considered a suitable target for palaeomagnetic investigation, as previously reported palynological studies from the same locality show well-preserved microfossils. Samples from this unit were drilled in grey fine- to medium-grained sandstones. Measurement of initial NRM intensities show

that fresh grey samples are weakly magnetised (0.2-0.6 mA/m), while the more weathered grey with reddish spots or reddish rocks have intensities ranging between 3 mA/m and 6 mA/m.

Both thermal and alternating field demagnetisations of the weakly magnetised samples show erratic directional behaviour. Possible directions were calculated from data points (below 450°C) apparently converging toward the origin on orthogonal projection (Fig. 8.6a), but these are highly scattered. In opposition, 22 samples from the more weathered sites (N= 4) yield a stable remanence. The identified direction has a site-level mean of D= 005.4°; I= -26.7° (α_{95}= 30°; k= 10) *in-situ* and D= 356.7°; I= -37.5° (α_{95}= 7.0°; k= 167) after bedding-correction (Tab. 8.3). This remanence passes the fold test of McElhinny (1964) at the 99% confidence level (Fig. 8.5). Therefore, it is assumed to be a pre-folding remanence. However, the observe direction deviates from all expected directions for the Carboniferous. Instead, it is similar to the expected Early Cretaceous direction at the sampling location (Randall, 1998). This remanence is obviously an Early Cretaceous overprint, acquired prior to the Cenozoic Andean deformation. It is likely a chemical remanent magnetisation (CRM) related to rock weathering.

Site	n	Dg(°)	Ig(°)	Ds(°)	Is(°)	α_{95}(°)	k	P_{lat}(°S)	P_{long}(°E)	dp	dm	dipdir	dip
LAJ1	8	18.0	-11.8	352.3	-30.1	90.1	37.8	82.4	40.2	5.6	9.1	80	62
LAJ2	6	29.8	-15.4	354.3	-42.0	9.0	55.9	81.9	336.4	6.8	11.0	80	62
LAJ14	4	342.5	-35.0	358.8	-37.5	15	38.5	86.9	317.7	10.4	17.7	267	22
LAJ16	4	343.6	-38.5	1.9	-40.2	8.4	120.6	84.9	276.2	10.9	18.1	267	22
LAJ6-9	6					Incoherent data							
Mean	N	Dg(°)	Ig(°)	α_{95}(°)	kg	Ds(°)	Is(°)	α_{95}(°)	ks	λ(°S)	ϕ(°E)	A_{95}(°)	K
	4	5.4	-26.7	30.0	10.3	356.7	-37.5	7.1	167	85.7	341.1	6.1	227

Tab. 8.3. Site-level palaeomagnetic data from the Lower Carboniferous Los Monos Formation (Subandean Zone, Bolivia). This remanence is considered pre-folding. The listed VGPs (P_{lat}/P_{long}) and the mean palaeomagnetic south pole (λ°S/ ϕ°E), therefore, correspond to the bedding-corrected mean directions.

Initial NRM intensities of the Uppermost Devonian Iquiri Formation range between 0.06 to 0.35 mA/m. Stepwise demagnetisation of representative samples from each sampling site (ANG) yield a soft magnetic component defined below 300°C. This component is identified in 18 samples from five sites (Tab. 8.4), yielding an overall site-mean direction of D= 349°; I= -18° (α_{95}= 9.7°; k= 40) *in-situ* and D= 354°; I= -13°; (α_{95}= 10.9°; k= 32) after bedding-correction. The increasing scattering of the site-level directions after bedding correction indicates a post-folding nature of this remanence. As the *in-situ* coordinate mean direction is statistically indistinguishable from the expected present magnetic field (D= 352°; I= -12°), this low unblocking

temperature magnetisation is interpreted as a VRM acquired under the present geomagnetic field.
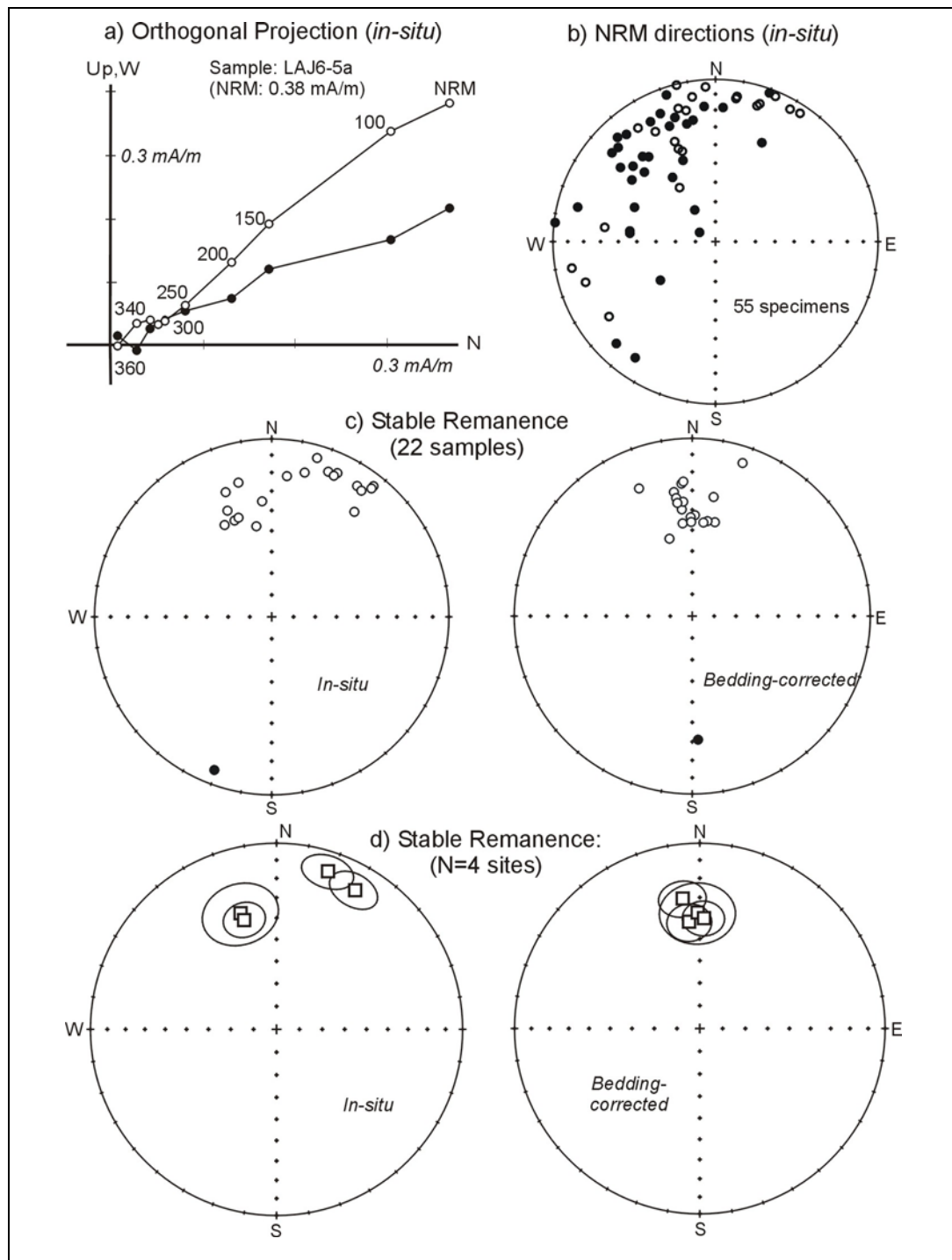
Fig. 8.6. Palaeomagnetic results from the Los Monos Formation. **a)** Orthogonal projection of typical behaviour during stepwise thermal demagnetisation. **b)** Equal area projection of individual NRM directions (55 specimens). **c)** and **d)** Equal area projection of the distribution of individual samples **(c)** and site-level mean directions **(d)** for the isolated stable remanence. This remanence yields a positive fold test significant at the 99% confidence level, therefore, considered to be pre-folding.

Site	n	Dg(°)	Ig(°)	Ds(°)	Is(°)	α_{95}(°)	k	P_{lat}(°S)	P_{long}(°E)	dp	dm	dipdir	dip
ANG1	5	342.6	-20.0	349.9	-12.1	7.7	62.0	71.5	49.4	4.2	8.1	239	26
ANG2	3	355.1	-13.8	359.4	-6.7	9.6	49.6	77.8	92.8	5.0	9.8	253	24
ANG3	3	352.3	-11.6	5.8	-1.8	17.9	19.2	75.4	83.3	9.2	18.2	256	31
ANG4	4	351.4	-17.9	357.8	-10.3	14.2	42.9	77.7	72.6	7.6	14.7	251	26
ANG5	3	329.3	-13.2	355.5	-12.0	26.7	12.7	57.6	43.6	13.5	26.5	240	27
Mean	N	Dg(°)	Ig(°)	α_{95}(°)	k	Ds(°)	Is(°)	α_{95}(°)	k	λ(°S)	ϕ(°E)	A_{95}(°)	K
	5	348.8	-18.0	9.7	40	354.3	-13.1	10.9	32	73.0	62.0	10.1	58

Tab. 8.4. Palaeomagnetic results from the Upper Devonian Iquiri Formation. P_{lat} and P_{long} are latitude (degrees south) and longitude (degrees east) position of VGPs calculated from *in-situ* site-level mean directions. Position of the mean palaeomagnetic south pole is designated by λ(°S): latitude in degrees south and ϕ(°E): longitude in degrees east. This remanence is interpreted as being a post-folding overprint.
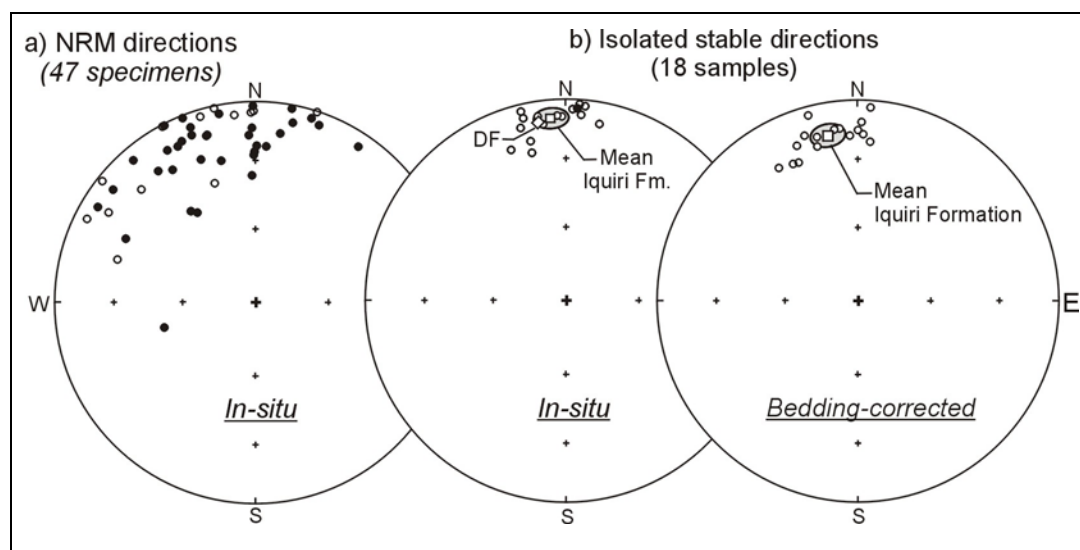
Fig. 8.7. Equal area projection of the palaeomagnetic results obtain from the Iquiri Formation. **a)** Distribution of the individual initial NRM directions (48 specimens). **b)** Distribution of the isolated stable directions from 18 samples.

8.1.3 Huamampampa Formation (mid-Devonian, SAZ, Bolivia)

The investigated samples from Huamampampa Formation include 23 oriented cores drilled in the Mataral area (MAT; Tab. 8.1; Fig. 8.1). Magnetic measurements of 36 specimens demonstrate that sandstones of this Formation are also weakly magnetised, with initial NRM intensities below 3 mA/m. Individual demagnetisation results from most samples show unstable directions after 350°C. Six samples from sites MAT2 and MAT4, however, yield a soft magnetisation (below 300°C). The overall mean of this component (D= 352.7°; I= -21.5°; α_{95}= 9.6; k= 50) is undistinguishable from the present day magnetic field at the sampling area (D= 352°; I= -12°), therefore it is obviously a VRM magnetisation.

Samples collected in the area near Yerba Buena (YER; Fig. 8.1; Tab. 8.1) yield average quality demagnetisation results. Stable remanences were identified in 22 samples out of the 36 analysed samples. The overall directions show poor grouping on within-site level ($\alpha_{95} > 17°$). However, the overall site means are cluster around the mean direction D= 344°; I= +45° (α_{95}= 14°, k= 31) *in-situ*, and D= 319°; I= +33° (α_{95}= 13.8°; k= 32) after bedding correction (Fig. 8.8; Tab. 8.5). Stepwise unfolding (Enkin, 2003) demonstrates an optimal grouping at 50%, suggesting the syn-folding nature of this remanence. It is difficult to constrain the relative age of this remanence because all directions in *in-situ*, 50% unfolding, and bedding-corrected co-ordinates deviate from all reference directions in the sampling area. This discrepancy may indicate local rotation in the sampling area, but the grouping of data is also very poor and no further interpretation can be placed on the results.
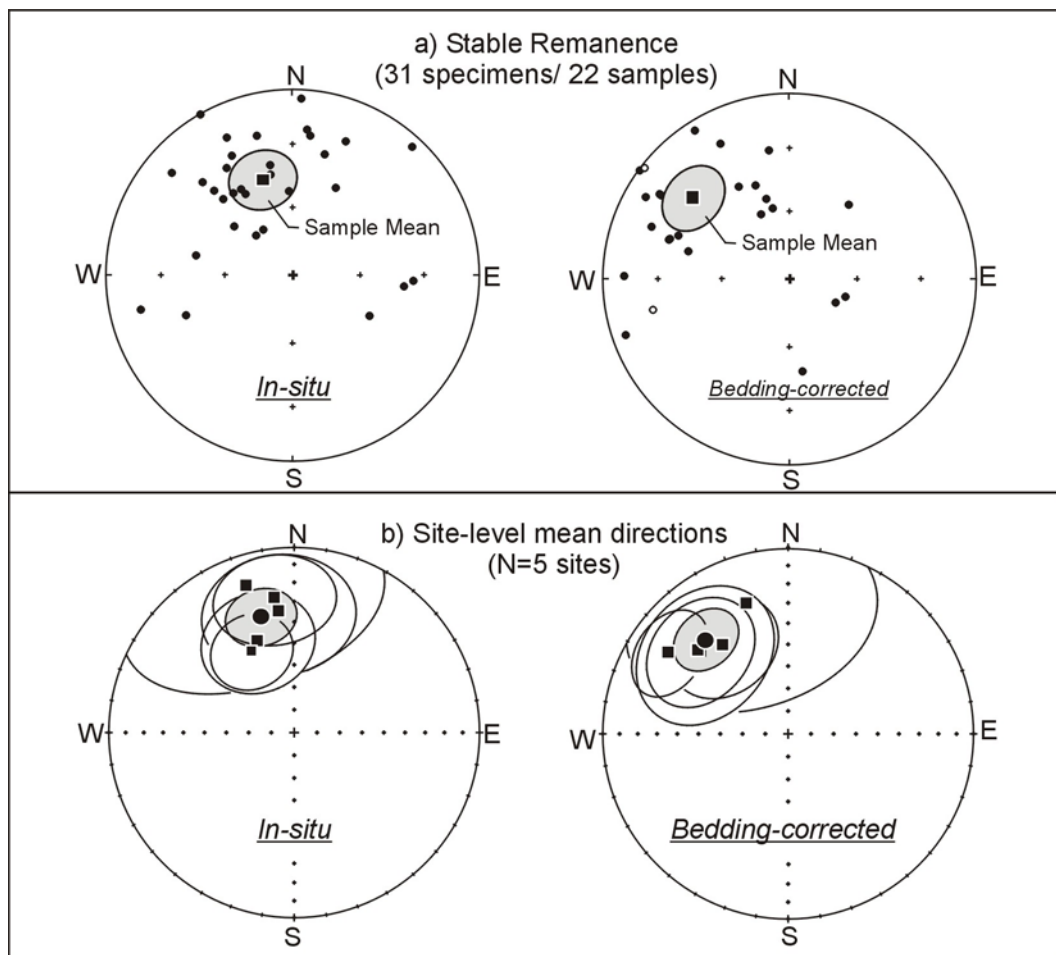
Fig. 8.8. Equal area projection of the palaeomagnetic data from the Middle Devonian Huamampampa Formation. **a)** Distribution of the individual directions isolated in 31 specimens cut from 22 samples. **b)** Site-level mean palaeomagnetic directions along with their 95% confidence circles. Shaded area represents confidence circle about overall mean direction.

Site	n	Dg(°)	Ig(°)	Ds(°)	Is(°)	α_{95}(°)	k	P_{lat}(°S)	P_{long}(°E)	dp	dm	dipdir	dip
YER2	4	351.6	27.1	323.4	39.9	23.3	16.5	35.8	253.2	16.8	28.0	231	42
YER3	3	341.9	17.4	342.4	26.8	49.3	7.2	42.4	246.0	29.4	54.1	231	42
YER4	4	352.5	34.1	313.4	36.1	30.3	10.1	30.6	243.5	20.5	35.3	241	51
YER7	5	338.1	45.6	313.0	34.3	23.7	11.4	30.9	242.1	15.5	27.1	256	31
YER9	6	332.3	48.8	304.3	22.8	17.4	20.4	27.4	230.2	9.8	18.1	262	44
Mean	N	Dg(°)	Ig(°)	α_{95}(°)	kg	Ds(°)	Is(°)	α_{95}(°)	ks	λ(°S)	ϕ(°E)	A_{95}(°)	K
	5	344.0	34.8	14.1	30.5	319.2	32.7	13.8	31.7	-	-	-	-
50% unfolding						331.1	35.9	11.9	43.6	33.4	242.6	8.6	79

Tab. 8.5. Site-mean palaeomagnetic directions from the Huamampampa Formation (YER, Santa Cruz, Bolivia). The listed VGPs (P_{lat}/P_{long}) correspond to the bedding-corrected site-level mean directions. λ(°S) and ϕ(°E) designate the latitude and longitude position of the mean palaeomagnetic pole calculated from the 50% unfolded directions. The YER remanence is considered as being syn-folding.

8.1.4   Other Palaeozoic rock units

Most of the Early Palaeozoic marine sandstones of the Subandean Zone and the Eastern Cordillera are very weakly magnetised. Magnetic intensities of these rocks are generally below 0.3 mA/m and as low as 0.02 mA/m in some units. Apart from the units discussed above, other 296 specimens cut from about 200 oriented core drilled in 52 sampling sites were analysed using AF demagnetisation, thermal demagnetisation or both techniques.

Despite the attempt to isolate stable remanence components in these rocks, demagnetisation results of individual samples from all locations listed in Table 8.6 commonly show erratic directional behaviour after few demagnetisation steps. Consequently, no palaeomagnetic direction could be defined from most of the samples. Some units, however, yield occasional stable remanences but these directions are inconsistent in both within-site and between-site level.

Moreover, poorly defined stable directions calculated from data points showing apparent linear segments on orthogonal projection yields highly dispersed overall directions in both sample and site-level. These data are, therefore, considered palaeomagnetically unreliable. Some examples of demagnetisation results and distributions of the isolated directions are shown in Fig. 8.9 (Tarma Group; Late Carboniferous) and Fig. 8.10 (Catavi Formation, Middle Silurian).

Rock Unit	Site	Age	Location	S_{lat}(°S)	S_{long}(°E)	N	n	n*	Lithology
Tarma Group	MTA	Cl	Pongo de Mainiqui, Cuzco, Peru	12.25	287.18	6	32	24	Green and grey fine-grained sandstones
Ambo Group	MAM	Ce	Pongo de Mainiqui, Cuzco, Peru	12.25	287.17	8	46	53	Grey massive medium to fine-grained sandstonces
	ATA9	Ce	Coñec, Cuzco, Peru	12.90	288.63	7	40	19	Grey shales and sandstones
Cabanillas Group	ATA1	De	Coñec, Cuzco, Peru	12.90	288.63	10	50	27	Cross-bedded fine-grained sandstones, shales, carbonate lenses
	MTC	De	Pongo de Mainiqui, Cuzco, Peru	12.25	288.18	7	36	30	Intercalated grey sandstone and shales
Catavi Formation	BOM	Sm	Bombeo, Cochabamba, Bolivia	17.67	293.54	3	15	45	Grey massive sandstones
Cacañiri Formation	TUN	Ol	Tunel, Cochabamba, Bolivia	17.21	294.54	7	36	62	Grey medium-grained sandstones
Anzaldo Formation	POL	Ol	Polvorin, Cochabamba, Bolivia	17.67	293.75	4	22	36	Grey medium-grained sandstones

Tab. 8.6. Sampling details for the Palaeozoic sedimentary units from the Subandean Zone and the Eastern Cordillera. The listed units are very weakly magnetised and did not provide reliable palaeomagnetic data. Sampling sites are shown in Fig. 8.1. Age of the units are: Cl: Late Carboniferous; Ce: Early Carboniferous; De: Early Devonian; Sm: Middle Silurian; Ol: Late Ordovician. N: number of palaeomagnetic sites; n: number of collected core samples; n*: number specimens analysed.
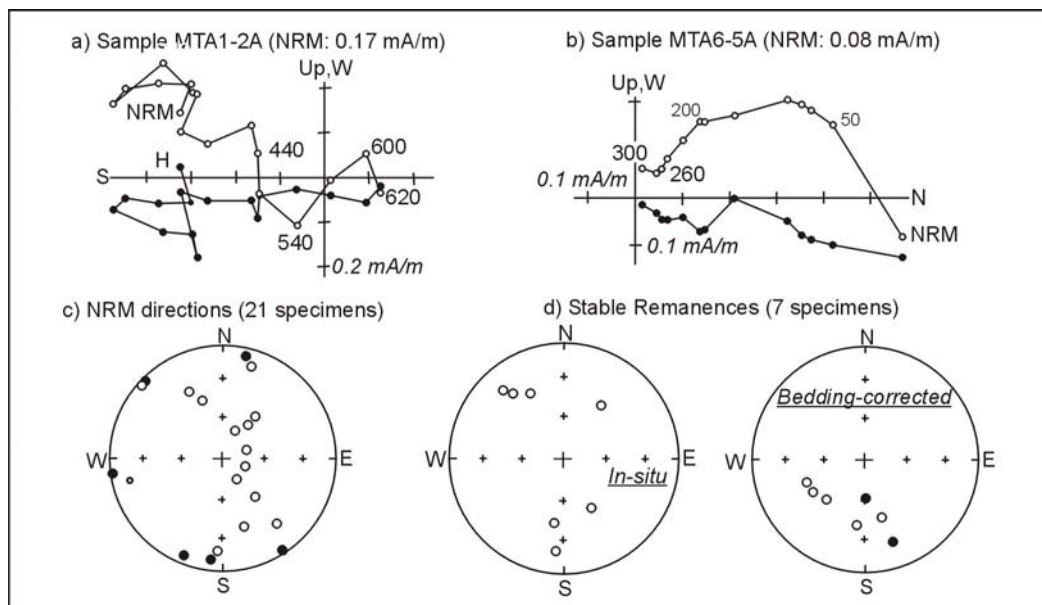
Fig. 8.9. Palaeomagnetic results for the Tarma Group (Subandean Zone, Peru). a) and b) orthogonal projections showing directional behaviour of representative samples during stepwise demagnetisation. c) Equal area projection of the distribution of the initial NRM. d) and e) Distribution of the probable stable component (7 samples) in *in-situ* and bedding-corrected co-ordinates.
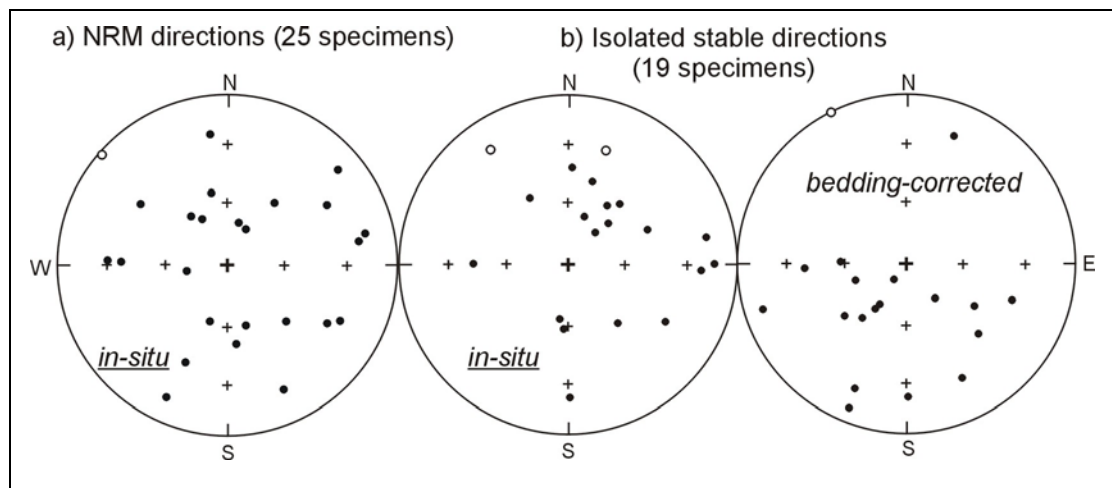
Fig. 8.10. Equal area projection showing distribution of the initial NRM directions (a) and the isolated directions (b) from the Middle Silurian Catavi Formation (Subandean Zone, Bolivia). As the isolated directions show large scatter in both sample- and site-level, palaeomagnetic data from this unit is considered unreliable.

8.2   Conclusion

Despite the extensive sampling of Palaeozoic rocks exposed in the Subandean Zone and the Eastern Cordillera, the majority of the palaeomagnetic results are unsatisfying. This is due to the weak magnetisation of most of the studied units and their relatively small amount of ferromagnetic minerals. Nevertheless, the component B direction from the Taiguati Formation (Subandean Zone) is interpreted to be a remagnetisation acquired in the Late carboniferous. This remanence is exclusively carried by magnetites, and significantly different from the Cenozoic remagnetisation (component A) carried by haematite.

Comparison with the previously published palaeomagnetic data from stable South America obtained from well-dated Late Carboniferous rocks having a quality factor Q≥3 (Van der Voo, 1990) shows reasonable agreement between the palaeopole obtained from Taiguati Formation (λ= 58.3°S; ϕ= 348.9°E; A_{95}= 6.0°) and the coeval selected poles (Tab. 8.7; Fig. 8.11). Integration of the pole from Taiguati Formation in the published poles results in a mean Late Carboniferous pole for South America situated at λ= 53.0°S; ϕ= 348.4°E (A_{95}= 6.0°; K= 86.4; N= 8 studies). Palaeopoles corresponding to the remagnetised Iquiri and Los Monos Formations plot on the Cretaceous segment of the APW path, thus providing further evidence that no rotation of the sampling area occurred during the Andean orogeny.

	Location	Age (Ma)	λ (°S)	ϕ (°E)	$\lambda*$ (°S)	$\phi*$ (°E)	A_{95}(°)	Ref.
PC	Pilar and Cas Formations	290-323	57.0	350.0	23.3	053.3	9.0	(1)
IT	Itarare Subgroup, Tubarao Gp.	290-323	56.0	357.0	20.7	056.5	11.0	(2)
CB	La Colina Basalt, Combined	295-305	66.0	348.0	31.5	057.8	5.0	(3)
CF	La Colina Formation	290-300	49.0	343.0	18.7	045.0	5.0	(4)
PF	Piaui Formation	300-323	50.0	345.0	18.9	046.7	16.0	(5)
HV	Hoyda Verde	330-323	41.9	356.2	8.2	049.8	5.7	(6)
TF	Taiguati Formation	290-323	45.0	340.0	16.5	040.9	8.0	(5)
BUT	Taiguati Formation	290-323	58.3	348.9	25.1	054.2	6.0	(7)
	Mean (N=8 studies)	**290-323**	**53.0**	**348.4**	**20.4**	**50.3**	**6.0**	**K=86.4**

Tab. 8.7. Late Carboniferous palaeomagnetic data with quality index Q≥3 (Van der Voo, 1990) and good age control from South America. λ(°S)/ϕ(°S): pole position in South American co-ordinates. $\lambda*$(°S)/$\phi*$(°S): pole position in African co-ordinates following the reconstruction parameters of Lawver & Scotese (1987). References are (1) Jesinkey *et al.* (1987); (2) Valencio *et al.* (1975); (3) Thompson & Mitchell (1972); (4) Sinito *et al.*, (1979); (5) Créer (1970); (6) Rapalini & Vilas (1991); (7) This study.
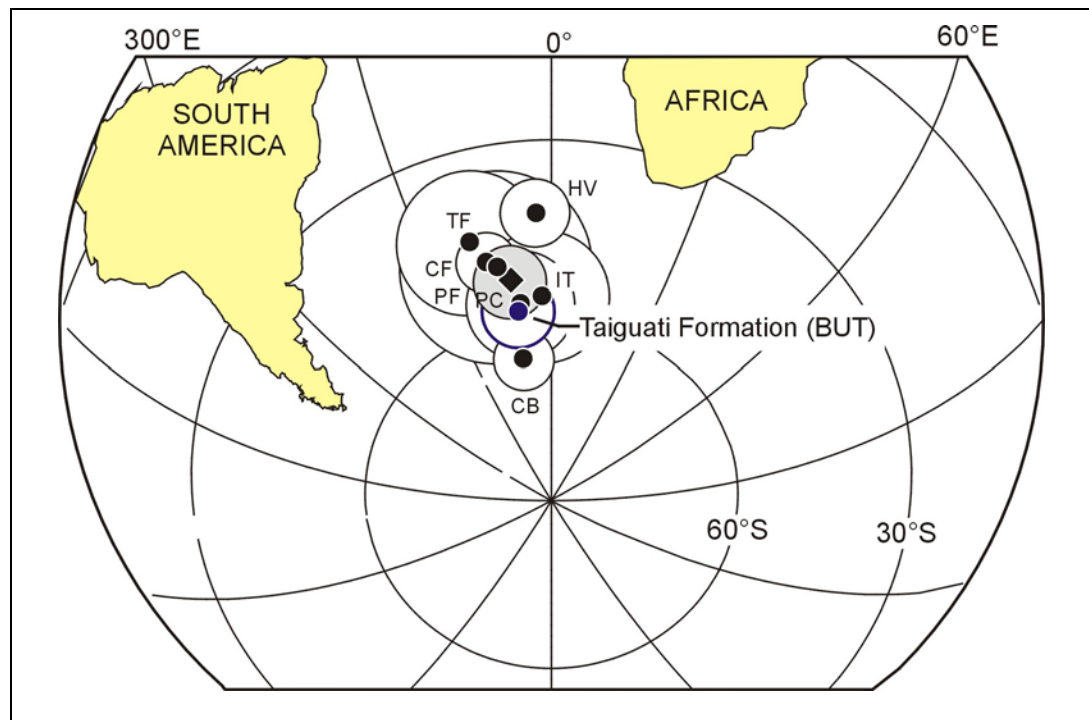
Fig. 8.11. Position of the palaeomagnetic south pole from Taiguati Formation (bleu circle) compared with the selected published poles for stable South America (black circles) listed in Table 8.7. The overall mean pole calculated from 8 studies (λ= 53.0°S; ϕ= 348.4°E; A_{95}= 6.0°) is presented by diamond with grey confidence circle.

Chapter 9

Palaeomagnetism of the Permian and Carboniferous rock units of the Pampean Ranges and the Paganzo Basin, NW Argentina

9.1   Introduction

Palaeomagnetic results presented in this chapter are based on investigation of 124 oriented cores drilled in 22 sites. Late Carboniferous and Early Permian ages are respectively attributed to the studied units, based on published palaeontological data. Results from the Stephanian Solca Formation, the Namurian-Early Westphalian Malanzán Formation sampled in the Paganzo Basin, and the Early Permian La Antigua Formation from the Pampean Range are discussed (Fig. 9.1; Tab. 9.1). Geological background of the sampling area (Fig. 9.1 inset) is given in section 2.3.4.
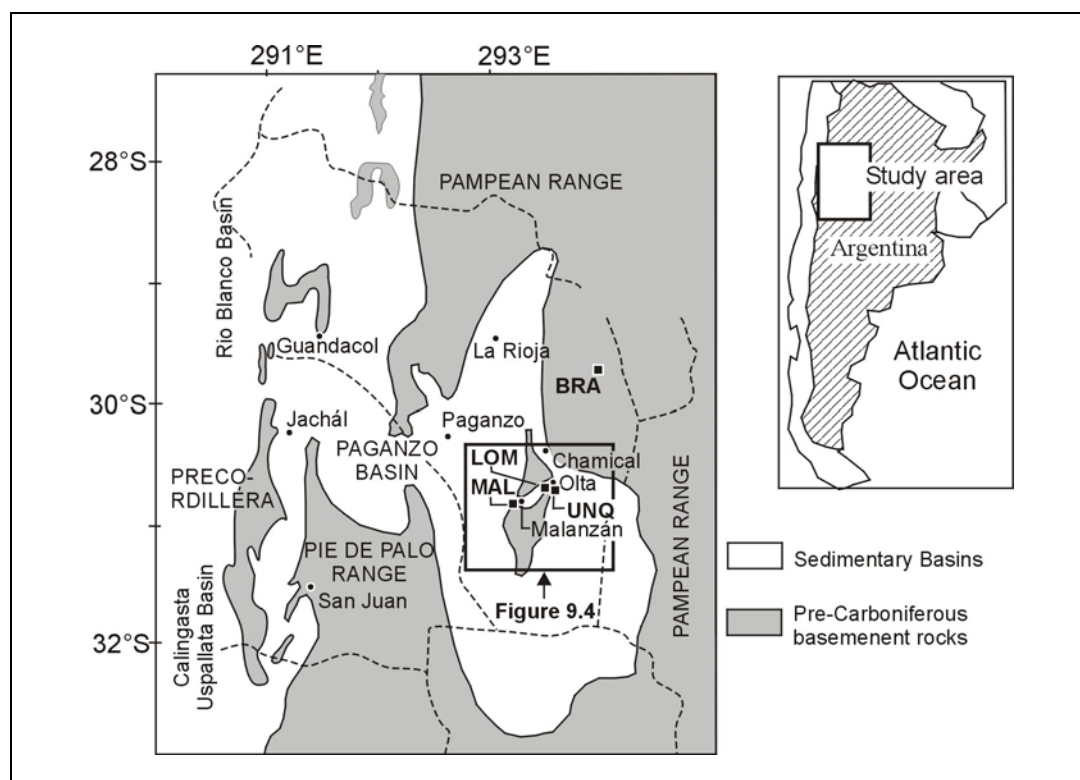
Fig. 9.1. Simplified sketch map (modified from Limarino *et al.*, 2002) showing sampling locations (filled squares) for the investigated Permian and Carboniferous sedimentary units. See Table 9.1 for location names and sampling details.

Formation	Age	Location	Site	S_{lat}(°S)	S_{long}(°E)	N (s/c)
La Antigua	L. Permian	Sierra Brava, La Rioja	BRA	29.72	293.97	6/29
Solca	U. Car-L. Per	Loma Larga, La Rioja	LOM	30.77	293.52	5/29
Malanzàn	U. Carbon.	Malanzàn-Solca, La Rioja	MAL	30.81	293.43	6/30
Malanzàn	U. Carbon.	Unquillal, La Rioja	UNQ	30.78	293.64	6/36

Total: 22 sites; 124 oriented cores

Tab. 9.1. Sampling details of the investigated Permian and Carboniferous rock units in NW Argentina. S_{lat} (°S) and S_{long} (°E) are latitude and longitude position of the sampling location in degrees south and east, respectively. N/n: Number of studied cores/samples.

9.2 Pampean Ranges

9.2.1. La Antigua Formation (Early Permian)

The La Antigua Formation was sampled on both limbs of a gently folded structure exposed in Sierra Brava (location BRA, Fig. 9.1). Shallowly NE and SW dipping beds (6°-24°) of reddish fine-grained sandstone, yellowish to pink siltstone, and volcano-clastic deposits were drilled in six sampling sites. An Early Permian age is attributed to the La Antigua Formation based on palaeontology and stratigraphic correlation (Coira & Koukharsky; 1968).

Fifty-three specimens cut from 29 cores were thermally demagnetised in 10 to 18 steps, with maximum temperatures of 700°C. Demagnetisation results of individual samples reveal two distinct magnetic components: a low unblocking temperature magnetisation (A) erased below 300°C, and a high unblocking temperature remanence. The soft magnetic A direction, generally representing less than 10% of the initial NRM intensity, is identified in 9 cores from sites BRA3, BRA4 and BRA5. It consists of normal polarity magnetisation with northerly declination, yielding an overall *in-situ* site-mean of D= 017.7°; I= -34.7° (α_{95}= 12.0°; k= 107). The significant increase of directional scattering, at both the sample and site level (Tab. 9.2a; Fig. 9.3), after bedding correction indicates the post-folding nature of this magnetisation. Component A is interpreted to be a viscous magnetisation.

The high unblocking temperature component B was identified in 25 samples from six sampling sites. B direction constitutes more than 90% of the initial NRM in almost all samples. A best-fit line passing through vector end points that converges toward the origin on orthogonal projection generally defines this remanence. Directions from individual specimens were calculated between 400° and 680° demagnetisation steps (Fig. 9.2). Intensity decay curves suggest that component B is carried in various proportion by both

magnetite and hematite, with unblocking temperature about 580°C and above 650°C, respectively.
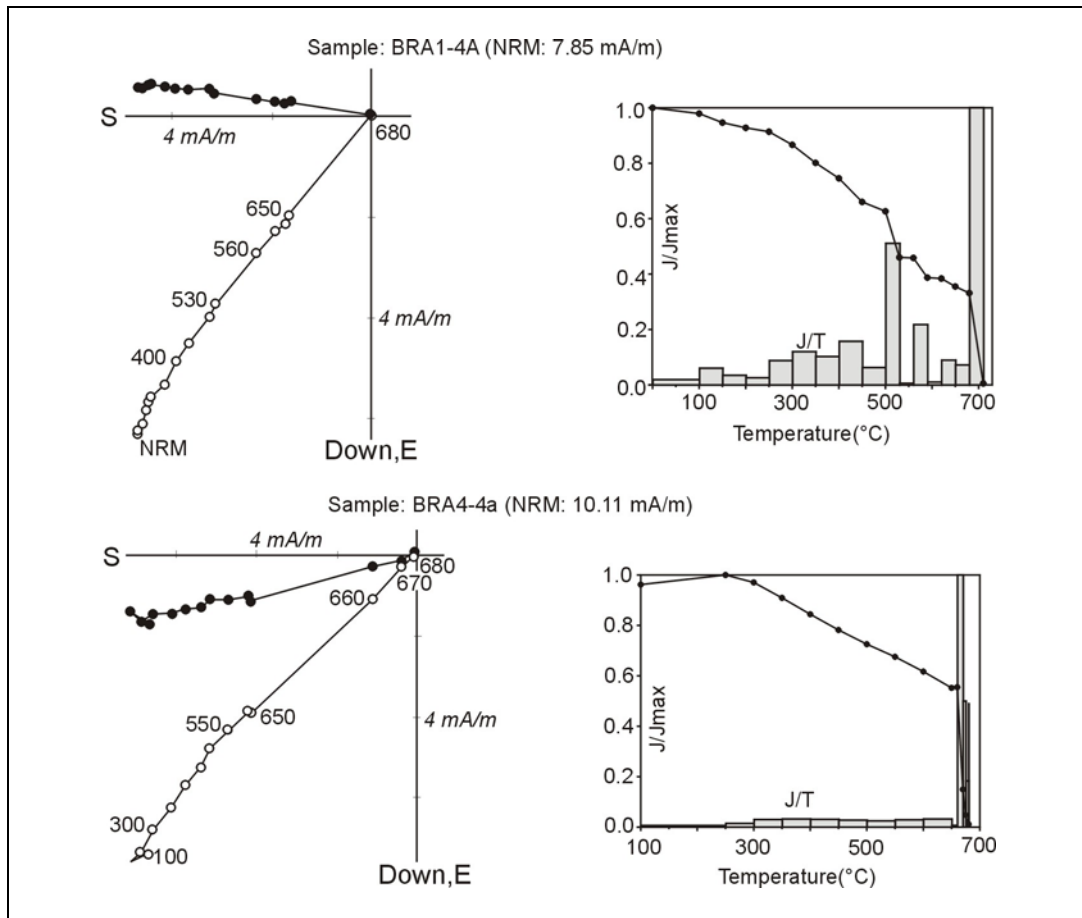
Fig. 9.2. Representative examples of thermal demagnetisation results from the La Antigua Formation. Orthogonal projection of samples from sites BRA1 and BRA4 are shown in bedding-corrected co-ordinates. The stable remanence is generally identified between 400°C and 680°C step. Intensity decay curves illustrate stable remanence mainly carried either by haematite (sample BRA4-4a) or both haematite and magnetite (sample1-4a). Closed/open circles in orthogonal projections are projection onto horizontal/vertical planes; numbers adjacent to data points are demagnetisation steps in degrees Celsius.

The B remanence is a reverse polarity magnetisation with southeasterly declination, yielding an overall site-mean directions (N= 6) of D= 153.5°; I= +55.4° (α_{95}= 5.5°; k= 192) *in-situ* and D= 166.6°; I= +54.1° (α_{95}= 8.2°; k= 87.8) after bedding correction. There is a noticeable decrease in directional grouping in both sample- and site-level directions after bedding correction (Fig. 9.3). Stepwise unfolding (Enkin, 2003) of the site-level mean directions show maximum grouping at 20% unfolding (α_{95}= 4.2° and k= 259), indicating the syn-folding nature of this remanence. Folding of La Antigua Formation is thought to have occurred during the Late Carboniferous-Early Permian (Limarino *et al*., 2002), thus the B remanence may have been acquired in Early Permian times, shortly after rock deposition.

The palaeomagnetic south pole calculated from 6 site-level VGPs, corresponding to the 20% unfolding directions is located at $\lambda= 65.8°S$; $\phi= 5.6°E$ ($A_{95}= 5.4°$; $K= 152$). It is situated at $\lambda= 31.0°S$; $\phi= 65.6°E$ when transferred into African co-ordinates (Lottes & Rowley, 1990). This pole is similar to the mean Early Permian poles for Gondwana reported by Torsvik & Van der Voo (2002; 270 Ma; $\lambda = 33.6°S$; $\phi= 62.1°E$) and McElhinny *et al.* (2003; 280 Ma; $\lambda= 34.7°S$; $\phi = 64.7°E$).
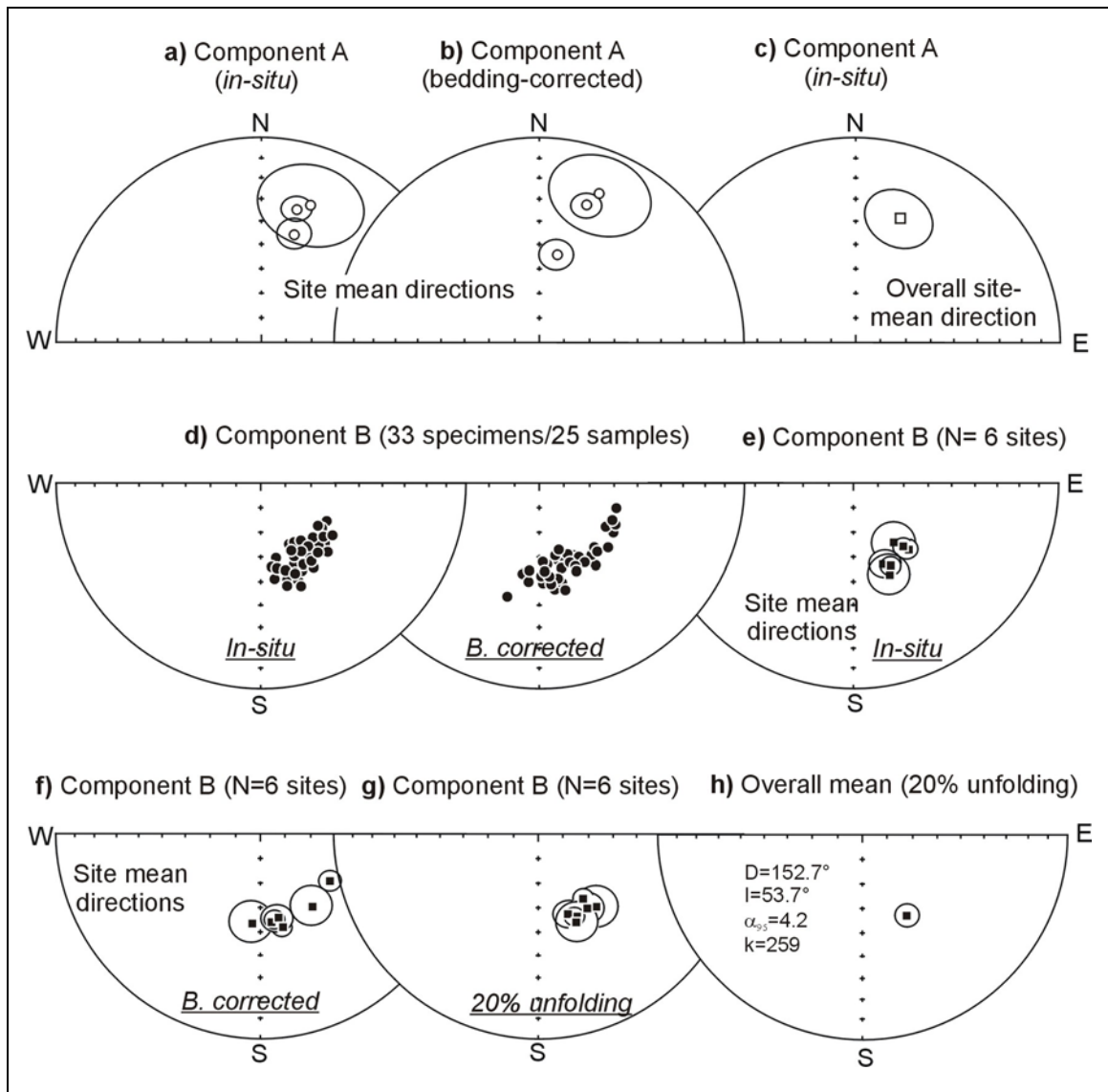
Fig. 9.3. Equal area projection of the palaeomagnetic data from the La Antigua Formation. **a)** and **b)** Equal area projection of the *in-situ* and bedding-corrected mean directions for the low unblocking temperature A direction from sites BRA3, BRA4 and BRA5. **c)** Overall site-level (3 sites) mean for component A. **d)** I*n-situ* and bedding-corrected distribution of B remanence obtained from specimens cut from 25 samples. **e)**, **f)** and **g)** Site mean directions for component B in I*n-situ*, bedding-corrected and 20% unfolding co-ordinates. The component B magnetisation is considered to be a syn-folding acquired in Early Permian.

a) Component A

Site	n	D_g(°)	I_g(°)	D_s(°)	I_s(°)	α_{95}(°)	k	P_{lat}(°S)	P_{long}(°E)	dp	dm	Dir	Dip
BRA3	2	19.9	-28.6	21.9	-21.9	18.3	189.3	67.7	174.1	11.0	20.1	234	8
BRA4	4	15.4	-32.3	18.3	-28.9	5.1	320.4	72.6	171.6	3.2	5.8	252	6
BRA5	3	17.7	-43.2	11.1	-53.8	6.1	409.2	73.5	232.1	5.0	7.1	43	12

Mean	N	D_g(°)	I_g(°)	α_{95}(°)	k_g	D_s(°)	I_s(°)	α_{95}(°)	k_s	λ(°S)	ϕ(°E)	A_{95}(°)	K
	3	17.7	-34.7	12.0	107.4	17.9	-34.9	26.8	22.1	72.2	161.2	12.0	107

c) Component B

Site	n	D_g(°)	I_g(°)	D_s(°)	I_s(°)	α_{95}(°)	k	Dir(°E)	Dip(°)
BRA1	3	145.2	58.1	180.1	52.5	6.0	62.2	240	24
BRA2	5	143.4	57.7	170.1	54.3	3.7	193.0	236	18
BRA3	4	156.2	52.9	166.0	50.5	3.8	248.2	234	8
BRA4	5	159.6	54.8	168.1	54.6	5.5	102.5	252	6
BRA5	5	158.7	50.0	144.1	53.8	8.2	55.6	43	12
BRA6	3	141.6	55.4	124.0	55.4	4.0	373.0	43	12

Mean	N	D_g(°)	I_g(°)	α_{95}(°)	k_g	D_s(°)	I_s(°)	α_{95}(°)	k_s
	6	153.5	55.4	5.5	191.8	166.6	54.1	8.2	87.8

d) Component B (20% unfolding)

Site	n	D(°)	I(°)	α_{95}(°)	k	P_{lat}(°S)	P_{long}(°E)	dp	dm	Dir(°E)	Dip(°)
BRA1	3	147.4	53.5	6.3	94.2	62.1	6.5	8.8	6.1	240	24
BRA2	5	146.2	57.8	3.7	193.0	60.9	357.5	5.4	4.0	236	18
BRA3	4	157.3	52.7	3.8	248.2	70.4	7.7	5.2	3.6	234	8
BRA4	5	160.4	54.8	5.5	102.5	72.6	360	7.8	5.5	252	6
BRA5	5	157.4	50.5	8.2	55.6	70.5	13.8	11.0	7.4	43	12
BRA6	3	142.7	52.0	8.7	60.5	58.1	9.1	11.9	8.1	43	12

Mean	N	D(°)	I(°)	α_{95}(°)	k	λ(°S)	ϕ(°E)	A_{95}(°)	K
	6	152.7	53.7	4.2	259.0	65.8	5.6	5.4	152

Tab. 9.2. Palaeomagnetic results from the Early Permian La Antigua Formation. Heading explanation are as follows: n: number of samples; Dg/Ig: declination/inclination of the magnetic remanence in *in-situ* (geographic) co-ordinates. Ds°/Is°: declination/inclination in bedding-corrected (stratigraphic) co-ordinates; α_{95}: calculated radius of cone of 95% confidence about the mean direction (Fisher, 1953) in degrees; k: Fisher (1953) precision parameter; P_{lat} (°S)/P_{long}(°E): latitude/longitude position of VGP corresponding to the *in-situ* (a) and bedding-corrected (b) site mean directions; dp/dm: semi-axes of the oval of 95% confidence about the VGP. Dir/Dip: dip direction /dip of bedding plane; kg/ks: precision parameters for the *in-situ*/bedding-corrected site mean directions; λ (°S) and ϕ (°E): latitude and longitude position of the mean palaeosouth pole calculated from site level VGPs in degrees south and east, respectively. The mean palaeomagnetic pole corresponding to the 20% unfolding site-mean directions (component B) is situated at λ=3.0°S; ϕ=65.6°E when transferred into African co-ordinates (Lottes & Rowley, 1990).

9.3   Paganzo Basin

9.3.1. Malanzán Formation (Namurian-Westphalian)

a) Sampling

Samples from the Malanzán Formation were collected in the Los Llanos Range within the eastern domain of Paganzo Basin. The exposures, which corresponds to the uppermost part of the Malanzán Formation, comprises massive conglomeratic beds with frequent intercalation of coarse-grained sandstones and lens of fine-grained sandstones and mudstones rich in plant remains. The Malanzán Formation was formerly interpreted to be a glacio-lacustrine deposit (Andreis *et al*., 1986; Net & Limarino, 1999). However, the recently discovered marine microplankton (Limarino *et al*., 2002) suggests a shallow marine depositional environment for this unit. These authors interpreted the facies association of the uppermost unit to represent a subaerial delta plain deposit. The studied samples from Malanzán Formation include 66 cores drilled in 12 palaeomagnetic sites situated in the Malanzán valley (UNQ1-6 and MAL1-6; Fig. 9.4; Tab. 9.1).
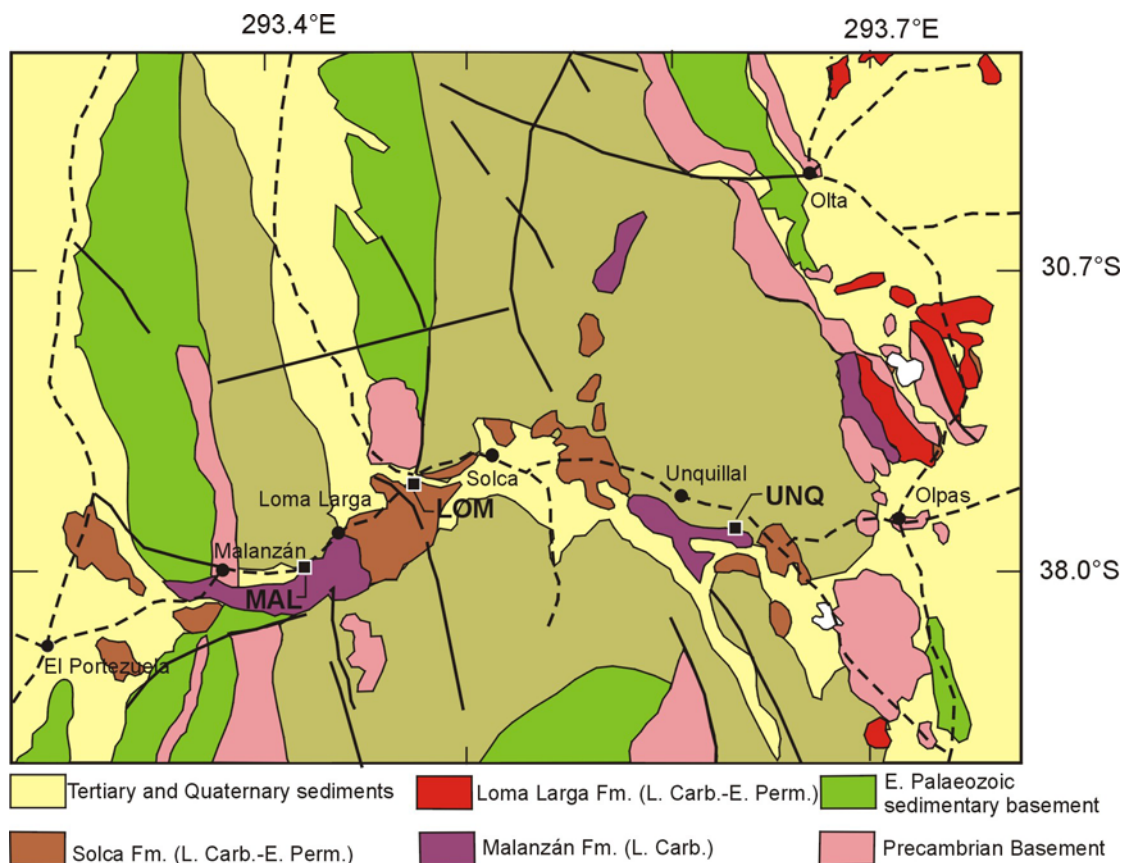
Fig. 9.4. Simplified geological map (modified from Net & Limarino, 1999) of the sampling area (box in Fig. 9.1). Sampling locations are indicated by filled squares. See Table 9.1 for name code and sampling details.

b) Results

Samples collected from the location UNQ have initial NRM intensity ranging between 10 mA/m and 50 mA/m. Stepwise thermal demagnetisations of these samples illustrate a single stable high unblocking temperature direction, recognised in 7 samples from sites UNQ4 and UNQ5. Stable remanence for individual specimens were calculated between 300°C and 700°C steps. Intensity decay curves indicate that the stable direction is mainly carried by haematite. The isolated directions are well grouped with southeasterly declinations and positive inclinations (Fig. 9.5), yielding a sample-mean of D= 150.0°; I= +50.4°; (α_{95}= 5.8°; k= 134) *in-situ* and D= 156.7°; I= +55.2° after bedding correction.

Magnetic measurements show very weakly magnetised rock with initial NRM intensities below 0.5 mA/m for the samples from location MAL (Fig. 9.4). Demagnetisation results of most these samples show erratic directional behaviour. However, stable magnetic component could be identified in 8 specimens cut from 5 samples. Individual directions from these samples were calculated between 300°C and 500°C steps. The overall directions yield a sample-level mean of D= 145.0°; I= +48.5° (α_{95}= 11.9°; k= 22.6) *in-situ* and D= 147.2°; I= +48.5° (α_{95}= 10.9°; k= 26.6) after bedding correction.

Combining the results from localities MAL and UNQ of the Malanzán Formation (n= 12 samples ; Tab. 9.4) yields an overall site mean direction of D= 150.6°; I= +49.5° (α_{95}= 5.6; k= 485.6) *in-situ* and D= 155.6°; I= +52.8°; (α_{95}= 9.3°; k= 179) after bedding correction. There is an increase in directional scattering after bedding correction, and stepwise unfolding shows optimal grouping in *in-situ* co-ordinates. Therefore, the Malanzán remanence was likely acquired posterior to the rock tilting, which is thought to have occurred during the Late Carboniferous tectonic movement (Net & Limarino, 1999). Therefore, the stable remanence of the Malanzán Formation is post-Carboniferous in age.

The mean palaeosouth pole calculated from the *in-situ* site-level VGPs (Tab. 9.3) is located at λ= 64.8°S; ϕ= 16.8°E (A$_{95}$= 7°; K= 309; N= 3) in South American co-ordinates. This pole is comparable with some published Early Permian poles for stable South America. When rotated into African co-ordinates (Lottes & Rowley, 1990), the pole from Malanzán Formation (λ= 28.6°S; ϕ= 70.3°E; A$_{95}$= 7.2°) is comparable with the Early Permian mean poles for Gondwana reported by Torsvik & Van der Voo (2002; 270 Ma; λ= 34.8°S; ϕ= 62.0°E; A$_{95}$= 9.3°) and McElhinny *et al*. (2003; 280 Ma; λ= 34.7°S; ϕ= 64.7°E; A$_{95}$= 3.8°). Therefore, the Malanzán remanence is

probably of Early Permian age. Notice that this remanence deviates from all expected reference directions younger than Permian.

Site	n	D_g(°)	I_g(°)	D_s(°)	I_s(°)	α_{95}(°)	k	P_{lat}(°S)	P_{long}(°E)	dp	dm	Dir	Dip
UNQ4	3	152.3	51.3	159.4	55.9	4.7	267	66.4	13.5	6.4	4.3	287	8
UNQ5	4	154.7	48.8	161.4	53.2	6.3	149	68.2	19.9	8.3	5.5	287	8
MAL	5	145.0	48.3	147.2	48.5	10.9	23	59.2	17.1	14.3	9.4	274/139	8/5
Mean	N	D_g(°)	I_g(°)	α_{95}(°)	k_g	D_s(°)	I_s(°)	α_{95}(°)	k_s	λ(°S)	ϕ(°E)	A_{95}(°)	K
	3	150.6	49.5	5.6	485.6	155.7	52.8	9.3	178.6	64.8	16.6	7.2	309

Tab. 9.3. Site-level palaeomagnetic results from the Malanzán Formation, interpreted to be post-folding remanence acquired in Early Permian. Site-level VGPs and mean palaeosouth pole are calculated from the *in-situ* mean directions.
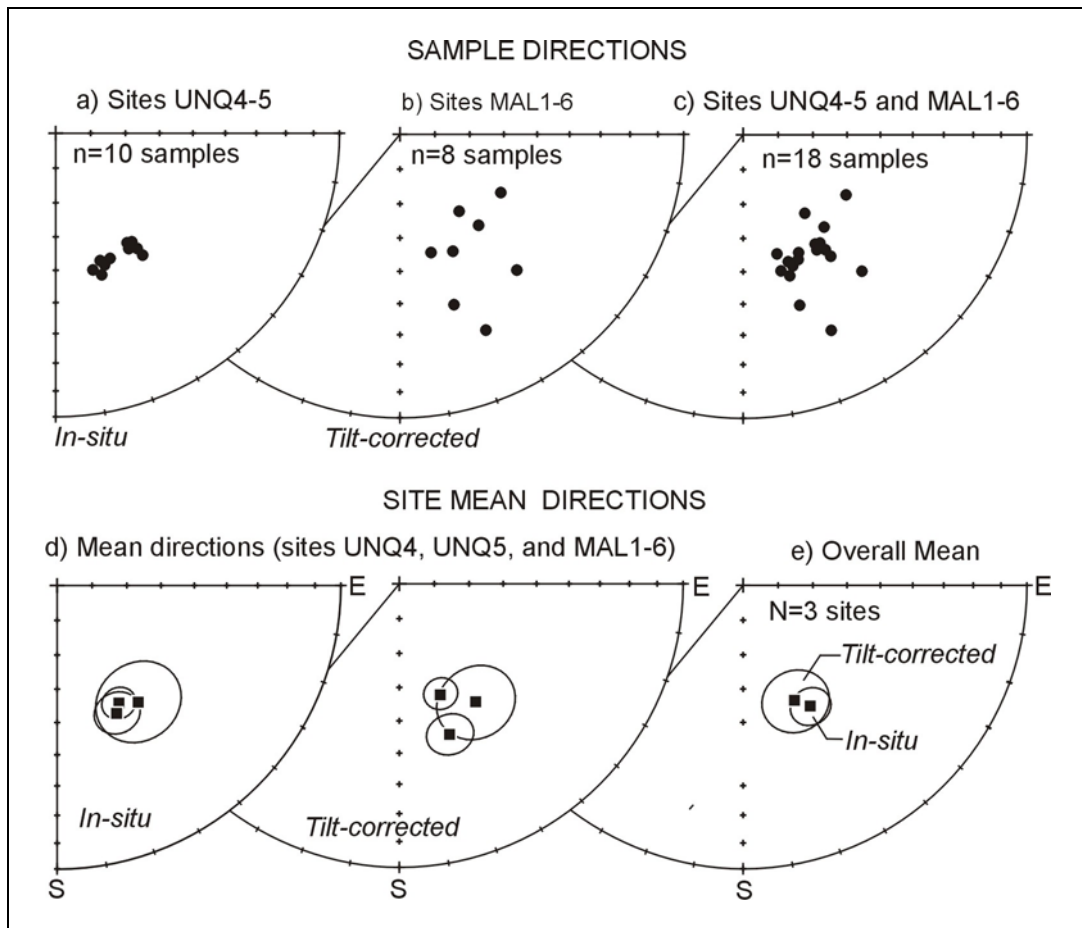
Fig. 9.5. Equal area projection of the palaeomagnetic result from Malanzán Formation. **a)** *in-situ* samples directions for sites UNQ4 and UNQ5. **b)** tilt-corrected directions for samples from sites MAL1-MAL6. **c)** Individual directions for 18 samples from all 3 sites. **d)** and **e)** *in-sit*u and tilt-corrected site mean directions. **f)** *in-situ* and tilt-corrected overall mean direction. Note that the *in-sit*u and tilt-corrected mean directions are statistically indistinguishable.

9.3.2. Solca Formation (Late Carboniferous)

a) Sampling

The Solca Formation, which forms the base of the Upper Paganzo Group (Paganzo II; Andreis *et al*., 1986), is considered to be a Late Carboniferous (Stephanian) deposit based on palynology and stratigraphy correlation (Net & Limarino, 1999). The Solca Formation was sampled in the eastern domain of the Paganzo basin, on a road cut between Solca and Loma Larga (Location LOM, Fig. 9.4). Rock exposure in this area consists mainly of very coarse-grained to conglomeratic sandstones with frequent alternating thin layers of fine-grained sandstones. The studied samples (n= 29, Tab. 9.1) were drilled in various stratigraphic levels, including grey mudstone beds (sites LOM1-2) and thin layers of reddish fine-grained sandstones (LOM3-5). All samples were drilled in flat-lying beds.

b) Results

Measurement of initial NRM show that the grey mudstone beds drilled in site LOM1 are very weakly magnetised. Initial NRM intensities of the samples collected from this location are below 0.35 mA/m. Stepwise thermal demagnetisation up to 690°C of these samples illustrates a single normal polarity magnetic direction (Fig. 9.10). The samples from sites LOM4-5 have initial NRM intensities range between 1.2 mA/m and 5mA/m. As well, a single normal polarity magnetisation, similar to that of the site LOM1, is identified in the samples from these sites (Fig. 9.6; Tab. 9.4). The overall directions derived from sites LOM1, LOM4, and LOM5 yield a sample-level mean direction of D= 000.3°; I= -40.6° (α_{95}= 3.6°; k= 101; n= 10).

On the other hand, a reverse polarity magnetisation is recognised in 7 samples from sites LOM2-3 between 600°C and 690°C. The directions from these samples yield a mean of D= 173.4°; I= +43.6° (α_{95}= 3.2°; k= 301). This direction is antipodal to the normal direction discussed above. The overall (n= 17) dual polarity magnetisation from Solca Formation passes the reversal test of McFadden (1990).

The overall site mean direction (N= 5, both polarities) is D= 358.7°; I= -40.9° (α_{95}= 6.9°; k= 123.5), and the corresponding palaeomagnetic south pole is located at λ= 82.6°S; ϕ= 102.3°E (A_{95}= 7.5°; K= 106; Tab. 9.4). There is no field test to constrain the relative age of this remanence because all samples were collected from horizontal beds. However, comparison with the expected younger direction at the sampling area indicates that this remanence may represent a secondary Cretaceous magnetisation (Fig. 9.7). Unblocking temperatures above 650°C inferred from intensity decay curves demonstrate remanence carried by haematite. These haematites are likely of

secondary origin resulting from weathering. An intermediate unblocking temperature remanence, probably carried by magnetite, is identified in some samples from site LOM2 and LOM3 (ex. LOM2-2a; Fig. 9.10), but these directions are statistically incoherent.

Site	n	D($°$)	I($°$)	α_{95}($°$)	k	P_{lat}($°$S)	P_{long}($°$E)	dp	dm
LOM1	3	11.6	-35.1	13.6	83.2	74.5	159.6	15.7	9.0
LOM2	3	172.3	46.3	2.3	1532	82.3	46.0	2.9	1.9
LOM3	4	174.4	40.8	5.7	259.3	80.8	76.5	6.9	4.2
LOM4	3	356.1	-38.3	1.0	14242	80.1	91.4	1.2	0.7
LOM5	4	357.6	-42.9	3.3	244.5	83.9	96.3	4.1	2.5
Mean	N	D($°$)	I($°$)	α_{95}($°$)	k	λ ($°$S)	ϕ($°$E)	A_{95}	K
	5	358.7	-40.9	6.9	123.5	82.6	102.3	7.5	106

Tab. 9.4. Site-mean palaeomagnetic results from the Solca Formation. n: number of samples. N: number of sites; D/I: declination and inclination in degrees; P_{lat}($°$S)/P_{long}($°$E): latitude/longitude position of the site-level VGPs in degrees south and east, respectively. λ($°$S)/ϕ($°$E): latitude and longitude position of the palaeomagnetic pole calculated from the listed VGPs. Sampling location: S_{lat}=30.8$°$S, S_{long}=293.5$°$E. Bedding attitudes are horizontal for all sampling sites.
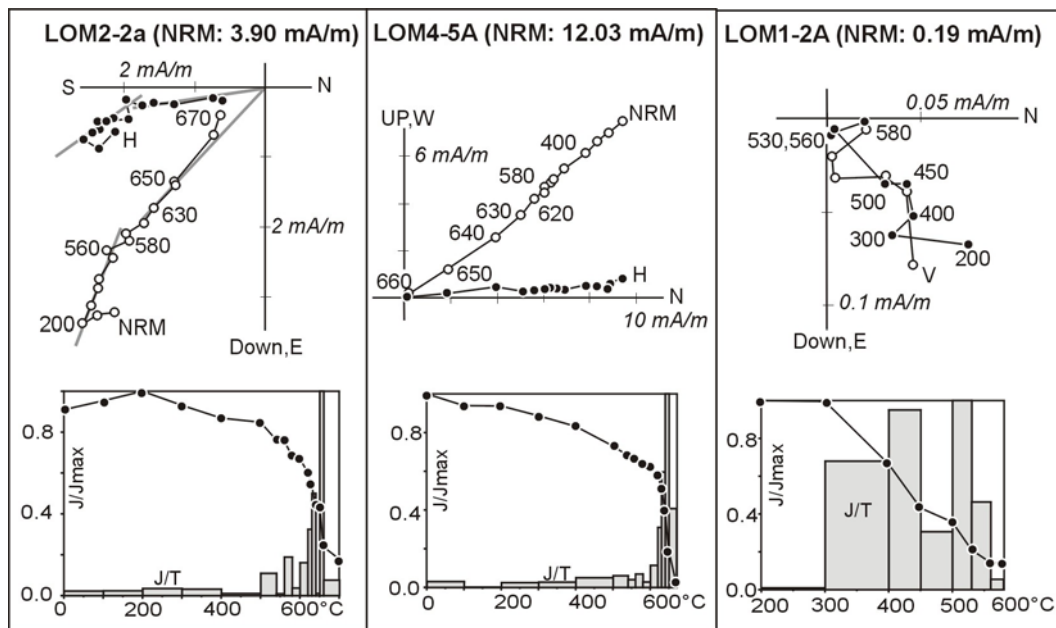
Fig. 9.6. Demagnetisation results from the Solca Formation. Presentation on orthogonal projections of the directional behaviour during thermal demagnetisation and the corresponding decay in magnetic intensities are shown. On orthogonal projections: numbers beside vector data points are demagnetisation steps in degrees Celsius; scales along axis represent intensity in mA/m; open/closed symbols are data point projections onto vertical/horizontal plane. Scales on horizontal and vertical axis of the intensity decay curves respectively represent temperature (in degree Celsius) and ration between the initial and remaining magnetisation (J_o/J) after each step.
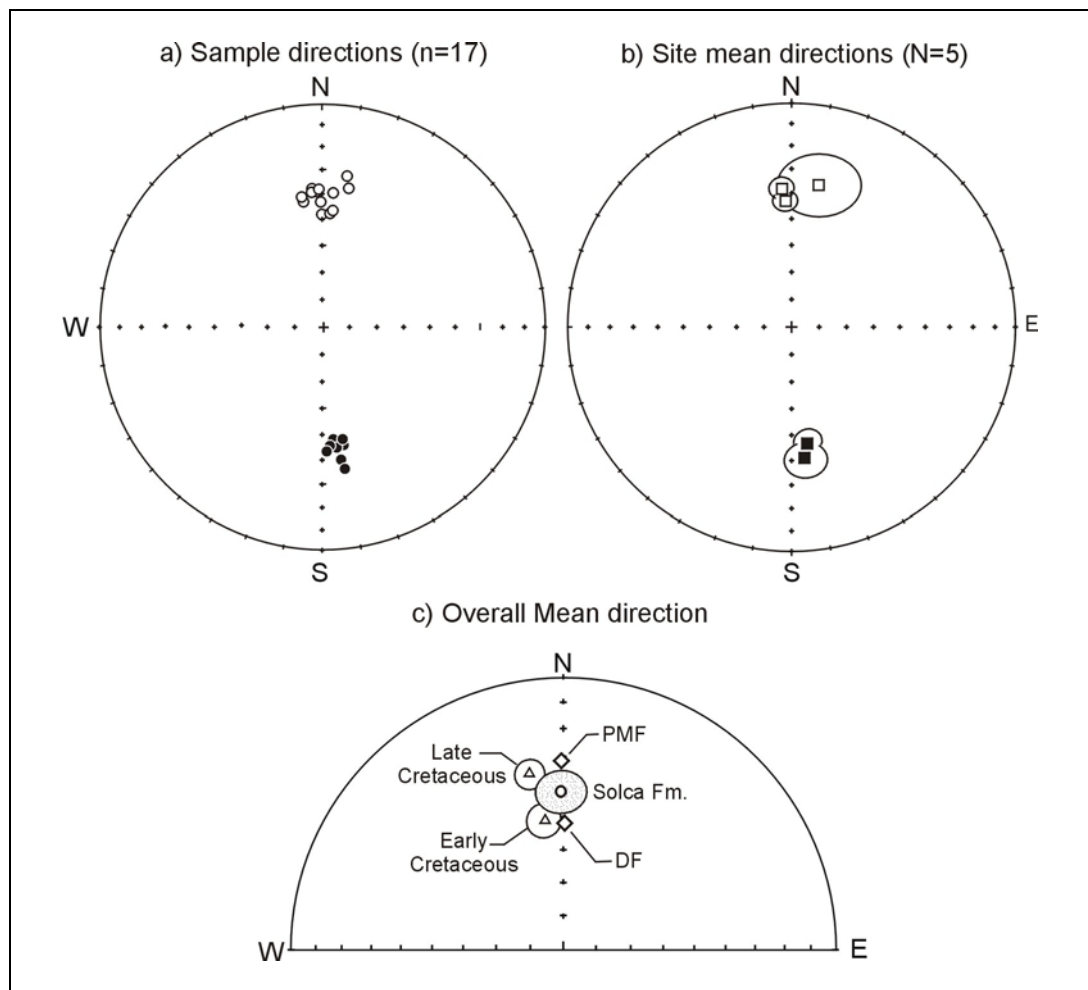
Fig. 9.7. Equal area projections of the palaeomagnetic results from the Solca Formation. **a)** sample directions. **b)** site means. **c)** site mean directions compared with the expected Early and Late Cretaceous directions at the sampling location (recalculated from Randall, 1998). The palaeomagnetic result from the Solca Formation is a secondary remanence probably acquired in Cretaceous times.

9.4 Summary and conclusion

Palaeomagnetic direction from the Permian sediments exposed in the Pampean ranges (La Antigua Formation) is interpreted to be a syn-folding remanence acquired in Early Permian time. The positions of the palaeomagnetic south poles from this unit are comparable with that of the published coeval poles for South America and for Gondwana (Fig. 9.8). The Malanzán Formation (Paganzo Basin) yields a remanence assumed to be post-folding, probably acquired in Early Permian. Both poles from NW Argentina are comparable with reference directions for stable South America and those for Gondwana (Fig. 9.8). This suggests the stability of the sampling area at least since the Permian. Palaeomagnetic data from this study

134

are also similar to some previously published data from the Paganzo Basin (Fig. 9.9; Tab. 9.6).
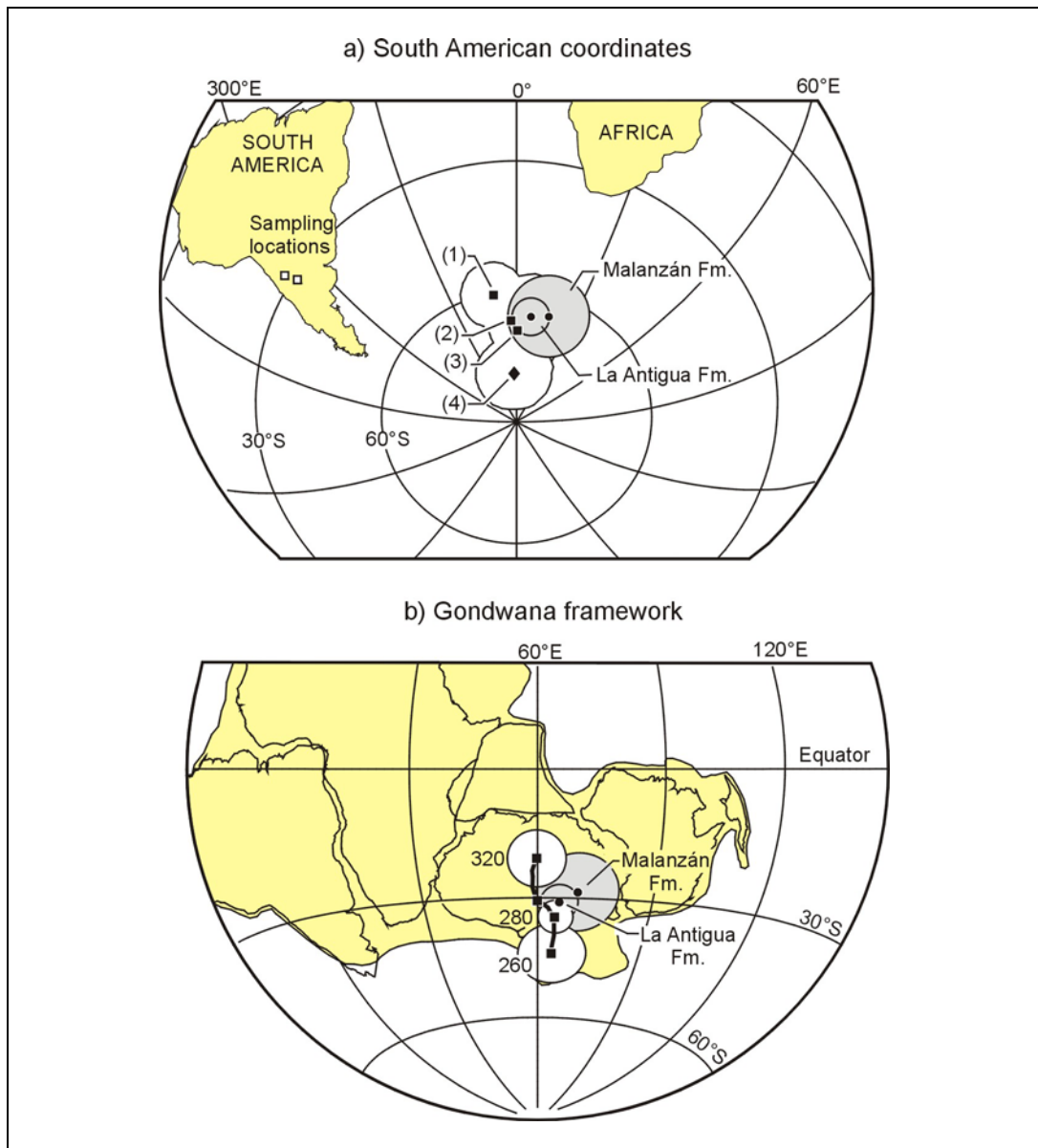
Fig. 9.8. Equal area projection of the palaeomagnetic south pole from La Antigua and Malanzán Formations. **(a)** Pole positions in South American co-ordinates compared with published Early Permian reference poles for stable South America (diamond) and Gondwana (square). (1) Torsvik & Van der Voo (2002; 280 Ma); (2) Torsvik & Van der Voo (2002; 270 Ma); (3) McElhinny *et al*. (2003; 280 Ma). (4) Mean South American poles Gilder *et al*., (2003). **b)** Comparison of the Malanzán and La Antigua poles with the 320 Ma to 260 Ma APWP for Gondwana proposed by McElhinny *et al*. (2003). The palaeomagnetic directions from the La Antigua and the Malanzán Formations are considered, respectively, to be syn-folding and post-folding remanences acquired in Early Permian.

Formation	Age (Ma)	Loc.	λ(°S)	ϕ(°E)	A_{95}(°)	K	N	λ^*(°S)	ϕ^*(°E)	Interpretation
La Antigua	260-290	PR	65.8	5.6	4.2	152	6	31.0	65.6	E. Permian-syn-folding
Malanzán	303-327	PA	64.8	16.6	7.0	309	3	28.6	70.3	E. Permian-post-folding
Solca	290-303	PA	82.6	102.3	7.5	106	5	-	-	E. Cretaceous overprint ?

Tab. 9.5. Summary of the palaeomagnetic data from NW Argentina. PR: Pampean ranges. PA: Paganzo Basin. λ(°S)/ϕ(°E): latitude/longitude position of the palaeomagnetic pole in degrees south and east, respectively. A_{95}(°): confidence circle about pole in degrees; K: precision parameter (Fisher, 1953). N: number of site-level VGPs used when calculating palaeopole. λ^*(°S)/ϕ^*(°E): position of palaeosouth pole in African co-ordinates. Rotation parameters used to transfer poles from South American to African co-ordinates are from Lottes & Rowley (1990; Lat= 46.8°N; Long= 329.5°E; angle = 55.9°).
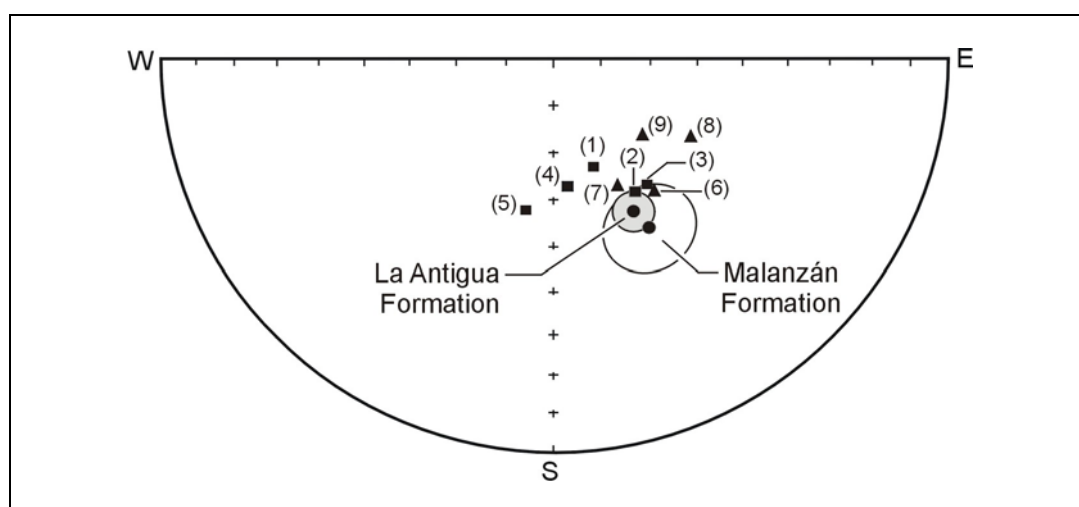
Fig. 9.9. Equal area projection of mean palaeomagnetic directions from this study (circles with 95% confidences) compared with the previously published Early Permian (squares) and Late Carboniferous (triangles) data from the Paganzo Basin. All directions are recalculated at the sampling site for La Antigua Formation (S_{lat}= 30°S; S_{long}= 293°E). (1) Lowest Middle Paganzo (256-290 Ma; Creer, 1965); (2) Middle Paganzo II, Huaco (256-290 Ma; Embleton,1970); (3) Lower Los Colorados Formation (256-290 Ma, Embleton, 1970); (4) Upper Los Colorados Formation, 256-290 Ma, Embleton (1970) (5) La Colina Formation (266-290 Ma, Valencio & Vilas, 1977); (6) La Colina Basalt (295-305 Ma, Embleton, 1970) (7) Combined La Colina Basalt (295-305 Ma, Thompson & Mitchell, 1972); (8) Hoyada Verde Formation (290-323 Ma, Rapalini & Vilas, 1991) (9) La Colina Formation (290-323 Ma, Sinito *et al.*, 1979)

Chapter 10

Palaeomagnetic data from the Argentine Precordillera and Famatina Ranges, NW Argentina

10.1 Introduction

The Argentine Precordillera (AP), bounded by the Frontal Cordillera to the West, and the Pampean and Famatina Ranges to the East, presents striking lithological and structural differences compared to the surrounding geological provinces. This exotic character is discussed in several publications and it is comprehensively accepted that the AP is a terrane. However, the provenance of this terrane and the mode of transfer to its present position are still debated. On one hand, the "exotic terrane" hypothesis (Astini *et al.*, 1995; Dalziel, 1997; Pankhurst *et al.*, 1998) considers the AP as a terrane derived from Laurentia in Cambrian-Ordovician times and accreted to the western margin of Gondwana. On the other hand, the "para-autochthonous terrane" hypothesis (Baldis *et al.*, 1989; Aceňolaza & Toselli, 2000; Aceňolaza *et al.*, 2002; Finney *et al.*, 2003) considers the AP as originating in southern Gondwana. This model assumes that the AP was part of a hypothetical SAFRAN plateau that developed between South America, Africa and Antarctica. The terrane is suggested to have reached its present position in Devonian by strike-slip displacement along the present day Pacific margin of Gondwana during the Ordovician-Silurian.

Although the Laurentia-derived terrane hypothesis is widely accepted by many in the literature, the evidence supporting this model is still disputed. For instance, the Greenvillian age of the basement rock underlying the AP, which is stated as evidence of its exotic origin, is challenged by Finney *et al.* (2003) who argued that Early Cambrian detrital zircon grains from the Cerro Totora Formation indicate Gondwanan provenance and have no affinity to any known Laurentian sources. Palaeomagnetic data from this Formation have been interpreted as confirming the Laurentian origin of the AP (Rapalini & Astini, 1998). However, this argument is disputable because of the lack of longitudinal constrain in palaeomagnetic data. Discussion of the various palaeontological, geochemical, isotopic and structural evidences supporting the Laurentian and Gondwanan origin of the AP, respectively, are given in

the recently published papers of Aceňolaza *et al.* (2002) and Thomas & Astini (1996).

For the Laurentia-derived terrane model, different scenarios have been proposed concerning the mode of transfer to Gondwana. Some authors (Dalla Salda *et al.*, 1992; Dalziel *et al.*, 1994, Dalziel, 1997) suggested that the AP was transferred to Gondwana's margin during a rifting event that followed a Middle Ordovician collision between Laurentia and Gondwana. In opposition, the scenario proposed by Astini *et al.* (1995) and Thomas & Astini (1996) consider the AP as an independent crustal plate that drifted across the Iapetus to reach the western margin of Gondwana. Timing of the rifting off of the AP from Laurentia and its accretion to Gondwana in this scenario remains a matter of dispute. The separation of the Precordillera from Laurentia is variably interpreted as having occurred in the Early Cambrian (*e.g.* Thomas & Astini, 1996) or the Middle-Late Ordovician (*e.g.* Keller, 1999). While, the accretional time has been differently proposed as being Middle-Late Ordovician in age (*e.g.* Dalla Salda *et al.*, 1992; Dalziel *et al.*, 1994; Astini *et al.*, 1995) or Silurian-Devonian in age (*e.g.* Keller *et al.*, 1998; Pankhurst & Rapela, 1998; Rapela *et al.*, 1998; Keller, 1999).

The present palaeomagnetic investigation of the AP and the neighbouring Famatina range were carried out to provide information about the Early Palaeozoic palaeoposition of the AP relative to Gondwana. Palaeomagnetic data from Ordovician to Permian rock units from the AP, and Early Ordovician and Late Permian rocks from the Famatina range are presented. Implication of the palaeomagnetic data to the drift history of the AP from the Early Ordovician to Late Devonian is discussed. The investigated samples include 291 cores drilled in 57 palaeomagnetic sites (Tab. 10.1).

Formation	Age (Ma)	Location	Site	S_{lat}(°S)	S_{long}(°E)	N	n
De la Cuesta (FA)	250-260	Fiambalá	CHA	27.70	292.04	5	27
Suri (FA)	485-478	Valle chachuil	SUR	27.80	291.94	5	25
Patquia (AP)	250-260	Huaco-Jáchal	HUP	30.13	291.47	5	25
Tupe (AP)	290-323	Huaco-Jáchal	HUC	30.14	291.46	5	25
Guandacol (AP)	290-323	Huaco-Jáchal	HUG	30.15	291.46	5	25
Punilla (AP)	370-354	Rodeo,Jáchal	PUN	30.18	290.81	4	25
Talacasto (AP)	412-391	Rodeo,Jáchal	JAT	30.22	291.02	5	25
Los Espejos (AP)	423-417	Rodeo, Jáchal	JAE	30.20	291.16	5	25
Yearba Loca (AP)	458-443	Rodeo, Jáchal	ROO	30.21	290.95	7	34
San Juan (AP)	495-485	Huaco-Jáchal	HUO	30.14	291.46	6	30
La Silla (AP)	495-485	Niquivil, Jáchal	NIQ	30.40	291.32	5	25

Tab. 10.1. Sampling details for the Palaeozoic rock units of the Famatina Ranges (FA) and the Argentine Precordillera (AP). S_{lat}(°S)/S_{long}(°E): latitude/longitude position of sampling locations. N/n: number of sites/core samples.
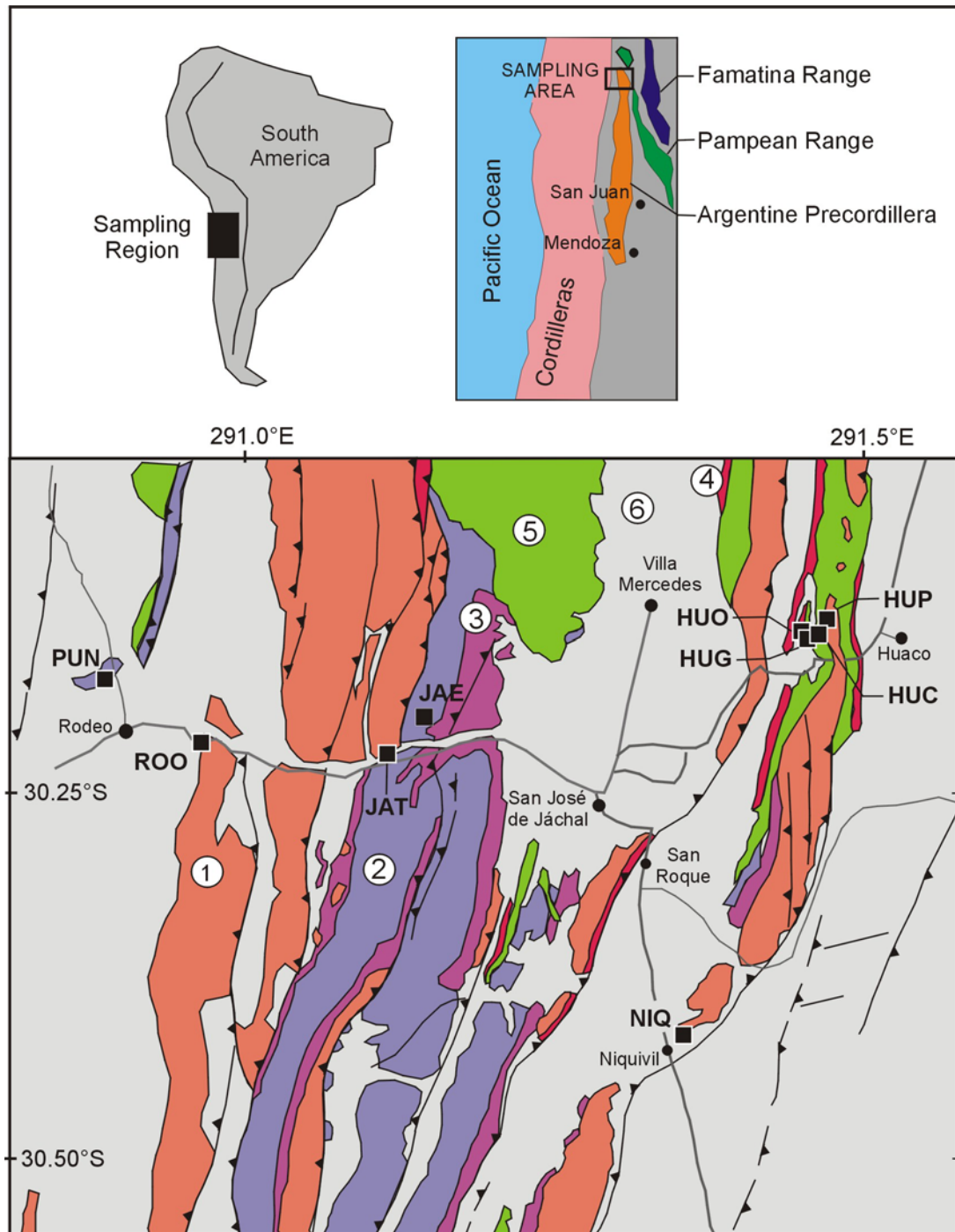
Fig. 10.1. Simplified geological map of the northern Argentine Precordillera (modified from Ragona *et al.*, 1995). Filled squares show sampling locations. (1) San Juan, La Silla, Yerba Loca Formations (Ordovician); (2) Los Espejos Formation (Silurian); (3) Callingasta Formation (Silurian); (4) Talasco, Punilla Formations (Devonian); (5) Guandacol, Tupe, Panacán Formation (Permian-Carboniferous); (6) Undifferentiated Tertiary and Quaternary. See Table 10.1 for details.

10.2 Palaeomagnetism of the Argentine Precordillera

10.2.1 Patquia Formation (Late Permian)

The Patquia Formation is defined by Milani & Thomaz Filho (2000) as being part of an up to 1300 meters thick succession referred to as the Patquia-De la Cuesta Supersequence. The authors describe the Patquia-De la Cuesta as Late Permian continental red beds comprising fluvial and playa lake facies. In the literature, the Patquia Formation exposed in the eastern Argentine Precordillera is considered equivalent in age to the De la Cuesta Formation of the Famatina Range. Sampling for the Patquia Formation was carried out east in the area near Huaco (location HUP; Fig. 10.1). The unit sampled for palaeomagnetic investigation involves red sandstones with local intercalation of greyish sandy calcareous mudrocks and conglomerates. Samples were drilled in intercalated pale and reddish fine-grained sandstone beds, and mudstones.

Samples from the Patquia Formation have NRM intensities ranging between 0.3 mA/m and 16 mA/m. Stepwise thermal demagnetisation results demonstrate single component magnetisation, stable up to 700°C (Fig. 10.2). Unblocking temperatures inferred from intensity decay curves suggest that haematite is the dominant remanence carrier in all samples. Stable magnetisation directions can be identified in 12 samples between the 200°C and 700°C demagnetisation steps. The *in-situ* sample directions have negative inclination values with south-westerly declinations, yielding an overall sample mean direction of D= 255.6°; I= -25° (α_{95}= 3.0°; k= 215). This direction is not comparable with any expected post-Permian directions at the sampling location. The bedding-corrected direction (D= 225.8°; I= +61.8°; α_{95}= 3.0°; k= 215) also deviates from all expected magnetisations. The discrepancy of both *in-situ* and bedding-corrected directions indicates that the sampling area has been rotated after remanence acquisition. There is no field test to constrain the relative age of this magnetisation. In terms of the inclination values, however, the *in-situ* direction has shallow inclinations unlike all post-Permian directions at the sampling location. On the other hand, the steep inclination in bedding-corrected co-ordinates is comparable with the reference Late Permian inclinations of the reference direction for stable South America recalculated from Van der Voo (1993; 246-256±10 Ma; I= +60.2°) and Gilder *et al*. (2003; 235±14 Ma; I= +59.3°). Hence, this magnetisation is likely a pre-tilting remanence acquired in Late Permian times. Considering the bedding-corrected direction, the declination discrepancy indicates an at least 60° clockwise rotation of the sampling area after remanence acquisition (Fig. 10.3).
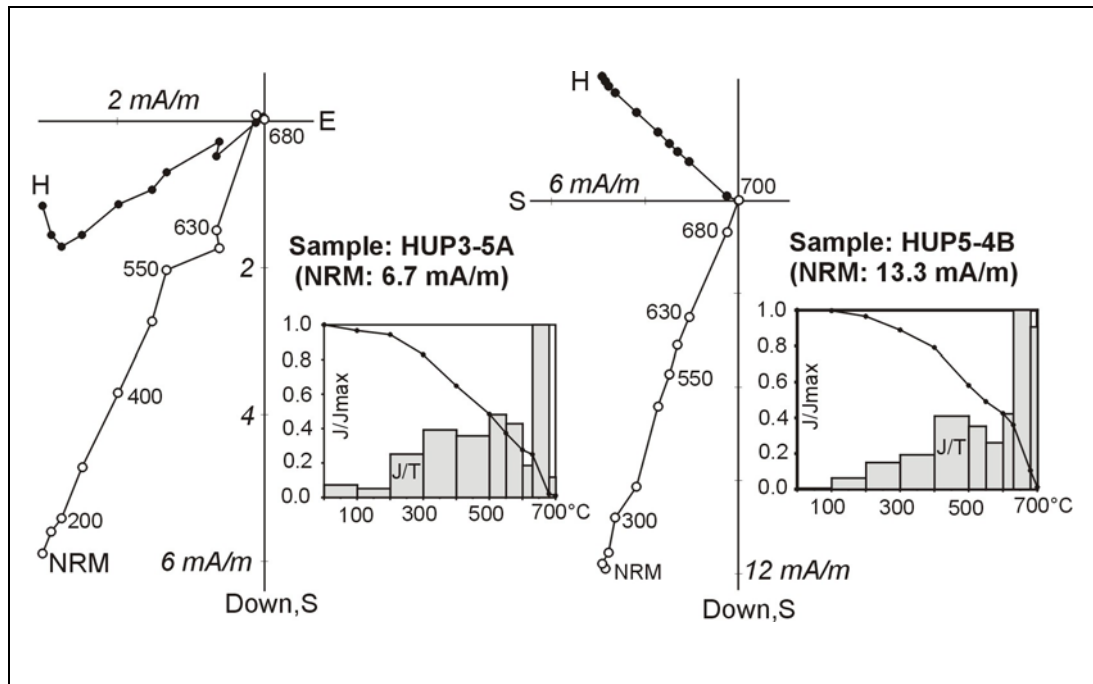
Fig. 10.2. Representative examples of thermal demagnetisation results from the Patquia Formation. Orthogonal projection of samples from sites HUP3 and HUP5 are shown in bedding-corrected co-ordinates. Stable remanence is generally identified between 300°C and 700°C step. Intensity decay curves indicate high unblocking temperature remanence mainly carried by haematite. Closed/open circles are projections onto horizontal/vertical planes. Numbers adjacent to data points indicate demagnetisation steps in degrees Celsius.
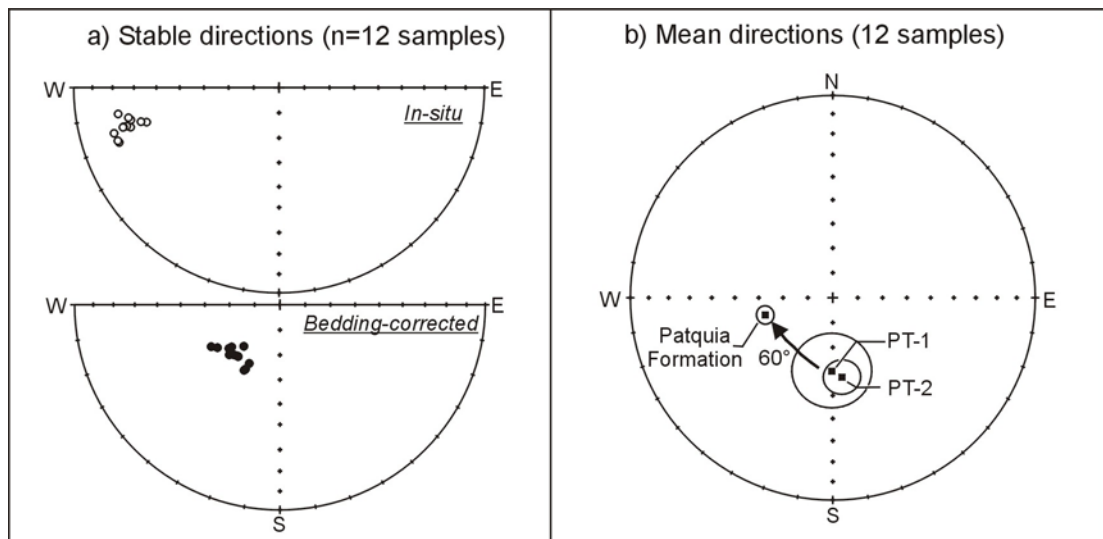
Fig. 10.3. Equal area projection of the palaeomagnetic data from Patquia Formation. **a)** Distribution of sample directions in *in-situ* and bedding-corrected co-ordinates. **b)** Sample-level mean direction compared with the expected Permian-Triassic directions recalculated at location (S_{lat}= 30°S; S_{long}= 291.5°E). PT-1: 235±14 Ma; Gilder *et al*., 2003; PT-2: 256±10; Vander Voo; 1993). An at least 60° clockwise rotation of the sampling area is assumed based on this palaeomagnetic data.

The palaeosouth pole calculated from the observe palaeomagnetic data from Patquia Formation is located at λ= 51.6°S; ϕ= 234.0°E (dp= 3.5°; dm= 4.5°). Correction for the assumed 60° clockwise rotation brings this pole at λ= 73.5°S; ϕ= 331.4°E in South American co-ordinates and at λ= 44.0°S; ϕ= 59.3°E when transferred into African co-ordinates (Lottes & Rowley, 1990).

10.2.2 Guandacol Formation (Late Carbonifereous)

The Guandacol Formation, exposed in the eastern Argentine Precordillera (HUG; Fig. 10.1), is considered equivalent to the Malanzán Formation in the eastern Paganzo Basin. A Namurian-Early Westphalian age (311-323 Ma) is attributed to the Formation, based on marine fossils and palynology (Limarino *et al*. 2002). Samples for the present palaeomagnetic study (Tab. 10.1) were drilled in northeast to east dipping sedimentary sequence comprising intercalated grey finely laminated shales and massive sandstones.

Laboratory experiments demonstrate that these lithologies are very weakly magnetised, with initial NRM intensities below 1 mA/m for almost all samples. As a result, most samples are unstable during demagnetisation above 350°C. However, two distinct magnetic directions are identified in few relatively strongly magnetised samples, generally with NRM intensities between 1mA/m and 1.7mA/m. A low unblocking temperature component (A) is identified in 9 samples. Component A yields and an overall mean of D= 326.0°; I= -29.0° (α_{95}= 9.8°; k= 29.1) *in-situ* and D= 311.5°; I= -11.5° (α_{95}= 10.6°; k= 25.2) after bedding correction. The increase in directional scattering after bedding correction suggests that this magnetisation was acquired after folding of the rock unit.

A relatively high unblocking temperature direction (B) is identified in 8 samples between 350°C and 550°C steps. Component B from individual specimens was calculated from demagnetisation data points that do not converge toward the origin on orthogonal projections. Although these samples are not totally demagnetised, no stable direction could be calculated above 550°C due to the viscous effects and the extremely weak magnetic remanence. Nevertheless, the overall B directions which has an *in-situ* sample-mean of D= 218.9°; I= +46.4° (α_{95}= 10.2°; k= 32.0) and D= 194.1°; I= 59.8° (α_{95}= 4.4°; k= 279) after bedding correction, thus passing the fold test at the 99% confidence level (McElhinny, 1964). Hence, B direction is considered to be pre-folding. As the folding occurred in Late Carboniferous-Early Permian times (Limarino *et al*., 2002), the reported palaeomagnetic data from Guandacol is likely acquired during or shortly after the rock deposition. Note that the *in-situ* direction is not similar to any expected

younger magnetic direction at the sampling location. The palaeosouth pole corresponding to the bedding-corrected direction is situated at λ=74.5°S; φ= 247.9°E (dp= 3.9°; dm= 5.2°) in South American co-ordinates.

Similarly to the Patquia direction discussed above, the remanence from the Guandacol deviates from the expected Late Carboniferous direction at the sampling area. Comparison with the published reference directions indicates at least 45° clockwise rotation of the sampling area (Fig. 10.4).
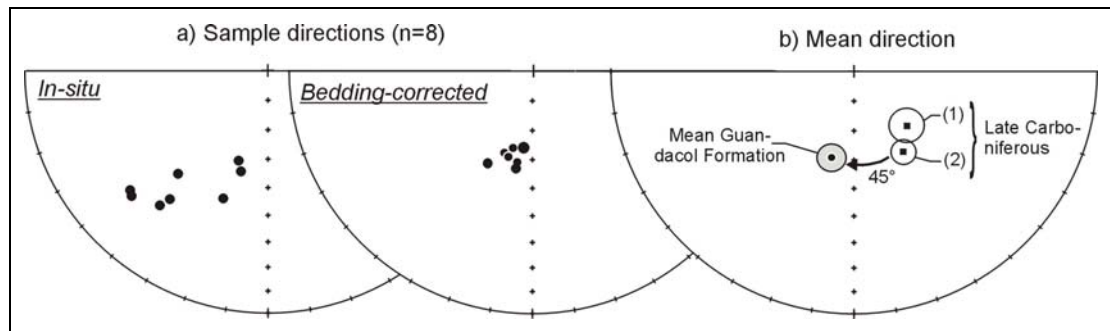
Fig. 10.4. Palaeomagnetic results from the Guandacol Formation. **a)** I*n-situ* and bedding-corrected of the 8 sample directions. **b)** Sample-level mean direction (HUG) compared with the reference Late Carboniferous directions for Gondwana recalculated from (1) Van der Voo (1993) and (2) McElhinny *et al.* (2003). Assuming a primary origin, the observed direction suggest that the sampling area experienced an at least 45° clockwise rotation.

10.2.3 San Juan Formation (Early Ordovician)

The carbonate samples from the Early Ordovician San Juan Formation (HUO1-6; Table 10.1; Fig. 10.1) are weakly magnetised, with initial NRM intensities below 0.1 mA/m. Stepwise thermal demagnetisation experiments were performed up to 560°C with a minimum of 15 steps. Demagnetisation results are characterised by rapid intensity decrease below 300°C. A soft magnetic component, constituting approximately 80% of the initial NRM was isolated at this stage. Most samples are totally demagnetised or have less than 15% of their initial NRM between 380°C to 460°C. However, a high unblocking temperature direction was isolated in some samples (Fig. 10.5).

The low unblocking temperature direction (HUO-A) is identified in 7 samples. This component consists of normal polarity magnetisation, yielding a mean direction of D= 355.5°; I= -47.6° (α₉₅= 10.9°; k= 31.4). This direction is statistically undistinguished from the present dipole field (D= 360.0°; I= -51.5°) at the sampling location and, therefore, represents a viscous remanent magnetisation. The relatively high unblocking temperature component (HUO-B) is well defined by data points converging towards the origin in orthogonal projection in some samples, but was determined by the

great circle method in most of the samples (Fig. 10.5). Component B is defined in 7 samples and is of reversed polarity. The overall mean sample direction is D= 028.2°; I= +61.9° (α_{95}= 7.4°; k= 82,4) *in-situ* and D= 015.0°; I= +60.2° (α_{95}= 6.8°; k= 97.6) after bedding-correction. There is an increase in directional clustering following bedding-correction, but this is not statistically significant. However, the in-situ direction is not similar to any expected direction at the sampling area. The palaeosouth pole corresponding to the bedding-corrected direction is located at λ= 17.4°N; ϕ= 303.3°E (dp= 7.8°; dm= 10.3°) in South American co-ordinates and λ= 11°N; ϕ= 336°E when transferred into African co-ordinates (Lottes & Rowley, 1990). This pole plots away from the Cambrian-Ordovician segment of Gondwana's APWP.
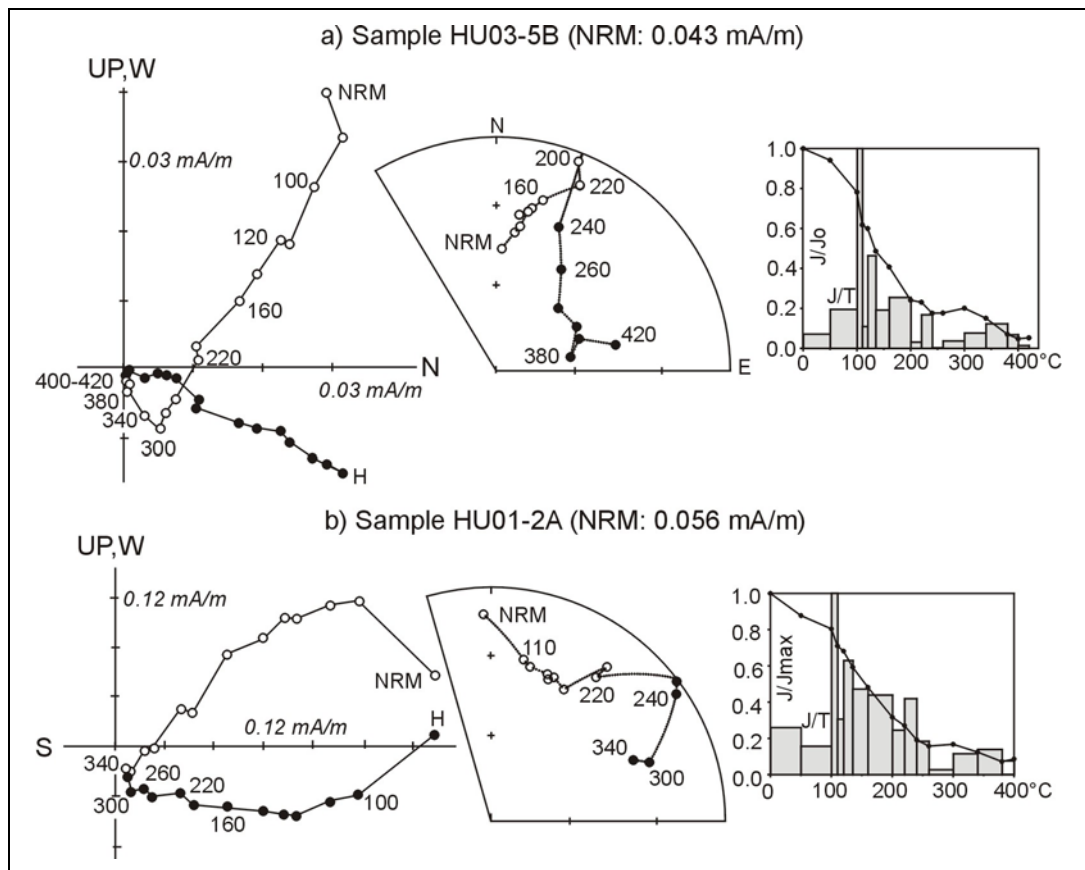
Fig. 10.5. Demagnetisation results of representative samples from the San Juan Formation (sites HUO1-3). Data points in orthogonal and equal area projections are in bedding-corrected (stratigraphic) co-ordinates.
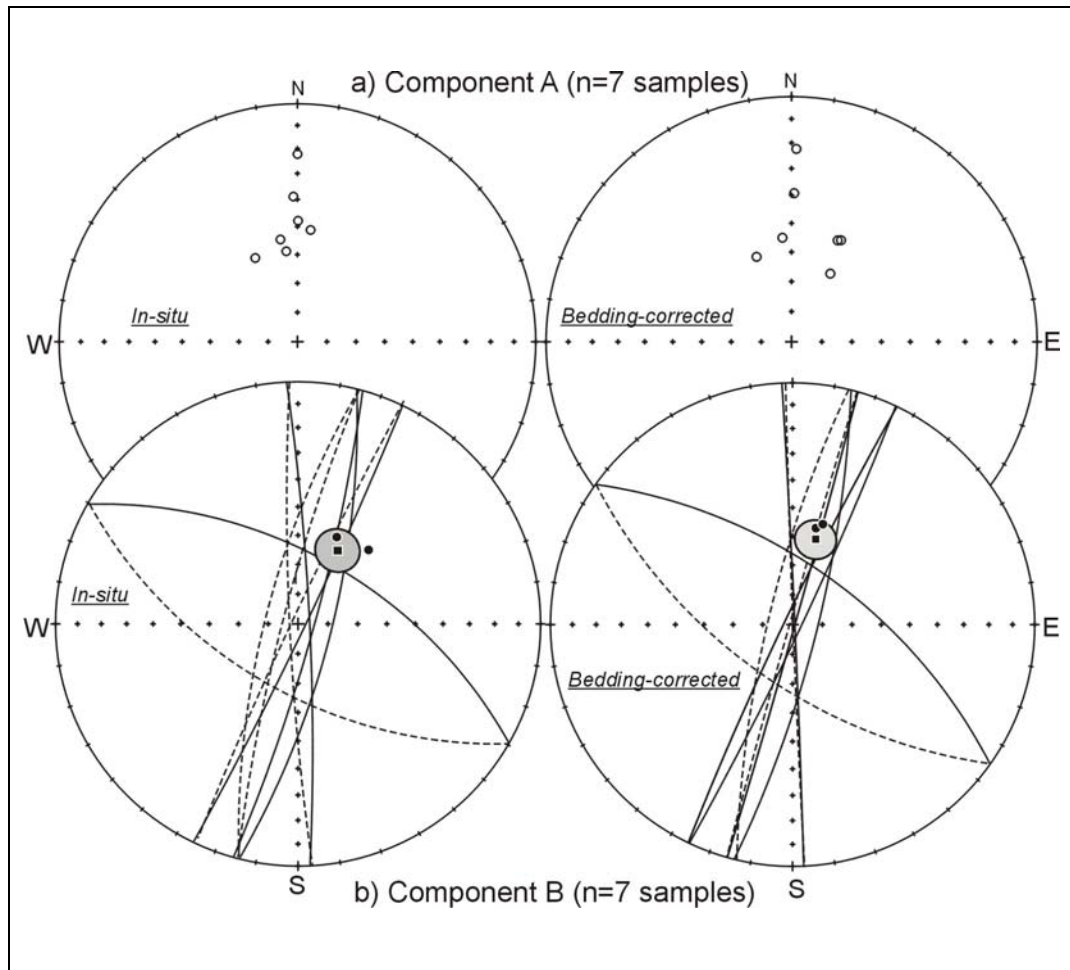
Fig. 10.6. Equal area stereographic projection of sample directions obtain from San Juan Formation (sites HUO1-6). The component A is interpreted as an overprint. Component B is a probable Early Ordovician magnetisation. Square with confidence circle represents mean direction calculated from 6 samples.

10.2.4 La Silla Formation (Early Ordovician)

The La Silla Formation was sampled in Cerro de la Silla, near Niquivil (NIQ, Tab. 10.1; Fig. 10.1). The carbonates from La Silla Formation are also very weakly magnetised, with initial NRM intensities ranging from 0.03 to 0.7 mA/m. The La Silla Formation yields 3 distinct magnetic components (Fig. 10.7): a low unblocking temperature component erased below 200°C; an intermediate component generally defined between 240°C and 300°C; and a high unblocking temperature component (C) isolated above 340°C, and stable up to 460°C.

The soft component (A) yields an overall sample mean direction (D= 002.0°; I= -36.7° (α_{95}= 3.9°; k= 52.4) *in-situ* similar to the present day local field and is clearly of VRM nature. The intermediate unblocking temperature component (NIQ-B) is identified in 18 samples, yielding an overall mean direction of D= 133.8°; I= +64.1° (α_{95}= 3.9°; k= 78.8) *in-situ*, and D=

273.2°; I= +82.9° (α_{95}= 4.5°; k= 60.1) after bedding correction. As there is a decrease of the directional clustering after bedding correction and stepwise unfolding shows maximum grouping in geographic co-ordinates, this component is considered post-folding in age. Therefore, the *in-situ* mean direction will be considered for interpretation.
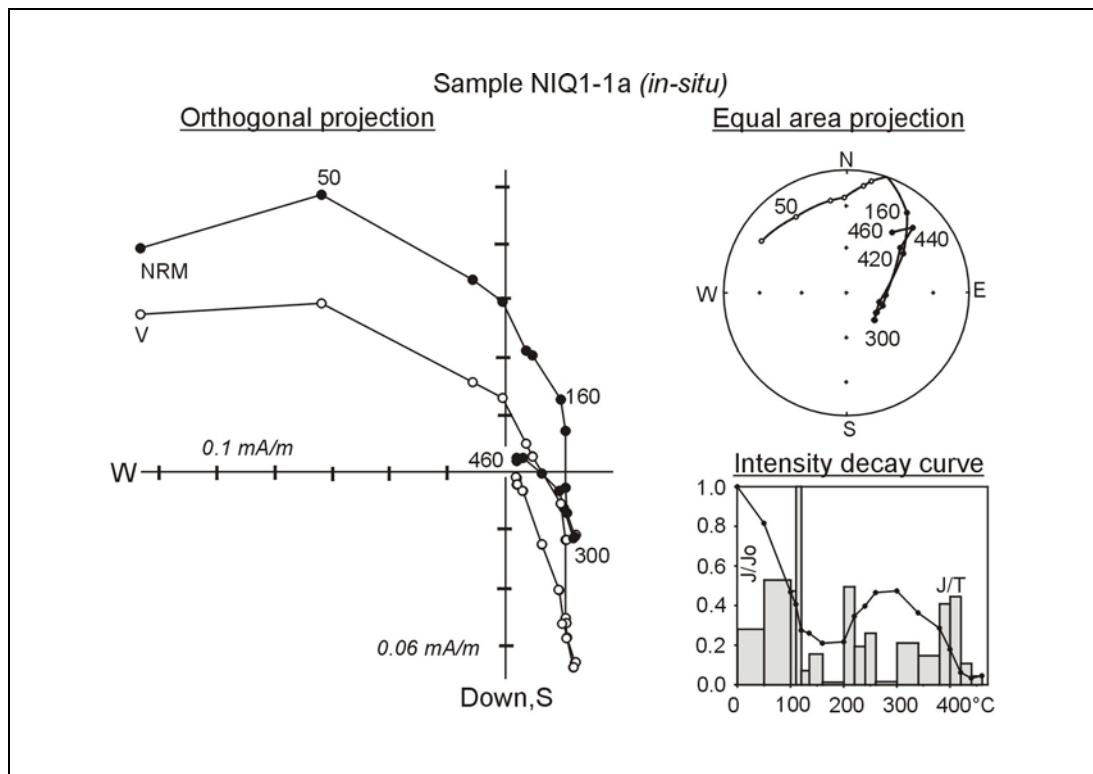
Fig. 10.7. Typical example of thermal demagnetisation results from La Silla Formation (Site NIQ1). Two distinct magnetic components with partially overlapping unblocking temperature spectra were identified. Closed/open circles are projection onto horizontal/vertical planes. Numbers adjacent to data points on orthogonal and stereographic projections indicate demagnetisation steps in degrees Celsius.

The highest unblocking temperature component (NIQ-C), recognised in 10 samples, yields and overall mean of D= 065.5°; I= +57.9° (α_{95}= 6.9; k= 49.5) *in-situ* and D= 009.0°; I= +57.9° (α_{95}= 5.7°; k= 73.9) after bedding correction. This remanence shows slight improvement of statistical precision parameters after bedding correction, but this is not statistically significant. However, when compared with the component A and B, which become scattered after bedding correction, this improvement of the directional grouping may be an indication of the pre-folding nature of the component C. For these reasons, the bedding-corrected direction is considered for further interpretation.
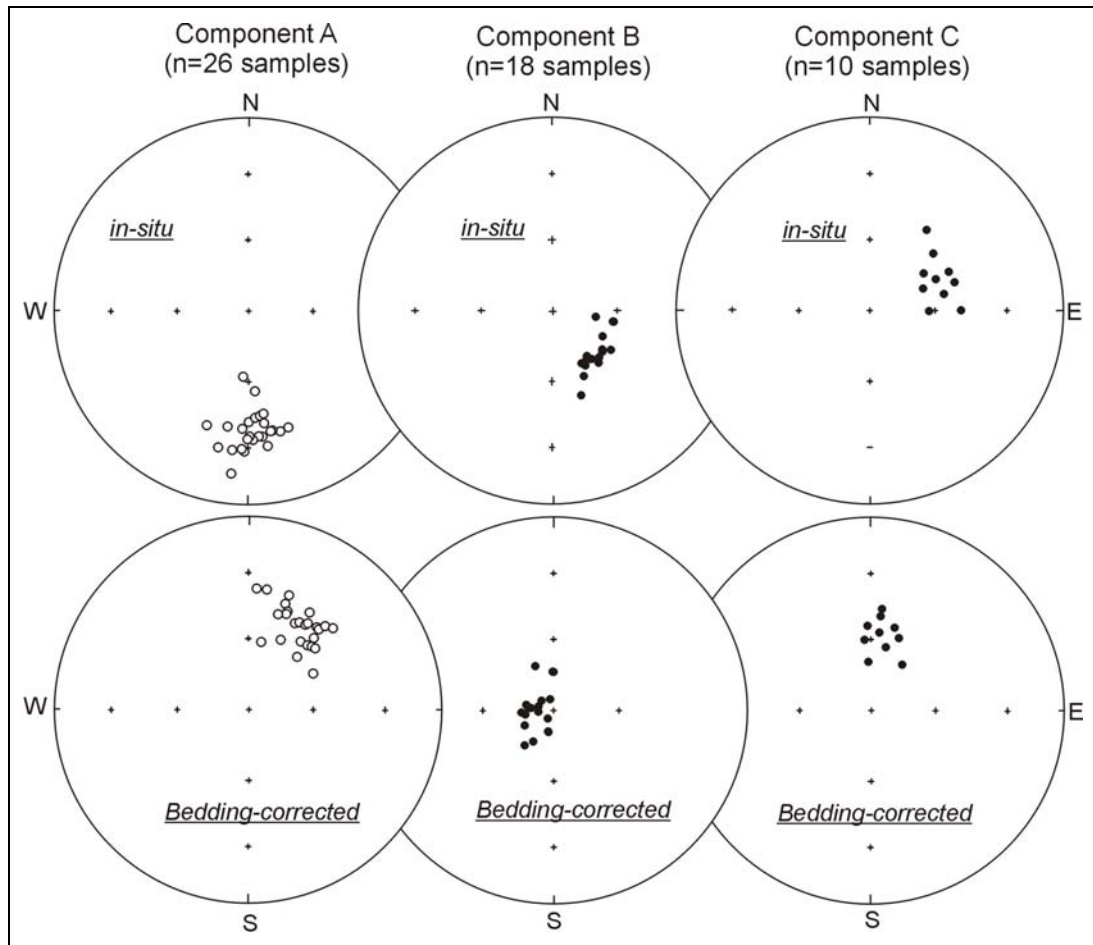
Fig. 10.8. Directional distribution (Equal area) of the results from the La Silla Fm.

NIQ	Dg(°)	Ig(°)	α_{95}(°)	kg	P_{lat}(°N)	P_{long}(°E)	Dg(°)	Ig(°)	α_{95}(°)	ks	P_{lat}(°N)	P_{long}(°E)	dp	dm
B	133.8	64.1	3.9	78.8	**-51.2**	**344.6**	273.2	82.9	4.5	60.1	-28.7	275.4	8.6	8.8
C	65.5	57.9	6.9	49.5	-2.0	336.7	9.0	57.9	5.7	73.3	**+20.5**	**298.9**	6.1	8.4

Tab. 10.2. Summary of the palaeomagnetic results from the Lower Ordovician La Silla Formation. The magnetic component B (n=18 samples) is interpreted as being a post folding remanence, while compoment C (n=10 samples) is assumed to be primary in origin. Hence, the respective poles (bold) corresponding to the *in-situ* and bedding-corrected mean directions are considered in this study. When transferred in African co-ordinates (Lawver & Scotese, 1987), these poles are situated at λ= -20.4°N; ϕ= 047.9°E (B), and at λ= +11.1°N; ϕ= 330.6°E (C).

Altogether, the combined high unblocking temperature components obtained from both San Juan and La Silla Formations (n= 17 samples), yield an overall direction of D= 054.5°; I= +61.5° (α_{95}= 6.3°; k= 33.0) *in-situ* and (D= 011.1°; I= +58.4°; α_{95}= 4.0°; k= 81.5) after bedding correction (Fig 10.8). The combined sample-level direction passes the fold test of McElhinny (1964) at 99% level of confidence. This component was, therefore, acquired before the

folding. The palaeosouth pole position corresponding to the bedding-corrected direction is $\lambda= 19°N$; $\phi= 301.1°E$ (dp= 4.4°; dm= 5.9°) in South American co-ordinates, and $\lambda= 11.3°N$; $\phi= 333.3°E$ when transferred in African co-ordinates according to the reconstruction parameters of Lawver & Scotese (1987). This pole also diverges from all Ordovician reference poles for Gondwana.
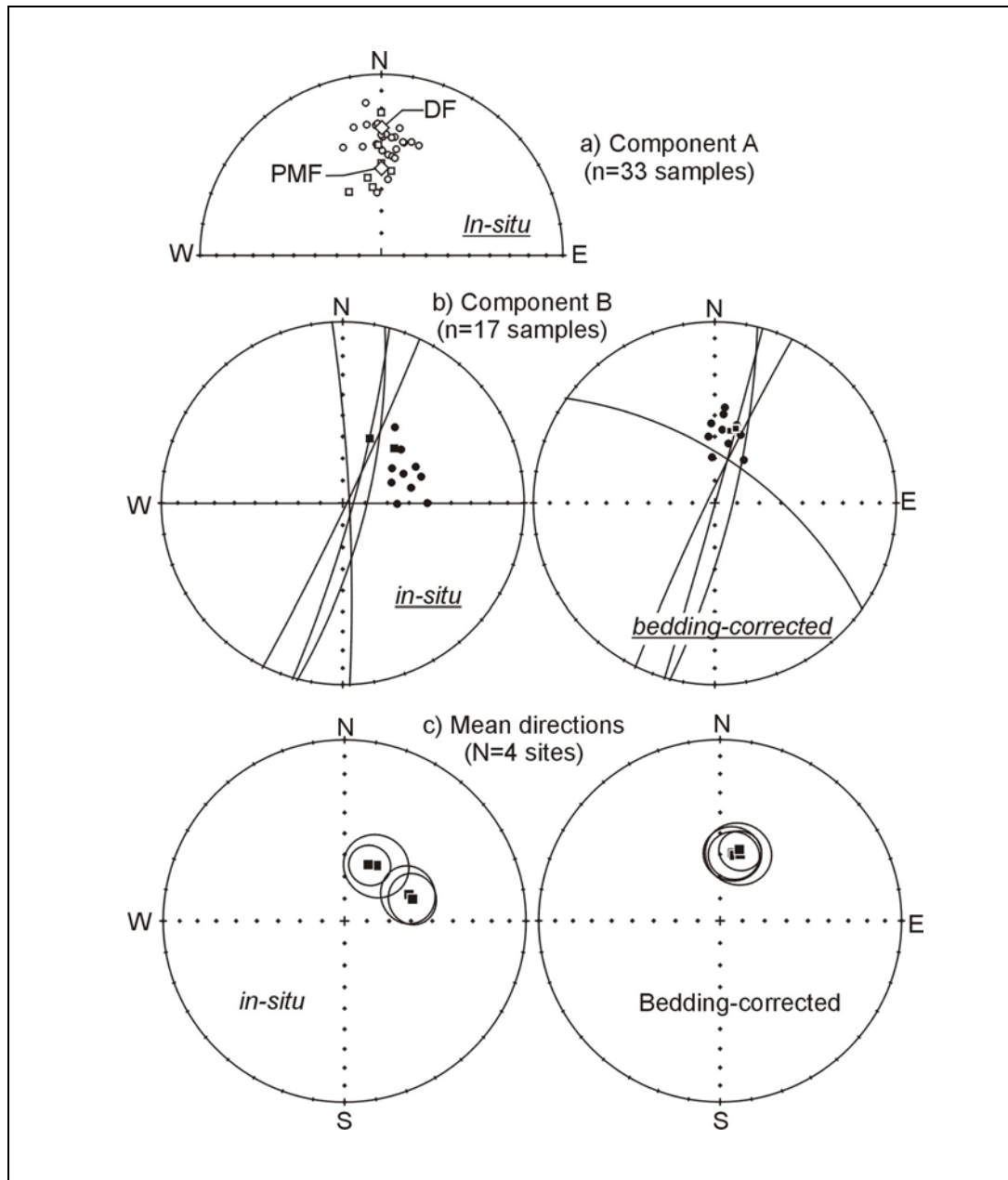
Fig. 10.9. Equal projection of the palaeomagnetic results from the Early Ordovician San Juan Formation (square) and La Silla Formation (circles). **a)** Samples directions for the soft component A interpreted as being a VRM. **b)** *in-situ* and bedding-corrected distribution of individual sample directions. The sample directions for la Silla Formation (n= 10) are well defined, whilst 5 of the 7 sample directions from the San Juan Fm were calculated using great circles. **c)** Distribution of the site-level mean directions in *in-situ* and bedding-corrected co-ordinates.

10.2.5 Los Espejos Formation (Late Silurian)

Samples from the Los Espejos Formation were drilled in grey siltstone/shale, and in some massive fine-grained sandstone beds, exposed along the road between Rodeo and Jachál (Fig. 10.1). Twenty-five samples collected in 5 palaeomagnetic sites were demagnetised. Stepwise thermal demagnetisations were performed in 15 to 18 steps. Initial NRM intensities generally range between 1.0 mA/m to 6.0 mA/m. Samples are either totally demagnetised at 590°C or have remaining magnetisation of less than 10% of their initial NRM. Demagnetisation steps above this temperature yield unstable directions in all samples.

Two distinct magnetic directions are isolated from the Los Espejos Formation. A low unblocking temperature direction (A) is defined in 9 samples between 100°C and 400°C. Direction A is exclusively of normal polarity, yielding an overall sample mean direction of D= 327.4°; I= -22.3°; (α_{95}= 10.5°; k= 25.1) *in-situ*. The decrease in directional grouping after bedding correction (α_{95}= 15.7°; k= 13.5) indicates that this direction is post-folding. It is likely a VRM magnetisation acquired under the present day magnetic field.

The stable direction (B) is characterised by maximum unblocking temperatures of 580°C, suggesting a remanence carried mainly by magnetite, and is isolated in 20 samples. In 14 samples, the stable remanence is well defined by linear trend of demagnetisation data points. However, the direction A and B have overlapping temperature spectra in some samples. The great circle method (McFadden & McElhinny, 1990) was, therefore, used to estimate the remanence direction in 6 samples.

The overall site-level mean (N= 3) for the B direction is D= 290.7°; I= 33.4° (α_{95}= 14.8°; k= 71) *in-situ*, and D= 289.8°; I= -29.9° (α_{95}= 17.6°; k= 50) after bedding correction (Tab. 10.4). While component A is clearly a magnetic overprint, there is no hint about the relative age of the component B. Both the *in-situ* and bedding-corrected directions deviate from all expected directions at the sampling location. However, the deviation of the bedding-corrected direction from the proposed APWP for Gondwana can be explained as a result of the clockwise rotation of the sampling area deduced from the above-mentioned Permian and Carboniferous palaeomagnetic data. Whereas, there is no explanation for the divergence of the *in-situ* mean direction. For this reason, the bedding-corrected mean direction is considered for further interpretation. The corresponding palaeosouth pole position is situated at λ= 24.6°S; ϕ= 16.2°E (A$_{95}$= 14.2°; K= 76.4) and λ= 10.4°N; ϕ= 60.2°E when rotated into African co-ordinates (Lottes & Rowley, 1990).

Site	n	Dg(°)	Ig(°)	Ds(°)	Is(°)	α_{95}(°)	k	P_{lat}(°S)	P_{long}(°E)	dp	dm	Dir(°E)	Dip
JAE1	9	282.5	37.8	282.5	-38.1	7.6	47.3	21.0	7.9	5.3	9.0	271	77
JAE2*	6	154.9	44.1	227.7	34.6	56.4	2.4	-	-	-	-	276	72
JAE3	3	302.0	33.2	297.2	-19.4	4.7	189.6	28.0	26.6	2.5	4.9	265	62
JAE4*	2	305.0	23.2	306.4	-26.3	171	22.6	-	-	-	-	261	66
JAE5	6	287.3	28.4	288.3	-31.8	10.3	49.3	24.1	14.6	6.5	11.6	261	66

Mean	N	Dg(°)	Ig(°)	α_{95}(°)	kg	Dg(°)	Ig(°)	α_{95}(°)	ks	λ(°S)	ϕ(°E)	A_{95}(°)	K
	3	290.7	33.4	14.8	70.6	289.8	-29.9	17.6	49.9	-24.6	16.2	14.2	76.4

Tab. 10.3. Palaeomagnetic data from the Los Espejos Formation (Component B). n: number of samples. * Sites JAE-2 and JAE-4, which show poor within site grouping, were not used when calculating site mean direction. The listed site-level VGPs were calculated from the bedding-corrected mean directions.
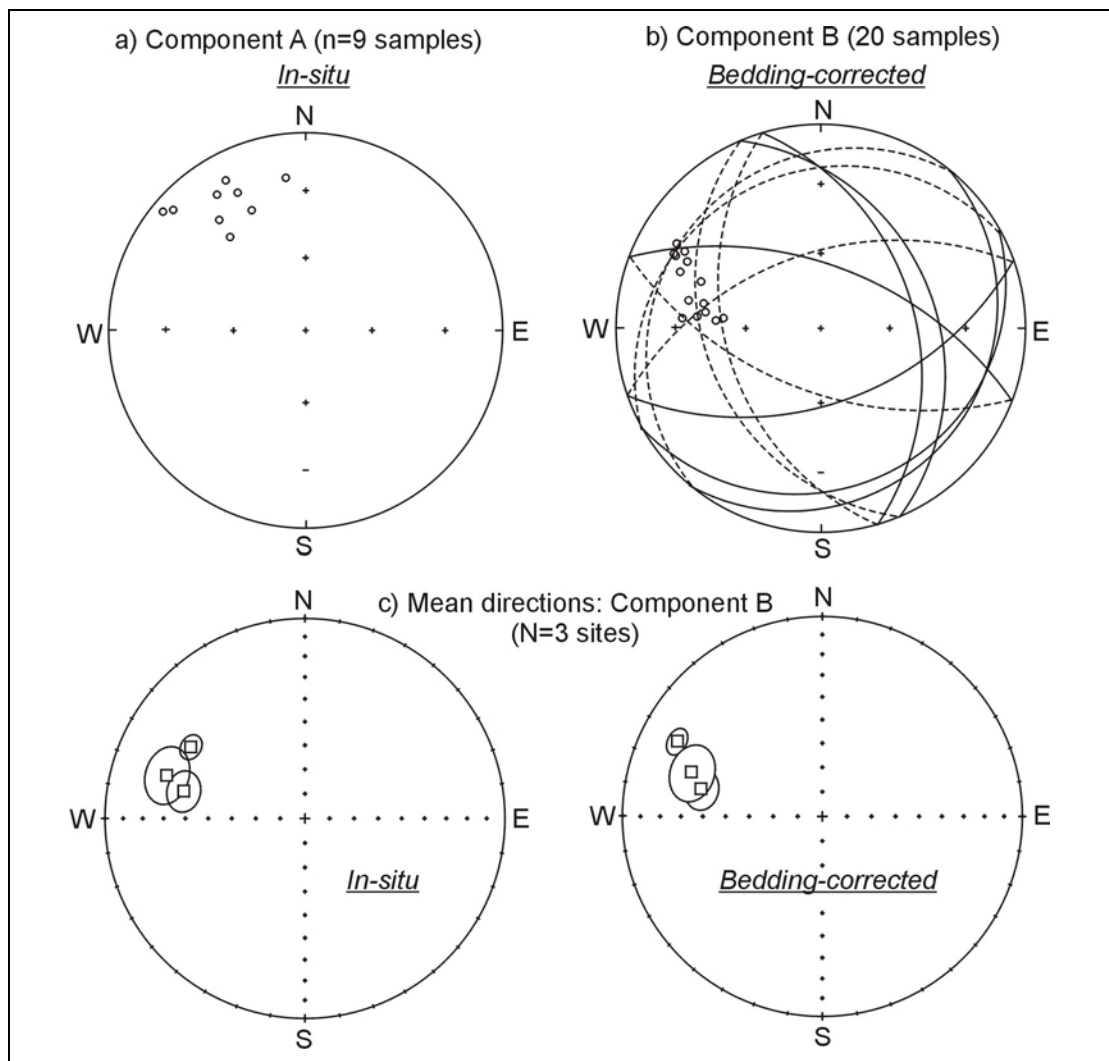
Fig. 10.10. Equal area projection of the palaeomagnetic data from the Silurian Los Espejos Formation (sites JAE1-5).

10.2.6 Other sedimentary rock units

As shown in figure 10.1 and table 10.1, other units covering the Ordovician to the Devonian times were collected in the Argentine Precordillera. Unfortunately most of these Palaeozoic rocks did not provide any interpretable palaeomagnetic data. For instance, the green shales and siltstones of the Early Devonian Talasco Formation drilled in a road-cut between Huaco and Jachál (location JAT) yield an overall direction with unsatisfactory grouping in both samples (n= 22) and sites (N= 5) levels, although, thermal demagnetisation of individual samples reveals fairly well defined single component magnetisation (Fig. 10.11).

Similarly, the samples drilled in the sandstone units of the Late Devonian Punilla Formation (location PUN) are very weakly magnetised and did not provide any interpretable demagnetisation data. Low unblocking temperature magnetisations calculated from some samples with average quality demagnetisation are incoherent. As well, the Ordovician Yerba Loca Formation Drilled in 7 sites near Rodeo village (ROO) shows erratic directional behaviour during stepwise demagnetisation experiments, and no stable end points could be calculated.
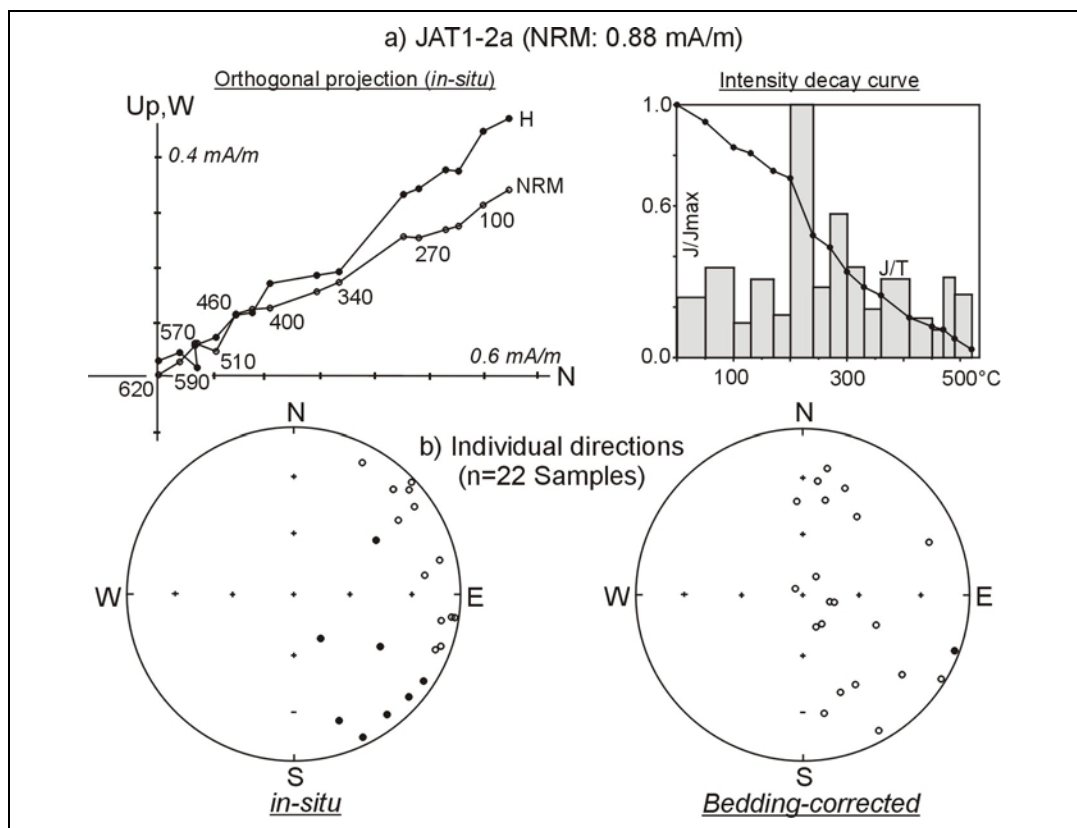
Fig. 10.11. a) Example of demagnetisation results for the Punilla Formation. **b)** Equal area projection showing distribution of the individual sample directions.

10.2.7 Interpretations

The stable remanences of the Patquia Formation and the Guandacol Formation are interpreted as being primary, acquired in the Late Permian and Late Carboniferous, respectively. These palaeomagnetic data indicate possible rotation of the sampling area (eastern Argentine Precordillera) during the Andean thrusting. A clockwise rotation of at least 45°clockwise is assumed from these data. Assuming this rotation, the corrected palaeopoles from the Patquia and Guandacol Formations coincide with the coeval reference poles for stable South America and for Gondwana (Fig. 10.12). When also corrected for similar rotations, the palaeopole obtained from the Los Espejos Formation falls on the Ordovician-Silurian part of the APWP for Gondwana. However, the Early Ordovician pole from the La Silla and San Juan Formation diverges from all reference poles for Gondwana even after correction for a clockwise rotation of approximately 45°. The secondary component B direction identified in these samples, however, falls on the Devonian segment of the APW path after rotational correction. This remanence may, therefore, be a Devonian overprint. The palaeogeographic implication of the identified primary Ordovician direction is further discussed in section 10.4.

10.3 Palaeomagnetism of the Famatina Range

10.3.1 De la Cuesta Formation (Late Permian)

The De la Cuesta Formation was first described by Freguelli (1946) as Patquia Formation, and later defined by Turner (1960) to be De la Cuesta Formation (Duran *et al.*, 1996). In the literature, the De la Cuesta Formation is considered equivalent of the Patquia Formation within the Paganzo basin. Turner (1967) suggested that the De la Cuesta Formation (up to 1600 m thick) was deposited during the whole of the Permian. Lately, a Lower Early Permian age is attributed to the De La Cuesta Formation (Aceñolaza & Vergel, 1987; Vergel, 1996) based on palynology. Stratigraphically, the De La Cuesta Formation overlies the palynologically dated Late Carboniferous Agua Colarada Formation.

Samples from the De La Cuesta Formation were collected within the Famatina geological province. The sampling sites are situated west of Fiambalá in the Las Angosturas area (Fig. 10.13), the exposure of La Cuesta Formation consists mainly of red cross-bedded sandstones, with conglomeratic beds. Twenty-seven drill cores were drilled in reddish fine to medium-grained sandstone beds.
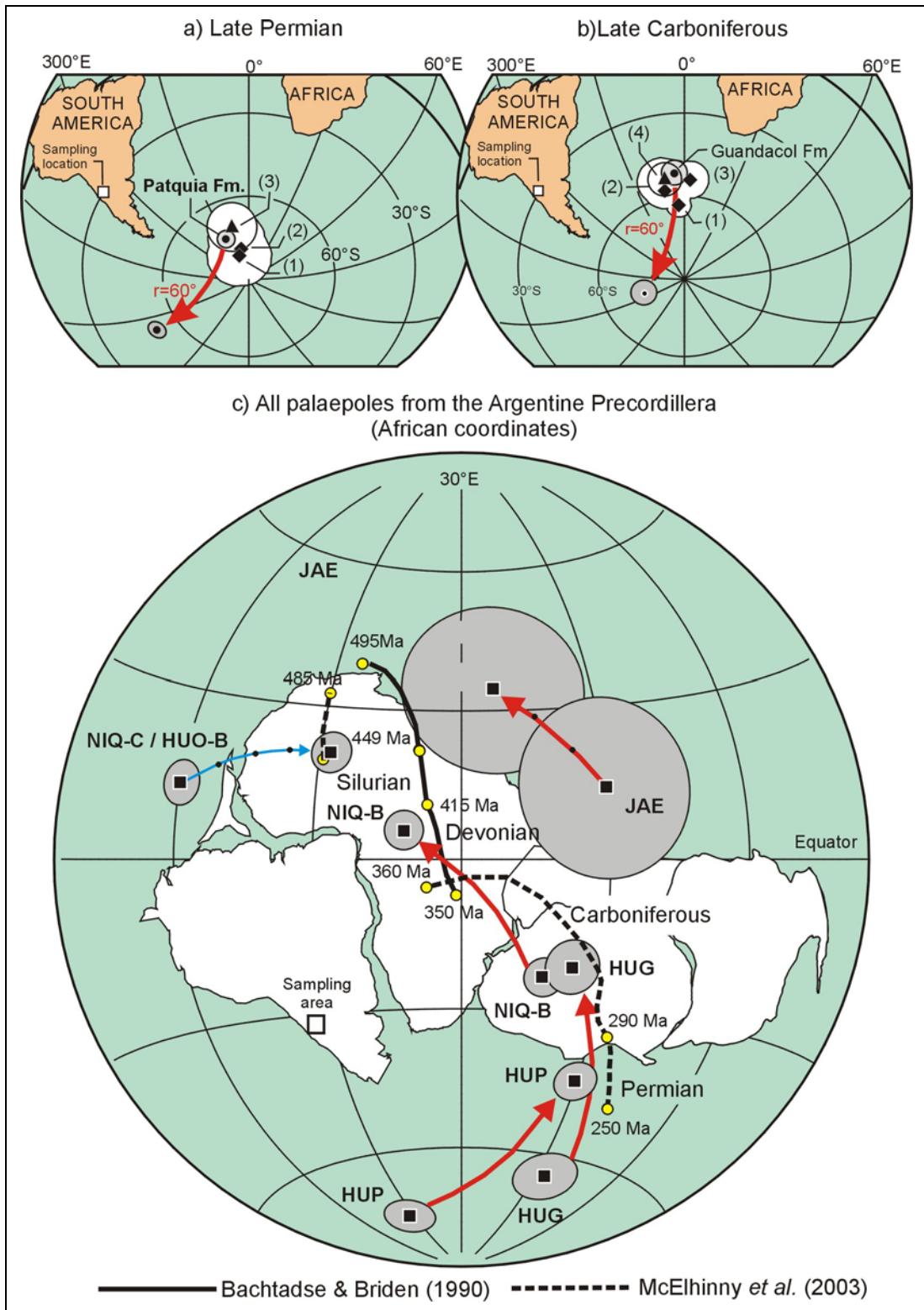
Fig. 10.12. a) and **b)** Late Permian (Patquia Formation) and Late Carboniferous (Guandacol Formation) poles from the Argentine Precordillera compared with the coeval reference poles from stable South America (triangle) and Gondwana (diamond). Reference poles are: <u>Late Permian</u>: (1) Torsvik & Van der Voo (2002; 260 Ma), (2) McElhinny *et al*. (2003; 260 Ma), (3) Mean South American poles. <u>Late Carboniferous</u>: (1) McElhinny *et al*. (2003; 320 Ma), (2) Torsvik & Van der Voo (2002; 310 Ma), (3) McElhinny *et al*. (2003; 300 Ma), (4) Mean South American poles.

Fig. 10.12 *(continued)* **c)** Equal area projection of all palaeopoles from the Argentine Precordillera compared with the proposed Palaeozoic APWPs for Gondwana. Pole positions before and after correction for 60° anticlockwise (red arrow) and 45° clockwise (bleu arrow) rotations are shown.
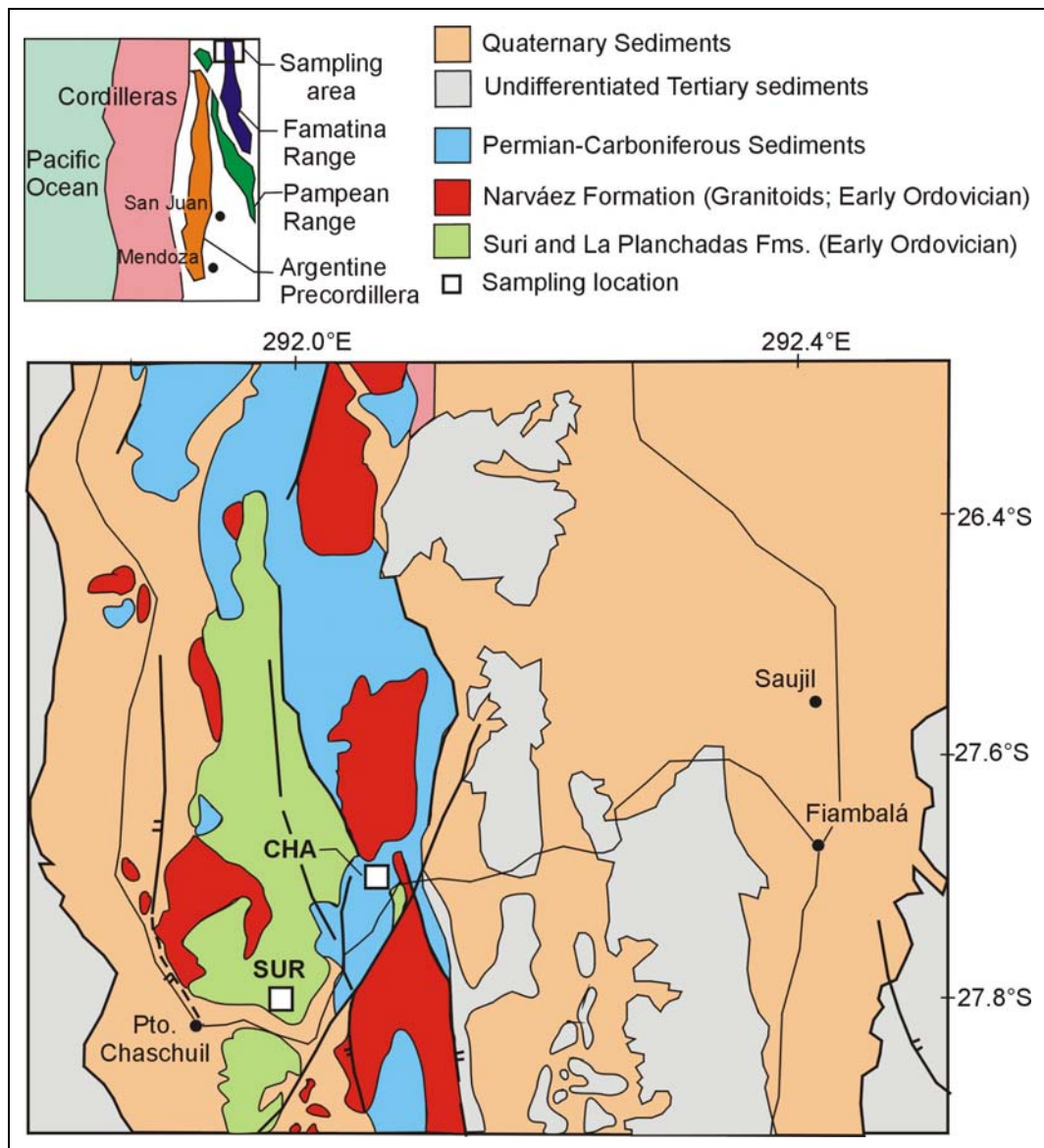
Fig. 10.13. Simplified geological map of the northern Famatina (box, inset) showing sampling locations for the De la Cuesta (CHA) and Suri (SUR) Formations (map after Duran, 1996).

These samples have NRM intensities ranging between 1.4 and 5.6 mA/m. Forty-four specimens cut from 26 drill cores were thermally demagnetisation up to 700°C. Stepwise demagnetisations isolated two distinct magnetic directions. A low unblocking temperature direction (A) was generally erased below 400°C (Fig. 10.14). The direction A is identified in 21 samples (10 great circles), yielding an overall mean of D= 354.7°; I= -39.0° (α₉₅= 11.5°; k= 13.7). The rather large confidence circle of the mean direction includes both the expected present dipole field (D= 360°; I= -48°) and the present

154

magnetic field (D= 359°; I= -26.0°) at sampling area. The soft magnetisation A is therefore interpreted to be of viscous in origin.

Intermediate and high unblocking temperature directions were identified in 23 samples from all sites. Unblocking temperature referred from intensity decay curves suggest that magnetite (T_b= 580°C) and haematite (T_b>650°C) are the main remanence carriers (Fig. 10.14). Both the magnetite and haematite remanences are of reversed polarity with southeasterly declinations. These directions are slightly different in individual samples, but statistically indistinguishable at both within- and between-sites level (Fig. 10.15; Tab. 10.4).
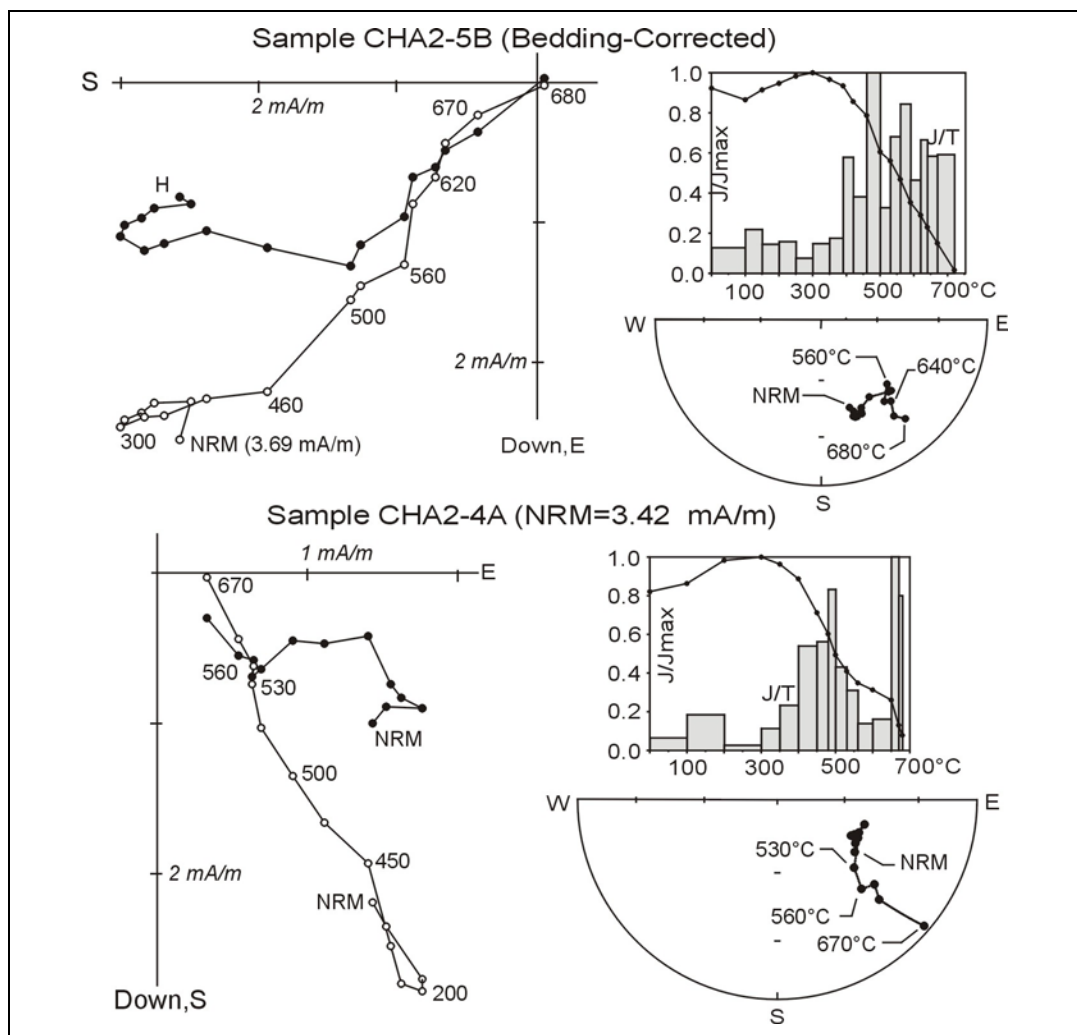
Fig. 10.14. Representative examples of thermal demagnetisation results from the De La Cuesta Formation. Orthogonal projection and equal area stereographic projection are shown in bedding-corrected co-ordinates. Closed/open circles are projections onto horizontal/vertical planes. Numbers adjacent to data points on orthogonal projections indicate demagnetisation steps in degrees Celsius. Intensity decay curves illustrate remanence carriers dominated by haematite in some samples and by both magnetite and haematite in others.

The overall B remanence from the Lower Permian age De la Cuesta Formation yields a site-mean direction of D= 185.4°; I= +41.8° (α_{95}= 14.3°; k= 29.5; N= 5) *in-situ* and D= 163.2°; I= +43.8°; α_{95}= 10.0°; k= 59.5) after bedding correction (Tab. 10.4). There is an increase in directional grouping (k-ratio: 2.0) after bedding correction but this is not statistically significant according to the fold test of McElhinny (1964). However, stepwise unfolding demonstrates an optimal grouping of the site-mean directions at 107% unfolding (Fig. 10.16), and it passes the Direction-Correction fold test of Enkin (2003). Therefore, the B direction is considered as being a pre-folding remanence. The mean of five VGPs corresponding to the bedding-corrected directions yield a pole located at λ= 75.0°S; ϕ= 25.9°E (A$_{95}$= 12.4°; K= 38.9), comparable with the mean Late Permian pole from previously published data from South Africa (λ= 75°S; ϕ= 344°E; Tab. 10.4), and the mean 260 Ma poles for Gondwana reported in Torsvik & Van der Voo (2002; λ= 80.5°S; ϕ= 340°E) and McElhinny *et al*. (2003; λ = 78.5°S; ϕ= 347.5°E). The palaeomagnetic south pole from De la Cuesta pole is situated at λ= 37.9°S; ϕ= 76.6°E (A$_{95}$= 12.4°) when rotated into African co-ordinates according to the reconstruction parameters of Lottes & Rowley (1990).
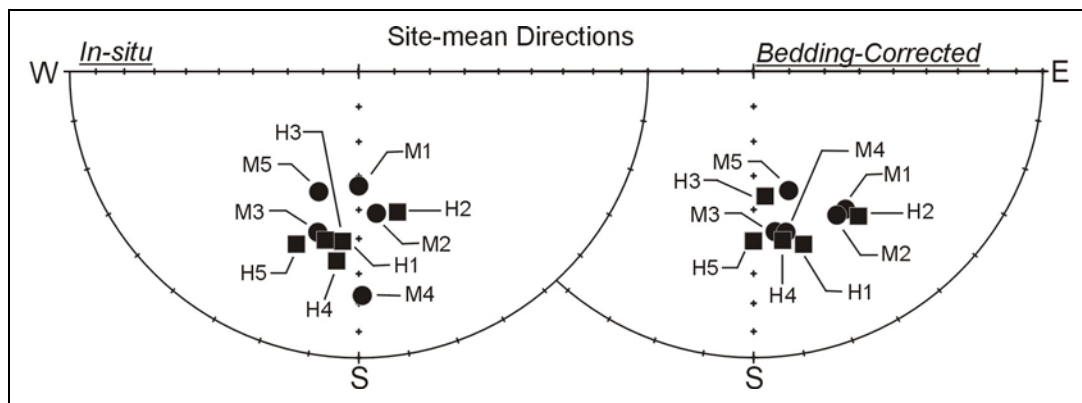
Fig. 10.15. Site mean directions of the remanences carried by magnetite (M) and haematite (H). Numbers 1 to 5 designate site numbers. Confidence circles (Table 6.2) are not shown for clearness. The magnetite and haematite directions (B1 and B2) are statistically indistinguishable in both within- and between-site levels.
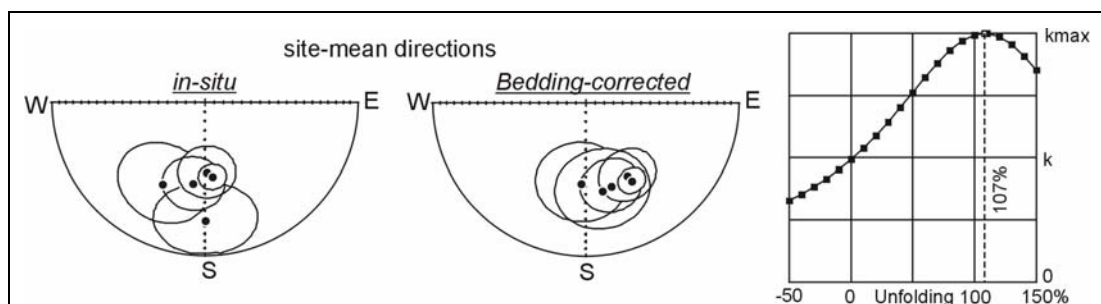
Fig. 10.16. Equal area projection of the stable remanence (B) from the De La Cuesta Formation. Variation of the precision parameter k (Fisher, 1953) illustrating optimal directional grouping at 107% unfolding is shown on right panel.

Magnetite remanence (B1)

Site	Dg(°)	Ig(°)	Ds(°)	Is(°)	α95(°)	
CHA1	180.3	57.1	146.6	41.1	10.9	
CHA2	173.7	48.9	149.2	41.1	10.9	
CHA3	194.8	41.2	171.7	43.1	16.6	
CHA4	179.4	22.6	169.7	41.3	23.3	
CHA5	198.7	53.4	163.4	54.3	29.1	
Mean	Dg(°)	Ig(°)	α95(°) kg		Ds(°) Is(°)	α95(°) ks
5 sites	185.1	45.1	14.9 27.4	159.9 44.7	9.7 63.2	

Haematite Remanence (B2)

Site	Dg(°)	Ig(°)	Ds(°)	Is(°)	α95(°)	
CHA1	185.5	40.1	163.9	37.9	18.6	
CHA2	165.1	47.9	143.8	37.2	8.1	
CHA3	191.4	40.0	169.7	40.7	23.6	
CHA4	186.7	33.3	173.9	53.5	16.2	
CHA5	199.4	35.8	179.7	40.5	17.4	
Mean	D_g(°)	I_g(°)	α95(°) kg		Ds(°) Is(°)	α95(°) ks
5 sites	186.4	39.9	10.4 55.3	165.7 42.6	11.7 43.4	

Overall B remanence

Site	n	Dg(°)	Ig(°)	Ds(°)	Is(°)	α95(°)	k	P_{lat}(°S)	P_{long}(°E)	dp	dm	Dir(°E)	Dip
CHA1	4	187.6	44.3	163.4	42.7	15.3	41.2	74.8	29.4	18.9	11.7	89	25
CHA2	4	173.9	48.6	149.7	40.9	7.1	169.0	62.4	24.0	8.6	5.2	89	25
CHA3	3	206.5	38.8	184.0	46.1	22.8	30.2	86.4	199.0	29.2	18.7	89	25
CHA4	7	186.7	33.3	173.9	53.5	16.2	13.3	79.9	42.9	28.4	17.3	34	25
CHA5	5	177.9	51.3	150.4	44.6	14.6	28.4	63.6	18.2	18.4	11.6	89	25
Mean	N	Dg(°)	Ig(°)	α95(°)	kg	Ds(°)	Is(°)	α95(°)	ks	λ(°S)	φ(°E)	A_{95}(°)	K
	5	185.4	41.8	14.3	29.5	163.2	43.8	10.0	59.5	75.0	25.9	12.4	38.9

Tab. 10.4. Palaeomagnetic site-mean directions from the De La Cuesta Formation. Site mean directions of the magnetisation dominantly carried by magnetite (B1) and haematite (B2) are listed separately. B1 and B2 are statistically indistinguishable in both site-level and overall mean directions (see Fig.6.4). P_{lat}/P_{long}: latitude/longitude position of the palaeomagnetic poles calculated from *in-situ* site means. N: number of sites; n: number of samples used when computing the listed site means.

10.3.2 Suri Formation (Early Ordovician)

a) Sampling

The Ordovician in the Famatina range is represented by the Suri and Molles Formations. These units comprise up to 2000 meters of mixed silici-clastic and volcano-clastic sediments (Astini, 1999). The Suri Formation exposed in Chaschuil area, in the northern part of the Famatina Range is the subject of the present study and comprises marine sediments representing a shallowing-upward depositional environment, from slope apron, shelf, to fan-delta (Waisfeld *et al.*, 2003). The upwards-increasing volcanic content of the

Formation indicates contemporaneous active volcanism. Based upon evidence from the Loma del Kilómetro Member, it has been suggested that the associated volcanic arc has developed on a narrow and geographically restricted shelf (Astini, 1998; Mángano & Buatois, 1997). A Middle Arenig age is attributed to the Suri Formation, based upon trilobite fauna from Loma del Kilómetro Member exposed in Chaschuil area (Vaccari & Waisfeld, 1994; Albanesi & Vaccari, 1994). Toro & Brussa (1996) dated the lower graptolite rich part of the Suri Formation as Lower Middle Arenig in age, and Middle Arenig conodonts in both the upper part of Suri Formation and the base of the overlying Los Molles Formation is reported in Albanesi & Astini (2000). These palaeontological data indicate an age range between 478 and 485 Ma, following the geological timescale of Gradstein & Ogg (1996). Twenty-five samples were sampled within an approximately 10 meters thick sequence of volcano-clastic sediments of the Suri Formation exposed in Chaschuil area (Fig. 10.13). Five core samples were drilled in different horizon separated by 2–3 meters, considered as palaeomagnetic sites.

b) Results and Interpretations

Initial intensities of the remanence in Suri Formation range between 1.4 and 27.4 mA/m. Stepwise demagnetisations of all 25 samples were performed in 15 to 18 steps, with maximum temperature of 600°C. Two palaeomagnetic directions, either well defined or showing partial overlap of unblocking temperature spectra, were isolated during demagnetisation (Fig. 10.17).

The soft magnetic direction (A), well defined in 15 samples for 4 sites, is completely erased after 370°C demagnetisation step. The A direction is of normal polarity yielding an overall mean site direction of D= 355.0°; I= -45.3° (α_{95}= 12.0°; k= 59.8) *in-situ*. This direction is indistinguishable at the 95% confidence level from the expected present dipole field direction at the sampling area (D= 360°; I= -49°), and thus represents an overprint magnetisation acquired under the present geomagnetic field.

The high unblocking temperature B direction is identified in 15 samples and is stable up to 590°C. Individual sample directions from these samples were calculated from at least the 6 last data points, clearly converging toward the origin on orthogonal projection. The great circle method (McFadden & McElhinny, 1988) was used to calculate individual directions for the 10 samples wherein A and B directions overlap (Fig. 10.17c,d). Intensity decay curves indicate that this stable direction is dominantly carried by magnetite with unblocking temperature ranging between 580 and 590°C.

The stable remanence from Suri Formation is exclusively of reverse polarity and well grouped in both samples and site levels (Fig. 10.18). The mean-site

direction is D= 117.2°; I= 52.7° (α_{95}= 7.1°; k= 97.3; N= 5) *in-situ*, and D= 107.0°; I= 30.6° (α_{95}= 7.1°; k= 97.3) after bedding correction (Tab. 10.5). No change in directional grouping was expected because all sites have the same bedding attitude. Consequently, there is no field test to establish the acquisition time of this magnetisation. Both the *in-situ* and the bedding-corrected directions deviate from all references recalculated from Ordovician and younger magnetisation for stable South America and for Gondwana. The bedding-corrected B direction is, however, similar to the previously published Early Ordovician data from Puna oriental-Famatina reported (Conti *et al.*, 1996). These authors found a reversed polarity magnetisation that passes the McFadden (1990) fold test at the 99% level of confidence.
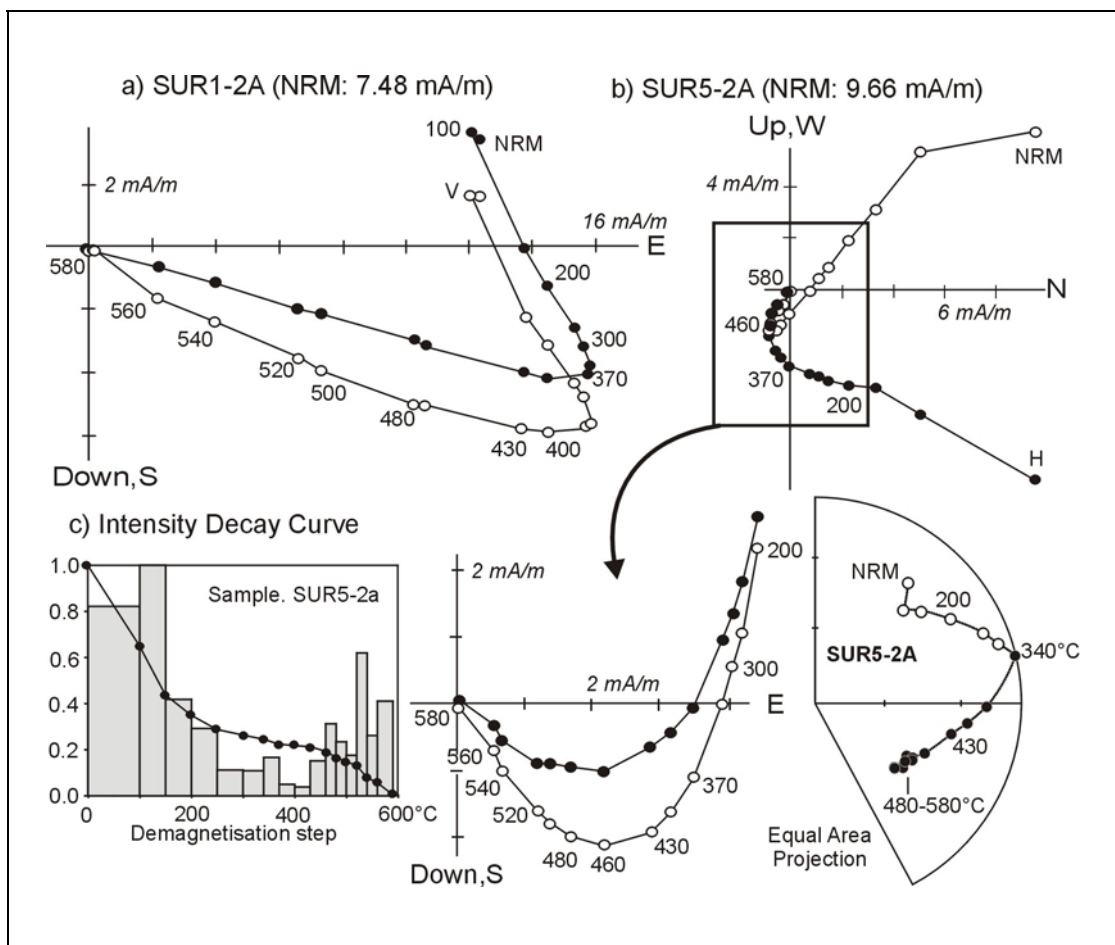
Fig. 10.17. Representative examples of thermal demagnetisation results from Suri Formation. **a)** and **b)** Orthogonal projection for samples SUR1-2A and SUR5-2A. **c)** Close-up view corresponding to the box in B. E: Equal area projection showing directional change (SUR5-2A) during demagnetisation. **d)** Intensity decay during stepwise demagnetisation. Two distinct directions either well-isolated or showing overlap of stability spectra were identified. Closed/open circles are projection onto horizontal/vertical planes. Numbers adjacent to data points indicate temperature steps in degree Celsius.

Assuming that the Suri remanence is also of pre-folding nature, the corresponding palaeopole is situated at $\lambda= 21.6°$S; $\phi= 14.0°$E ($A_{95}= 4.5°$; K= 293) and at $\lambda= 12.8°$N; $\phi= 57.4°$E when rotated into African co-ordinates and the Gondwana framework (Tab. 10.5). This pole clearly diverges from all proposed APWPs for Gondwana. As the palaeomagnetic data from the De La Cuesta Formation indicates stability of the northern Famatina since the Late Permian, this discrepancy is not the result of rotation during the Andean deformation. In contrast, the Suri pole plots on the Cambrian-Ordovician segment of the Laurentian APWP (Fig. 10.19).

Component A

Site	n	Dg(°)	Ig(°)	Ds(°)	Is(°)	α_{95}(°)	k	P_{lat}(°S)	P_{long}(°E)	dp	dm	Dir(°E)	Dip
SUR1	5	351.4	-34.5	337.0	-28.2	9.1	70.9	78.2	68.5	6.0	10.5		
SUR2	4	348.3	-51.0	324.6	-41.5	7.1	168.9	79.1	358.0	6.5	9.6		
SUR3	4	354.4	-41.4	335.5	-35.4	7.7	142.3	83.6	58.8	5.8	9.4	89	24
SUR5	3	7.9	-53.6	336.5	-50.6	9.6	167.2	80.7	246.8	9.3	13.3		

Mean	N	Dg(°)	Ig(°)	α_{95}(°)	kg	Ds(°)	Is(°)	α_{95}(°)	ks	λ (°S)	ϕ(°E)	A_{95}(°)	K
	4	355.0	-45.3	12.0	59.8	333.5	-39.0	12.0	59.8	85.8	26.8	11.7	62.6

Component B

Site	n	Dg(°)	Ig(°)	Ds(°)	Is(°)	α_{95}(°)	k	P_{lat}(°S)	P_{long}(°E)	dp	dm	Dir(°E)	Dip
SUR1	5	123.8	56.7	116.6	35.4	5.8	234.9	27.6	13.2	3.3	5.0		
SUR2	4	112.2	51.0	105.3	28.3	5.7	357.4	20.3	15.2	3.1	5.2		
SUR3	8	111.3	56.9	103.5	34.0	4.4	224.9	20.2	10.9	2.5	3.8	89	24
SUR4	5	133.3	56.8	104.8	34.2	5.1	458.5	21.3	11.3	2.9	4.5		
SUR5	3	110.3	43.8	105.3	21.0	12.2	309.3	18.5	19.2	6.4	11.6		

Mean	N	Dg(°)	Ig(°)	α_{95}(°)	kg	Ds(°)	Is(°)	α_{95}(°)	ks	λ(°S)	ϕ(°E)	A_{95}(°)	K
	5	117.2	52.7	7.1	97.3	107.0	30.6	7.1	97.3	21.6	14.0	4.5	293.1

Tab. 10.5. Site-level palaeomagnetic data from the Suri Formation. The Component B is considered to be a post-folding remanence. Hence, the listed VGPs (P_{lat}/P_{long}) and the mean palaeomagnetic south pole (λ°S /ϕ°E) correspond to the bedding-corrected direction. Contrarily, the site-level VGPs and mean palaeopole for the overprint component A are calculated from the mean directions in *in-situ* co-ordinates.
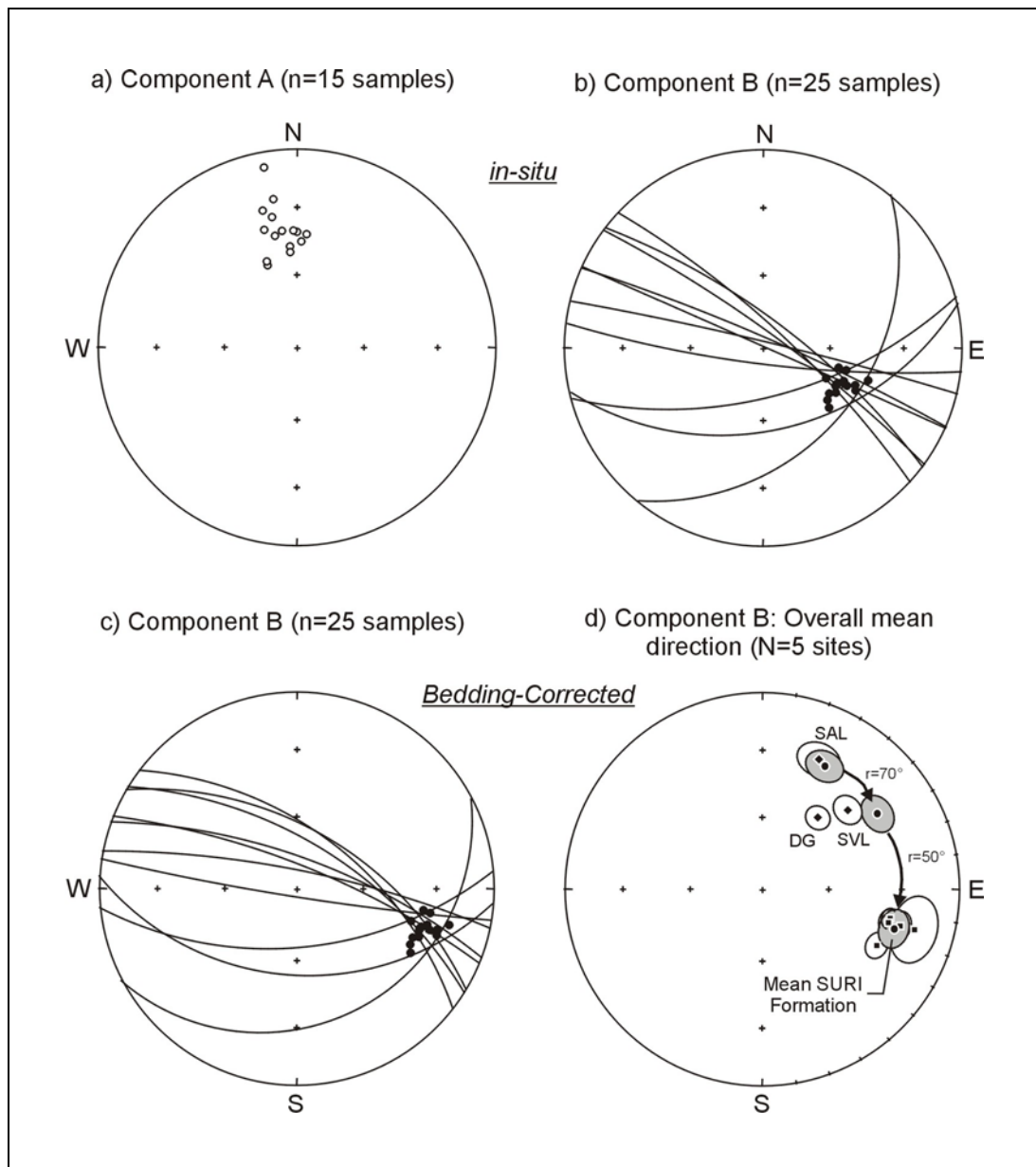
Fig. 10.18. Equal area projection of the palaeomagnetic directions from the Suri Formation. **a)** Distribution of the of low temperature remanence A from15 samples. **b)** Distribution of the stable remanence B identified in 25 samples. Great circles method were used to calculate the high unblocking temperature component in 10 samples wherein the direction B was not completely isolated as a result of overlapping unblocking temperatures with the component A. **c)** Distribution of the bedding-corrected directions for component B. **d)** Site-level means and overall mean directions for component B compared with the reference directions recalculated from the published African poles (DG; SAL; SVL).
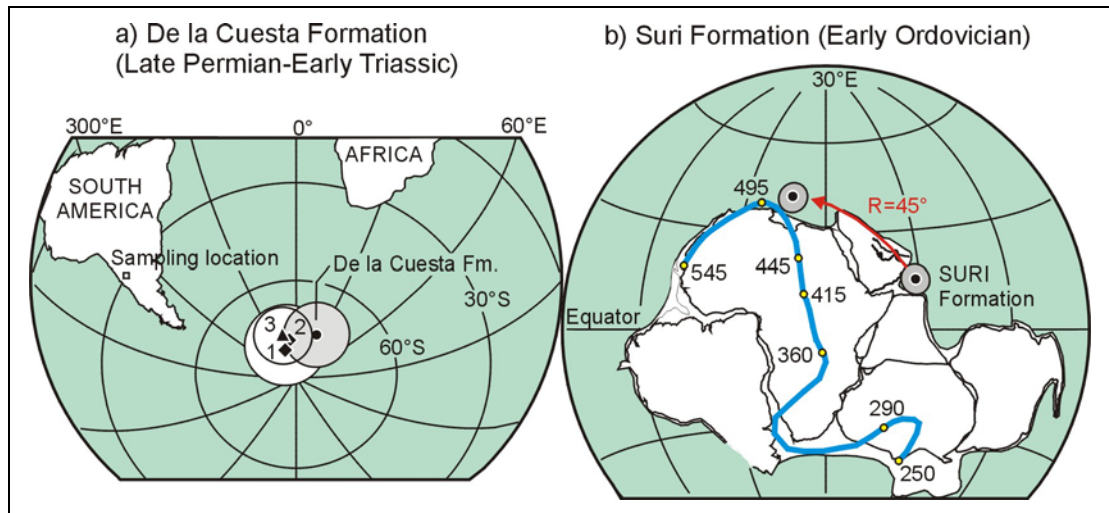
Fig. 10.19. Equal area projection of the palaeopoles from the northern Famatina. **a)** Comparison of the De la Cuesta pole (South American co-ordinates) with the reference poles for stable South America and for Gondwana. 1: Torsvik & Van der Voo (2002; 260 Ma); 2: McElhinny *et al.* (2003; 260 Ma). 3: Mean South American poles reported in this study (Chapter 6). **b)** Position of the Suri pole (in African co-ordinates) compared with the APWP for Gondwana (Bachtadse & Briden, 1990).

10.4 Discussion and conclusion

a) The Argentine Precodillera

Primary palaeomagnetic directions have been obtained from Lower Ordovician (San Juan and Silla Formations), Early Silurian (Espejos Formation), Late Carboniferous (Guandacol Formation), and Late Permian (Patquia Formation) age sequences. All resulting palaeopoles are in discordance with the APW path for Gondwana. However, applying a clockwise rotation of approx. 45° brings the Silurian to Permian age results into reasonable agreement with the APW path for Gondwana. This is a clear indication that the region as a whole has undergone rotation with respect to stable South America in post Permian times, and most likely in relation to the Andean deformation. After correction for this regional rotation, however, the Ordovician palaeopole obtained from the Precordillera diverges significantly from the Early Ordovician segment of the APW path for Gondwana indicating a complex tectonic history involving a pre-Silurian rotation of the Argentine Precordillera. Nevertheless, palaeolatitude information from the Early Ordovician data indicates a palaeoposition of 39.5±4°S for the Precordillera. This is consistent with the latitudinal position of the western border of South America in the Early Ordovician Gondwana (Fig. 10.20). The presented palaeomagnetic data, therefore, suggests that the Precordillera was part of Gondwana in Early Ordovician. Considering the palaeolatitude information and the associated errors on the palaeomagnetic data, The

162

Argentine Precordillera has probably been located at its present position relative to South America since the Early Ordovician.

However, as mentioned above (section 10.2.7), if the Precordillera was part of Gondwana in the Early Ordovician, then it must have rotated anticlockwise up to 105° in Ordovician-Permian times. This rotation possible occurred during the Late Ordovician-Early Silurian Oclóyic orogeny, which resulted eastward thrusting and subsequent closure of the Puna Basin (Bahlburg *et al.*, 2000).

b) The Famatina Ranges

Palaeomagnetic results from the De la Cuesta Formation suggest that the northern Famatina was stable since at least the Late Permian. The Early Ordovician pole from Suri Formation, however, deviates from the Gondwanan APWP. Nevertheless, palaeomagnetic data from Suri Formation places the sampling area at latitude 16.5±3°S during the Early Ordovician. This is not significantly different from the palaeolatitude positions of Famatina calculated from the mean Early Ordovician poles of Bachtadse & Briden (1991), Van der Voo (1993), Smith *et al.*, (1999), Grunow (1999), and McElhinny *et al.* (2003) for Gondwana, which range between 21°S and 36°S. Given the errors associated with these mean poles and the general scatter of the Early Ordovician poles for Gondwana, from which the calculated palaeolatitudes for Famatina range between 7°S to 35°S, the result from Suri Formation is in good agreement with the palaeolatitude location of the Gondwana margin in Early Ordovician times. This suggests that the Famatina Range was part of Gondwana in Early Ordovician times.

Therefore, the present palaeomagnetic data supports the model based on geochemical data (Pankhurst *et al.* 1998) wherein the Famatina Arc is considered as being a continental arc developed on the Gondwana margin during the Early Ordovician. The discrepancy of the palaeomagnetic data from the Suri Formation and the Early Ordovician data for Gondwana is interpreted as a result of an approximately 60° clockwise rotation of Famatina with respect to Gondwana after the Early Ordovician. Results from De la Cuesta Formation suggest that this rotation occurred prior to the Late Permian. Similarly to the rotation of the Precordillera, the Famatina may also have rotated during the Oclóyic orogeny. Further detailed investigation is, however, required to provide firm timing of this rotation.
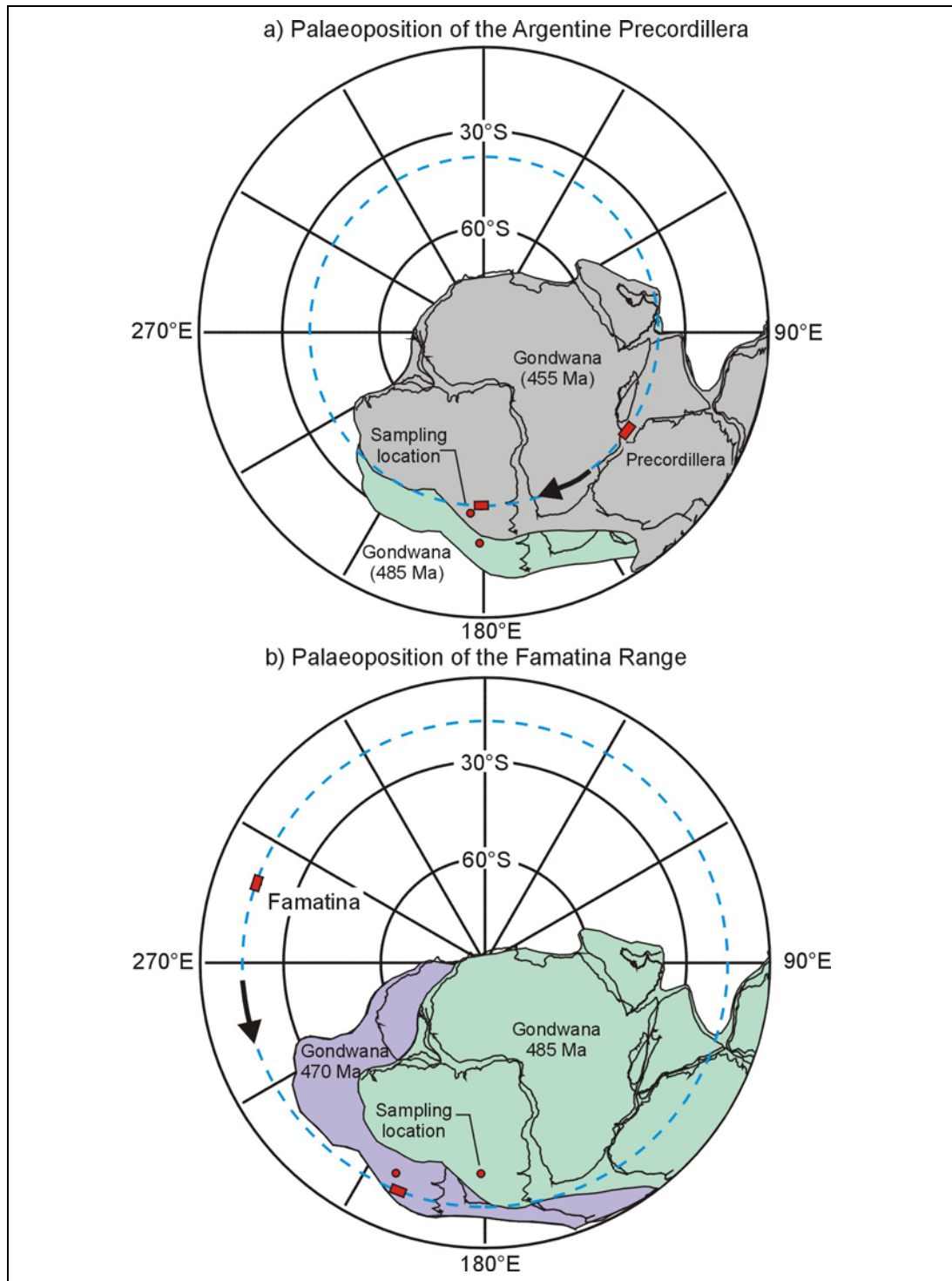
Fig. 10.20. Early Ordovician relative palaeoposition of the Argentine Precordillera and the Famatina Ranges (red boxes) based on the presented palaeomagnetic data. Both positions before and after correction for a 45° clockwise rotation (Precordillera) and a 60° anticlockwise rotation (Famatina) are shown. Palaeoreconstructions of Gondwana are based on (a) mean Early and Mid-Ordovician poles (green: 485 Ma and grey: 455 Ma) from McElhinny *et al.* (2003), and on (b) mean Early Ordovician poles from McElhinny *et al.* (2003; 485 Ma) and Smith (1999, 470 Ma). Blue stippled lines represent the calculated palaeolatitudes for Precordillera and Famatina. Red dots represent position of sampling location with respect to Gondwana (see text).

Chapter 11

Summary and conclusions

---

11. 1 New Mesozoic and Palaeozoic Poles from South America

This study provides a new Early Cretaceous Palaeomagnetic pole ($\lambda = 84°S$; $\phi = 89°E$; $A_{95} = 2.5°$) for the South American plate. This pole is derived from well-dated (120-130Ma) rocks from stable areas in NE Brazil. The presented pole is of good quality (Q= 5) and is similar to the previously published poles with good age constraint from Brazil. The overall mean calculated from 6 studies yields a palaeopole situated at $\lambda = 84.3°S$; $\phi = 067.7°E$ ($A_{95} = 2.3°$; K= 866) for the period between 115 and 133 Ma. This new pole is similar to the Lower Cretaceous (98-142 Ma) reference pole calculated from combined South American and African data (Randall, 1998), and not significantly different from other previously reported Lower Cretaceous reference palaeomagnetic pole for the South American plate.

Investigation of the Palaeozoic rocks from the southern Peruvian Andes yields stable remanences interpreted as being primary in origin, which were acquired in the Early Triassic and Early Permian times, respectively. The Early Triassic data from the Mitu Group is from well-dated volcanic units and passes at the 99% level the fold test of McElhinny (1964) and the reversal test of McFadden & McElhinny (1990) with classification B. The Early Permian remanence from Copacabana Group is exclusively of reversed polarity consistent with the Permian-Carboniferous Reverse Superchron (PCRS), and also passes the fold test of McElhinny (1964) at the 99% confidence level.

Combining the reported palaeomagnetic results from southern Peru with the selected (Q≥3) well-dated published data from stable south America results in a palaeopole located at $\lambda = 76.5°S$; $\phi = 306.2°E$ ($A_{95} = 8.3°$) in Early Triassic times, and at $\lambda = 70.4°S$; $\phi = 341.8°E$ ($A_{95} = 8.8°$) during the Early Permian. In view of the Pangaean palaeogeography, therefore, Permo-Triassic palaeomagnetic data are in disagreement with the Pangaea A configuration, in which South America and Africa are respectively facing North America and Europe. Rather, the new mean Permian-Triassic pole using the new data presented in this study, a new mean Early Triassic pole ($\lambda = 48.3°S$; $\phi = 058.9°E$; $A_{95} = 8.3°$; in African co-ordinates) places

Gondwana in a palaeoposition which is similar to the Pangaea A2 configuration of Van der Voo & French (1974). Palaeoreconstruction based on the combined Early Permian data from Africa, South America and Australia (λ= 34.8°S; ϕ= 063°E; A_{95}= 4.6°; in African co-ordinates) clearly supports the Pangaea B configuration as proposed by Morel & Irving (1981), placing Gondwana further east relative to its position in Pangaea A2 (Fig. 11.1).
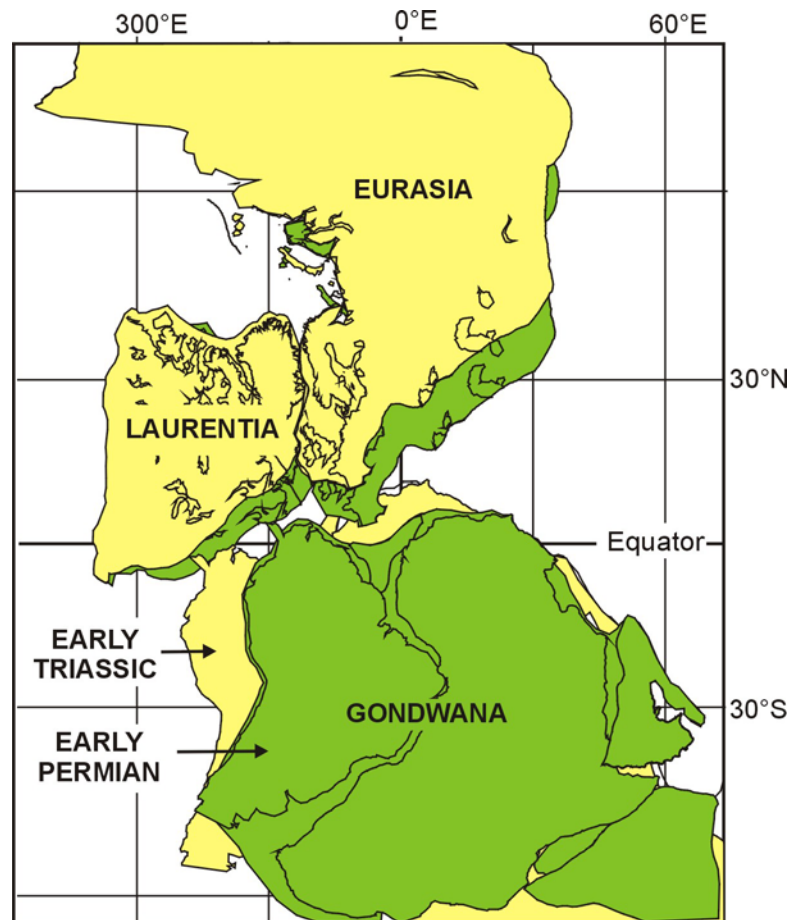
Fig. 11.1. Palaeogeographic reconstruction based on the palaeomagnetic results from South America (Early Triassic; pole: λ= 48°S; ϕ= 058.9°E; α_{95}= 8.3°) and combined data from Africa, South America and Australia (Early Permian; λ= 34.8°S; ϕ= 063.0°E; α_{95}= 4.6°). Palaeopositions of Laurentia and Eurasia are based on the Late Permian-Early Triassic (λ= 51.2°S; ϕ= 294.2°E) and the Early Permian (λ= 46.0°S; ϕ= 304.0°E) palaeomagnetic poles from Van der Voo (1993).

These data, therefore, indicate major dextral shear between Gondwana and Laurasia from an Early Permian Pangaea B configuration, to an Early Triassic Pangaea A2 type reconstruction, i.e., the Pangaea configuration evolved from Pangaea B to Pangaea A2 during Permian times. Muttoni *et al.* (1996; 2003), based on palaeomagnetic data and some geological supports, has been proposed this Permian transformation of Pangaea. The authors

166

suggested that the post-Variscan dextral shear system, which developped between Gondwana and Laurussia, was responsible for this relative translation. Evidence for this shear zone is presented in Arthaud & Matte (1977). This westward relative translation may have continued during the Triassic time (Irving, 1977; Morel and Irving, 1981) until Gondwana reached its position facing Laurentia such as in the well accepted Jurassic Pangaea A (Bullard *et al.*, 1965).

The new palaeopoles presented in this study from South America also suggests that the palaeomagnetic mismatch in Pangaea A reconstruction is not an artefact of the poor quality of the existing palaeomagnetic dataset. Effects such as inclination shallowing in sediments (Van der Voo, 1993; Rochette & Vandamme, 2001) can also be ruled out as comparison of results from red beds, carbonates and extrusive volcanics, from which the mean Early Permian pole for South America was calculated, show no significant difference in inclination. Regarding the possible significant non-dipole contamination of the Earth's geocentric dipole field (Van der Voo & Torsvik, 2001; Torsvik & Van der Voo, 2002), as palaeomagnetic data used in this study come from a broad palaeolatitudinal band (3°S to 67°S for Early Permian and 32°S-66°S for the Early Triassic), the proposed zonal octupole effect are unlikely to cause this mismatch. Thus, strong geological evidences supporting an up to 3500 km relative westward translation of Gondwana during the Permo-Triassic times is required to resolve the Pangaea problem.

For the Carboniferous times, palaeomagnetic result from the Early Carboniferous Taiguati Formation exposed in the Bolivian Subandean Zone is interpreted as a pre-folding remagnetisation acquired in Late Carboniferous (290-323 Ma) times. Although no field test could be carried out due to the exposure conditions, a slight improvement of the directional statistics of this remanence is observed after bedding correction, and the corresponding palaeopole (λ= 58.3°S; ϕ= 348.9°E (A_{95}= 6.0°) compares favourably with the previously well-dated published coeval poles from stable South America and those from high quality data from Africa. Combining the pole from the Taiguati Formation with the previously reported poles obtained from palaeomagnetic data having a quality factor Q≥3 (Van der Voo, 1990), yields a new Late Carboniferous pole for South America located at λ= 53.0°S; ϕ= 348.4°E; A_{95}= 6.0°; K= 86.4; N= 8 studies). This new South American pole (λ= 20.8°S; ϕ= 50.1°E in African co-ordinates) is consistent with the Carboniferous-Permian segment of the APWP of Schmidt *et al.* (1990) and that of Torsvik and Van der Voo (2002).

Altogether, combination of the palaeomagnetic data presented in this manuscript with the selected previously published data yield new Late

Carboniferous, Early Permian and Late Permian-Early Triassic poles for stable South America. The proposed Upper Carboniferous to Early Triassic APWP for South America drawn from these poles is shown in figure 11.3. When transferred in African co-ordinates according to the reconstruction parameters of Lawver & Scotese (1987), the proposed APWP for South America, and by proxy for Gondwana, suggests that the south pole for Gondwana was located in northern Antarctica in the Late Carboniferous, shifted south towards southern Antarctica during the Permian, and situated south of Antarctica in Early Triassic times. This implies that Gondwana moved northward with an average velocity of 7.2 cm/year during Late Carboniferous to Early Permian times, and 4.6 cm/year during the Permian. The presented path supports the Permian segment of the proposed paths shown in Figure 11.3, and the Carboniferous to Triassic segment of path proposed by Torsvik and Van der Voo (2002) and McElhinny *et al.* (2003). Conversely, the data from South America do not agree with the Carboniferous segment of the paths proposed by Bachtadse & Briden (1990), Schmidt *et al.* (1990) and Smith (1998).
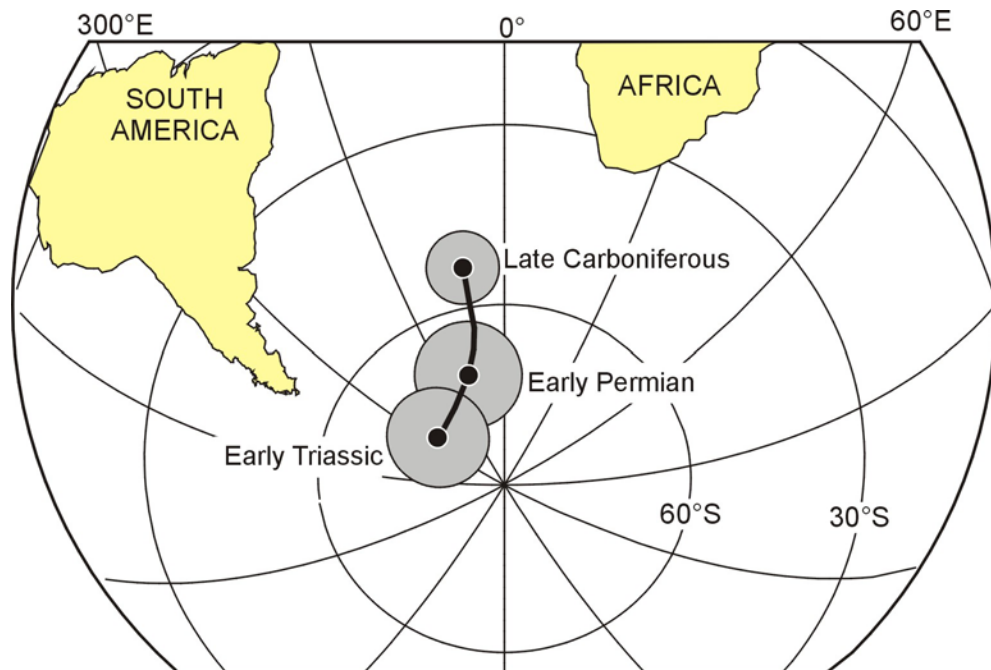
Fig. 11.2. Proposed Late Carboniferous to Early Triassic APWP for South America (equal area projection). Palaeosouth poles (circles with grey A_{95}) were calculated from combined results from this study and selected published data from South America. Selected data include results from well dated rocks with age uncertainty equal or less than a half period, and have a quality factor $Q \geq 3$ (Van der Voo, 1990). The Mean palaeopoles for South America are: Late Carboniferous $\lambda = 53.0°S$; $\phi = 348.4°E$ ($A_{95} = 6.0°$; N= 8 studies); Early Permian $\lambda = 70.4°S$; $\phi = 341.8°E$ ($A_{95} = 8.8°$; N= 7 studies); Early Triassic $\lambda = 76.5°S$; $\phi = 306.2°E$ ($A_{95} = 8.3°$; N= 6 studies).
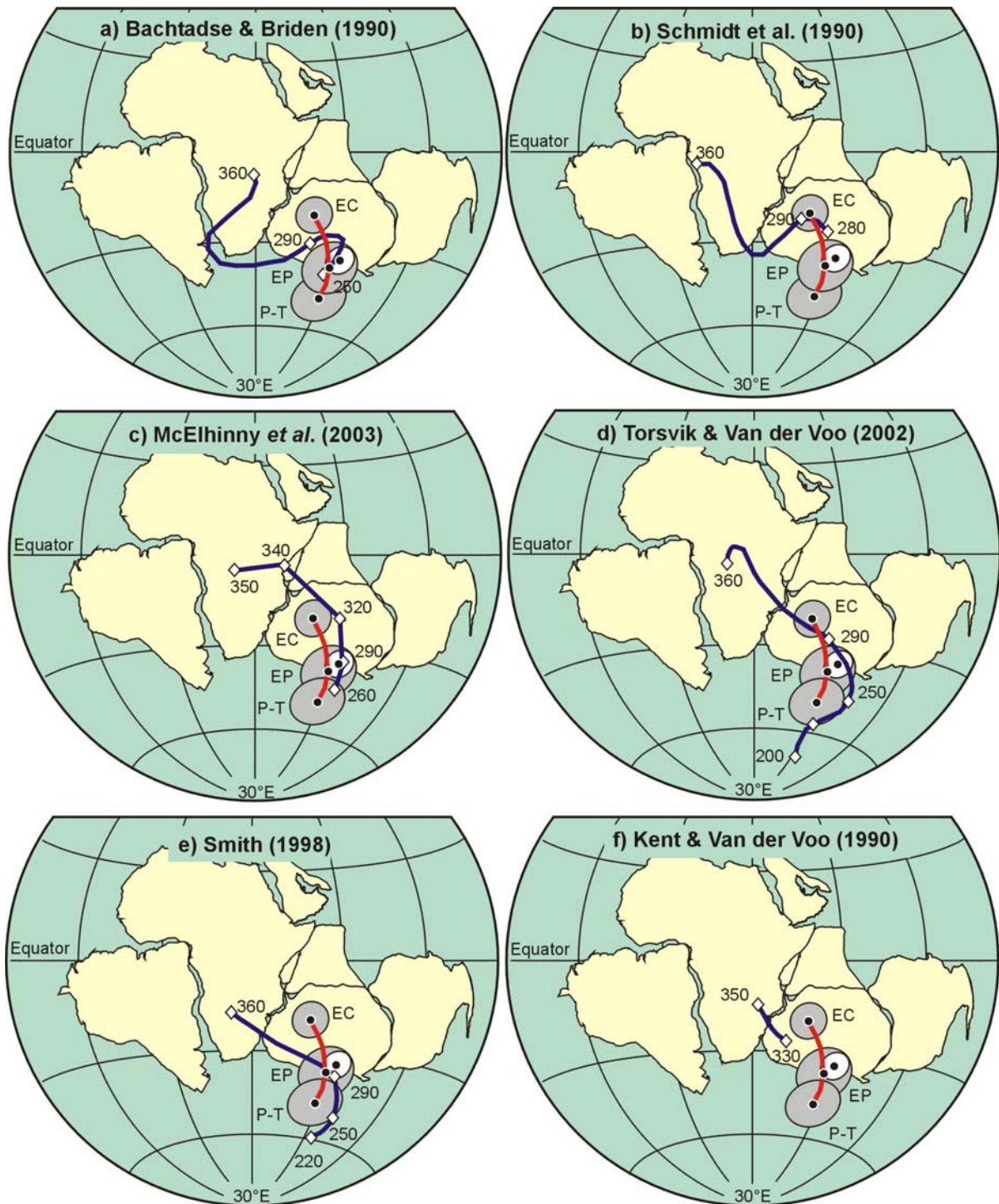
Fig. 11.3. Late Carboniferous to Early Triassic poles (circles with grey A₉₅) and APWP for Gondwna (red) based on results from South America compared with the previously proposed APW paths for Gondwana (blue). The combined mean Early Permian pole from Africa, South America and Australia (white confidence oval) is also shown for comparison. The overall palaeomagnetic results from South America supports a Late Carboniferous-Early Triassic path running south from northern Antarctica to off its southern shoreline (see text). Diamonds and adjacent numbers represent poles used to reconstruct APW paths and their corresponding age in million years (Ma). Projection are on equal area and all poles are plotted in African co-ordinates following the reconstruction paramemeters of Lawver & Scotese (1987).

11. 2 Permian and Mesozoic Remagnetisations

The present study demonstrates widespread Permian and Early Cretaceous remagnetisations of the Palaeozoic rock units exposed the Paganzo Basin and in the Pampean range (NW Argentina). Palaeomagnetic results from La Antigua Formation and the Malanzán Formation are interpreted to be an Early Permian syn-folding and post-folding remanences, respectively (c in Fig. 11.4b,c). Conversely, the secondary magnetisation observed in the Late Carboniferous Solca Formation is a probable Early Cretaceous overprint (Fig. 11.4l). The calculated palaeopoles corresponding to these remanences are consistent with the Late Carboiferous to Early Triassic APWP for South America and the newly defined Early Cretaceous poles for stable South America described above.

Similarly, Palaeozoic rock units sampled in the Parnaíba Basin of NE Brazil did not provide any primary magnetisation. These rocks were either remagnetised during the Permian (Itaim and Tiangua Formations) or Mesozoic (Pimenteiras, Piauí, and Pedra de Fogo Formations). The Early Cretaceous overprint in the Piauí Formation is likely a TRM related to Mesozoic magmatic intrusion that occurred prior to the opening of the Atlantic Ocean. Whereas, the mixed normal and reversed polarity Jurassic and Permian remagnetisations are likely of chemical origin (CRM) related to rock weathering.

Results from Lower Palaeozoic rocks from the Subandean Zone and the Eastern Cordillera are disappointing although fresh and apparently unaltered rocks were sampled. These rocks provide very poor palaeomagnetic data and record various Mesozoic and Cenozoic secondary magnetisations. The origin and processes of these remagnetisations are not clear. However, secondary haematite resulting from rock weathering seems to be the main cause. Another problem is fact that these Palaeozoic clastic marine sediments are very weakly magnetised due to the relative small amount of ferromagnetic mineral contents. As a result, unstable directions carried by paramagnetic minerals dominate their bulk magnetisations, and stepwise demagnetisation techniques were not successful to isolate any stable primary directions.

11. 3 Palaeomagnetism of the Famatina and the Precordillera

Magnetic remanences carried by Early Ordovician sequences suggest that both the Famatina and the Argentine Precordillera was part of Gondwana and was located at their present positions relative to South America in Early Ordovician times. The overall results suggest that the Famatina Ranges has

been stable since at least the Late Permian, while the Argentine Precordillera experienced rotation during the Andean Orogeny.

The Famatina, which is inboard of the Precordillera, indicates significant (approximately 60°) anticlockwise rotation, which affected Ordovician age rocks but not the Permian, thus the rotations is constrained as having occurred between Early Ordovician and Late Permian. The Precordillera on the other hand, results show an anticlockwise rotation of about 45° which affects Ordovician rocks and an approximately 60° clockwise rotation affecting Late Silurian to Late Permian age sequences. Thus, the Precordillera experienced an up to 105° anticlockwise rotation between the Early Ordovician to Late Silurian times and then an about 60° clockwise rotation during the Andean deformation. Further detailed investigation is, however, required to provide firm timing of these rotations.

	Formation/Gp.	Age	Location	Pol.	λ(°S)	ϕ(°E)	A_{95}(°)	Field test	Interpretation
(a)	Taiguati (B)	Cl	SAZ-Bol	R	58	349	6.0	F^o	Primary, E. Carboniferous
(b)	La Antigua	Cl	SP-Arg	R	30	-66	5.4	50% unf.	Synfold, E. Permian?
(c)	Malanzán	Cl	PNG-Arg	R	65	17	7.0	F^-	Secondary, E. Permian?
(d)	Copacabana (B)	Pe	SAZ-Per	R	68	321	5.2	F^+	Primary, E. Permian
(e)	Itaim	De	PB-Braz	R	75	331	3.4	F^-	Secondary, L. Permian
(f)	Tiangua	Se	PB-Braz	M	77	345	6.9	F^-	Secondary, L. Permian
(g)	Mitu (B)	Te	ALT-Per	M	79	352	3.7	F^+, R^+	Primary, E. Triassic
(h)	De la Cuesta	Pl	FA-Arg	R	75	26	12.4	107% unf.	Primary, L. Permian
(i)	Pimenteiras	De	PB-Braz	R	75	241	4.3	F^o	Secondary, E. Jurassic
(j)	Piauí	Cl	PB-Braz	R	86	117	2.5	F^-	Secondary, E. Cretaceous
(k)	Los Monos	Cl	SAZ-Bol	N	86	341	6.1	F^+	Secondary, E. Cretaceous
(l)	Solca	Cl	PNG-Arg	M	83	102	7.5	R^+	Secondary, E. Cretaceous
(m)	Sardinha	Cre	PB-Braz	R	84	89	2.3	F^o	Primary, E. Cretaceous
(n)	Tiangua (A)	De	SAZ-Bol	R	80	58	3.0	F^o	Secondary, E. Cretaceous
(o)	Iquiri	De	SAZ-Bol	N	73	62	10.1	F^-	Secondary, L. Cretaceous
(p)	Pedra de Fogo	Pe	PB-Braz	R	59	268	4.9	F^o	Secondary, E. Jurassic

Tab. 11.1. Summary of the palaeomagnetic data from stable South America. Rock ages are: Oe: Early Ordovician; Cl: Late Carboniferous; Pe: Early Permian; Pl: Late Permian; Te: Early Triassic; Cre: Early Cretaceous. Sampling locations are: SAZ: Subandean Zone; SP: Pampean Ranges; PB: Parnaíba Basin; ALT: Altiplano; FA: Famatina Ranges; PNG: Paganzo Basin; Bol.: Bolivia; Per.: Peru; Arg.: Argentina. Magnetic polarity are: N: Normal; R: reversed; M: mixed. F^+, F^o, F^-, represent positive, indeterminate and negative fold test, respectively.
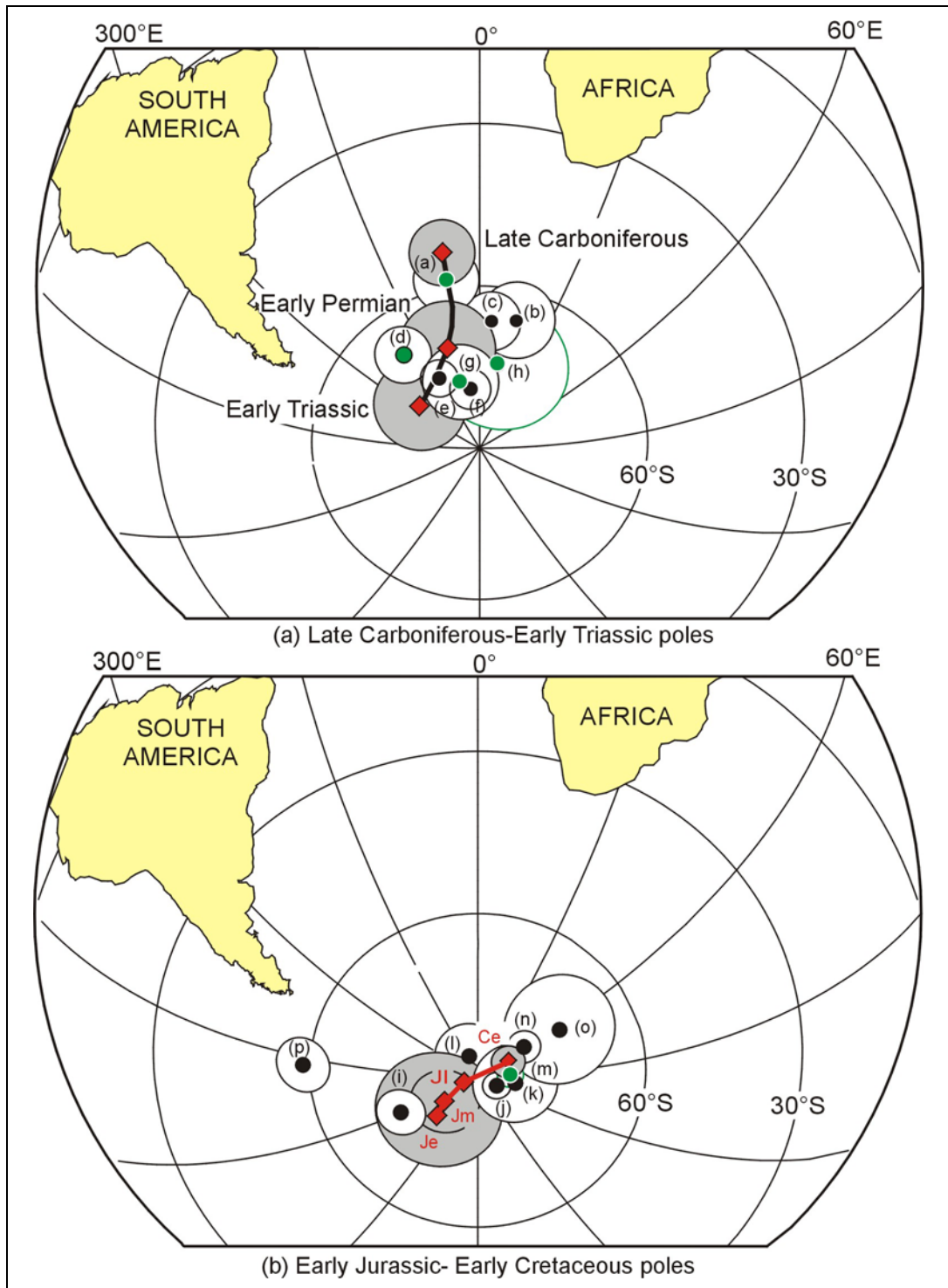
Fig. 11.4 Equal area projection of the palaeomagnetic poles (South American co-ordinates) obtained from stable South America interpreted as primary in origin (green), and probable Late carboniferous-Late Permian **(a)** and Early Jurassic to Early Cretaceous remagnetisations **(b)**. Early, middle and Late Jurassic reference poles (Je, Jm, Jl) for the south American plate are from Randall (1998). Late Carboniferous, Early Permian, Early Triassic and Early Cretaceous reference poles are from this study. See Table 11.1 for details and pole names.

References

Aceňolaza, F.G., Durand, F.R., 1986. Upper precambrian-lower Cambrian biota from the northwest of Argentina. *Geological Magazin, 123(4): 367-375*.

Aceňolaza, F.G., Vergel, M., 1987. Hallazco del Pérmico superior fosilífero en el Sistem de Famatina. *10th Congreso Geológico Argentino, Tucumán, Actas, 3: 125-129*.

Aceňolaza, F.G., Miller, H., Toselli, A.J., 1990. El Ciclo Pampeanoen el Noroeste Argentino. *Correlacion Geologica, 4: 227 p*.

Aceňolaza, F.G., Toselli, A.J., 2000. Argentine Precordillera: allochthonous or autochthonous Gondwanic? *Zentralblatt fuer Geologie und Palaeontologie, Teil I: Allgemeine, Angewandte, Regionale und Historische Geologie, 1999(7-8): 743-756*.

Aceňolaza, F.G., Miller, H., Toselli, A.J., 2002. Proterozoic-early Paleozoic evolution in western South America; a discussion. *Tectonophysics, 354(1-2): 121-137*.

Albanesi, G.L., Vaccari, N.E., 1994. Conodontos del Arenig en la Formación Suri, Sistema de Famatina, Argentina. *Revista Espaňola de Micropaleontologia, 26: 125-146*.

Albanesi, G.L., Astini, R.A., 2000. New conodont fauna from Suri Formation (Early-Middle Ordovician), Famatina System, western Argentina. *Ameghiniana, 37(4): 68*

Albertão, G.A., Martins, P.P.J., 1996. A possible tsunami deposit at the Cretaceous-Tertiary boundary in Pernambuco, northeastern Brazil. *Sedimentary Geology, 104(1-4): 189-201*.

Allmendiger, R.W., 1983. Tectonic developmemt, southestern border of the puna Plateau, northwest Argentina Andes. *Geological Society of America, Bulletin, 97: 1070-1082*.

Allmendinger, R.W., Gubbels, T., 1996. Pure and simple shear plateau uplift, Altiplano-Puna, Argentina and Bolivia. *Tectonophysics, 259: 1-13*.

Almeida, F.F.M., Brito Neves, B.B., Carneiro, C.D.R., 2000. The origin and evolution of the South American Platform. *Earth-Science Reviews, 50: 77-111*.

Andreis, R.R., Leguizamón, R., Archangelsky, S., 1986. El paleovalle de Malanzán: Nuevos criterios para la estratigrafía del Neopaleozoico de la Sierra de Los Llanos, La Rioja, Repúblic argentina. *Bolétin de la Academia Nacional de Ciencias, 57(1-2): 3-119*.

Arthaud, F., Matte, P., 1977. Late Paleozoic strike-slip faulting in southern Europe and northern Africa: Result of a right-lateral shear zone between the Appalachians and the Urals. *Bulletin of the Geological Society of America, 88: 1305-1320*.

Astini, R.A., Benedetto, J.L., Vaccari, N.E., 1995. The early Paleozoic evolution of the Argentine Precordillera as a Laurentian rifted, drifted, and collided terrane; a geodynamic model. *Geological Society of America, Bulletin, 107(3): 253-273*.

Astini, R.A., 1998. El Ordovicico de la region central del Famatina (provincia de La Rioja, Argentina); aspectos estratigraficos, geologicos y geotectonicos. The Ordovician of the central region of the Famatina Ranges (La Rioja Province); stratigraphic, geologic and geotectonic considerations. *Revista de la Asociacion Geologica Argentina, 53(4): 445-460*.

Astini, R.A., 1999. Sedimentary record, volcano-tectonic cyclicity and progressive emergence of an Early Ordovician perigondwanan volcanic arc; the Famatina System. *Acta Universitatis Carolinae, Geologica, 43(1-2): 115-118.*

Azcuy, C.L., Tarazona A., Valdivia, H., 1992. Palynología del Paleozoico Superior en las nacientes del río Urubamba, Pongo de Mainique, Perú. *Convenio de cooperación Técnica Petroperú, Univerisdad de Buenos Aires. Petroperú, Lima,*10p.

Baby, P., Moretti, I., Guillier, B., Limachi, R., Méndez, R., Oller, E.J., Specht, M., 1995. Petroleum system of the northern and central Bolivian Subandean Zone. In: Tankard, A.J., Suárez Soruco, R., Welsink, H.J., (Editors), Petroleum Basins of South America. *American Association of Petroleum Geologists, Memoir, 62: 445-458.*

Baby, P., Rivadeneira, M., Christophoul, F., Barragan, R., 1999. Style and timing of deformation in the Oriente basin of Ecuador. *4th International Symposium on Andean Geodynamics (ISAG'99), Extended Abstracts Volume, Universtity of Göttingen, Germany, 68-72.*

Bachtadse, V., Van der Voo, R., Haelbich, I.W., 1987. Paleozoic paleomagnetism of the western Cape Fold Belt, South Africa, and its bearing on the Paleozoic apparent polar wander path for Gondwana. *Earth and Planetary Science Letters, 84: 487-499.*

Bachtadse, V., Briden, J.C., 1989. Palaeomagnetic results from Devonian volcanics from the Gilif Hills, Bayuda Desert, Sudan. *Terra, 1: 85.*

Bachtadse, V., Briden, J.C., 1990. Palaeomagnetic constraints on the position of Gondwana during Ordovician to Devonian Times. In: W.S. McKerrow,C.R. Scotese (Editors), Palaeozoic Biogeography and Palaeobiogeography. *Geological Society of London, Memoir, 12: 43-48.*

Bachtadse, V., Briden, J.C., 1991. Palaeomagnetism of Devonian ring complexes from the Bayuda Desert, Sudan - new constraints on the apparent polar wander path for Gondwanaland. *Geophysical Journal International, 104: 635-646.*

Bachtadse, V., Zanglein, R., Tait, J., Soffel, H.C., 2002. Palaeomagnetism of the permo/carboniferous (280 Ma) Jebel Nehoud ring complex, Kordofan, Central Sudan. *Journal of African Earth Sciences, 35(1): 89-97.*

Bahlburg, H., 1990. The Ordovician basin in the Puna of NW Argentina and N Chile Geodynamic evolution from back arc to foreland basin. *Geotektonische Forschungen, 75: 1-107.*

Bahlburg, H., Breitkreuz, C., 1991. The evolution of marginal basins in the southern Central Andes of Argentina and Chile during the Paleozoic. *Journal of South American Earth Sciences, 4: 171-188.*

Bahlburg, H., Hervé, F., 1997. Geodynamic evolution and tectonostratigraphic terranes of northwestern Argentina and northern Chilie. *Geological Society of America,Bulletin, 109(7): 869-884.*

Bahlburg, H., Moya, M.C., Zimmermann, U., Bock, B., Hervé, F., 2000. Paleozoic Plate Tectonic Evoulution of the Western Gondwana Margin in Northern Chile and Northwestern Argentina. *Zeitschrift für Angewandte Geologie, Sonderheft, 1: 345-353.*

Baldis, B.B., Armella, C., Beresi, M, Cabaleri, N. Peralta, S.H, Bastias, H., 1989. La cuenca Paleozoica inferior de la Precordillera Argentina. The lower Paleozoic basin of the Argentine Precordillera. Cuencas sedimentarias argentinas. *Argentine sedimentary basins, 6: 101-121.*

Beck, M.E.J., 1988. Analysis of late Jurassic-recent paleomagnetic data from active plate margins of South America. *Journal of South American Earth Sciences*, *1(1): 39-52*.

Beck., M.E.J., 1998. On the mechanism of crustal block rotations in the central Andes. *Tectonophysics, 299: 75-92*.

Beck, M.E.J., Burmester, R.F., Drake, R., Riley, P., 1994. A tale of two continents : Some tectonic contrasts between the Central Andes and the North American Cordillera as illlustrated by their palaeomagnetic signatures. *Tectonics*, 13: 215-224.

Bellieni, G., Montes-Lauar, C.R., Min, A.D., Piccirillo, E.M., Cavazzini, G., Melfi, A.J., Pacca, I.G., 1990. Early and late cretaceous magmatism from sao sebastiao island (SE-Brazil): geochemistry and petrology. G*eochim. Brazil, 4(1): 59-83*.

Bellieni, G., Piccirillo, E.M., Gavazzini; G., Petrini, R., Comin-Chiaramonti, A., Nardy, A.J.R., Civetta, L., Melfi, A.J., Zantedeschi, P., 1990. Low-and high-TiO2 Mesozoic tholeiitic magmatism of the Maranhao basin (NE-Brazil): K/Ar age, geochemistry, petrology, isotope characteristics and relationships with Mesozoic low-and high-TiO2 flood basalts of the Paranà basin (SE-Brazil). *Neues Jahrbuch für Mineralogie, 162(1): 1-33*.

Bellieni, G., Macedo, M.H.F., Petrini, R., Piccirillo, E.M., Cavazzini, G., Comin-Chiaramonti, P., Ernesto, M., Macedo, J.W.P., Martins, G., Melfi, A.J., Pacca, I.G., Min, A.D., 1992. Evidence of magmatic activity related to Middle Jurassic and Lower Cretaceous rifting from northestern Brazil (Ceará-Mirim): K/Ar age. palaeomagnetism, petrology and Sr-Nd isotope characteristics. *Chemical Geology*, 97: 9-32.

Benedetto, J.L., 1998. Early Palaeozoic brachiopods and associated shelly fauna from western Gondwana: their bearing on the geodynamic history of the pre-Andean margin. In: Pankhurst, R.J., Rapela, C.W. (Editors), The proto-Andean margin of Gondwana. *Geological Society of London, London, pp. 57-83*.

Bullard, E.C., Everett, J., Smith, A.G., 1965. The fit of the continents around the Atlantic. *Philosophical Transactions of the Royal Society London*, A258: 41-45.

Butler, R.F., Herve, F., Munizaga, F., Beck(Jr), M.E., Burmester, R.F.,Oviedo, E.S., 1991. Paleomagnetism of the Patagonian plateau basalts, southern Chile and Argentina. *Journal of Geophysical Research, 96: 6023-6034*.

Clark, D.A., Lackie, M.A., 2003. Palaeomagnetism of the Early Permian Mount Leyshon Intrusive Complex and Tuckers Igneous Complex, North Queensland, Australia. *Geophysical Journal International, 153: 523-547*.

Coimbra, J.C., Mitsuru, A., Carreño, A.L., 2002. Biostratigraphy of Lower Cretaceous microfossils from Araripa basin, northeastern Brazil. *Geobios, 35: 687-698*.

Coira, B.L. and Koukharsky, M., 1968. Descripción Geològica de la Hoja 17f, Sierra Brava, Buenos Aires.

Coira, B.L., Davidson, J., Mpodozis, C., Ramos, V.A., 1982. Tectonic and magmatic evolution of the Andes of northern Argentina and Chile. *Earth Science Reviews, 18: 303-332*.

Coira, B.L., Mahlburg Kay, S., Pérez, B., Woll, B., Hanning, M., Flores, P., 1999. Magmatic sources and tectonic setting of Gondwana margin Ordovician magmas, northern Puna of Argentina and Chile. In: Ramos, V.A., Keppie D.

(Editors), Laurentia Gondwana connections defore Pangea. *Geological Society of America, Special Paper, pp. 145-170.*

Conti, C.M., Rapalini, A.E., 1990. Paleomagnetismo de la formacion Choique Mahuida, aflorante en la Sierra Homonina, Provincia de la Pampa, Republica Argentina. *XI Congresso Geológico .Argentina, San Juan 2, 235-238.*

Conti, C.M., Rapalini, A.E., Vilas, J.F., 1995 Palaeomagnetism of the Silurian Lipeon Formation, NW Argentina, and the Gondwana apparent polar wander path. *Geophyscal Journal International, 121: 848-862.*

Conti, C.M., Rapalini, A.E., Coira, B., Koukharsky, M., 1996. Paleomagnetic evidence of an early Paleozoic rotated terrane in northwest Argentina: a clue for Gondwana-Laurentia interaction? *Geology 24 (10): 953-956.*

Cordani, U.G., Torquato, J.R., 1981. Brazil-Africa Geological links. *Earth Sciences Reviews, 17(155-176).*

Cordani, U.G., Sato, K., Teixeira, W., Tassinari, C.C.G., Basei, A.S., 2000. Crustal evolution of the South American Platform. In: Cordani, U. G., Milani, E. J., Thomaz Filho, A., and Campos D. A., (Editors), Tectonic evolution of South America. *31st International Geological Congress, Rio de Janeiro, Brazil. August 6-17, 19-40.*

Corner, B., Henthorn, D.I., 1978. Results of a palaeomagnetic survey undertaken in the Damara Mobile Belt, South West Africa, with special reference to the magnetisation of the uraniferous pegmatitic granites. *Pel-260, Atomic Energy Board, Pretoria.*

Creer, K.M., 1965. A Symposium on Continental Drift - III. Palaeomagnetic data from the Gondwanic continents. *Philosophical Transactions of the Royal Society, London, Ser.A, 258: 27-40*

Dalla Salda, L., Cingolani, C., Varela, R., 1992. Early Paleozoic orogenic belt of the Andes in southwestern South America: Result of Laurentia-Gondwana collision? *Geology, 20: 617-620.*

Dalmayrac, B., Laubacher, G., Marocco, R., Martinez, C., Tomasi, P., 1980. La chaine hercynienne d'amerique du sud; structure et evolution d'un orogene intracratonique. The Hercynian fold belt of South America; structure and evolution of an intracratonic orogeny. *Geologische Rundschau, 69(1): 1-21.*

Daly, L., Pozzi, J.P., 1976. Résultats paléomagnetiques du Permien inférieur et du Trias Marocain: comparaison avec les donnéss africaines et sud-americaines. *Earth and Planetary Science Letters, 29: 71-80.*

Daly, L., Irving, E., 1983. Paleomagnetism des roches carbonifere du Shara central; analyse des aimantations juxtaposes; configuration de la Pangee. *Ann. Geophys., 1: 207-216.*

Dalziel, I.W.D., 1997. Neoproterozoic-Paleozoic Geography and Tectonics: Review, Hypothesis, Environmental Speculation. *Geological Society of America Bulletin, 109(1): 16 - 42.*

Dalziel, I.W.D., Dalla, S.L.H., Gahagan, L.M., 1994. Paleozoic Laurentia-Gondwana interaction and the origin of the Appalachian-Andean mountain system. *Geological Society of America, Bulletin, 106(2): 243-252.*

Day, R., 1977. TRM and its variation with grain size. *Advances in Earth and Planetary Sciences, 1: 1–33.*

De la Cruz, N.B., Zapata, A. M., Larico, W. C., 1998. Geología de los cuadrángulos de timpia, Calangato y Río Providencia. *INGEMMET Boletín, 121, Ser. A, 223p.*

Derder, M.E.M., Smith, B., Hery, B., Yelle, A.K., Bayou, B., Djellit; H., Ait ouali, R., Gandriche, H., 2001. Juxtaposed and superimposed paleomagnetic primary and secondary components from the folded middle carboniferous sediments in the Reggane Basin (Sahara craton, Algeria). *Tectonophysics 332, 403-422.*

Derder, M.E., Henry, B., Merabet, N.E., Daly, L., 1994. Palaeomagnetism of the Stephano-Autunian Lower Tiguentourine formations from stable Sharan craton (Algeria). *Geophysical Journal International, 116: 12-22.*

Durand, F.R., 1996. La tectonica cenozoica en el Sistema de Famatina. Cenozoic tectonics of the Famatina System. In: Acenolaza, F G; Miller, H; Toselli, A (Editors) Geologia del sistema de Famatina. Geology of the Famatina System. *Muenchner Geologische Hefte. Reihe A, Allgemeine Geologie, 19: 343-357.*

Embleton, B.J.J., 1970. Palaeomagnetic results for the Permian of South America and a comparison with the African and Australian data. *Geophysical Journal of the Royal Astronomical Society, 21(2): 105-118.*

Enkin, R.J., 2003. The direction-correction tilt test: an all-purpose tilt/fold test for paleomagnetic studies. *Earth and Planetary Science Letters, 212: 151-166.*

Ernesto, M., Pacca, I.G., Hiodo, F.Y., Nardy, A.J.R., 1990. Palaeomagnetism of the Mesozoic Serra Geral Formation, southern Brazil. *Physics of the Earth and Planetary Interiors, 64: 153-175.*

Ernesto, M., Raposo, M.I.B., Marques, L.S., Renne, P.R., Diogo, L.A., de Min, A., 1999. Paleomagnetism, geochemistry and Ar-40/Ar-39 dating of the North-eastern Parana Magmatic Province: tectonic implications. *Journal of Geodynamics, 28(4-5): 321-340.*

Finney, S., Gleason, J., Gehrels, G., Peralta, S., Acenolaza, G., 2003. Early Gondwanan connection for the Argentine Precordillera terrane. *Earth and Planetary Science Letters, 205(3-4): 349-359.*

Fisher, R.A., 1953. Dispersion on a sphere. *Proceedings of the Royal Society London A, 217: 295-305.*

Flint, S., Turner, P., Jolley, E.J., Hartley, E.J., 1993. Extensional tectonics in convergent margin basins: An example from the Salar de Atacama, Chilean Andes. *Geological Society of America, Bulletin, 105: 603-617.*

Forsythe, R.D., Davidson, J., Mpodozis, C., Jesinkey, C., 1993. Lower Paleozoic relative motion of the Arequipa Block and Gondwana; paleomagnetic evidence from Sierra de Almeida of northern Chile. *Tectonics, 12(1): 219-236.*

Frenguelli, J., 1946. Consideraciones acerca de la "Serie de Paganzo" en las provincias de San Juan y La Rioja. Rev. *Mus. La Plata (N.S.), secc. Geol. II: 313-376.*

Gil, W., Baby P., Marocco R., Ballard, J.F., 1999. North-South structural evolution of the Peruvian subandean zone. *4th ISAG, Goettingen.Germany: 278-282.*

Gilder, S., Rousse, S., Farber, D., McNulty. B., Sempere, T., Torres, V., Palacios, O., 2003. Post-Middle Oligocene origin of palaeomagnetic rotations in Upper Permian to Lower Jurassic rocks from northern Peru. *Earth and Planetary Science Letters, 210: 233-248.*

Góes, A.M.O., Feijó, F.J., 1994. Bacia do Parnaíba. *Boletim de Geociências da Petrobras, 8: 57-67.*

González Bonorino, G. and Eyles, N., 1995. Inverse relation between ice extent and the late Paleozoic glacial record of Gondwana. *Geology, 23: 1015-1018.*

Gradstein, F.M., Ogg, J., 1996. A Phanerozoic time scale. *Episodes, 19(1-2): 3-5.*

Grunow, A.M., 1995. Implications for Gondwana of new Ordovician paleomagnetic data from igneous rocks in southern Victoria Land, East Antarctica**.** *Journal of Geophysical Research, 100 (7): 12589-12603***.**

Geuna, S.E., Vizan, H., 1998. New Early Cretaceous palaeomagnetic pole from Cordoba Province (Argentina); revision of previous studies and implications for the South American database. *Geophysical Journal International, 135(3): 1085-1100.*

Guena, S.E., Somoza, R., Vizán, H., Figari, A.G., Rinaldi, C.A., 2000. Paleomagnetism of Jurassic and Cretaceous rocks in central Patagonia: a key to contrain the timing of rotations during the breakup of southwestern Gondwana? *Earth and Planetary Science Letters, 181: 145-160.*

Henry, B., Merabet, N., Yelles, A., Derder, M.M., Daly, L., 1992. Geodynamical implications of a Moscovian palaeomagnetic pole from the stable Sahara craton (Illizi basin, Algeria). *Tectonophysics, 201: 83-96.*

Irving, E., Irving, G.A., 1982. Apparent polar wander paths Carboniferous through Cenozoic and the assembly of Gondwana. *Geophys. Survey*s, *5: 141- 188.*

Isaacson, P. E., Diaz-Martinez, E., 1995. Evidence for a Middle-Late Paleozoic Foreland Basin and significant Paleolatitudinal Shift, Central Andes. In: A.J. Tankard, R. Suarez, H.J. Welsink (Editors). Petroleum Basin of South America*, American Association of Petroleum Geologists, Memoir, 231-249.*

Isacks, B.L., 1988. Uplift of the Central Andean Plateau and Bending of the Bolivian Orocline. *Journal of Geodynamics, 2: 183-192.*

Jackson, M., 1990. Diagenetic sources of stable remanence in remagnetized Paleozoic cratonic carbonates; a rock magnetic study. *Journal of Geophysical Research, 95(B3): 2753-2761.*

Jaillard E., Hérail, G., Monfret, T., Diáz-Martinez, E., Baby, P., Lavenu A., Dumont, J.F., 2000. Tectonic evolution of the Andes of Ecuador, Peru, Bolivia and Northernmost Chile. In Cordani, U. G., Milani, E. J., Thomaz Filho, A., and Campos D. A., (eds), Tectonic evolution of South America. *31st International Geological Congress, Rio de Janeiro, Brazil. August 6-17, 481-559.*

Jesinkey, C., Forsythe, R.D., Mpodozis, C., Davidson, J., 1987. Concordant late Paleozoic paleomagnetizations from the Atacama desert: implications for tectonic models of the Chilean Andes . *Earth and Planetary Science Letters, 85: 461-472.*

Jordan, T.E., Alonso, R.N., 1987. Cenozoic stratigraphy and basin tectonics of the Andes mountains, 20-28° south latitude. *American Association of Petroleum Geologists, Bulletin, 71: 49-74.*

Jordan, T.E., Gardeweg, P.M., 1989. Tectonic evolution of the late Cenozoic central Andes (20°-33°S). In: Ben-Avraham, Z. (Editor). The evolution of the Pacific ocean margins. *Oxford University Press, New york, 193-207.*

Keller, M.L., O, 1998. The Rio Sassito sedimentary succession (Ordovician); a pinpoint in the geodynamic evolution of the Argentine Precordillera. *Geologische Rundschau, 87(3): 326-344.*

Keller, M., Buggish W., Lehnert O., 1998. The stratigraphical record of the Argentina Precordillera and its plate-tectonic background. In Pankhurst, R. J.

& Rapela C.W.(eds): The Proto-Andean Margin of Gondwana. *Geological Society of London, Special Publications, 142: 35-56.*

Keller, M., 1999. Argentine Precordillera; sedimentary and plate tectonic history of a Laurentian crustal fragment in South America. *Geological Society of America, Special Paper, 341: 131pp.*

Kent, D.V., Van der Voo, R., 1990. Palaeozoic palaeogeography from palaeomagnetism of the Atlantic-bordering continents. In: McKerrow, W.S. Scotese, C.R. (Editors), Palaeozoic Palaeogeography and Biogeography. *Geological Society, London, 12: 49-56.*

Kirschvink, J.L., 1980. The least square lie and plane and the analysis of paleomagnetic data. *Geophysical Journal of the Royal Astronomical Society, 62: 699-718*

Kley, J., Reinhardt, M., 1994. Geothermal and tectonic evolution of the Eastern Cordillera and Subandean Ranges of Southern Bolivia. In: K. J., Scheuber, E., and Wigger, R. J. (Editors). *Tectonics of Southern Central Andes, Springer Verlag, 155-170.*

Klootwijk, C. T., Giddings, J. W., Percival, P., 1993. Palaeomagnetic reconnaissance of Upper Palaeozoic volcanics, northeastern Queensland. *Australian Geological Survey Organisation, 88 p.*

Kontak, D.J., Clark, A.H., Farrar, E., Strong, D.F., 1985. The rift associated Permo-Triassic magnmatism of the Eastern Cordillera: a precursor of the Andean orogeny. In: Pitcher, W.S., Atherton, M.P., Cobbing, E.J., Beckinsale, R.D. (Editors). Magmatism at a plate edge: the Peruvian Andes. *Blackie & Halsted Press, 36-44.*

Keppie, J.D., Ramos, V.A., 1999. Odyssey of terranes in the Iapetus and Rheic oceans during the Paleozoic. In: V.A. Ramos,J.D. Keppie (Editors), Laurentia- Gondwana connection before Pangea. *Geological Society of America, Special Paper, pp. 267-276.*

Kramer, P.E., Escayola, M.P., Martino, R.D., 1995. Hipótesis sobre la evoulición tectónica neoproterozoica de las sierras pampeanas de córdoba (30°40'-32°40'), Argentina. *Associacíon Geológica Argentina, Buenos Aires, Revista, 50(1-4): 47-59.*

Lanza, R., Tonarini, S., 1998. Palaeomagnetic and geochronological results from the Cambro-Ordovician Granite Harbour Intrusives inland of Terra Nova Bay (Victoria Land, Antarctica). *Geophysical Journal International, 135(3): 1019-1027.*

Lawver, L. A. Scotese, C. R., 1987. A revised reconstruction of Gondwanaland. In: Mckenzie, G. D. (Editor), Gondwana Six: Stratigraphy, Sedimentology and Paleontology. *Geophysical Monograph, Washington, 17-23.*

Lehnert, O., Keller, M., 1994. The Conodont record of the Argentine Precordillera: problems and Possibilities. *Zbl. Geol. Paläont. Teil 1, H. 1/2: 231-244.*

Libarkin, J.C., Butler, R.F., Richards, D.R.,1998. Tertiary remagnetization of Paleozoic rocks from the Eastern Cordillera and sub-Andean Belt of Bolivia. *Journal of Geophysical Research, 103: 30417-30429.*

Limarino, C.O, Césari, S.N., Net, L.I., Marenssi, S.A., Gutierrez, R.P., Tripaldi, A., 2002. The Upper Carboniferous postglacial transgression in the Paganzo Basin and Río Blanco basins (northwestern argentina): facies and stratigraphic significance. *Journal of South American Earth Sciences, 15: 445-460.*

Lopez Gamundì, O.R., Espejo, I.S., Conaghan, P.J., Powel, C.A., 1994. Southern South America. In: Veevers, J.J., Powell, C.A. (Editors), Permian-Triassic Pangea Basins and Foldbelts along the Panthalassan Margin of Gondwanaland. *Geological Society of America, Memoir, pp. 281-329.*

Lottes, A. L., Rowley, D. B., 1990. Reconstruction of Laurasian an Gondwana segments of Permian Pangea. In: McKerrow, W.S., Scotese, C.R., (Editors). Paleozoic Paleogeography and Biogeography: *Geological Society of London, Memoir, 12: 383-395.*

Maisey, J.G., 2000. Continental break up and the distribution of fishes of Western Gondwnana during the Early Cretaceous. *Cretaceous Research, 21: 281-314.*

Mángano, M.G., Buatois, L.B., 1997. Slope-apron deposition in an Ordovician arc-related setting: the Vuelta de Las Tolas Menber (Suri Formation), Famatina Basin, northwest Argentine. *Sedimentary Geology, 109(1-2): 155-180.*

McElhinny, M.W., 1964. Statistical significance of the fold test in palaeomagnetism. *Geophysical Journal of the Royal Astronomical Society, 8: 338-340.*

McElhinny, M.W., Powel, C.M., Pisarevsky, S.A., 2003. Paleozoic terranes of eastern Australia and the drift history of Gondwana. *Tectonophysics, 362: 41-65.*

McFadden, P.L., McElhinny, M.W., 1988. The combined analysis of remagnetization circles and direct observations in paleomagnetism. *Earth and Planetary Science Letters, 87(1-2): 161-172.*

McFadden, P.L., 1990. A new fold test for palaeomagnetic studies. *Geophysical Journal International, 103: 163–169.*

McFadden, P.L., McElhinny, M.W., 1990. Classification of the reversal test in palaeomagnetism. *Geophysical Journal International, 103: 725-729.*

Meert, J.G., Van der Voo, R., 1997. The assembly of Gondwana 800-550 Ma. *Journal of Geodynamics, 23(3-4): 223-35.*

Merabet, N., Bouabdallah, H., Henry, B., 1998. Paleomagnetism of the Lower Permian redbeds of the Abadla Basin, Algeria). *Tectonophysics, 293(1-2): 127-136.*

Milani, E.J., Thomaz Filho, A., 2000. Sedimentary Basin in South America. In: Cordani, U.G., Milani, E.J. Thomaz Filho, A., Campos, D.A. (Editors). Tectonic evolution of South America. *31st Geological Congress, Rio de Janeiro, 389-449.*

Mingramm, A., Russo, A., Pozzo, A., Casau, L., 1979. Sierras subandinas. Secundo simposio de geologia regional Argentina. *Academia Nacional de Ciencias, Còrdoba: 95-138.*

Morel, P., Irving, E., 1978. Tentative paleocintinental maps for the early Phanerozoic and Proterozoic. Journal of Geology, 86: 535-561.

Morel, P., Irving, E., 1981. Paleomagnetism and the evolution of Pangea. *Journal Geophysical Research, 86: 1858-1872.*

Moya, M.C., Malanca, S., Hongn, F.D., Bahlburg, H., 1993. El Tremadoc temprano en la Puna Occidenta Argentina. *XII Congresso Geológico Argentino y II Congreso Exploración de Hidrocarburos (Mendoza). Actas, 2: 20-30.*

Muttoni, G., Kent, D. V., Garzanti, E., Brack, P., Abrahamsen, N., Gaetani, M. 2003. Early Permian Pangea B to late Permian Pangea A. *Earth and Planetary Letters, 215: 379-394.*

Net, L.I., Limarino, C.O., 1999. Paleogeografía y correlación estratigrafica del Paleozoico Tradio de la Sierra de Los Llanos, Provincia de La Rioja, Argentina. *Revista de la Asociacion Geologica Argentina, 54(3): 229-239.*

Neumann, V.H., Borrego, A.G., Cabrera, L., Dino, R., 2003. Organic matter composition and distribution of through the Atian-Albiabn lacustrine sequences of the Araripe Basin, northeastern Brazil. *International Journal of Coal Geology, 54: 21-40.*

Opdyke, N. D., Mushayandebvu, M., De Wit, M. J., 2001. A new palaeomagnetic pole for the Dwyka System and correlative sediments in sub-Saharan Africa. *Journal of African Earth Sciences, 33(1): 143-153.*

Oviedo, E.S., Valencio, D.A., Vilas, J.F., 1991. Palaeomagnetism of Jurassic and Cretaceous rocks from South America and the tectonics of the Central Andes. In: Harmon, R.S., Rapela, C.W. (Editors). Andean magmatism and its tectonic setting. *Geological Society of America, Special Paper, 265: 291-299.*

Pacca, I.G., Hiodo, F.Y., 1976. Paleomagnetic analysis of Mesozoic Serra Geral basaltic lava flows in southern Brazil. Annales .*Acad. Brasil Cienc., 48: 207-214.*

Palacios, O., De la Cruz, J., De la Cruz, N., Klinck, B.A., Allison, R.A., Hawkins, M.P., 1993. Geología de la Cordillera Occidental y Altiplano al oeste del lago Titicaca-sur del Peru. *Carta geológica Nacional, INGEMMET, Bolétin, 42, Ser. A:, 257p.*

Pankhurst, R. J., Rapela C.W., 1998. The Proto-Andean margin of Gondwana: an introduction. In Pankhurst, R. J., Rapela C.W. (Editors): The Proto-Andean Margin of Gondwana. *Geological society, London, Special Publications, 142: 1-9.*

Quiñones, L., 1990. Estudio palinoestratigráfico del Paleozoico del Pongo de Mainique, provincia de la Convencíon, Cuzco. *Universidad de San Marcos, Geológica, Lima, 101p.*

Ragona, D., Anselmi, G., González, P., Vujovich, G., 1995. Mapa Geológico de la provincia de San Juan, República Argentina. Escala 1:500.000. *Secretaría de Minería, Direcíon Nacional del Servicio Geológico, Argentina.*

Ramos, V. A., Jordan, T. E., Allmendinger, R. W., Mpodozis, C., Kay, S. M., Cortes, J. M., Palma, M. A., 1986. Paleozoic terranes of the central Argentine-Chilean Andes. *Tectonics, 5: 855-880.*

Ramos, V. A., 1988. Late Proterozoic-Early Paleozoic of south America- A collisional history. *Episodes, 11: 168-174*

Ramos, V.A., 1988. The tectonics of the Central Andes; 30° to 35°S latitude. In: Clark S.P. Jr. (Editor), Processes in continental lithospheric deformation. *Geological Society of America, Colorado, Special Paper, 218: 31-54.*

Ramos, V.A., Vujovich, G.I., 1995. New appraisal on the southwestern Gondwanan terranes and their Laurentian affinities. In: Laurentia-Gondwanan connections before Pangea, *IGCP field Conference Project 376, pp. 31-32.*

Ramos, V.A., Vujovich, G., 1993. Las Orogénesis de Grenville en las Sierras Pampeanas Occidentales: Sierra de Pié de Palo y su integración al Supercontinente Proterozoico. *12th Congreso Geológico Argentino, Mendoza, Actas 3: 343-357.*

Ramos, V.A., 1994. Terranes of southern Gondwanaland and their control in the Andean structure (30 degrees -33 degrees S latitude). In: Reutter, K J; Scheuber, E; Wigger, Peter J. Tectonics of the southern Central Andes;

structure and evolution of an active continental margin. *Springer-Verlag, Berlin, Federal Republic of Germany: 249-261.*

Ramos, V.A., 1995. Evolucion tectonica del segmento de subduccion horizontal de los Andes Centrales (27-34°S) y su control en las manifestaciones auriferas epitermales. Fifth Congreso Nacional de Geologia Economica, San Juan, 1995, *Actas, (82-95).*

Ramos, V.A., 2000. The Southern Central Andes. In: Cordani, U.G., Milani, E.J. Thomaz Filho, A., Campos, D.A. (Editors), Tectonic Evolution of South America. *31st Geological Congress, Rio de Janeiro, pp. 561-604.*

Ramos, V.A., Basei, M., 1997. The basement of Chilenia: an exotic continental terrane to Gondwana during the Early Paleozoic. *Symposium on Terrane Dynamics'97, Chistchurch: 140-143.*

Ramos, V.A., Basei, M., 1997. Gondwanan, PeriGondwanan, and exotic terranes of southern South America. South American *Symposium on Isotope Geology, Sao Paolo, Abstract: 250-252.*

Ramos, V.A., Aleman, A., 2000. Tectonic Evolution of the Andes. In: Cordani, U.G., Milani, E.J. Thomaz Filho, A., Campos, D.A. (Editors). Tectonic Evolution of South America. 31st *International Geological Congress, Rio de Janeiro, Brazil. August 6-17: 635-685.*

Ramos, V.A., Escayola, M., Mutti, D.I., Vujovich, G.I., 2000. Proterozoic-Early Palaeozoic ophiolites of the Andean basemen of southern South America. *Geological society of America, Special Paper, 349: 331-349.*

Randall, D. E., 1998. A new Jurassic-Recent apparent polar wander path for South America and a review of central Andean tectonic model. *Tectonophysics, 299: 49-74.*

Rapalini, A.E., Tarling, D.H., 1993. Multiple magnetizations in the Cambrian-Ordovician carbonate paltform of the Argentine Precordillera and their tectonic implications. *Tectonophysics, 227: 49-62.*

Rapalini, A.E., Tarling, D.H., Turner, P., Flint, S., Vilas, J.F., 1994. Paleomagnetism of the Carboniferous Tepuel Group, central Patagonia, tina. *Tectonics, 13(5): 1277-1294.*

Rapalini, A.E., Vilas, J.F.A., 1991. Tectonic rotations in the late Palaeozoic continental margin of southern South America determined and dated by palaeomagnetism. *Geophysical Journal International, 107(2): 333-351.*

Rapalini, A.E., 1998. Syntectonic magnetization of the mid-Palaeozoic Sierra Grande Formation: Further constraints on the tectonic evolution of Patagonia. *Journal of the Geological Society of London, 155(1): 105-114.*

Rapalini, A.E., Astini, R.A., 1998. Paleomagnetic confirmation of the Laurentian origin of the Argentine Precordillera. *Earth and Planetary Science Letters, 155(1-2): 1-14.*

Rapela, C.W., Coira, B.L., Toselli, A.J., Saavedra, J., 1992. El magmatismo del Paleozoico Inferior en el Sudoesto de Gondwana. In: Gutiérrez, J.G.M., Saavedra, J. and Rábano, I. (Editors). *Paleozoico Inferior de Ibero-América. Univeridad de Extramadura, pp. 21-68.*

Rapela, L.W., 1998. Early evolution of the proto-Andean margin of Gondwana. *Geology, 26 (8): 707-710.*

Rapela, C.W., Pankhurst, R.J., Casquet, C., Baldo, E., Saavedra, J., Galindo, C., Fanning, C.M., 1998. The Pampean Orogeny of the southern proto-Andes: Cambrian continental collision in the Sierras de Córdoba. In: Pankhurst, R.J,

Rapela, C. W. (Editors).The proto-Andean margin of Gondwana. *Geological Society, Special Publications, 142: 181-217.*

Raposo, M.I.B., Ernesto, M., 1995. Anisotropy of magnetic susceptibility in the Ponta Grossa dyke swarm (Brazil) and its relationship with magma flow direction. *Physics of the Earth and Planetary Interiors, 87: 183–196.*

Raposo, M.I.B., Ernesto, M., 1995. An early Cretaceous paleomagnetic pole from Ponta Grossa dykes (Brazil): implications for the South American Mesozoic APWP. Journal of Geophysical Research, 100 (B10): 20095-20109.

Riley, P.D., Beck, M.E., Jr, Burmester, R.F., Mpodozis, C., Garcia, A., 1993. Paleomagnetic evidence of vertical axis block rotations from the Mesozoic of northern Chile. *Journal of Geophysical Research, B, Solid Earth and Planets, 98(5): 8321-8333.*

Rochette, P., Vandamme, D., 2001. Pangea B; an artifact of incorrect paleomagnetic assumptions? *Annali di Geofisica, 44(3): 649-658.*

Roeder, D., 1988 Andean-age structure of Eastern Cordillera (Province of La Paz, Bolivia)

Roperch, P., Carlier, G., 1992. Paleomagnetism of Mesozoic Rocks from the Central Andes of Southern Peru: Importance of Rotations in the Development of the Bolivian Orocline. *Journal of Geophysical Research, 97: 17233-17249.*

Royer, J.Y., Müller, R,D., Gahagan, L.M., Lawver, L.A., Mayes, C.L., Nürnberg, D., Sclater, J.G., 1992. A Global isochron. University of Texas, Institute for Geophysics, Technical Report No. 177.

Schmidt, P.W., Powell, C.M., Li, Z.X., Thrupp, G.A., 1990. Reliability of Palaeozoic palaeomagnetic poles and APWP of Gondwanaland. *Tectonophysics, 184: 87-100.*

Sempere T., 1995. Phanerozoic evolution of Bolivia and adjacent regions. *American Association of Petroleum Geologists, Memoir, 62 : 207-230*

Sinito, A.M., Valencio, D. A., Vilas, J. F.,1979. Palaeomagnetism of a sequence of upper Palaeozoic-lower Mesozoic red beds from Argentina. *Geophysical Journal of the Royal Astronomical Society, 58: 237-247.*

Schult, A., Guerreiro, S.D.C., 1979. Palaeomagnetism of Mesozoic igneous rocks from the Maranhão Basin, Brazil, and the time of opening of the South Atlantic. *Earth and Planetary Science Letters, 42(3): 427-436.*

Smith, A.G., Hurley, A.M., Briden, J.C., 1981. Phanerozoic paleocontinental world maps. *Cambridge University Press, Cambridge, 102 pp.*

Smith, A.G., 1999. Gondwana: its shape, size and position from Cambrian to Triassic times. *Journal of African Earth Sciences, 28(1): 71-97.*

Somoza, R., 1985. Paleomagnetismo de rocas cretácias de la Patagonia y la curva de deriva polar aparente de América del Sur. *PHD Thesis, Universidad de Buenos Aires: 238 pp.*

Somozo, R., Singer, S., Coira, B., 1996. Paleomagnetism of Upper Miocene ignimbrites at the Puna: an analysis of vertical-axis rotations in the Central Andes. J*ournal of Geophysical Research, 101: 11387-11400.*

Tait, J., Schätz, M., Bachtadse, V. and Soffel, H., 2000. Paleomagnetism and Paleozoic paleogeography. In: W. Franke, V. Haak, O. Oncken and D. Tanner (Editors), Orogenic Processes: Quantification and Modelling in the Variscan Belt. *Special Publications of the Geological Society. Geological Society of London, London, 21-34.*

Thomas, W.A. and Astini, R.A., 1996. The Argentine Precordillera; a traveler from the Ouachita Embayment of North American Laurentia. *Science, 273(5276): 752-757.*

Thompson, R., Mitchell, J.G., 1972. Palaeomagnetic and radiometric evidence for the age of the lower boundary of the Kiaman Magnetic Interval in South America. *Geophysical Journal of the Royal Astronomical Society, 29: 107-214.*

Tomezzoli, R.N., Vilas, J.F., 1999. Paleomagnetic constraints on age of deformation of the Sierras Australes thrust an fold belt. *Geophysical Journal of the Royal Astronomical Society, 51: 59-74.*

Tomezzoli, R. N., 2001. Further palaeomagnetic results from the Sierras Australes fold and thrust belt, Aargentina. *Geophysical Journal International, 147: 356-366.*

Torsvik, T.H., Carter, L.M., Ashwal, L.D., Bhushan, S.K., Pandit, M.K., Jamtveit, B., 2001. Rodinia refined or obscured: paleomangnetism of the Malani igneous suite (NW India). *Precambrian Research, 108: 850-856.*

Torsvik, T.H., Van der Voo, R., 2002. Refining Gondwana and Pangea palaeogeography: estimates of Phanerozoic non-dipole (octupole) fields. *Geophysical Journal International, 151 : 771-794.*

Tosdal, R.M., 1996. The Amazon-Laurentian connection as viewed from the Middle Proterozoic rocks in the Central Andes, western Peru and Northern Chile. *Tectonics, 15: 827-842.*

Toro, B.A., Brussa, E.D., 1996. Graptolitos de la Formacion Suri (Arenigiano) en la Sierra de Famatina, Argentina; importancia bioestratigrafica y paleobiogeografica. Graptolites from the Suri Formation (Arenigian) in the Sierra de Famatina, Argentina; biostratigraphic and paleobiogeographic importance. *Ameghiniana, 33(2): 232-233.*

Turner, J.C., 1960. Las Sierras Traspampeanas como unidad estructural. *Ann. J. Geol. Arg., Buenos Aires, 1.*

Turner, J.C. 1967. Descripción geológica de la hoja 13b, Chaschuil (Provincias de Catamarca y La Rioja). *Dir. Nac. Geol. y Min. Bol., 106.*

Vaccari, N.E., Waisfeld, B.G., 1994. Nuevos trilobites de la Formacion Suri (Ordovicico temprano) en la region de Chaschuil, Provincia de Catamarca, implicancias bioestratigraficas. New trilobites from Suri Formation (Lower Ordovician) from Chaschuil region, Catamarca Province; biostratigraphic implications. *Ameghiniana, 31(1): 73-86.*

Valencio,D.A., Mendia, J.E., Vilas, J.F., 1975. Palaeomagnetism and K-Ar ages of Triassic igneous rocks from the Ischigualasto-Ischichuca Basin and Puesto Viejo formation, Argentina. *Earth and Planetary Sciences.Letters 26, 319-330.*

Valencio, D.A., Vilas, J.F.A., Mendia, J.E., 1977. Palaeomagnetism of a sequence of redbeds of the Middle and Upper Sections of Paganzo Group (Argentina) and the correlation of Upper Palaeozoic-Lower Mesozoic rocks. *Geophysical Journal of the Royal Astronomical Society, 51: 59-74.*

Valencio,D.A., Vilas, J.F.A., 1985. Evidence of a microplate in the southern Andes. *Journal of Geodynamics, 2: 183-192.*

Van der Voo, R. and French, R.B., 1974. Apparent polar wandering for the Atlantic-bordering continents: Late Carboniferous to Eocene. *Earth-Science Reviews, 10: 99-119.*

Van der Voo, R., 1990. The reliability of paleomagnetic data. *Tectonophysics, 184: 1-10.*

Van der Voo, R., 1993. Paleomagnetism of the Atlantic, Tethys and Iapetus Oceans. *Cambridge University Press, Cambridge, 411 pp.*

Van der Voo, R., Torsvik, T., 2001. Evidence for late Paleozoic and Mesozoic non-dipole fields provides an explanation for the Pangea reconstruction problems. *Earth and Planetary Science Letters, 187(1-2): 55-69.*

Vergel, M.M., 1996. Palinologia des Sistema de Famatina. Palynology of the Famatina System. In: Acenolaza, F G, Miller, H, Toselli, A. (Editors) Geologia del sistema de Famatina. Geology of the Famatina System. *Muenchner Geologische Hefte. Reihe A, Allgemeine Geologie, 19: 145-155.*

Waisfeld, B.G., Sanchez, T.M., Benedetto, J.L., Carrera, M.G., 2003. Early Ordovician (Arenig) faunal assemblages from western Argentina; biodiversification trends in different geodynamic and palaeogeographic settings. *Palaeogeography, Palaeoclimatology, Palaeoecology, 196(3-4): 343-373.*

Watson, G.S., Enkin, R.J., 1993. The fold test in paleomagnetism as parameter estimation problem. *Geophysical Research Letters, 20(19): 2135-2137.*

Wasteneys, H.A., Clark, A.H., Farrar, E., Lagridge, R.J., 1995. Genvillian granulite-facies metamorphism in the Arequipa Massif, Peru: a Laurentia-Gondwana link. *Earth and Planetary Letters, 132: 63-73.*

Zijderveld, J.D.A., 1967. Demagnetization Analysis of results. In: Collinson D.W., Creer K.M., Runcorn S.K. (Editors.). Methods of Paleomagnetism. *Elsevier, Amsterdam, New York, 254-286.*

Lebenslauf

Name: Nicolas Albert Rakotosolofo
Geburtsdatum: 28 November 1965
Geburtsort: Fianarantsoa, Madagaskar
Familienstand: Ledig
Staatsangehörigkeit: Madagassisch

Schulbildung

1970-1976   Grundschule Saint Charles, Madagaskar
1976   Abschluß, „Certificat d'Etudes Primaires Elémentaires" (CEPE)
1977-1980   "Collège d'Enseignement General Mahamanina", Madagaskar
1980   Abschluß "Brevet des Collèges (BEPC)
1981-1984   Gymnasium "Lycée Raherivelo Ramamonjy", Madagaskar
August 1984   Abschluß, Baccalauréat D: Mathématiques et Sciences de la Nature
               (Abitur)

Universitäre Ausbildung

1986-1989   Studium der Naturwissenschaft an der Université d'Antananarivo,
               Madagaskar
Juli 1989   Abschluß, Diplôme Universitaire d'Étude Scientifiques" (DUES)
1990-1992   Studium der Naturwissenschaft an der Université d'Antananarivo,
               Madagaskar
Juni 1992   Abschluß, "Licence d'Enseignement es Sciences Naturelles"
1992-1993   Studium der Geologie, Geochemie und Pädologie an der Université
               d'Antananarivo, Madagaskar
Juli 1993   Abschluß, Maîtrise de Recherche en Geologie, option Geochimie"
1995-1996   Mitarbeiter in der Abteilung für Geologie der Université
               d'Antananarivo in Zusammenarbeit mit der Randse Afrikaans
               Universiteit und der University of Cape Town im Rahmen des
               Projekts "Madagascar in Gondwana Project" gefördert von der
               südafrikanischen "Founds for Research and Development"
1996-1999   Studium der Geologie an der Randse Afrikaans Universiteit, Südafrika
August 1999   Abschluß, "Magister Scientiae, Geologie"
               Titel der Abschlußarbeit: "*Sedimentology, structural geology and
               Palaeomagnetism of the Morondava Basin, SW Madagascar*";
               Betreuer: Prof. Lewis Ashwall, Prof. Maarten de Wit.
2000-heute   Wissenschaficher Angestellter an der Ludwig-Maximilians-
               Universität München (LMU), Department für Geo- und
               Umweltwissenschaften, Sektion Geophysik, im Rahmen des
               Projektes "Gondwana "gefördert von der VW-Stiftung.
               Titel der Doktorarbeit: "*Paläomagnetismus des Paläozoikums und
               Mesozoikums von Südamerika: Ergebnisse von Peru, Bolivien,
               Argentinien und Brasilien*"; Betreuer Dr. Jennifer Tait (LMU
               München).